A Petrological and Geochemical Reconnaissance of the Moor of Rannoch Pluton, South-West Highlands, Scotland.

CERTIFICATE

I certify that Philip S. Leighton has been engaged in research for 9 terms at the University of St. Andrews, that he has fulfilled the conditions of Regulation No. 12 (St. Andrews) and the Resolution of the University Court, 1974, No.2, and that he is qualified to submit this thesis for the degree of Master of Science.

W.E. Stephens.

I certify that the following thesis is based on the results of research carried out by me, that it is my own composition, and that it has not previously been presented for a higher degree.

P.S. Leighton.

This thesis is dedicated to Susanne, Jack and Jerry for their quiet yet insistent encouragement when it was most required.

ABSTRACT

The Moor of Rannoch granitoid is a composite pluton forcefully intruded into a structurally complex nappe root zone involving Moine and Lower Dalradian metasediments. Internal variation is extensive, from monzodiorites through to syenogranites with a concommitant geochemical variation, from 52.6 to 75.7 wt% SiO_2 in a high-K calc-alkaline trend. The major and trace element abundances are consistent with an I-type origin, but the syenogranites exhibit characteristics intermediate between I- and A- type granitoids. Distinctive high Ba and Sr concentrations, characteristic of the southwest Highland Caledonian granites, are contrasted with significantly lower abundances in the Strath Ossian Caledonian granitoid and coupled with isotopic evidence, indicates the two intrusions to be distinct in terms of source and age of emplacement.

The chemical and petrographic variation is accounted for by a multi-episodic intrusion model involving a change in source material and with limited crustal contamination. The syenogranites have low absolute Rb abundances and are isotopically distinct . The Laidon-Ericht fault, (subparallel to the Great Glen Fault), cuts the pluton and is considered to have greater horizontal displacement than previously thought. Evidence is presented to support a possible 30 - 40 km sinistral displacement by comparing petrographically and geochemically similar rock types from the southeastern and eastern part of the Etive intrusive complex with the eastern part of the Moor of Rannoch complex and Loch Tulla outlier.

CONTENTS

INTRODUCTION

The objective of this project was the reconnaissance of a poorly studied granitoid in the Central Highlands of Scotland, the Moor of Rannoch pluton. Initial work was to discover the extent of exposure and sample sufficient to determine field, petrologic and chemical variations present. A secondary objective, isotopic analysis of representative samples of the rock types mapped, could not be completely carried out due to pressure of existing work at the SURRC at East Kilbride. From these, an attempt to outline magma source, the evolution of magmatism and level of emplacement has been made.

Comparison between the Moor of Rannoch and Strath Ossian plutons has been made using published and unpublished data for the latter. Reconnaissance samples of Strath Ossian collected in the course of field work have been used to expand the data base for this 'satellite' pluton.

Using the petrogenetic 'I-' and 'S-' type classification of Chappell and White (1974), together with a review of the Scottish Caledonian by Stephens and Halliday (1984), as models, similarities and dissimilarities between models and the data presented here are thought adequately accounted for. An attempt to classify and explain a common petrographic texture (biotite cores within amphibole) using microprobe data has been made.

Regional Geology

2.0 Introduction.

The Moor of Rannoch granite is hosted by the metasediments of the Central Highlands Group (Figs. 2.1 & 2.2), which form a complex structural sequence within the region. The south-eastern margin lies close to the juncture between the Moine and the Dalradian, at the present level of exposure. Due to the structural relationships proposed for the Moine and Dalradian, both formations may be considered as the 'host' to the intrusion. A detailed summary of their depositional and deformational histories is presented here, in an attempt to outline the pre-intrusive sequence of events prior to emplacement of the Moor of Rannoch pluton.

2.1 The Moines.

The Moine metasediments of the region have been referred to as the 'younger Moines' (Hinxman et al., 1923; Powell, 1978). Within the areas of Ben Alder, Ben Dorian and Meall Beag early workers considered their outcrop too complex for sedimentological or chronological study. Recent structural and isotopic work gives evidence for two distinct divisions within the Central Highland Moines (Piasecki 1975; Johnstone 1975; Piasecki & van Breemen, 1979a, 1979b). These workers recognise a basement of high grade gneissic migmatites (the Central Highland Division), overlain by medium grade cover (Grampian Division)

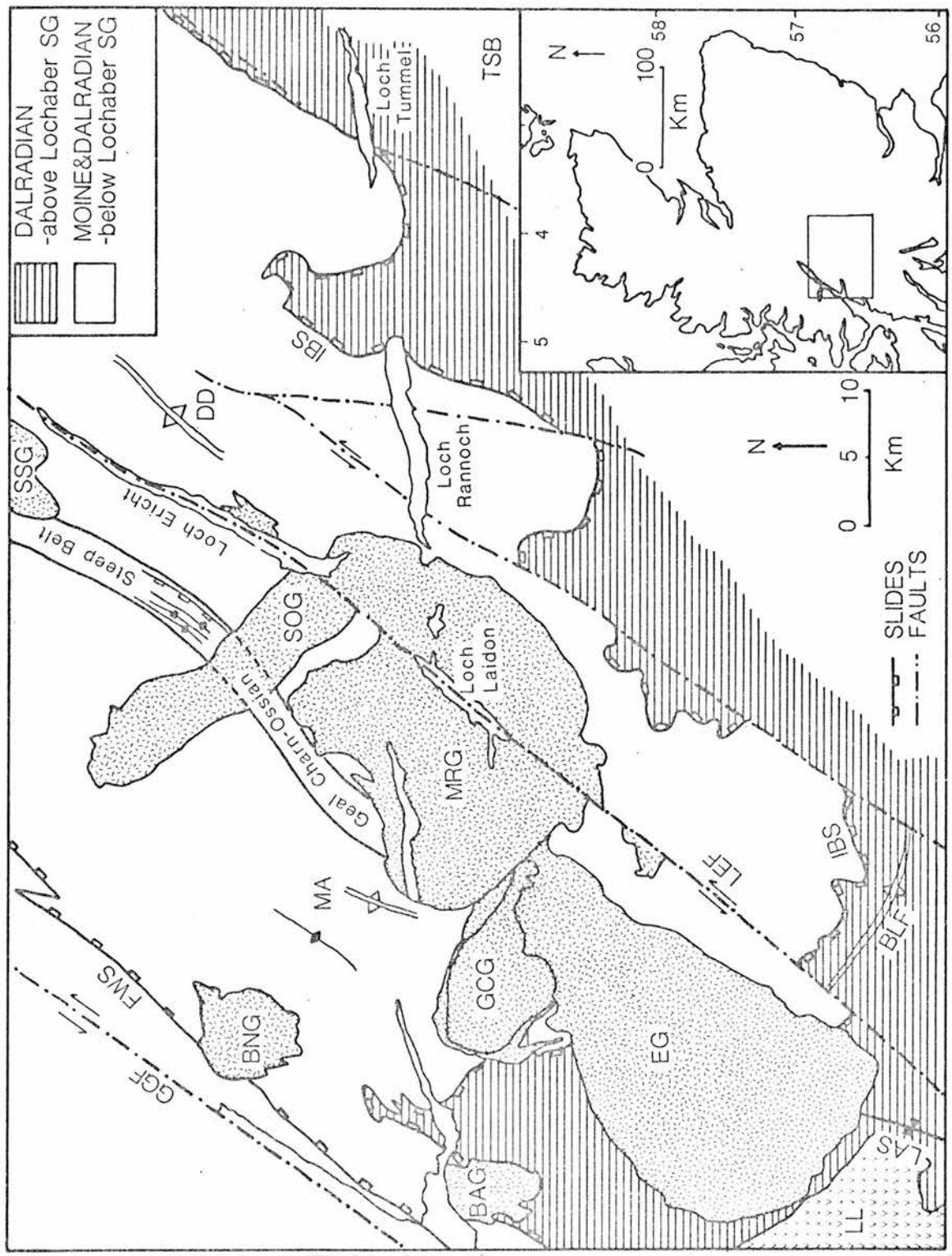

Diagram adapted from THOMAS (1979)

Figure 2.1 Location map and simplified structural map showing major faults, folds, slides and granitoid intrusions in the western Central Highlands. Key for abbreviations: BAG Ballachulish granite, BNG Ben Nevis granite, EG Etive granite, GCG Glen Coe granite, MRG Moor of Rannoch granite, SOG Strath Ossian granite, SSG Strathspey granite; BLF Ben Lui fold, DD Drumochter dome, FWS Fort William slide, GGF Great Glen fault, IBS Iltay boundary slide, LAS Loch Awe syncline, LEF Laidon-Ericht fault, LL Lorne lavas, MA Mamore anticline, TSB Tummel steep belt.

and separated by a zone of tectonic sliding termed the 'Grampian Slide'. This slide is marked in the field by a zone of ductile thrusting tectonised schists.

Syntectonic pegmatite veins occurring in the slide zone have yielded ages of 718+/-19 Ma to 573+/-13 Ma. (Piasecki & van Breemen, 1979b). This range of dates is considered to be the result of D3 Caledonian deformation on the pegmatites, with pegmatite emplacement occurring wholly before the oldest date given. Further unpublished pegmatite ages from slides subparallel and close to the Grampian Slide have a range of 730 - 780 Ma (Piasecki et al., 1981). This suggests a Morarian age for the slide and thus allows a minimum age for the Grampian group cover and Central Highland Division basement to be proposed.

The Central Highland Division basement is composed of medium to coarse grained gneissic psammitic metasediments with concordant migmatites (Piasecki & van Breemen 1979). This has been tentatively correlated with the Glenfinnan Division west of the Great Glen Fault, a structurally and lithologically similar division dated at 1030+/-50 Ma (Brook et al., 1976). The cover rocks of the Grampian Division are non-migmatitic, non-gneissic medium-grade metasediments with relict sedimentary structures. They are thought to be older than the Morarian pegmatites, yet younger than the Central Highland Division basement.

Thus the lower part (c. 1.5km) of the Grampian Division is assumed to comprise sediments deposited in the Grenville - Morarian interval and have been only weakly folded in the pre-Caledonian (Piasecki & van Breemen, 1979). These lower Grampian Division rocks are tentatively correlated with the Loch Eil and Morar divisions and Tarskavaig Moines in Scotland and with the North East Ox mountains and Loch Dearg inliers in Ireland. Analyses of Rb/Sr isotopic ratios in the Irish formations give ages of 860+/-115 Ma (Piasecki & van Breemen, 1979b) which correspond to a post-Grenville age. The lower cover rocks of the Grampian Division are considered by the above authors to be related to the Torridonian arkoses.

Acceptance of this proposed subdivision of the Moines east of the Great Glen Fault is dependent on the recognition of the Grampian Slide. This concept of a slide zone with restricted temporal occurrence of pegmatites is questioned by Ramsay (in Zaleski 1982) who indicates difficulties in recognition of the tectonised schists as a major slide in the field. A summary of the structural work of Piasecki on the Central Highland Moines is given below.

Three major pre-Cambrian deformations in the Central Highland Division are recognised; the earliest is of gneissosity and migmatisation subsequently affected by two later episodes of penetrative isoclinal folding. The first of these latter events resulted in further migmatisation, the second and youngest giving regional recumbent folding. Within the Grampian Division, two major pre-Cambrian deformations and one major Caledonian defromation are

inferred.

The first pre-Cambrian, D1, resulted in a penetrative schistosity and low grade metamorphism which was overprinted by a later regional D2 schistosity event with associated kyanite grade amphibolite facies metamorphism. Sliding within the basement/cover contact zone is considered to have occurred during the D2 deformation. A subsequent D3 folding event of inferred Caledonian age, (573+/- 13 Ma from deformed pegmatites), resulted in a new regional schistosity with attendant lower grade amphibolite facies metamorphism and major movements on the Grampian Slide. In recent work, Thomas (1979) has presented evidence for two contrasting Moine successions, one of which is closely related to the overlying Dalradian.

2.2 Dalradian Supergroup.

The Dalradian of the Central Highlands is regarded as being a continuous sedimentary succession from the Moines and having greater lithological variety than the latter. There is no evidence for, or against, unconformities within the Dalradian. The common field definition used is "where the monotonous psammites change to the more lithologically diverse pelites and quartzites" (Johnstone 1975). Harris (1978) ascribes this change in lithology to an increasing basin maturity with deposits changing from poorly sorted feldspathic sands (Moine) to turbidites. The boundary between the Moine and Dalradian is continuous in the northern Grampian region and discontinuous in Perthshire, where a boundary slide is inferred to separate them (Fig. 2.1). The term slide (Bailey, 1922) is used to describe a plane of

movement along the limbs of a major fold, while Fleuty (in Craig, 1964) suggests a slide represents a fault in connection with folding which is conformable with the fold limbs or axial surface.

The age of this boundary between the Moine and Dalradian sedimentation and of the younger 'Moines' is uncertain. The age of the Varranger Tillite in Norway, 668+/-23 Ma (Pringle 1972), which Johnstone (1975) considers as a time equivalent to the Portaskaig Tillite at the base of the Middle Dalradian, places a constraint on the possible age of these younger Moines. However, the Portsoy and Windyhills gneisses which intrude the Durnhill Quartzite, stratigraphically higher than the Portaskaig Tillite, have been dated at 669+/-17 Ma (Pankhurst 1975). This would imply emplacement after a rapidly accumulated sedimentary sequence of quartzites. Pankhurst (1975) interprets this as a break in the Middle Dalradian of the Argyll Group or that the Lower Dalradian is older than 700 Ma (no error qualification, Dunning, 1972).

The augen gneisses of Portsoy and Windyhills are thought to be evidence of an earlier Morarian orogeny, however Peach and Horne (1930) reported Planolite sp. trace fossils from the Appin Group on Islay. These are in keeping with Dalradian ages and would be unlikely to survive polyphase deformation and sliding. Harris et al. (1980) propose a "modified unconfromity" - a tectonised platy zone - between Grenville/Morarian basement and the younger cover, extending to the Dalradian. A possible correlation with the Sgurr Beag Slide west of the Great Glen Fault is suggested.

2.3 Dalradian Sedimentology.

The Dalradian Supergroup is considered as having a thickness of approximately 20km and despite deformation and metamorphism, determination of order of superposition is rarely difficult (Harris and Pitcher 1975). Subdivision of the supergroup is based on lithostratigraphical evidence and correlation of sedimentary associations as a result of consistency of detail along strike. The environment of deposition is interpreted as a basin of increasing maturity. This is based on the lateral and vertical changes from sorted quartzose sands and micaceous silts of the lower Lochaber group, through calcareous silts and clays of the Leven schists, to the closed basinal accumulation of argillaceous and carbonate muds of the Ballachulish slates. An accumulation of shallow water sands of the Appin quartzite terminated deposition prior to subsequent subsidence. Following this recommencement of deposition, intercalations of carbonate mud with sand wedges accumulated leading to final laminated lagoonal muds (Treagus, 1964;Treagus and Thomas, 1968;Harris and Pitcher, 1975). In the central and south-west Highlands, large areas have been metamorphosed to amphibolite or garnet amphibolite facies and Dunning (1972) considered the deformation and concomitant metamorphism probably occurred in the Lower Ordovician.

The lateral variations and facies changes between outcrop in Scotland and Ireland, eg. the Appin Limestone (Pitcher and Berger, 1972), suggest an elongated depositional trough to the south-east of the present outcrop. Litherland (1970) has demonstrated similar facies variation in the Glen Creran area, previously considered to be due to

tectonic attenuation (Bailey,1960). The Lochaber and Ballachulish subgroups appear to indicate rapid sedimentation in the early Dalradian period. For detailed lithological descriptions of the Dalradian see Harris and Pitcher (1975), Roberts and Treagus (1979) and Borradaile (1979).

2.4 Structural Synthesis and Regional Tectonic Relationships.

The pre-Caledonian and Caledonian structural history of the Dalradian and the underlying Moines is both complex and not yet fully understood. Bailey (1925), commenting on work by Barrow (1915), first proposed a series of large scale recumbent folds as part of a large nappe structure for the area east of Loch Rannoch. This nappe was later termed the Tay Nappe. Further work by Bailey and McCallien (1937), Treagus (1964) and Roberts and Treagus (1979), suggests that the Central Highlands area lies to the south-east of any postulated root zone for the Tay Nappe. Roberts and Treagus (1979) consider that both the south-west and central Highlands were affected by the same system of south-east facing nappes. These nappes, termed D1 and D2 (Roberts and Treagus 1977), are seen at various structural levels only as a result of later D4 cross-folding. The deformation style below the Perthshire succession is thought by Treagus (1964) to be controlled by competent Moine and thin 'strips' of Dalradian.

Roberts and Treagus (1979) also consider the boundary slide to be a diffuse D2 structure "of little mechanical importance", an idea at variance with many other workers in the area. The above authors also consider that sliding and attenuation of outcrop was important at

lower levels, but that no one slide can be shown to have a uniform effect on a specific stratigraphical horizon throughout the region. Large dome structures are postulated to underlie the Glen Orchy antiform, Ben Dorian, Schiehallion and Drumochter areas (Fig. 2.2).

A different interpretation of the structure of the central Highlands has also been proposed in the recent literature. This interpretation is based on the idea of divergent nappes facing in opposite directions - north-west and south-east - on either side of a central belt of upright F1 structures, the "root zone". Based on work by Sturt (1961), Rast (1958, 1963), Johnstone (1966), Thomas (1965, 1979), France (1971) and Borradaile (1973), this interpretation questions that of Bailey, Roberts and Treagus. The grounds for this are that the large scale D2 nappes proposed by the latter require large swings in strike, a feature not well supported by field evidence. A summary of the alternative hypothesis is given below.

The primary deformation (early Grampian) is thought to be development of D1 nappes diverging from a root zone at Ossian/Geal Charn (Fig 2.1) and lying below the Loch Awe syncline. As the large scale nappes developed, older Moine rocks were brought up to below the Sgoir Slide (equated with the Iltay boundary slide). These Moine rocks were in effect draped over the arched, deeper level domes (Fig. 2.2). To the north-west of the Ossian/Geal Chrarn root zone, nappe folds also developed, with the Aonach Beag slide (a possible Ballachulish Slide equivalent), forming a dislocation between the Moine and Lower Dalradian. Under increased pressure and temperature conditions, a D2 deformation led to the overturned folds in the

Diagram adapted from THOMAS(1979)

Figure 2.2 Idealised cross section across Geal Charn - Ossian steep belt showing the complex structural relationship of Moines and Lower Dalradian. The sheeted intrusive style of the Moor of Rannoch in the south-west may result from magma following these convoluted boudaries.

south-east and modified the nappe structures to the north-west of the root zone.

The secondary (late Grampian/Caledonian) deformation is not thought as consistent in style, plunge and areal occurrence as the preceeding D1 and D2 deformations. The pattern of folding was modified by major D3 folds in certain areas, eg. Glen Lyon to Glen Tilt. These D3 deformations may have been influenced by the presence of deeper seated domes. Final open monoform D4 deformations appear to be restricted to the east of the root zone, although extending to Strathspey in the north-east. These D3 and D4 deformations may have resulted from changes in the dominant stress field (from NW-SE to WNW-ESE) prior to D5 wrench faulting.

A U/Pb zircon date, 514+/-6 Ma for the emplacement of the synorogenic Ben Vuirich granite (Pankhurst and Pidgeon 1976), indicates a pre 514 Ma age for the D2 deformation and a post 514 Ma age for the D3 deformation. Bradbury et al. (1979) argue that granite emplacement was coeval with migmatisation in the Perthshire region. In the Moines north-west of the Great Glen, U/Pb zircon ages from the pre-metamorphic Glen Dessary syenite yield a 456+/-5 Ma maximum age for metamorphism (van Breemen et al. 1979). These authors propose a diachronous event across the Great Glen Fault. Lambert et al. (1982) regard the Grampian metamorphism as a 486+/-9 Ma event on the basis of work in the schists of the Grampian Division of the Moine. Late tectonic pegmatites at Glenfinnan and Loch Morar are recognised (van Breemen et al. 1974) and correlated with similar at Upper Findhorn to the east of the Great Glen Fault (van Breemen and Piasecki, 1983).

2.5 The Newer Granites of the Highlands.

The Caledonian granites of Scotland, emplaced between 560+/-10 Ma and 389+/-6 Ma, have been problematic with regard to their classification. Read (1956,1961) was the first to produce a modern overall classification and a brief summary of both his work and later contributions to the debate on origin and emplacement of these granites is presented here.

Read (1961) based his classification on the time and manner of emplacement of the plutons. Field work and petrological examination, led him to conclude a primary two-fold division existed; the 'Older Granites' and the 'Newer Granites'. The 'Older' granites he considered syntectonic (D1 - D3 deformations), while the 'Newer' granites were post tectonic. This group of 'Newer' granites he further subdivided, by intrusive style, into 'forceful' and 'permitted' intrusions; his subdivision was based on the results of field work on the southern and western margins of the Moor of Rannoch pluton, the Glen Coe and Etive intrusive complexes and the Lower Old Red Sandstone age lavas of the Lorne plateau. Thus he considered the Moor of Rannoch pluton to be an early, forcefully emplaced 'Newer' granite which was cut by the fault intrusion of the Glen Coe complex.

Recent attempts at classifying Caledonian granites have been made in the light of new geophysical, geochemical and isotope geochronological data (Brown & Locke, 1979; Pankhurst & Sutherland, 1980; van Breemen & Bluck, 1981). Read himself foresaw this as

refining and modifying his original ideas. In addition, new classifications for granites in general have been proposed by Chappell & White (1974) and Isihara (1976).

Brown and Locke (1979) proposed a two-fold temporal division in which the 'Older' syntectonic granites and the forceful 'Newer' granites of Read, formed one group. These, on the basis of magnetic and geochemical properties (high Sr & K/Rb ratios) were thought similar to their host metasediments, the Moine and Dalradian (Johnstone et al., 1979). The intrusions of this first group were low volume melts with a significant crustal contamination or crustal source component.

The second group proposed are the permitted 'Newer' granites of Read (1961) which feature large intrusive volumes, large aeromagnetic and gravity anomalies. Brown and Locke (1979) suggest that their geochemistry - low $^{87}Sr/^{86}Sr$ ratios, high incompatible element concentrations and concordant U/Pb systematics - is indicative of mantle derivation. This group were thought to be Siluro-Devonian in age, those of the first group pre-Silurian. This temporal division has been questioned by Pankhurst (1979) and considered untenable by Clayburn (1981).

Brown and Locke (1979) equate the change between source and intrusive style with a change in the regional tectonics; they consider the change from compressional movements to extensional movements gave rise to a different melting regime.

Pankhurst and Sutherland (1980) modified Read's classification by grouping the 'Newer' granites according to the time of emplacement, thus producing a three-fold division, ('groups' 1 to 3). The first group, early-mid Ordovician granites emplaced at the climax of deformation and metamorphism (c. 485+/-20 Ma) eg. Strichen, Glen Kyllachy, correspond to the first of the 'Older' granites of Read, (part of group 1 of Brown & Locke). The second group of Pankhurst and Sutherland consists of late Ordovician-early Silurian granites (440 -410 Ma) and are those that post-date the climax of deformation and metamorphism. These authors include some of the 'permitted' granites along with the 'forceful' granites. The third group comprises those granites younger than the arbitrary 410 Ma boundary together with some of Read's 'Last' granites and LORS granites.

The Caledonian granites may also be classified according to the model of Chapell and White (1974) - that of I and S types. Those granites of I-type, that is of igneous source rocks, are thought to be complex intrusions with a wide range of SiO2 values, low initial $^{87}Sr/^{86}Sr$ ratios (0.704-0.706) and high Ca and Na/K ratios. S-type granites are considered compositionally restricted, with high initial $^{87}Sr/^{86}Sr$ ratios (>0.707) and A/CNK values >= 1.10 (i.e. peraluminous granites). As with all classifications, not all granites studied in detail fall completely into any one particular classification.

2.6 Granites of the South-West Highlands.

The Caledonian granites of the south-west Highlands are Ben Nevis, Ballachulish, Glen Coe, Etive, Moor of Rannoch and Strath Ossian of which the Moor of Rannoch pluton is volumetrically the most significant. Although a wide range of rock types are present in the intrusions of this region, eg. diorite - biotite granite, granodiorite is predominant, followed by tonalites. As a general rule, the tonalites/granodiorites are emplaced first as marginal phases into which later, more acid magmas were intruded. Evidence will be presented later (chapter 7) to show that this general rule is not strictly adhered to and a multi-episodic model is erected to account for the large scale and detail differences.

Within the Moor of Rannoch and Strath Ossian intrusions, granodiorite and tonalite are the predominant rock types. Diorites and quartz diorites are present in significant volumes in both intrusions, while at Moor of Rannoch, granites (sensu stricto) are well exposed and may form up to 10% of the intrusive area. As a result of the survey work by Hinxman et al., (1923) and Read (1961), the Moor of Rannoch intrusion is considered the first of the 'Newer' granites along with the Strath Ossian intrusion.

Little published data is available on the Ballachulish intrusion, but it is comprised of an outer biotite quartz diorite with an inner adamellite, both types containing numerous xenoliths. The Glen Coe intrusion is perhaps the best known example of cauldron subsidence (Bailey and Maufe 1960). A ring fault, cutting both the Dalradian/Moine and the earlier Moor of Rannoch intrusion, is intruded

by granite which chilled against the Moor of Rannoch mass and that of Etive. Within the downfaulted block are stratified volcanics and granite of the Etive complex (Cruachan granite). These lavas are thought of LORS age, correlating with the LORS Lorne lavas of Argyllshire, and contain boulders of material very similar to the Moor of Rannoch granite (s.l.).

The Etive complex comprises the early Quarry intrusion followed by the Cruachan granite which varies from tonalite to adamellite. The Meall Odhar phase which followed is a mafic poor granite with sheeted form and limited outcrop. The final phases are those of the Porphyritic Starav and Central Starav granites; they have approximately concentric outcrop and are the most acid type found within the complex.

The Ben Nevis intrusion is again approximately concentric in outcrop, with a central core of downfaulted LORS volcanics (Haslam 1968). From the outside to centre there are outer and inner quartz diorites of early, possible ring dyke origin with a third of porphyritic granite which appears to cut the inner quartz diorite. The 'inner granite' is in fact granodiorite which has a chilled contact with the downfaulted volcanics.

2.7 Conclusions.

The pre-Caledonian history of the Moines and Dalradian are still not yet fully understood. The regional metamorphic compilations of Winchester (1974) and Fettes (1979) are "likely to be composites of polymetamorphic terranes" (Zaleski 1982), while intrusion of the Moor of Rannoch and Strath Ossian granites into a structurally critical area, removing regional rock outcrop, will preclude our understanding from being complete. Much work remains to be done in isotope systematics and classification of the granites before any one model accounts for their histories, present compositions and spatial distribution.

FIELD GEOLOGY

3.0 Introduction.

The margins of the Moor of Rannoch pluton exhibit one dominant intrusive style, detailed below, with different possible interpretations in particular areas. A brief description of the contact aureole is included and an attempt made to analyse the movements of the Laidon-Ericht wrench fault. The internal relationships within the pluton, noted in the course of sampling, are summarised but are necessarily incomplete due to the nature of the project. Reconnaisance of the pluton, some 240 kms^2, and sampling conducted on a grid basis but modified as a result of exposure, which in the central Black Corries and Moor area was very poor.

3.1 Eastern margins.

Based on Read's (1956,1961) interpretations of features of intrusion, the margins of the Moor of Rannoch pluton show evidence for a predominantly forceful style of intrusion. Along the river Ericht at the eastern part of the complex a 1000 metre traverse across the contact shows swing in strike and steepening of dip in the country rocks (Fig. 3.1). In this area no contact between the main intrusive mass and the Dalradian is seen. Between Loch Ericht and Gleann Chomraidh the arcuate outcrop of the pluton is controlled by a fault.

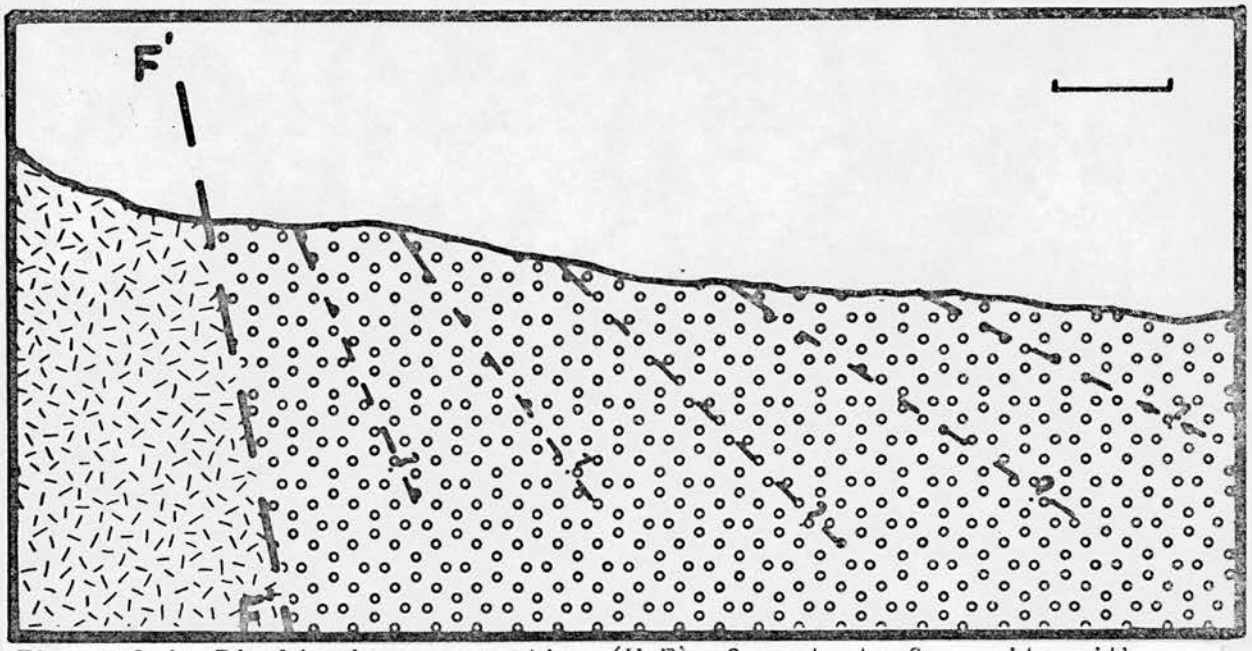

Figure 3.1 Idealised cross section (W-E) of contact of granite with country rock (Eastern margin). Dashed lines indicate steepening of dip in country rock as contact with granite is approached. Heavy dashed line (F - F') represents fault contact. Vertical scale exaggerated, horizontal scale bar represents 100 metres.

Figure 3.2 Detail of contact between Lower Dalradian xenolith and host quartz-monzodiorite(QMD). Distended and flattened amphibolite inclusions within the host are orientated parallel to the margin of the metasedimentary xenolith. The lack of deformation of the metasediment suggests that the amphibolite was incorporated into the ascending magma before it. A cross-cutting vein of later granodioritic material has disrupted the amphibolite inclusions and host but not the metasediment, suggesting the QMD was still a mobile mush. Scale bar represents 10cms. By Kingshouse.

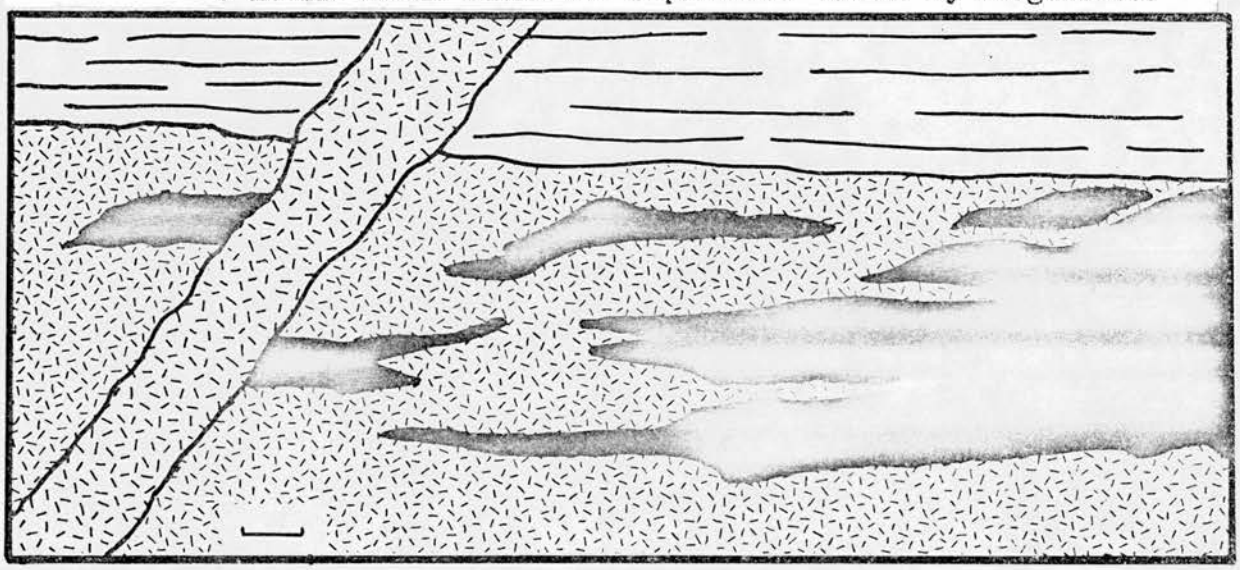

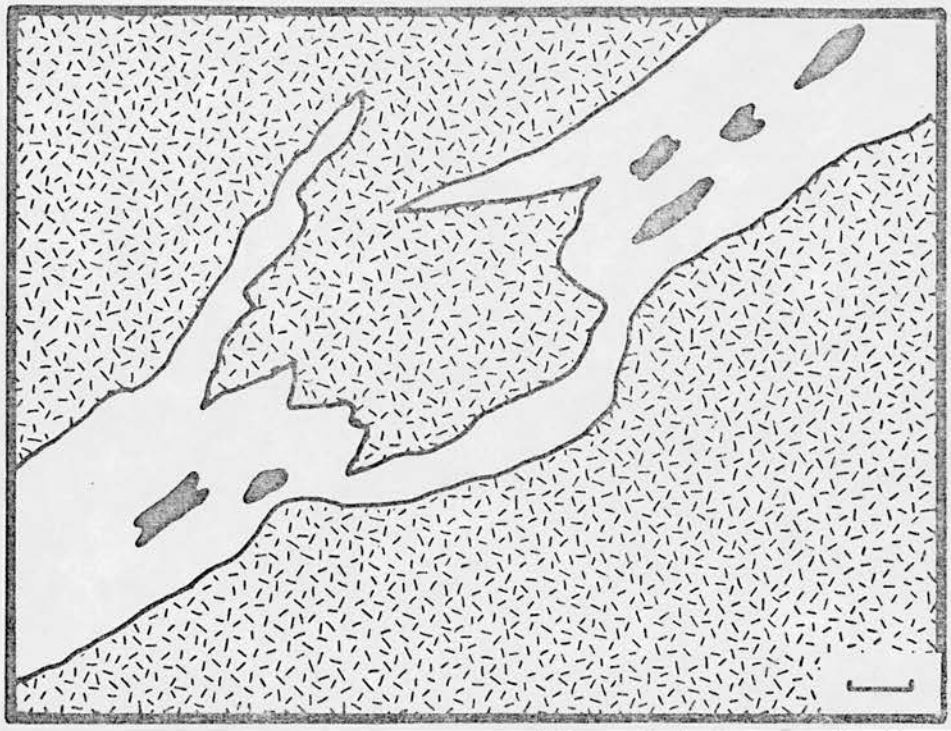

Figure 3.3 Amphibolite inclusions within a later, more basic phase cutting an earlier monzogranitic phase. Scale bar represents 10cms. Western shore, Loch Laidon.

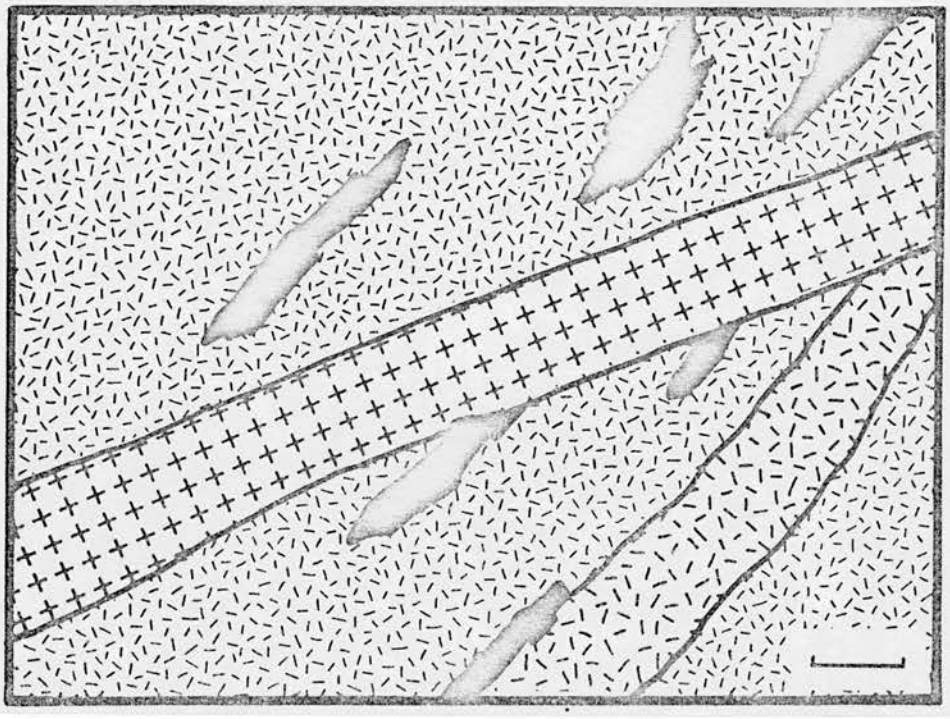

Figure 3.4 Amphibolite inclusions in quartz-monzodiorite, parallel to a vein of more leucocratic quartz-monzodiorite, showing extension and flattening. A later monzogranite vein cross cuts both. Scale bar represents 10cms. By Loch Eighach, eastern margin.

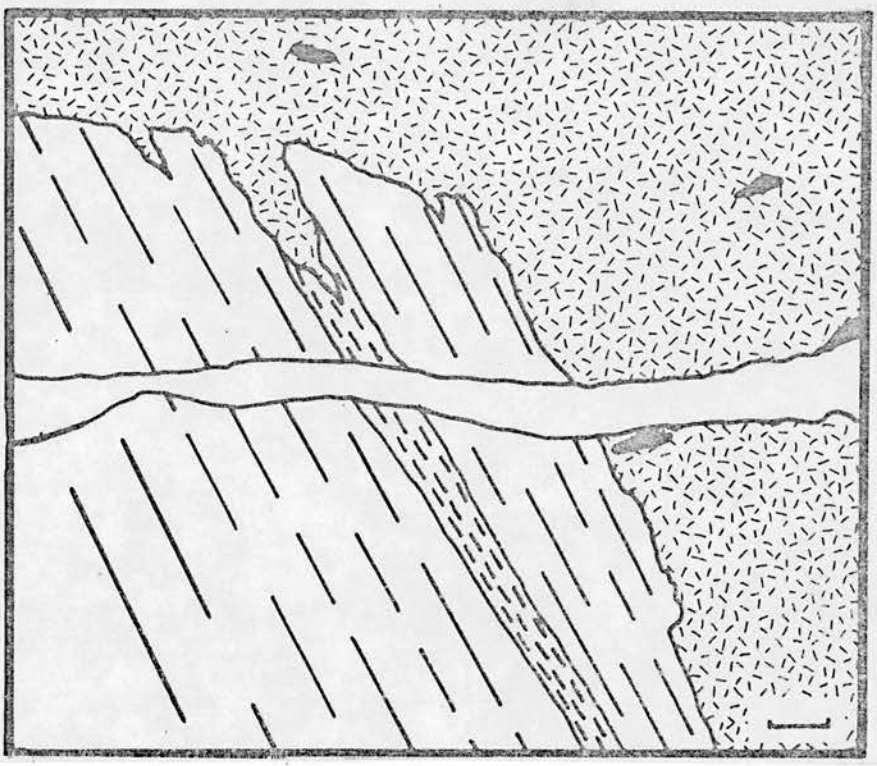

Figure 3.5 Detail of schist inclusion in quartz-monzodiorite with alignment of amphibolitic 'clots' parallel to a later, cross-cutting granodiorite vein. Preferential penetration of the quartz-monzodiorite along micaceous layers in the schist is also noted. Scale bar represents 1cm. By Kingshouse, weatern margin.

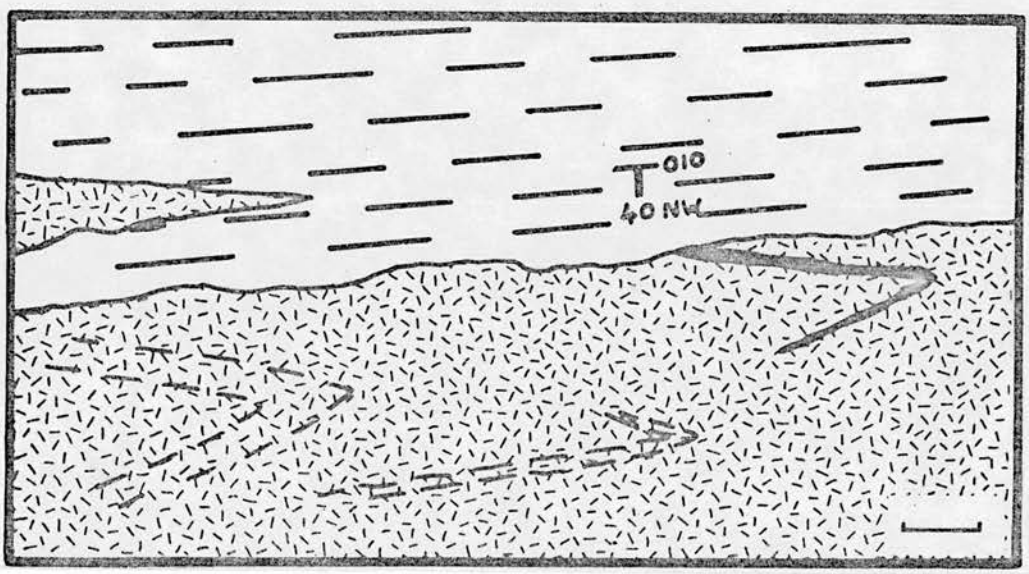

Figure 3.6 Detail of contact between metasedimentary xenolith and granite with deformed schlieren structures. Veining of the xenolith by granitic material is also noted. Scale bar represents 5cms. By Kingshouse, western margin.

Amphibolitic xenoliths within the granodiorite close to the margin are elongate, the long axes paralleling the orientation of 'ribbing' developed in the host. (These ribs may represent mineral alignment in response to intrusion tectonics, at local levels, throughout the pluton.) These xenoliths range in size from 10's of cms to 500m2 and details are shown in Figs. 3.2, 3.3, 3.4. Within the eastern marginal area, numerous schist/psammite inclusions up to 100 metres in length form a plexus paralleling the contact. The strike and dip of these have been altered with respect to regional values.

3.2 Eastern margins: sheeted intrusive style.

Evidence for sheeting of the intrusion can be seen in two places. The first is at the north-eastern margin by Old Corrour Lodge where the contact approximately follows the Dalradian/Moine junction which is within 500 metres of the pluton margins. Intrusion of the magma may have occurred preferentially along this junction from depth, aided by the regional structure (Fig. 2.2).

The second can be seen at the south-eastern margin where an irregular form of contact with the Dalradian schists and quartzites is developed (locality RM31). Gneissosity within pelitic inclusions in the granodiorite can be traced into the country rock (France, 1971). Many aplite veins and 'granitic' apophyses can be traced short distances into the schists and the contact is in places an intimate interfingering of country rock and intrusion.

Along the north-western margim, a sheeted contact style is noted with the sheets dipping into the main mass of the pluton. Outcrops of 'granitic' material in corrie Bhric Beag outwith the main intrusion confirm this interpretation.

3.3 Loch Tulla outlier of Moor of Rannoch.

The granodioritic outlier at Loch Tulla is at present considered part of the main Moor of Rannoch pluton and to be the result of movement along the Laidon-Ericht fault. Numerous parallel smale scale valleys indicate that the fault may be a large plane of movement with minor small planes associated (OS grid ref. NN 265416). Intrusive material is found to the west of these fault planes, but material is also found between the inferred minor planes. The implication is that magma intusion continued after tectonic movement along the fault or was possibly initiated by the fault activity 'tapping' a deep magma source.

The remainder of the outlier of Loch Tulla has a similar relationship with the country rock as found along the south-eastern margins of the main pluton, i.e. a sheeted contact. Enclaves of schist and quartzite in the area have undergone extensive recrystallisation. Contacts between the intrusive material and schist inclusions are sharp.

From the above a 'forceful' style of intrusion is inferred but, from evidence of sheeting along parts of the margin, is not exclusively developed.

3.4 Evidence for possible permitted intrusive style.

At the northern margins (localities RM22,22A,23,118,119,120), mineral foliation in the granite is subparallel to the strike and dip of bedding in the country rock. The joint pattern in the granite, both proximal and distant from the contact, is of two dominant directions - 100° and 140° . These are generally parallel/subparallel to the trace of the contact with the schists and psammites, the dip of the joints invariably into the pluton. Small scale lit-par-lit veining can be seen (RM 22,23) though it is not laterally extensive. Aplite veining of the country rock parallel to the contact is also seen. Inclusions of mica schist (ranging in size up to 10's of metres) are found within the granite but rarely further than 100 - 400 metres from the margins.

Recrystallistaion textures are frequently, but not uniformly, developed at the margins of these inclusions. Plastic deformation on a macroscopic scale is not common, though crystal realignment, strained extinction in biotite, feldspar and quartz suggests some re-equilibration to new stress directions on a microscopic scale. Parallelism of strike and dip with regional schist values is generally preserved.

These features are consistent with a possible 'permitted' style of magma intrusion involving little or no disruption of the country rocks.

3.5 Local thermal effects of intrusion.

A thermal aureole is developed around the pluton and has been described in detail for the south by France (1971), a brief summary of which is given here. France described a thermal aureole for the intrusion which, on the basis of thin section work, has a maximum extent of 700 metres. Within this area, biotite-cordierite hornfelsed schists are found up to 400 metres from the contact. Up to 200 metres from the contact, biotite recrystallisation is noted and cordierite predominates over andalusite. Within 5 metres of the intrusion, myrmekite textures are found in the country rock.

The western margins of the pluton abut against the Glen Coe fault intrusion and Moine quartzites. Hinxman et al. (1923) describe the fault intrusion as chilled against flinty crush material of the Moor of Rannoch pluton, indicating that the Moor of Rannoch was emplaced earlier. These workers also noted an absence of veining of the country rock in the western area, though a paucity of exposure may be have been misleading.

There is little chilling of the intrusion against the country rock which possibly indicates a small temperature difference between the the two. The observed aureole width could be due to the angle of contact subsurface between the intrusion and the host metasediments ie. a shallow outward dip. This is at variance with the noted steep inward dip of the granodioritic sheets in the northern and southeastern areas and the steep, almost vertical, dip of the contact by the river Ericht and at the western margins.

Clayburn (1981) suggests a regional temperature of 300 +/- 50 ^{o}C for the country rocks in this area but since such a low value would lead to an initially higher thermal gradient close to the intrusion, a more extensive aureole would be expected. Collins et al. (1982) describe narrow contact aureoles (10-20m wide) for southeastern Australian granites intruded into Ordovician country rocks and consider this a characteristic of sub-volcanic granites, ie. high level emplacement.

3.6 Inclusions.

Accidental xenoliths of Moine and Dalradian metasediments are found within the Moor of Rannoch pluton up to 4000 metres from the contact with these rocks. Deformation of Lower Dalradian inclusions in the granodiorite at the western margin is noted (Fig. 3.7), may indirectly evidence a forceful style of intrusion. As the country rock by this margin is Moine quartzite, the Lower Dalradian inclusions (Plate 4.24) may represent indirect evidence for the complex regional

Figure 3.7 Xenolith in marginal granodiorite, western Black Corries (by locality RM74). Plastic deformation of country rock material (Lower Dalradian semi-pelitic schist) and lack of chilled margin suggests arrested assimilation of the material. As noted in Figs. 3.2 and 3.6, movement within the ascending magma may also be responsible.

geology noted in Chapter 2 and Fig. 2.2.

By Kingshouse, amphibolitic xenoliths and mafic mineral clots close to the pluton margin (<1000 metres) occur as a series of small discrete elongate bodies, forming a xenolith train. The strike of their long axes is uniformly subparallel to the pluton margin and as they weather out easily, a train of holes marks their original extent. A further possible interpretation is that the xenoliths are mafic restite incorporated in to the ascending magma and found at the margins in response to magma convection.

3.7 The Laidon-Ericht Fault.

The Laidon-Ericht fault is a major structure subparallel to the Great Glen Fault and traceable for over 250 kms. The sinistral displacement of 6.5 kms is calculated from the offsetting of the Moor of Rannoch and Strath Ossian intrusions relative to each other (Hinxman et.al., 1923). Movement on the fault plane, either pre- or post solidification of the intrusions, appears to have induced quartz veining (locality RM44) while at Loch Tulla cataclastic mineral textures are present within the granodiorite close to the line of the fault. Widespread reddening of the granodioritic material is due to subsolidus fluid movement and Fe oxidation, facilitated by the crush zone.

Any previous lateral displacements along this fault have not been accounted for. Movement is assumed to have ceased prior to the Lower Old Red Sandstone as LORS lavas are not affected by the fault, but are affected by the later Fault Intrusion of Glen Coe. The inferred time interval is short.

Assuming the material exposed on both sides of the fault are of the same intrusion, the implication is of limited movement along a major crustal dislocation within a single event over a short time interval. This would be very different from the multi episodic movements thought to affect the Great Glen Fault. If the material across the fault was representative of more than one intrusion, then larger scale movement along the fault plane must be assumed (given no currently reliable estimate of vertical displacement). This would seem to be more likely as the fault is a laterally extensive major dislocation.

3.8 Internal relationships.

A complex series of cross-cutting temporal relationships have only partially been resolved in the course of field work, but from evidence noted an intrusive chronology has been tentatively erected.

The biotite syenogranites (Figs. 4.1, 5.0, Table 4.1 and Chapter 4.7) have a restricted occurrence within the Moor of Rannoch pluton, being confined to two major outcrops on either side of the Laidon-Ericht fault (east side - RM36- 38; west side - RM86, RM106-107)

and to a marginal facies prominent at the western and northern margins (RM30, RM22, RM119). Veins of similar material are found cross-cutting (and being cross-cut by) more basic rocks (Plate 3.1).

The outcrop of the amphibole-free syenogranite on the east side of the Laidon-Ericht fault suggests it has the form of an inward dipping sheet. This is contrasted with the more complex relationship of similar rocks exposed west of the fault (Plate 3.2). At this locality, where contacts between the types involved are seen in the field, there is a lack of a chilled margin between the later monzogranite and earlier syenogranite. However, there is ambiguous evidence to suggest the two types are contemporaneous. This is not confirmed by the initial Sr isotope ratios presented in Chapter 7.1.

Within the medium to coarse grained quartz-monzodiorites, preferred alignment of both mafic and felsic minerals is noted at outcrop (e.g. RM68) and in hand specimen orientation of smaller biotite crystals around the margins of plagioclase phenocrysts is seen. A distinctive fluxion texture is always developed in the monzodiorites and alignment of felsic minerals is ubiquitous.

A number of cross-cutting relationships have been noted for the intermediate to basic rocks and these have almost always indicated that the basic phase is later than an earlier, more intermediate to acidic phase. This sequence is repeated at a number of localitites, but appears confined to the east of the Laidon-Ericht fault and to a zone c. 2 kms. immediately to the west of the fault.

Plate 3.1 Intrusive vein of syenogranitic material, indicated by hammer head, cutting monzodiorite material; locality RM111. The vein material is a minimum of 7km from the nearest exposed similar syenogranite.

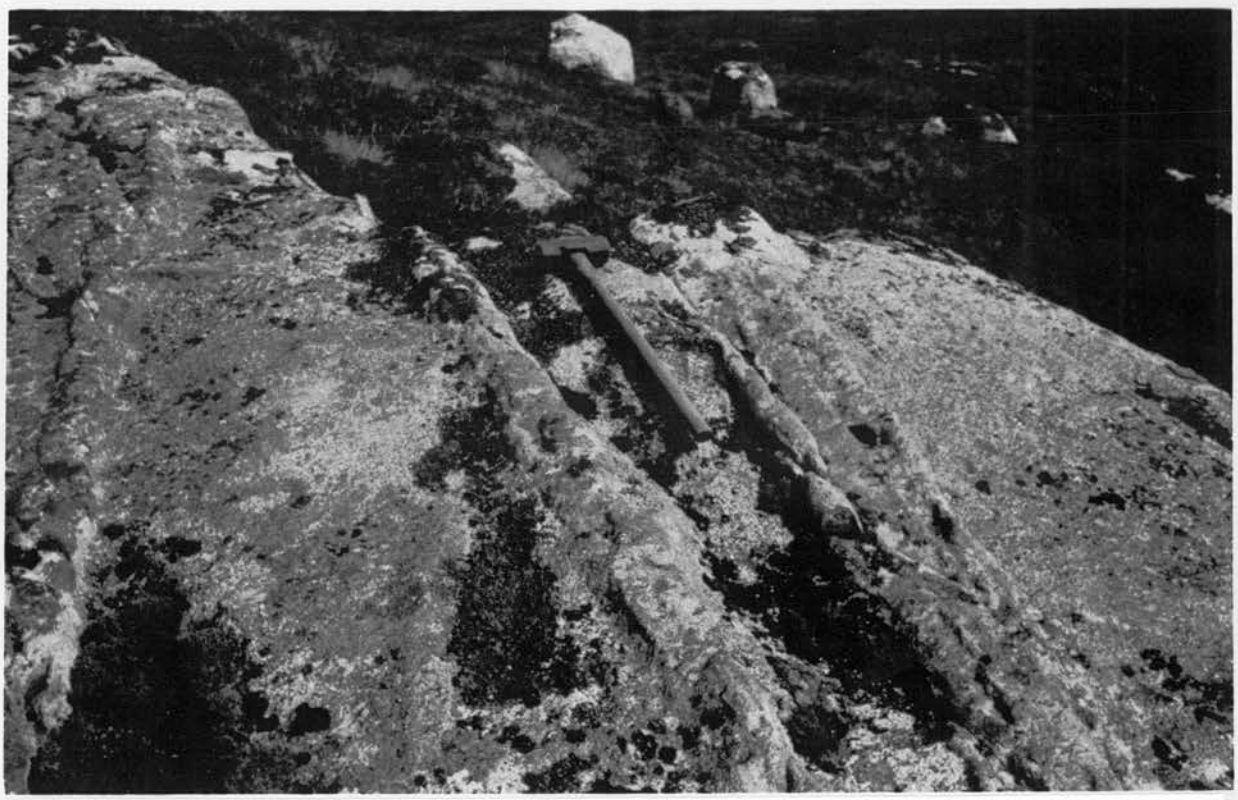

Plate 3.2 Quartz-monzodiorite/monzogranite veined by syenogranite. Veins associated with the main mass of syenogranite off to left of Plate. Grid ref. 380570.

On the western shore of Loch Laidon at two localitites - RM116 and 117 and RM103 and 103A - the more basic quartz-monzodioritic and quartz monzonitic phases respectively are seen cutting earlier monzogranitic material. Fig. 3.3 shows the relationships at locality RM116/117 where, as noted in section 3.1, the basic material contains amphibolitic inclusions and veins into the monzogranite, wedging off portions of the pre-existing rock.

Further examples of this temporal relationship can be seen in the railway snow tunnel at locality RM17 and 17A where the two rock types, though both modally monzogranites but of different geochemical groups (Chapter 5), are in contact. The later, more basic phase (RM17A) produces a domed contact structure 20m in section length, by intrusion into the earlier, more leucocratic phase.

3.9 Probable intrusive chronology.

As the common relationship between quartz monzodiorites and monzogranites of intermediate chemical compostion and monzodiorites and quartz monzodiorites of more basic composition (SiO_2 57-61 wt%) suggests, the more basic components are almost ubiquitously later. The concentration of these features east of, and along the line of, the Laidon-Ericht fault suggests that the fault may have been active during magma emplacement and simply tapped deeper, more basic, material within a vertically graded magma chamber. The implication of this is that all the material is of approximately the same intrusive age with only very minor, within pluton, differences.

The syenogranites appear to be the last major phase of intrusion, but the time 'gap' may again be small as no chilled margin has been noted between them and the quartz monzodiorites (Plate 3.2 and locality RM86 - RM89). Together with the marginal acidic phases, the syenogranites of the interior of the pluton may represent a part of an 'envelope' of acidic material which possibly preceeds the basic to intermediate material as it is intruded into the country rock.

An attempt to resolve the possible age differences between the different components is presented in Chapter 7.1.

PETROGRAPHY

4.0 Introduction.

The Moor of Rannoch granitoid was described by Hinxman et al. (1923) in terms of two main rock types. The first was a "hornblende-biotite-tonalite in which hornblende was always present" and sphene a common macroscopic accessory. The second was a "moderately coarse reddish biotite-granite or syenite often with large crystals of orthoclase".

As a result of field work, coupled with the use of a newer classification (Streckeisen, 1976), the intrusion can be described in terms of 6 distinct petrographic types. These show an extensive range of ternary Quartz - Alkali feldspar - Plagioclase (QAP) petrography (Figs. 4.1, 4.3, 5.0 and Table 4.1) from monzodiorites and quartz diorites through to monzogranites and syenogranites. This corresponds to the calc-alkaline-granodioritic (medium K) range with extension into the calc-alkaline monzonitic (high K) range, as descibed by Lameyre and Bowden (1982). Some overlap of the granites into the 'crustal granites' zone is noted. Within each group, fine through to coarse grained varieties are found. Modal distinctions in essential QAP mineralogy have limitations in the field for distinguishing rock type, but good correspondence between ternary QAP and geochemical classifications is observed.

TABLE 2

MODAL ANALYSES FOR MOOR OF RANNOCH AND STRATH OSSAIN PLUTONS

TYPE	MONZODIORITE		QUARTZ MONZODIORITE							
PHASE \ SAMPLE	RM109	RM111	RM68	RM11	RM69	RM89	RM102	RM103A	RM104	RM33
QUARTZ	1.30	1.70	4.95	6.00	6.60	13.50	7.35	11.60	9.95	16.10
ALKALI FELD	14.00	16.70	8.70	11.10	9.15	15.00	13.40	27.05	12.65	17.20
PLAG FELD	26.10	36.55	50.45	54.30	53.50	39.90	58.50	41.90	49.95	54.25
AMPHIBOLE	27.50	10.15	17.65	12.20	10.00	15.00	8.70	12.60	8.45	4.70
BIOTITE	26.25	32.25	16.90	16.00	19.70	16.40	10.80	10.95	18.20	6.85
SPHENE	0.05	1.90	0.20	0.20	-	0.20	-	-	0.15	0.70
OPAQUE	3.55	0.40	0.65	-	0.75	-	1.25	0.60	0.70	0.15
ZIRCON	-	0.1	0.05	0.15	0.05	-	-	-	-	-
APATITE	1.25	0.25	0.45	0.10	0.25	-	-	0.20	-	0.05
MUSCOVITE	-	-	-	-	-	-	-	-	-	-
Q	3.14	3.09	7.72	8.40	9.53	19.74	9.27	15.35	13.72	18.39
A	33.82	30.39	13.57	15.50	13.21	21.93	16.91	29.19	17.45	19.65
P	63.04	66.52	78.71	76.10	77.26	58.33	73.82	55.46	68.83	61.96

							QUARTZ MONZO-NITE	GRANODIORITE		
RM35	RM43	RM44	RM78	SOG7	RM81	RM79	RM66	RM34	RM51	RM54
12.85	14.00	9.20	16.81	8.10	5.85	11.75	10.05	24.15	24.30	24.75
23.30	18.15	14.15	26.63	6.65	15.65	10.70	16.65	20.10	13.15	16.25
44.05	52.60	57.30	44.50	46.60	52.15	49.30	28.50	38.30	39.25	43.00
9.95	4.50	5.10	4.25	15.85	10.20	11.85	21.50	5.95	9.10	6.85
9.45	8.80	12.95	9.81	22.80	15.65	15.25	21.55	9.70	11.30	8.65
0.05	1.15	0.10	0.56	-	-	-	0.25	0.30	0.60	0.10
0.35	0.55	1.10	0.44	-	0.5	1.15	0.05	0.50	1.50	0.40
-	-	-	-	-	-	-	-	-	0.15	-
-	0.25	0.10	-	-	-	-	1.45	-	0.50	-
-	-	-	-	-	-	-	-	-	RUTILE 0.15	-
16.02	16.52	11.41	19.79	13.20	7.94	16.39	18.21	28.90	31.68	29.46
29.05	21.42	18.77	27.82	10.84	21.25	14.91	30.16	24.66	17.14	19.35
65.95	62.06	69.82	52.39	75.96	70.81	68.72	51.63	45.54	41.13	51.19

	MONZOGRANITE								SYENOGRANITE		
RM55	RM17	RM17A	RM57	RM63	RM86	RM103	RM120	SOG9	RM36	RM38	RM107
29.85	16.95	16.50	23.90	29.05	32 75	22.27	22.00	23.95	31.60	34.40	31.86
17.50	28.50	20.45	21.60	19.80	40.15	37.47	25.60	29.00	42.60	42.20	42.83
35.25	37.60	35.10	35.70	36.20	22.75	22.59	25.00	31.25	19.30	19.05	15.38
6.9	5.80	13.70	5.00	5.40	-	-	13.75	2.90	0.30	0.10	1.58
9.95	9.25	12.65	12.50	8.35	4.00	16.00	13.25	11.95	5.25	3.35	7.20
0.55	0.70	0.60	0.20	-	0.05	0.27	0.05	0.55	-	0.10	0.17
-	1.00	1.00	0.70	1.04	0.30	1.00	-	0.20	0.95	0.70	0.75
-	-	-	-	-	-	-	0.15	-	-	-	-
-	0.20	-	0.40	0.15	-	0.40	0.20	-	-	0.10	0.23
-	-	-	-	-	-	-	-	0.20	-	-	-
36.14	20.41	22.90	29.43	34.15	33.16	27.05	30.30	28.44	33.80	35.96	35.37
23.18	34.32	28.38	26.60	23.29	42.05	45.51	35.26	34.44	45.56	44.12	47.55
40.68	45.27	48.72	43.97	42.56	24.79	27.44	34.44	37.12	20.64	19.92	17.08

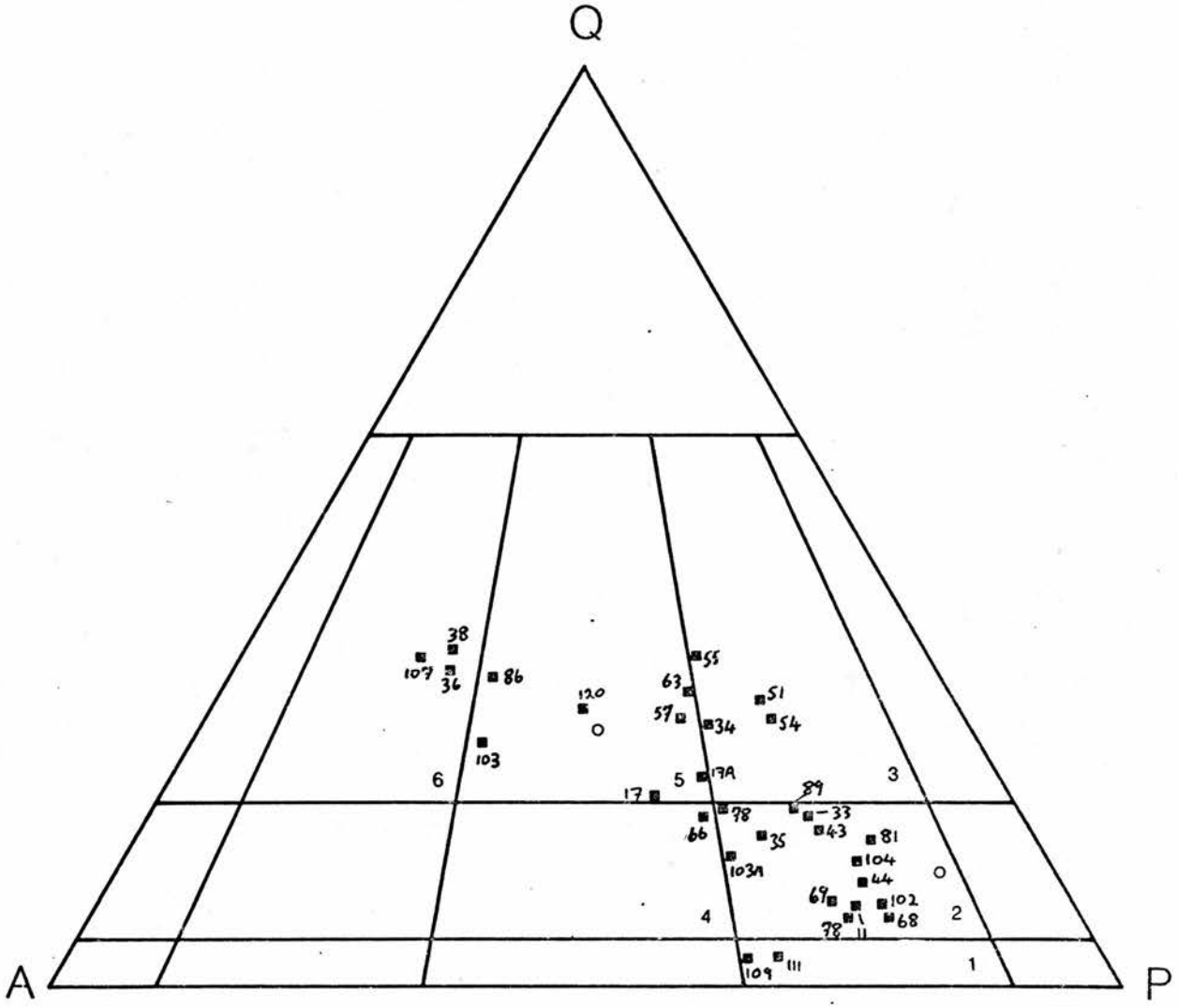

Figure 4.1 Ternary Quartz (Q)- Alkali feldspar (A)- Plagioclase (P). Adapted from Streckeisen (1976). Field numbers as below: 1- Monzodiorite, 2- Quartz-Monzodiorite, 3- Granodiorite 4- Quartz Monzonite, 5- Monzogranite, 6- Syenogranite Sample numbers as per Table 4.1.

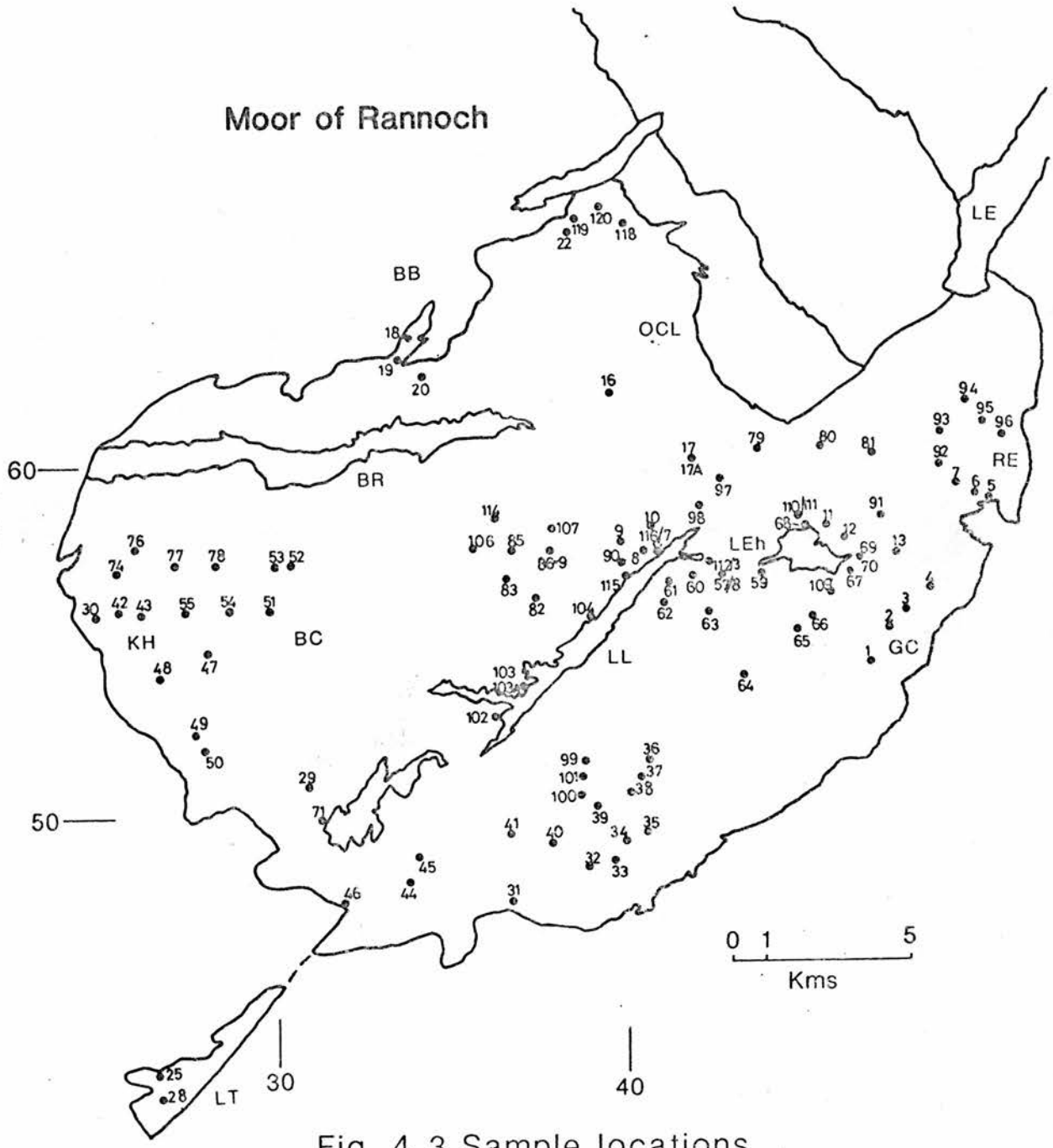

Fig. 4.3 Sample locations

RE - River Ericht LE - Loch Ericht GC - Gleann Chomraidh KH - Kingshouse
LL - Loch Laidon LEh - Loch Eighach OCL - Old Corrour Lodge BB - Bhric Beag
LT - Loch Tulla BR - Blackwater Reservoir BC - Black Corries

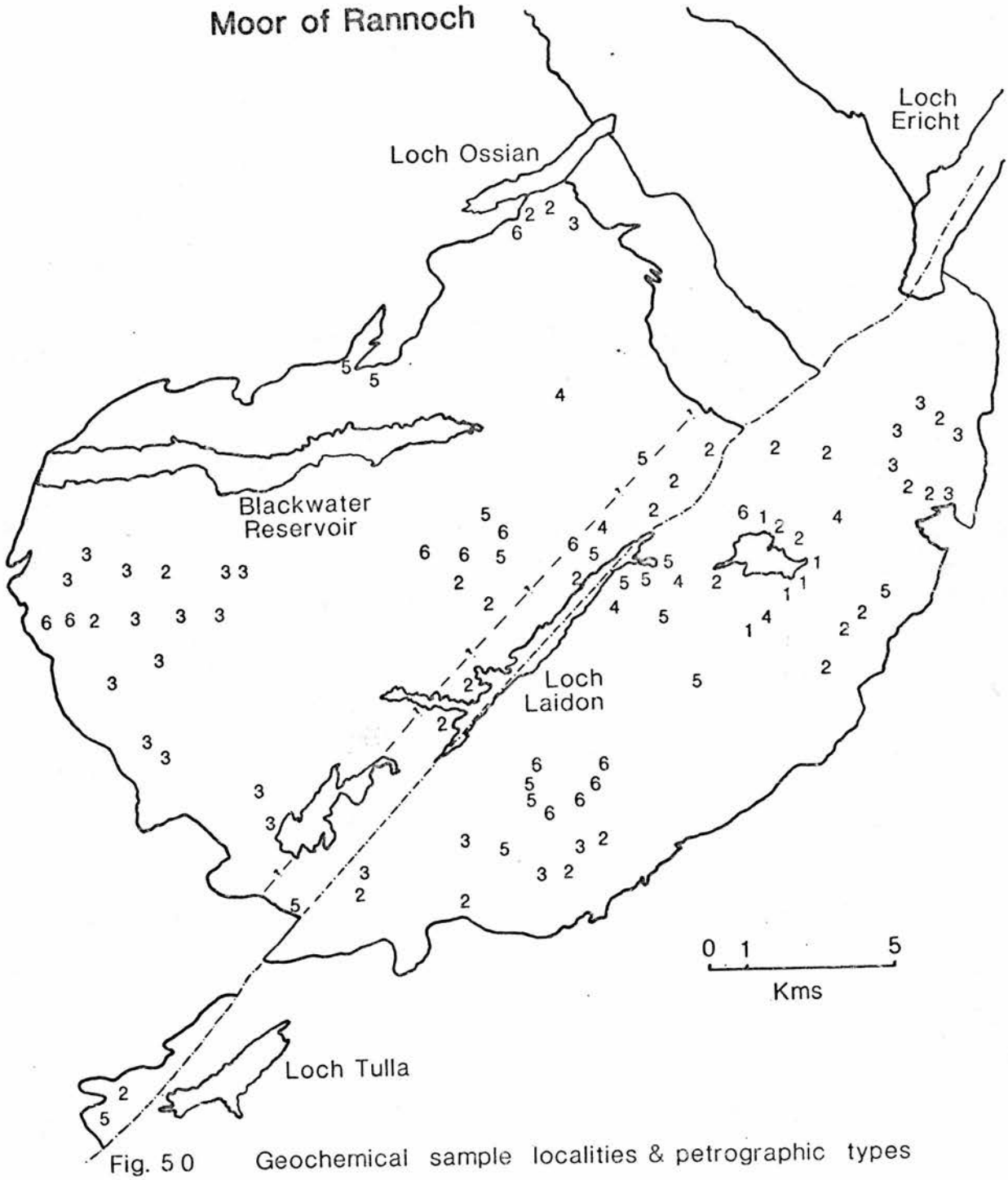

Fig. 5 0 Geochemical sample localities & petrographic types

Subdivision of the complex based on areas east and west of the Laidon-Ericht fault is useful. In the eastern part of the complex, the complete range of modal petrographic types is found (Fig. 5.0). Outwith the northern marginal area and a zone 1.5-2 kms wide to the west of the fault, the predominant type in the west is granodiorite with constituent variations in quartz and feldspars. These variations probably reflect very localised events in the cooling history of the pluton.

4.1 MONZODIORITES.

a) In hand specimen, the monzodiorites are dark-grey to greenish black, medium to coarse-grained rocks with a range of between 0-35% plagioclase phenocrysts. Where these phenocrysts occur, they are elongate between 5-15mm and are in a medium grained 'matrix' in which plagioclase is interstitial to the mafic minerals. Quartz content is always <5% and is frequently absent. A distinctive fluxion texture is always developed and can be seen on outcrop (Plate 4.25).

b) In thin section the predominant feature is a coarse porphyritic texture but a fabric of aligned ferromagnesian minerals is apparent (RM111). A further distingishing feature is the ubiquitous presence of biotite cores in amphibole (Plate 4.3). This texture is noted throughout the range of rock types at Moor of Rannoch excepting the syenogranites.

Biotite occurs as subhedral to elongated tabular crystals up to 3.5mm with moderate brown to dark-brown pleochroism. The larger crystals occassionally include plagioclase, alkali feldspar and acicular apatite. In sample RM109, biotite is always mantled by, or incorporated into, amphibole and also occurs as an interstitial mineral within felsic patches. Two types of biotite are identified:

i) Stubby or elongate crystals which poikilitically enclose, and are enclosed by, amphibole. The contact between the two minerals is frequently marked by opaque minerals.

ii) Later biotite overgrowing amphibole and earlier biotite.

The tabular biotites all show ragged edges due to chlorite or opaque oxide development at the rims and in cleavage traces. Combined optical and microprobe analysis shows the biotite compositions to be annite-phlogopite solid solutions with a strong annitic component and only limited siderophyllite content (probe data, Fig. 6.2.1).

Amphibole occurs in either elongated, twinned, prismatic habit up to 4mm in length or as overgrowths on biotite crystals, up to 2.5mm in size. Biotites within the former habit which is optically identified as actinolitic hornblende, possess common cleavage orientation with the host amphibole (Plate 4.4). This, together with the embayed margins of the overgrown biotites, indicates that the texture results from the replacement of biotite by amphibole. Inclusions of plagioclase, alkali feldspar are present (Plate 4.9) and growth of

secondary opaques occurs at biotite-amphibole interfaces in the 'overgrowth' amphibole.

Altered amphibole thought to be tremolitic hornblende, has an asbestiform appearance and opaque minerals are often associated with this habit when it occurs in aggregates of small amphibole and biotite crystals. Amphibole is also found as discrete inclusions in plagioclase phenocrysts (RM111).

Plagioclase, with normal and oscillatory zoning, ranges in composition from An35 to An15. Grain size varies from stubby, euhedral crystals approximately 1.5mm up to elongate phenocrysts 4mm in length. Lamellar twinning and zoning are often obsured by alteration, particularily in the cores of grains (RM109), which highlights compositional variations within oscillatory zoned crystals. Syenitic aggregates of plagioclase and alkali feldspar are mafic mineral free and usually composed of smaller grains.

Alkali feldspar (optically orthoclase) is interstitial to plagioclase and ferromagnesian minerals and occurs as subhedral grains up to 2mm in length. Zoning is frequently developed and inclusions of biotite and amphibole (up to 0.2mm) are noted. Patches of orthoclase and plagioclase reach 5mm in size and exhibit sericitisation. Armouring of smaller plagioclase grains by alkali feldspar is also seen in these patches.

Quartz is a minor constituent occurring as anhedral interstitial grains. Accessory constituents include abundant apatite (1.25% by mode, RM109) as acicular prisms up to 0.75mm predominantly in plagioclase. Sphene occurs as euhedral embayed crystals up to 4mm length, 1mm width and makes up 1.9% by mode of RM111 with apatite prism inclusions. It is faintly light-brown to brown pleochroic and is often altered to secondary opaques. Primary Fe-oxides, commonly magnetite with hematite, are present in variable amounts (Table 4.1). Subhedral-anhedral grains of zircon have been identified in biotite giving pleochroic haloes in sample RM111.

4.2 QUARTZ MONZODIORITES.

Two distinct varieties of quartz-monzodiorites are evident on the basis of amount of ferromagnesian minerals present. A division into 'mafic-rich' or melanocratic and 'mafic-poor' or leococratic varieties at 20% modal ferromagnesian minerals adequately serves to distinguish the two and fine to coarse grained varieties of each type are found in the field.

4.2.1 Melanocratic, fine-grained QUARTZ MONZODIORITES.

a) In hand specimen (Plate 4.26) the fine grained quartz monzodiorite is dark-grey to greenish-black with elongate acicular prisms of amphibole and aggregates of amphibole and biotite. Plagioclase is both phenocrystic and groundmass forming with quartz and alkali feldspar interstitial. A slight pinkish tinge is caused by

the alkali feldspar. Only minor mineral foliation is seen in the field and a strong relationship between this type and the mafic-rich, fine-grained monzogranites (RM112, Plate 4.31 and 4.12) is noted.

b) In thin section (Plate 4.10), biotite occurs as small, tabulate laths <0.5mm which are light to dark-brown pleochroic and which often appear interstitial. Few crystal laths are found outwith amphibole or biotite-amphibole aggregates; those that are, show extensive chlorite development in cleavage fractures and also appear to be a later interstitial phase. Biotite occurs as relict cores within euhedral to subhedral amphiboles or as a 'patchwork' within amphibole aggregates. A common cleavage development for biotite and amphibole is seen in compound aggregates and grains where haematisation of biotite has occurred at inter-grain contacts.

Amphibole almost ubiquitously contains biotite either as discrete tabulate laths or, texturally, as relict cores resulting from replacement of biotite by amphibole. Two distinct types of amphibole can be determined.

The first type are elongate prisms often reaching 4mm but generally only 0.5-1mm in length and light-green to brown pleochroic. On the basis of optical determinations (pleochroism, habit, cleavage, 2V) these are thought to be magnesio - actinolitic hornblende (Plate 4.11). Twinning is commonly developed in elongate crystals with length:breadth ratios >5:1 and biotite is frequently noted parallel to 110. The smaller prismatic crystals tend to form aggregates which poikilitically enclose plagioclase and alkali feldspar. These prisms

are often chloritised and have later overgrowth of amphibole. Discrete elongate prisms and subhedral tabular grains of actinolitic hornblende are often found within interstitial alkali feldspar or, rarely, plagioclase, along with biotite.

The second amphibole type forms subhedral to euhedral crystals up to 2mm length with biotite cores and resorbed primary opaque minerals. The inclusions of biotite show chlorite and opaque oxides developed in the cleavage traces, as does the surrounding amphibole. Its slight light-green to green pleochroism, cleavage and 2V indicate that it is intermediate between edenitic and tremolitic hornblende.

Plagioclase also exhibits three types of habit, the first of which is as subhedral to euhedral phenocrysts up to 2.5mm in length and normally zoned. The more sodic rims are frequently mantled by unzoned, untwinned plagioclase or alkali feldspar. Selective sericitisation of the cores or compositional steps within the zoning pattern often obscures albite and pericline twinning, but not carlsbad twinning which is poorly developed. Inclusions of biotite and amphibole are rarely found.

The second habit of plagioclase is tabular subhedral to elongate laths which are calcic oligoclase and generally <1mm in length. Lamellar twinning is present which does not extend into the rim overgrowth. The grains are ubiquitously normally zoned with variable alteration of the cores and are commonly free of inclusions. Interstitial plagioclase is the third habit developed and is present forming small anhedral grains.

Alkali feldspar is predominantly interstitial orthoclase enclosing discrete biotite, amphibole, oligoclase and occassional subhedral grains of sphene. Uniform extinction over grains of 2-2.5mm is noted and zoning (Chapter 6.4) seen in other crystals. Sericite alteration often obscures small inclusions of plagioclase and biotite.

Quartz is uniquely interstitial, forming anhedral grains with undulose extinction and only rarely forming aggregates. Common accessory constituents include sphene as interstitial grains with embayed outlines and apatite as very small acicular prisms. Primary and secondary opaque Fe-oxides are present in variable amounts.

4.2.2 Leucocratic, medium to coarse grained QUARTZ MONZODIORITES.

a) Hand specimens of this type are medium to coarse grained dark-grey with black ferromagnesian minerals. A frequently granular appearance on weathered surfaces is due to variable alteration of the mafic minerals. Tabular to equant plagioclase phenocrysts up to 1.5cm long are set in a groundmass of biotite and amphibole aggregates with smaller interstitial plagioclase and alkali feldspar. Quartz is present interstitially in varying amounts (Plate 4.27). Compositional zoning within the phenocrysts is readily visible and hematisation of the feldspars gives a pinkish tinge to the weathered surface (cf. RM69 & RM70).

b) Biotite in thin section forms subhedral to tabular crystals (rarely euhedral) with ragged edges which are normally 1.5-3mm long and smaller laths between 0.5-1.5mm in size. Pleochroism is normally tan to dark-brown, but secondary biotite is frequently brown, weakly pleochroic. Basal sections are more prolific in samples which display fluxion textures and are a function of orientation of the thin section cut (RM43).

Porphyritic examples with plagioclase phenocrysts often show a distinct bimodal size distribution of biotite and aggregates up to 1cm are formed. Inclusions of apatite needles, rounded sphene and plagioclase are irregularily found. Undulose extinction and bent crystal outlines are found (RM43, RM81) and chlorite development in cleavage fractures, though variable within one section, is common. Aggregates of small biotites are chloritised more extensively than single large crystals. Mantling of biotite by secondary Fe-oxide opaques, especially in mafic aggregates, together with development of opaques at grain boundaries and in cleavage traces is common.

Biotite appears interstitial to plagioclase, especially the smaller grains, but larger individual crystals appear to be contemporaneous with plagioclase phenocrysts.

Amphibole has two distinct habits both of which exhibit the intimate relationship with biotite described in 4.1(b). The first is a variably elongated prismatic habit, 0.4-2mm (4mm, RM81), which is commonly twinned and has green to tan-brown pleochroism. This is

thought to be actinolitic hornblende. Inclusions of plagioclase, biotite and opaques are usually orientated parallel to the twin plane, but rare apatite needles seem randomly orientated. Patchy zoning is visible in stubby crystals <1.5mm (RM68) and is noted throughout the size range. Sphene and opaque oxides are developed at grain contacts between amphibole and biotite.

Tremolitic hornlende forms anhedral to subhedral, occassionally elongate, crystals up to 1.5mm long which aggregate to form irregular patches. This amphibole is weakly pleochroic pale-green to green or non-pleochroic pale-green and frequently contains inclusions of biotite, opaques and allanite. It is commonly untwinned, except in more elongate examples, and rarely shows good cleavage. Optical continuity up to 1.5cm is noted (RM35). Chloritic alteration is variable within a single section from abundant to moderate.

Plagioclase, with normal, oscillatory and patchy zoning is compositionally variable between An 35-25 and An15-20. Twinning is on albite and carlsbad laws. Lamellar twinning and zoning are often highlighted by selective alteration which varies greatly even within a single section. Twinning is complex and myrmekite is developed as a minor texture at the margins of large plagioclase crystals. Complex plagioclase aggregates are interpreted as syneussis textures, after Vance (1969).

Large phenocrystic oligoclase/andesine crystals range in size from 3 to 10mm as tabular, rarely equant, crystals with inclusions of small discrete biotite, alkali feldspar and plagioclase grains (Plate 4.7). Mantling by untwinned sodic plagioclase (probe determination) is common on the smaller crystals.

Tabular, subhedral to euhedral laths of sodic oligoclase are usually 0.5 to 2.5mm and display strong albite and pericline twinning, though untwinned examples are also found. The more calcic cores in these grains are generally sericitised leaving alteration-free rims. Myrmekite and slight marginal intergrowth textures with alkali feldspar are found.

Alkali feldspar is predominantly interstitial to plagioclase, biotite and amphibole and is optically orthoclase with minor microcline present. Optical continuity up to 7mm is noted (RM35). Larger anhedral, occassionally subhedral, grains up to 3mm (RM81) are found which have inclusions of biotite and lamellar twinned, squat plagioclase laths. Perthite and intergrowths with interstitial quartz at corroded margins is noted. The perthite is commonly fine-braided and string type although patch perthite is occassionally found.

Quartz is interstitial but granular aggregates which show concertal textures and recrystallisation features occur (RM43). Undulose extinction is common in the larger grains, especially when these are close to mafic patches. Common accessory constituents are sphene, allanite, apatite, monazite, zircon and opaque Fe-oxides, both

primary and as secondary reaction rims to biotite and amphibole (Plate 4.8). Sphene has an embayed subhedral to euhedral habit up to 1.5mm in length and displays zoning (RM33). Secondary sphene is identified mantling biotite in mafic aggregates (RM43).

Apatite occurs as acicular prisms up to 0.25mm in ampibole and orthoclase. Allanite, monazite and zircon are found as subhedral to anhedral grains in biotite (Plate 4.18). Allanite has also been identified in amphibole (RM79).

4.2.3 Melanocratic, medium to coarse grained QUARTZ MONZODIORITES.

a) In hand specimen this variety is variably light to dark-grey with black interstitial ferromagnesian minerals. Plagioclase forms elongate tabular to equant phenocrysts up to 1.5cm long, but also occurs as inclusion-free turbid grains interstitial to the ferromagnesian minerals. On a sawn surface, the large plagioclase crystals can be seen to be zoned. Fluxion texture is evident from felsic and mafic mineral alignment at outcrop and where this does occur the samples are more weathered giving a granular appearance to the rock. Quartz is always interstitial (Plate 4.28).

b) In thin section biotite exhibits the same habit as for the leucocratic quartz monzodiorite but rarely exceeds 2mm as tabulate crystals with ragged edges. Rare muscovite alteration is noted (RM102) and preferred crystal orientation is accompanied by undulose extinction.

Amphibole in this rock type (eg. RM68) shows similar textures and habit to the leucocratic variety. Xenotime has been noted (RM102) along with more common apatite needles and plagioclase with quartz blebs in disequilibrium texture (Plate 4.14). Primary amphibole crystals appear broken and bent more than in the leucocratic type while the secondary amphibole grains are generally undisturbed.

Plagioclase features are common to both leucocratic and melanocratic types but in sample RM104, trains of small discrete biotite crystals are confined to the cores of oligoclase megacrysts leaving the rims inclusion free. These biotite crystals are <0.2mm and show orientation of longer axes about the core and zone boundaries. Larger subhedral to euhedral crystals also contain actinolitic hornblende, biotite and plagioclase grains as inclusions. Alteration of plagioclase grains is stronger closer to amphibolitic aggregates.

Alkali feldspar is interstitial with single crystal optical continuity up to 7mm (RM102) and together with plagioclase and quartz, forms fine-grained leucocratic patches within more basic members of the rock type. Micrographic intergrowths with quartz and oligoclase are common. Larger (up to 2mm) zoned anhedral crystals are noted poikilitically enclosing small subhedral amphibole and biotite grains and often show mantling by a more K-rich rim. The rim between the larger grains and interstitial alkali feldspars show resorption of the former (RM103A).

Quartz is interstitial and also forms multiple grain aggregates which exhibit both undulose extinction and uniform extinction up to 5mm in one section. Accessory phases are confined to sphene, apatite, xenotime (as noted above) and muscovite as a secondary alteration product. Secondary alteration products of sphene are seen where primary sphene is in contact with amphibole and plagioclase.

4.3 QUARTZ MONZONITES.

a) The quartz monzonites are light-grey to grey, medium to coarse-grained, leucocratic/mesocratic rock variously tinged pink due to feldspar colouration. There are gradations between plagioclase phenocrystic varieties which display fluxion texture in the melanocratic 'matrix' and heterogeneous, non-phenocrystic varieties which show markedly less aggregation of the mafic minerals. Both types are closely related, in the field and petrographically, to the quartz monzodiorites (Plate 4.29).

b) Biotite in thin section forms tabular to elongate crystals generally <1.5mm which often cluster with amphibole as mineral aggregates. Alteration to chlorite, zeolite and opaque occurs preferentially along cleavage fractures while complete replacement of biotite by chlorite and secondary amphibole (Plate 4.5) is seen in orientated mafic-rich aggregates (RM66). Biotite appears late as interstitial grains to plagioclase, amphibole and larger alkali feldspar crystals, but is also an early-formed mineral.

Amphibole has three distinct habits (elongate prismatic, corroded euhedral and subhedral to anhedral) in aggregates which have been described previously. Patchy zoning (RM66) is rarely seen and their composition is estimated optically as actinolitic hornblende.

Mantling of embayed euhedral crystals by secondary opaques, biotite, chlorite and amphibole is common (RM10, RM66, RM113). Amphibole is also found in mafic patches as described previously and is predominantly interstitial to plagioclase, biotite and alkali feldspar, but often contains inclusions of quartz and plagioclase. Mantling by secondary opaques is a common feature on all crystals (Plate 4.8).

Plagioclase displays fine albite and pericline twinning along with patchy and normal zoning. Size ranges from a maximum of 10mm as elongate phenocrysts (An26-28, RM66) to anhedral grains usually 0.4-0.75mm (An20-25). In RM10, a checkerboard texure is well developed and syneussis of grains is noted throughout the type. In more melanocratic samples, sericitisation of cores is common, highlighting calcic cores. Inclusions of amphibole and biotite as discrete non-orientated grains are found in finer grained melanocratic varieties (RM113). Vermicular intergrowths with quartz is a minor textural feature throughout the type.

In RM91, a large patch composed of two joined oligoclase/andesine megacrysts contains numerous, approximately concentrically orientated, biotite and euhedral amphibole crystals. These inclusions appear to be concentrated about the core of the joined crystals (Plate 4.23). Vermicular intergrowths with quartz are seen throughout the type as a minor textural feature.

Alkali feldpsar occurs as both an interstitial and early formed mineral as anhedral, occassionally subhedral, orthoclase crystals. Normal and patchy zoning is highlighted by sericitisation which can vary greatly within a section. String and braided perthite exsolution is common (RM10, RM66) and concertal margins where grains contact with plagioclase are also noted (RM113). As an interstitial phase, alkali feldspar encloses amphibole (second type), biotite and plagioclase , in grains up to 6mm in total area.

Quartz occurs predominantly as an interstitial mineral but also is found as individual crystals within plagioclase phenocrysts (RM66) and alkali feldpsar (RM113). Rare quartz-rich patches exhibit undulose extinction. Common accessory constituents are apatite (RM10), zircon as subhedral grains in biotite (RM113, RM16), and sphene. Sphene is found rarely as a primary phase but more commonly as a secondary alteration product mantling biotite, euhedral-habit amphibole and within biotite cleavage fractures.

4.4 GRANODIORITES.

a) These are a group of light-grey, medium to coarse grained, occassionally phenocrystic, leucocratic rocks. They show little change in modal mineralogy and appearance despite extensive outcrop in the western part of the pluton. A pinkish tinge is due to feldspar colouration while the quartz aggregates give a patchy glassy appearance. Mafic minerals are mainly interstitial to the felsic minerals. Average grain size is <2.5-3mm but occasional acicular amphibole prisms exceed 5mm. Fluxion texture is only rarely seen in hand specimen, but at outcrop a faint orientation of the mafic minerals is noted , especially towards the pluton margins. Rib structures are extensively developed on outcrop surfaces in granodiorites (Plate 4.30).

b) Although certain of the granodiorites appear more leucocratic in thin section (RM75,RM76,RM77), there is no significant difference in mineral habit between these and the remainder of the granodioritic suite eg. RM48,RM52,RM93. Biotite shows a bimodal size distribution. Large tabulate to equant crystals up to 3mm length, which have ragged outlines, display brown to dark-brown strong pleochroism and are thought to be annitic biotite. These crystals often have bent form and cleavage with chlorite, minor sphene and opaque phases developed in cleavage fracture. Concentric zoning is occassionally seen as are inclusions of zircon, zeolite blebs, apatite needles, primary opaque oxides and quartz grains. Aggregates of these larger crystals form melanocratic patches which frequently contain smaller secondary(?) biotite and amphibole.

Biotite also has an interstitial habit as small, anhedral to elongate crystals which rarely exceed 1.5mm and are more normally 0.5-1mm in length. Pleochroism is light-brown to brown and the grains are often extensively chloritised. Secondary sphene, amphibole and opaque oxides are found in deformed cleavage traces and at crystal margins (Plate 4.16). Where aggregates of this biotite occur, recrystallisation textures and later biotites are found. Muscovite is noted as a rare alteration product in these patches.

Amphibole in the granodiorite has similar habit to that of the quartz monzodiorites and quartz monzonites and in the granodiorites from the eastern margin (RM92, RM93, RM94, RM96) inclusions of quartz and plagioclase are common.

Plagioclase displays normal, oscillatory and patchy zoning with twinning on the albite, pericline and carlsbad laws. Core compositions are An25-30 with rim compositions more sodic An15-20 (combined optical and probe determinations). Large tabulate, subhedral megacrysts up to 8mm length are intergrown with smaller (1-2mm), anhedral to subhedral oligoclase laths which frequently contain small biotite and amphibole inclusions.

Selective sericitisation, variable within section, often highlights patchy and concentric zoning. Myrmekite is a common texture and armouring of smaller plagioclase grains by alkali feldspar and untwinned sodic plagioclase is noted.

Alkali feldspar is predominantly interstitial, enclosing prismatic and euhedral amphibole, tabular biotite, plagioclase and primary opaque oxides (Plate 4.15). Uniform extinction occurs over distances of 10mm. Anhedral crystals of orthoclase develop up to 1.5mm and form syennitic patches with smaller plagioclase and quartz. Braided perthite exsolution textures and vermicular intergrowths with quartz are common (RM51.RM54). Symplectic contacts and micrographic intergrowths with plagioclase are characteristic of the granodiorites. Microcline, identified optically and Or89 by microprobe, is most commonly seen in granodiorite from the western part of the pluton.

Quartz is interstitial, forming individual grains up to 2mm or aggregates of smaller grains. These patches display recrystallisation triple point junctions, undulose exctinction and in larger aggregates, consertal texture (RM47, RM55, RM76; Plate 4.17). Quartz also occurs as inclusions in biotite, plagioclase and in amphibole.

Accessory constituents identified are opaque oxides, apatite, zircon, allanite, monazite and sphene. Sphene occurs as a primary phase interstitial to plagioclase megacrysts and large, tabular biotites but is also found as a secondary alteration product in mafic patches. Secondary opaque oxides are associated with alteration of amphibole, biotite and primary sphene and their habit is similar to that decribed for the quartz monzodiorites. Zircon is found as subhedral grains <0.1mm giving pleochroic haloes in biotite (RM55) while anhedral allanite up to 0.5mm is noted in sample RM51.

4.5 MONZOGRANITES.

The monzogranites can be subdivided into two subgroups which are fine-grained, mesocratic to melanocratic or medium to coarse-grained, mesocratic to leucocratic in hand specimen.

Fine-grained, melanocratic MONZOGRANITES.

a) Hand specimens of this type have a range of colour, from dark-grey to greenish-black, dependent on the concentration of ferromagnesian minerals present (RM62, RM112). Plagioclase appears to be interstitial although the mafic aggregates may enhance this feature. Average grain size is again <1mm. Quartz and alkali feldspar in both are interstitial. These rocks are characteristically very hard in the field and ghost restitic(?) mafic patches or xenoliths are visible on outcrop surface (Plate 4.31).

b) Biotite in thin section forms predominantly subhedral laths 0.25-0.75mm in size and with faint preferred orientation. Pleochroism is moderate light-brown to brown. Alteration to chlorite is associated with very fine-grained crystal margins giving a mantled appearance and is dominantly developed in aggregates of biotite with amphibole.

A bimodal size range can be identified for amphibole. The first is a subhedral elongate habit with crystals up to 4mm length. These are pleochroic tan to green to dark-green with high birefringence colours (actinolitic/edenitic hornblende) and twinning is commonly

developed. Biotite inclusions and relict biotite cores are orientated parallel to the twin plane. Quartz grain aggregates up to 1mm in size are found within this elongate, prismatic amphibole.

The second type is of small, anhedral to subhedral grains, <0.5mm in length which have light-green to green pleochroism and are commonly twinned. These form aggregates along with biotite or are poikilitically enclosed in orthoclase. Where this type is matrix forming along with biotite, faint preferred mineral orientation is seen.

Plagioclase is normally zoned with An22-27 cores which are infrequently mantled by unaltered, untwinned sodic andesine or orthoclase. Grain size is <1.25mm and crystal habit is generally subhedral to anhedral.

Alkali feldspar is interstitial orthoclase(?) enclosing amphibole, biotite and plagioclase, with grains rarely exceeding 1mm. Syenitic patches composed of both interstitial and discrete orthoclase, plagioclase and quartz often contain small, non-orientated amphibole laths. Micrographic textures with plagiocase and quartz are developed.

Quartz is predominantly interstitial but does occasionally form aggregates, up to 3mm in radius, of larger discrete grains. These larger grains are mantled by small, elongate amphibole laths whose long axes are aligned parallel to the quartz grain margin. Inclusions of plagioclase and orthoclase are common in the syenitic patches.

Apatite is the most abundant accessory phase as acicular crystals in biotite, secondary amphibole and plagioclase. Apatite also forms fibrous, radiate growths into quartz, plagioclase and orthoclase from crystal boundaries.

Fine-grained, mesocratic MONZOGRANITES.

a) This type appears to be intermediate between the medium-grained, leucocratic and the fine-grained, melanocratic monzogranites. In hand specimen both are fine to medium-grained with small (1mm), acicular amphiboles (rarely up to 4mm) and elongate biotites randomly orientated. Plagioclase rarely exceeds 2mm and often has a pink tinge due to alteration (RM62).

b) In thin section both biotite and amphibole possess essentially the same variety of crystal habit as for the fine-grained melanocratic type (see above) with only their relative proportions varying. Biotite and amphibole are randomly orientated and may represent first crystallised phases incorporated into a more syenitic mush.

Plagioclase has the same habit as in the fine-grained, melanocratic type with a grain size <1.5mm. Compositionally oligoclase, zoning is ubiquitously developed and cores are selectively altered. Untwinned rims are either sodic oligoclase or alkali feldspar.

Alkali feldpsar occurs both a liquidus mineral up to 3mm in length and as an interstitial phase poikilitically enclosing biotite, amphibole and plagioclase over distances of 2-3cm. These crystals exhibit uniform extinction. Large orthoclase megacrysts exhibit concentric, normal zoning on resorbed cores and this feature is common to the smaller, anhedral grains. Acicular apatite crystals occur in the larger interstitial grains. Blebby and braided perthite exsolution textures are common in the larger (>1.5mm) orthoclase crystals

Quartz is mainly interstitial and has undegone annealing, giving large grains with uniform extincion alongside aggregates with serrate boundaries and undulose extinction.

Sphene and apatite are the commonest accessory constituents, but secondary opaque oxides and muscovite are also present. Secondary sphene is interstitial and is intimately associated with opaques as inclusions in, or mantling, biotite. Apatite forms elongate, acicular prisms, whose occurrence has been previously noted.

Medium to coarse-grained, mesocratic to leucocratic MONZOGRANITES.

a) These monzogranites are variable in hand specimen from grey, medium to coarse-grained mesocratic through to grey to cream, medium-grained, leucocratic rocks. Fluxion texture, where present, is seen in the more mafic varieties. The leucocratic type possesses more alkali feldspar, but the amount of quartz remains approximately

constant between the two (Plate 4.32).

b) The mesocratic type in thin section show biotite textures and features similar to those of the granodiorites and quartz monzodiorites. Infrequent inclusions of anhedral zircon give pleochroic haloes.

In sample RM17A, a unique "feather" texture is developed in the biotite (Plate 4.19) and many of the affected crystals appear to be secondary biotites. The texture has developed after secondary hematite formation in cleavage fractures as these elongate opaque grains have been subsequently deformed alomg with the remainder of the crystal. The sample RM17A (Plate 4.20), is taken from the core of an intruding later, more basic, phase (Plate 4.21) as noted in Chapter 3.8.

Amphibole displays the characteristic habits noted previously (Plate 4.6) with biotite a common inclusion (relict cores). High birefringence colours in the elongated and prismatic habits are distinctive.

Plagioclase forms subhedral to anhedral crystals up to 3mm in length and elongate tabular megacrysts up to 8mm. The plagioclase is variable between oligoclase and albite (combined optical and probe determinations) and shows features common to those of the quartz-monzodiorites and granodiorites. Where contact with alkali feldspar occurs, marginal exsolution textures into the plagioclase are seen. Myrmekite is not commonly found but occurs in the more syenitic patches preferentially.

Alkali feldspar is thought to be predominantly orthoclase and forms both anhedral rounded and subhedral crystals up to 2.5mm in length with exsolution and intergrowth features similar to those of the granodiorites.

Quartz is predominantly interstitial grains <0.5mm but also forms larger grains (up to 2mm) which appear framework forming and have undulose extinction. Concertal texture and triple point junctions are noted for the interstitial grains, especially where they are proximal to mafic patches which have undergone extensive alteration.

Accessory phases are secondary sphene associated with the alteration of amphibole and biotite; anhedral zircon up to 0.05mm in biotite and plagioclase (Plate 4.13); apatite in biotite and plagioclase. Secondary opaques also form in discrete biotite crystals alongside primary opaque phases and are found in mafic aggregates.

4.6 Medium-grained, leucocratic MONZOGRANITES.

a) These rocks exhibit a wide range of plagioclase/alkali feldspar ratios, from 60/40 (eg RM63) through to 37/63 (RM86, RM103) and the latter rocks are very similar to the syenogranites. Although modally monzogranites, the latter type can be distinguished by their lack of primary amphibole and are thus more closely related to the amphibole free syenogranites and may share a common origin. The presence of interstitial biotite (<1mm long) which has been extensively chloritised, along with alteration to secondary sphene and

opaque minerals, is diagnostic (Plate 4.33).

b) Thin sections of the medium to coarse-grained, leucocratic, primary amphibole bearing monzogranites display granitic textures similar to those of the mesocratic varieties. Biotite is predominantly interstitial, appearing to have often nucleated on subhedral, corroded sphene crystals. Tabular biotite, pleochroic light-brown to greenish-brown, show ragged edges with chlorite and opaques developed on the margins and in cleavage fractures. Interstitial biotite, often basal sections, show little marginal alteration but inclusions of sphene and opaques are found. This habit is thought to be exclusively later secondary in origin. The characteristic "feather-like" cataclastic texture, noted in RM17A, also occurs infrequently, along with kink-bands and deformed crystal outlines.

Amphibole habit is predominantly severely corroded, elongate subhedral crystals which have formed aggregates up to 5mm in size. These 'clots' are often extensively altered to opaque oxides and biotite. Biotite occurs as relict cores in single subhedral crystals but also forms intimate melanges with chlorite, earlier biotite, sphene and hematite.

Plagioclase is usually tabular to equant with elongate megacrysts up to 8mm length 2mm width. Compositionally calcic to sodic oligoclase (combined optic and probe determinations), these crystals infrequently display normal zoning and both albite and pericline twinning. Overgrowth by untwinned sodic plagioclase and alkali feldspar occurs on the elongate, larger crystals.

Selective sericitisation highlights zoning and twinning but is variable and often obscures these features. Myrmekite exsolution and intergrowth textures are developed at crystal margins but are not common. The smaller grains sometimes contain actinolitic hornblende and biotite inclusions.

Alkali feldspar is interstitial orthoclase (microcline?) but discrete anhedral to subhedral crystals of orthoclase, up to 3mm, also occur. Patch and lammellar perthite is commonly developed and zoning is occassionally present. Inclusions of plagioclase, quartz and altered biotite are often noted , especially in the anhedral interstitial grains.

Quartz has a granular appearance with larger interstitial grains (up to 4mm) often showing undulose extinction. Aggregates of small grains exhibit serrate boundaries and rare concertal texture but no triple point junctions have been recorded.

Accessory constituents are sphene as a common alteration product intimately associated with biotite, amphibole and opaque oxides. Apatite is present as small (<0.05mm) needles in biotite and plagioclase..

4.7 SYENOGRANITES.

These leucocratic rocks are characteristically pink coloured, fine to medium-grained with minor interstitial biotite. In medium-grained varieties, rare plagioclase megacrysts up to 1cm in length exhibit zoning and have inclusions of very fine biotite grains. Quartz forms glassy aggregates giving the rock a granular appearance. The average grain size is 2-2.5mm (Plate 4.34).

b) In thin section (Plate 4.22), biotite forms interstitial, stubby tabulate or slightly elongate, crystals with ragged edges , up to 1mm. Pleochroism is light to dark-brown. Alteration to chlorite and opaques is ubiquitous and secondary sphene is often associated with the sparse aggregates of biotite. Kink-structures and deformed elongate opaques in cleavage fractures show late-magmatic or sub-solidus movements have taken place. Inclusions of epidote and apatite are present.

Plagioclase is variable between An11-16 and An8 (optical and probe determinations). Crystal habit is predominantly subhedral tabular, up to 4mm and normally zoned with fine albite lamellar twinning always present. Resorbed crystal margins are frequently overgrown by more sodic plagioclase or alkali feldspar and sericitisation highlighting the more calcic zones but obscuring the fine lamellar twinning.

Alteration is very variable within section, and appears mainly confined to oligoclase cores. Micro-myrmekite and graphic intergrowths with alkali feldspar are common but not found at all crystal interfaces. Haematisation along crystal boundaries is present (RM107) as a very fine-grained alteration product. Limited deformation of twin planes indicates sub-solidus movements.

Alkali feldspar is present as anhedral orthoclase (up to 2.5mm) and as microcline (RM36-38). Simple twinning and optical zoning are common in discrete grains. Aggregates of orthoclase, mantled by interstitial (more potassic) alkali feldspar show alteration to marginal hematite, muscovite and epidote.

Coarse lamellar, bleb and rod perthite textures are well developed but they are, along with patchy discontinuous zoning, often obscured by alteration products. In large interstitial patches, optical continuity over 5-7mm is noted and inclusions of plagioclase, biotite and quartz are common.

Quartz occurs as granular aggregates, discrete grains and as interstitial patches with consertal textures. Inclusions of muscovite, orthoclase and oligoclase are present in both the interstitial material and the discrete grains. Recrystallisation has generated patches up to 5mm which display undulose extinction and have triple point junctions. Combined with the felsic minerals, a marked granular texture results.

Allanite, muscovite, epidote and apatite are the common accessory phases. Secondary opaques are ubiquitous as individual grains or as grain boundary and cleavage infill in biotite. Acicular apatite and epidote occur as inclusions in plagioclase, alkali feldspar and to a lesser extent biotite or as separate phases interstitial to large plagioclase crystals.

The marginal syenogranites are more syenitic in composition and exhibit greater alteration of plagioclase and alkali feldspars. The plagioclase appears to be slightly more sodic than that of the central syenogranites. Biotite, if present, is extensively to completely altered to chlorite minerals with mantling by secondary opaques and sphene common. The secondary sphene is often itself altered to opaque oxides.

A 6.5km traverse inwards from the western margin contact with Moine quartzites (Fig. 4.2) illustrates the change in essential mineralogy from the marginal syenogranites (RM30) to the granodiorites (RM55-52). The absence of primary amphibole in the acid phase is readily apparent while a minimum modal percentage of biotite appears to be a fundamental feature of all rock types.

4.8 Crystallisation history.

Figure 4.2 Variation in essential mineralogy with increasing distance from contact with country rock. Note amphibole-poor, K-feldspar-rich mineralogy of marginal acidic syenogranite phase. Quartz content of granodiorites decreases with distance from quartz-monzodiorite phase.

Considering the intermediate types (quartz-monzodiorites, granodiorites and monzogranites), biotite is mainly subhedral to euhedral and contains earlier accessory phases. The presence of these accessories, e.g. apatite needles, suggests that biotite was stable early in the sequence. Where biotite occurs as inclusions within plagioclase, it is itself free of accessory phase inclusions. Interstitial biotite is considered to result from crystallisation under late magmatic conditions or is secondary resulting from amphibole alteration.

Amphibole has three distinct crystal habits only one of which is predominantly free of inclusions. This latter type is the elongate, prismatic amphibole which often appears to be the first phase crystallised from the melt, followed closely by biotite and plagioclase. Patchy zoning is uncommon but where present does indicate short intervals of equilibration to changing conditions. The remaining two habits of amphibole commonly possess small irregular grains of quartz.

Several textural features of some amphiboles appear to be compatible with a post magmatic origin. The untwinned subhedral to anhedral habit, often enclosing quartz and feldspars, is usually restricted to areas of primary amphibole and biotite. Post-consolidation textures show the development of very fine-grained alteration products along cleavage fractures and grain boundaries together with variable chlorite mineral growth on biotite and in mafic aggregates. The distinctive "feather texture" of biotites in RM17 &

RM17A is also thought to result from post magmatic, post consolidation deformation, possibly aided by fluids.

The dominantly subhedral to euhedral habit of phenocrystic plagioclase indicates that it was one of the first major phases to crystallise. The presence of biotite, amphibole and rarer alkali feldspar inclusions does suggest that these ferromagnesian phases were also formed at an early stage. Phenocryst and groundmass textures of plagioclase indicates that at least two distinct periods of crystallisation occurred and are probably a function of intrusion, with the later part of the sequence occurring after emplacement.

Alkali feldspar occurs both as interstitial grains and as discrete crystals or occasionally as phenocrysts which contain small inclusions of plagioclase, biotite and amphibole which indicate a possible early crystallisation of the feldspar from the melt. Chemical zoning of the larger crystals is interpreted as due to magmatic diffusion processes.

The porphyritic habit can be regarded as resulting from sparse nucleation and high growth rates (Swanson, 1977) while the interstitial habit indicates a late magmatic growth. Those samples with optically continuous poikilitic alkali feldspar crystals suggest that rapid growth occurred, possibly simultaneously with earlier quartz.

Quartz as an early phase appears as small inclusions within plagioclase phenocrysts and also within secondary or late-magmatic amphibole, but the predominantly interstitial habit suggests a late magmatic origin. Undulose extinction indicates the presence of strain during crystallisation. Where both sharp and undulose extinction styles coexist, recrystallisation of the quartz may have occurred due to inversion strain in the transition from beta to alpha quartz. This is most likely to have occurred in the post magmatic phase.

Considering the syenogranites, these rocks have a different postulated paragenetic sequence reflecting their different essential mineralogy. Biotite contains few inclusions and although often elongate to subhedral, it occurs on grain boundaries of felsic phases or interstitially. Biotite occurs infrequently as inclusions in other phases and intimate relationships with secondary opaques and chlorite minerals suggests that it is predominantly a product of a late magmatic stage of consolidation. Primary amphibole is conspicuously absent.

Plagioclase phenocrysts and poorly zoned plagioclase with resorbed cores indicate that it was either the first major crystallising phase from the melt or that it crystallised simultaneously with potassic feldspar. Cores sometimes contain inclusions of biotite and apatite, often orientated parallel to the faces of the crystal. Chemical zoning is variably developed and is often restricted to only a narrow, more sodic rim found on the equant crystals. The presence of muscovite appears to be confined to the

areas of sericite alteration.

Alkali feldspar occurs both as phenocrysts and interstitial grains and is interpreted as having a long history. Large grains contain numerous inclusions of rounded quartz and these are joined by biotite and amphibole in those samples which are intermediate to the syenogranites and the monzogranites (eg. RM106,RM107). Chemical zoning is less markedly developed in this type but a strong domain texture with separation by braid perthite is noted for the earlier formed subhedral grains. Marginal exsolution textures appear to be confined to areas with little quartz present and are thought to be magmatic in origin, due to continuity of the exsolved feldspar with the host.

Quartz appears as inclusions in plagioclase and alkali feldspar but is predominantly developed as large, framework-forming rounded grains with embayed margins or as small interstitial grains. These larger grains are free of inclusions and are thus interpreted as forming later than the earlier feldspar phases but prior to the overgrowths on alkali feldspar, plagioclase and biotite.

4.9 Discussion of amphibole textures.

A texture displayed by amphibole throughout all rock types (except the syenogranites and marginal syenogranites/syenites) is the presence of more than one habit of biotite inclusions within different amphibole habits (Plate 4.3). Three varieties of this relationship are found but interpretation is difficult and will be discussed later,

in more detail in Chapters 6 and 7.

The first style of the texture is found predominantly within the most basic rock type (monzodiorite). It consists of knots of altered, chloritised biotite with opaques developed along cleavages and ragged edges, associated with later biotite, the whole of which is enclosed within a penetrative overgrowth of subhedral to euhedral pseudo-poikiltic amphibole (Plate 4.3).

The second and more common style consists of corroded subhedral or elongate, untwinned prismatic amphibole crystals enclosing disrupted biotite showing lobate, embayed contacts to the host. The biotite is almost always in single crystal optical continuity and is preferentially orientated parallel to the 110 cleavage of the surrounding amphibole (Plate 4.4).

The third texture is for late-stage amphibole growth within and surrounding mafic aggregates or discrete biotite grains. Where composed of small amphibole grains, this texture frequently has a 'granular' appearance (Plate 4.23). One interpretation of this texture is that they represent restite.

To account for the observed features where biotite is both earlier and later than amphibole, reference is initially made to Bowen's reaction series and recent work on experimental melting relationship phase diagrams. The published melting relationships assist interpretation of crystallisation relationships. For tonalite, data are published by Lambert & Wyllie, 1974; Piwinskii, 1975; Wyllie,

1975; Wyllie et.al., 1976.

It is noted that for a tonalite with excess H2O, the phase boundaries for hornblende and biotite do not cross for any given temperature and pressure (total) range. Thus the expected order of crystallisation from such a magma would be amphibole followed by biotite. In many sections, elongate prismatic amphibole, interpreted as a first-formed mineral, co-exists with the second type of textural relationship.

This implies that crystallisation followed the path predicted from the phase diagrams and that all amphibole subsequent to the biotite-free habit is of post magmatic origin, or that biotite occurring within amphibole was the product of crystallisation in 'hollow' crystals. The possibility that the texture results from simultaneous crystallisation of biotite and amphibole has been considered but rejected as it cannot account for two generations of biotite, one often greatly altered, within a sub-euhedral, unaltered enclosing amphibole (Plates 4.2 and 4.3).

The amphibole may therefor be considered as of either magmatic, subsolidus replacement or restitic origin, or as is more likely, some combination of these. This would more readily account for the noted differences in crystal habit of the amhiboles within chemically and petrographically similar rocks. Chemical variation between the different biotite and amphibole phases has been identified and is explained in Chapters 6 & 7.

4.10 Myrmekitic texture and its significance.

Myrmekitic intergrowth textures have restricted occurrence within the Moor of Rannoch and are characteristic of the granodiorites from the western part of the pluton (RM48-55, RM72-78) and the eastern margin (RM92-94, RM96). The symplectic intergrowth occurs either as extension of subhedral oligoclase crystals or as irregular wart-like growths out from plagioclase. Both coarse and fine vermicules of quartz are noted at crystal margins but, where replacement of original plagioclase inclusions within alkali feldspar has taken place, only coarse vermicules and blebs are seen.

Where myrmekite occurs as extensions to crystals, it is thought to be the result of expulsion of a K-rich phase (Hibbard, 1979). Simple exsolution interacting with sodic metasomatism could generate it as a replacive texture. The evidence for Na-metasomatism is seen as incipient checkerboard albite development (RM54). Development of untwinned, unzoned sodic-rich plagioclase rimming plagioclase phenocrysts may also represent sodic metasomatic efffects. This armouring may also be the product of magmatic processes controlled by external factors of pressure and temperature on intrusion as the compositional gap between the rim and phenocryst is too large to be explained by the constitutional supercooling growth scheme proposed by Sibley et al., (1976).

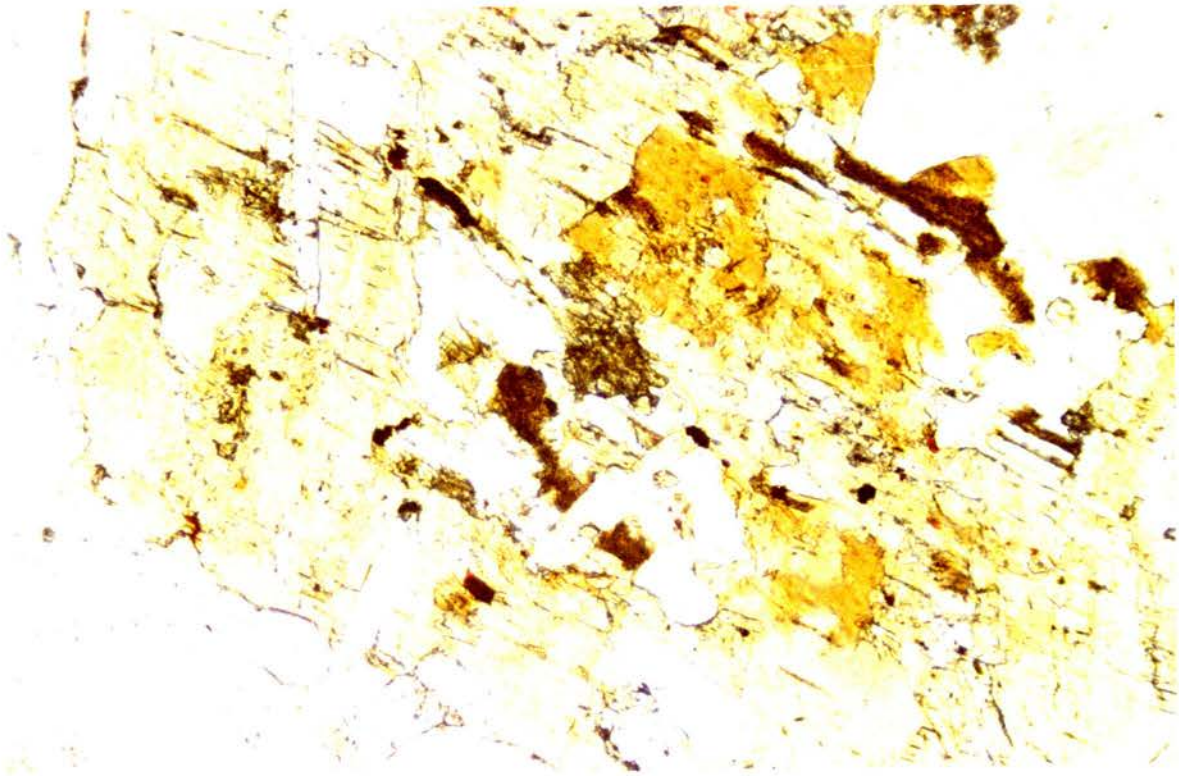

Plate 4.1 Intimate relationship of biotite in actinolitic hornblende RM100. XPL. x125.

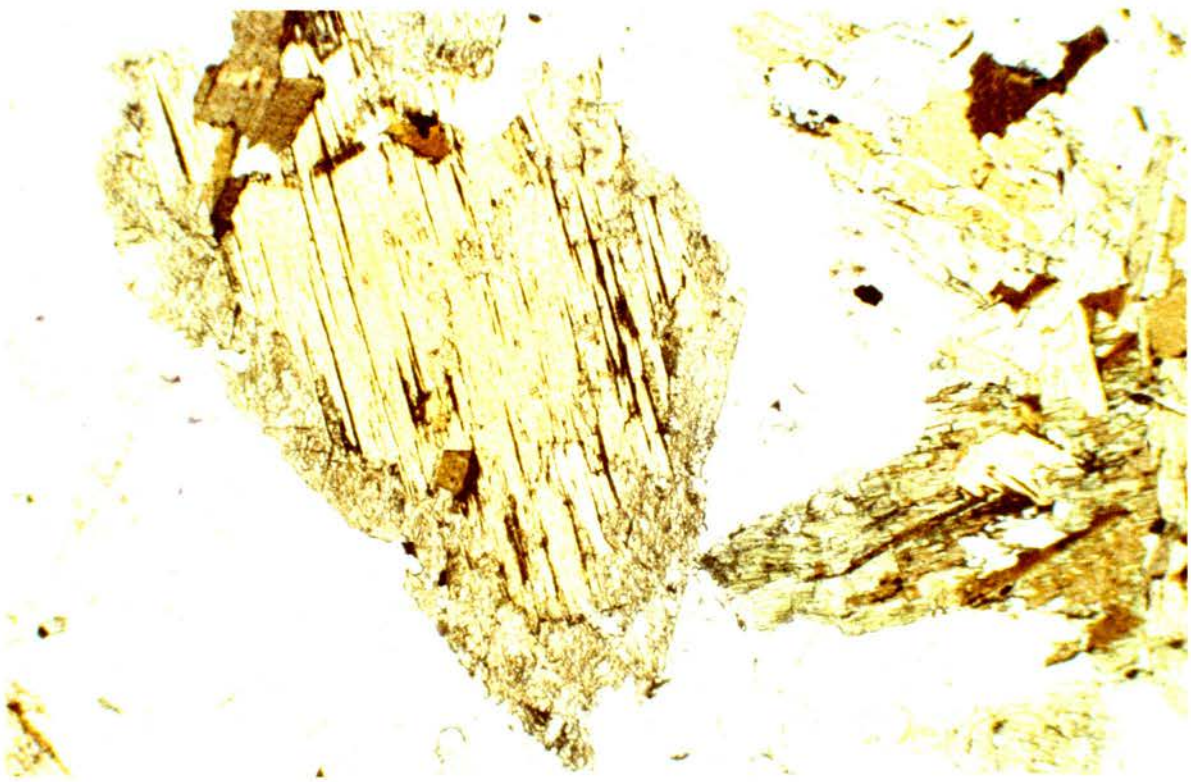

Plate 4.2 Ragged annitic biotite with opaques developed in cleavage and margins enclosed within euhedral actinolitic(?) hornblende (centre). Two generations of biotite are noted in actinolitic hornblende to right of field of view. RM100. PPL. x50

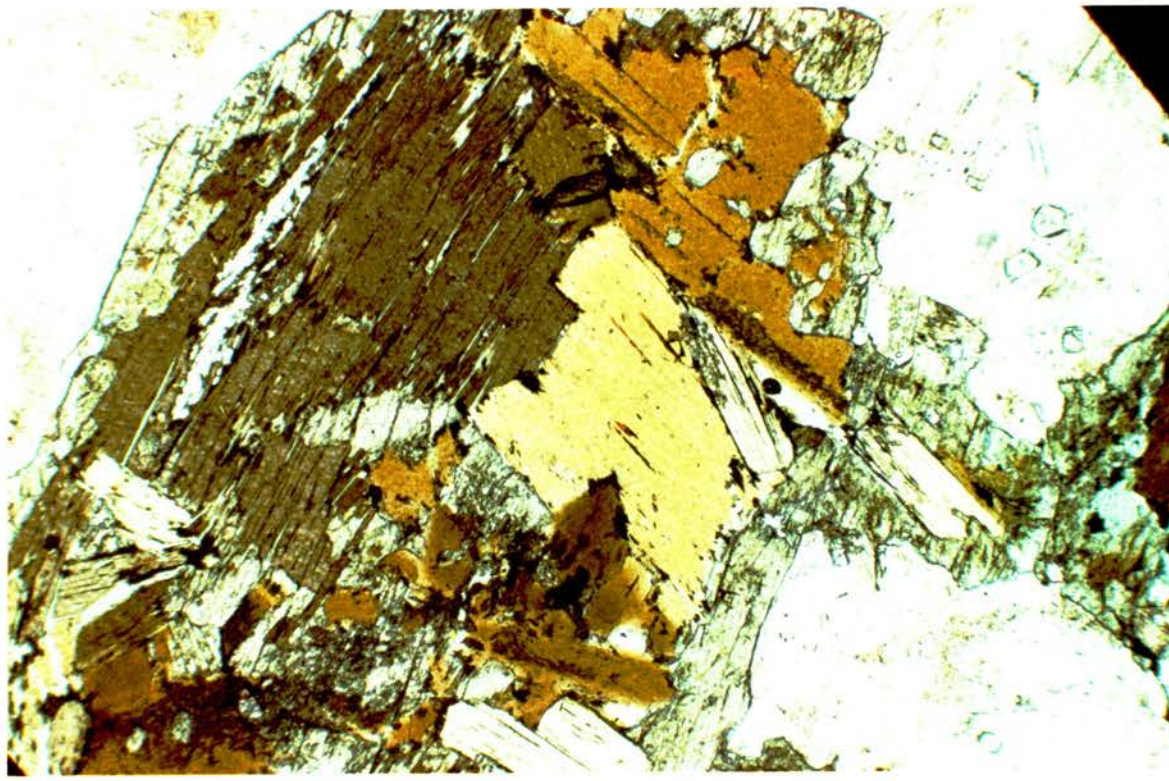

Plate 4.3 Two generations of biotite within euhedral hornblende. The earliest biotite phase has been kinked and disrupted the second shows weak cleavage development and mantling by opaque phases. RM111. PPL. x50.

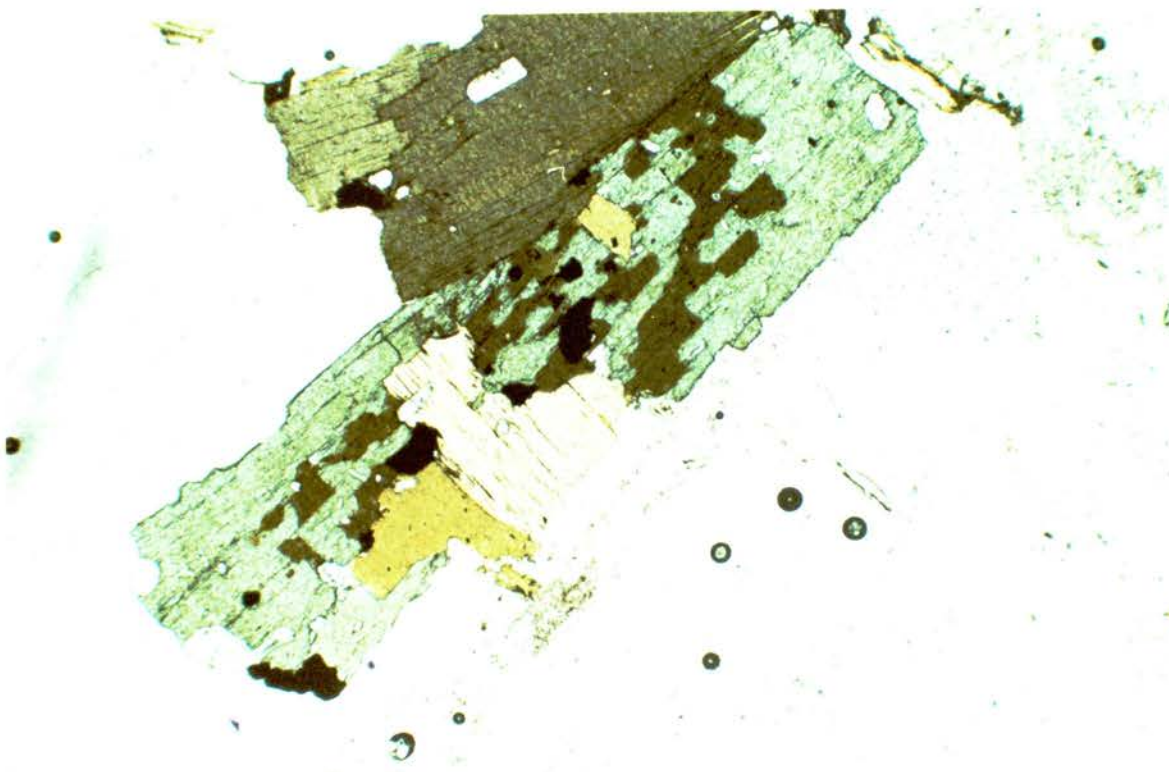

Plate 4.4 Two generations of biotite within magnesio-hornblende. The inferred earlier biotite possesses common cleavage with the host amphibole and has embayed crystal outlines. RM93. PPL. x50.

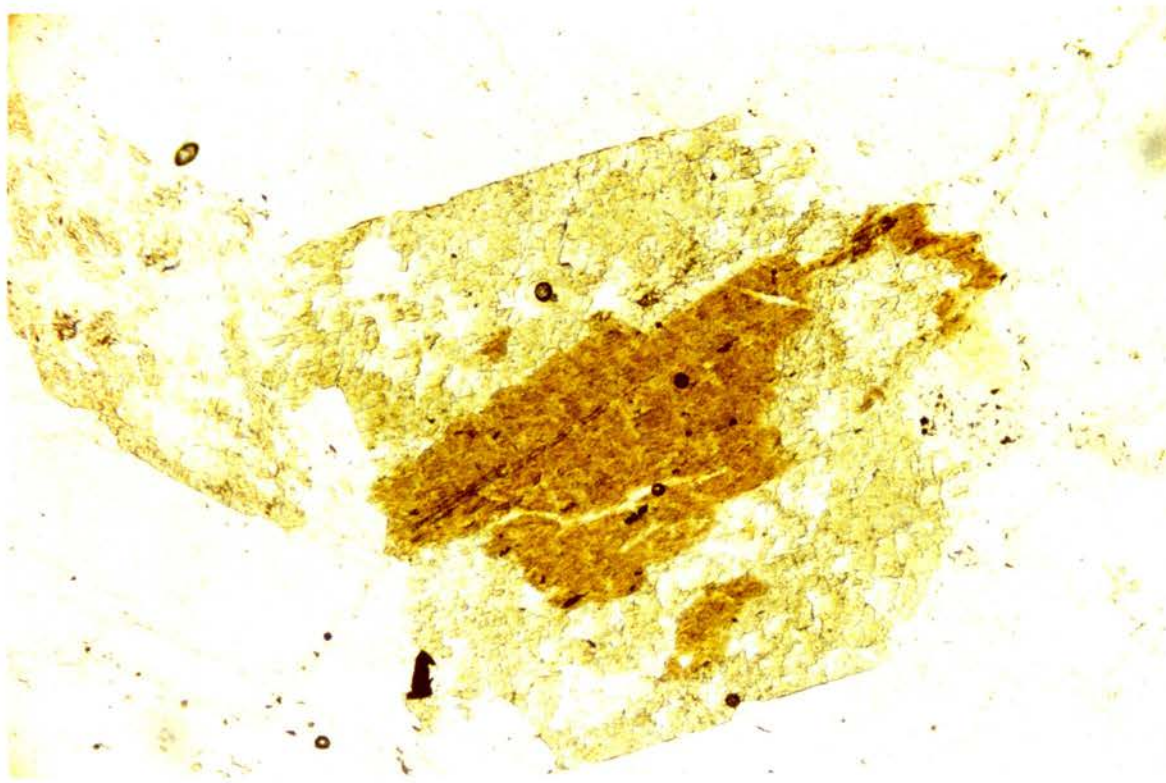

Plate 4.5 Extensively corroded amphibole (actinolitic hornblende?) with core of included biotite which has been partly replaced by amphibole. RM16. PPL. x125

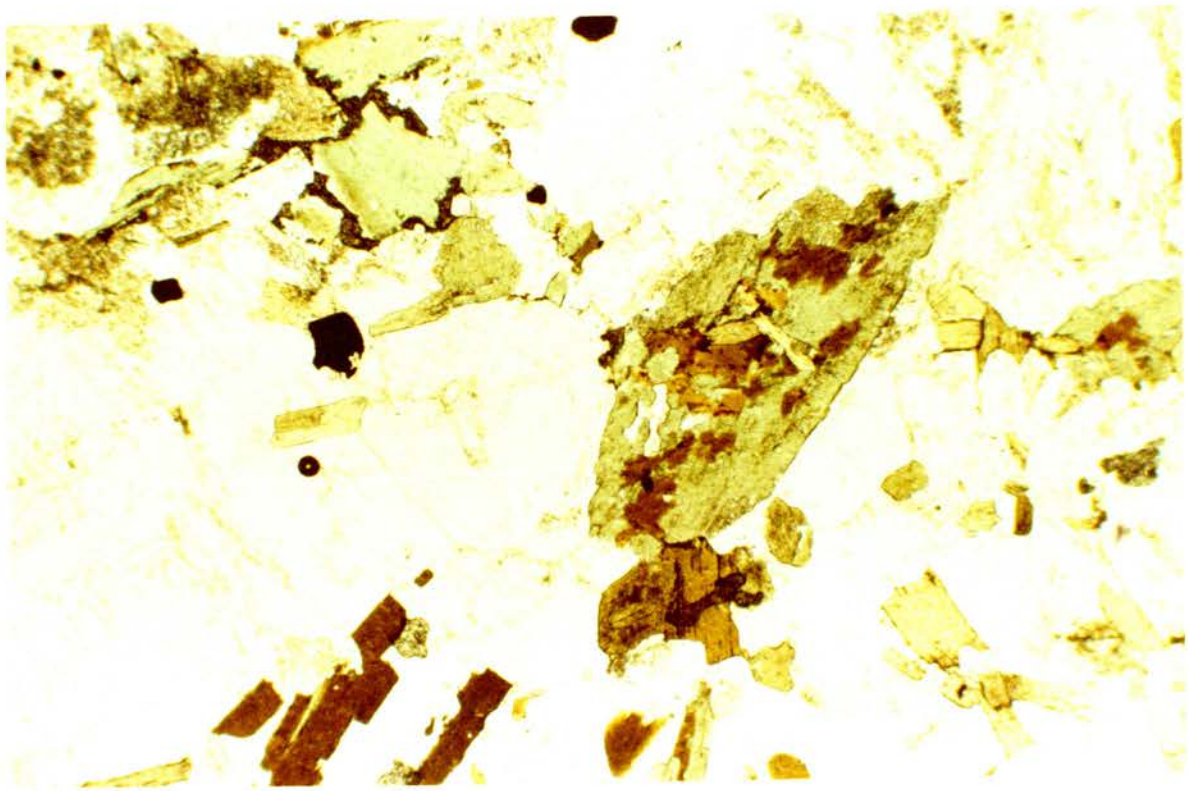

Plate 4.6 Three characteristic amphibole habits: euhedral hornblende (top left); inclusion-free, non-pleochroic actinolitic hornblende (mantled by opaques and secondary sphene); elongate actinolitic hornblende with two generations of biotite (right of centre). RM63. PPL. x50.

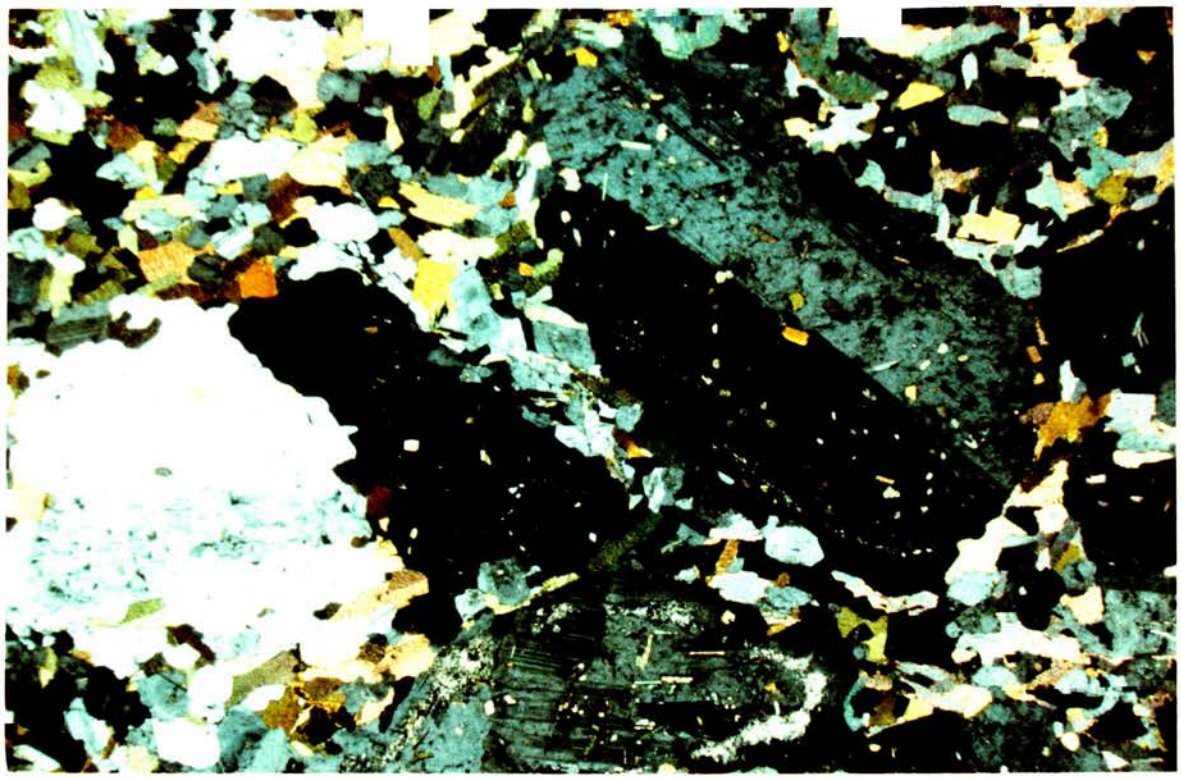

Plate 4.7 Andesine phenocrysts, with orientated orthoclase and biotite inclusions, in a groundmass of oligoclase and biotite with faint fabric noted in the groundmass. Biotite laths are orientated around phenocryst margins.
RM71A. XPL. x15.

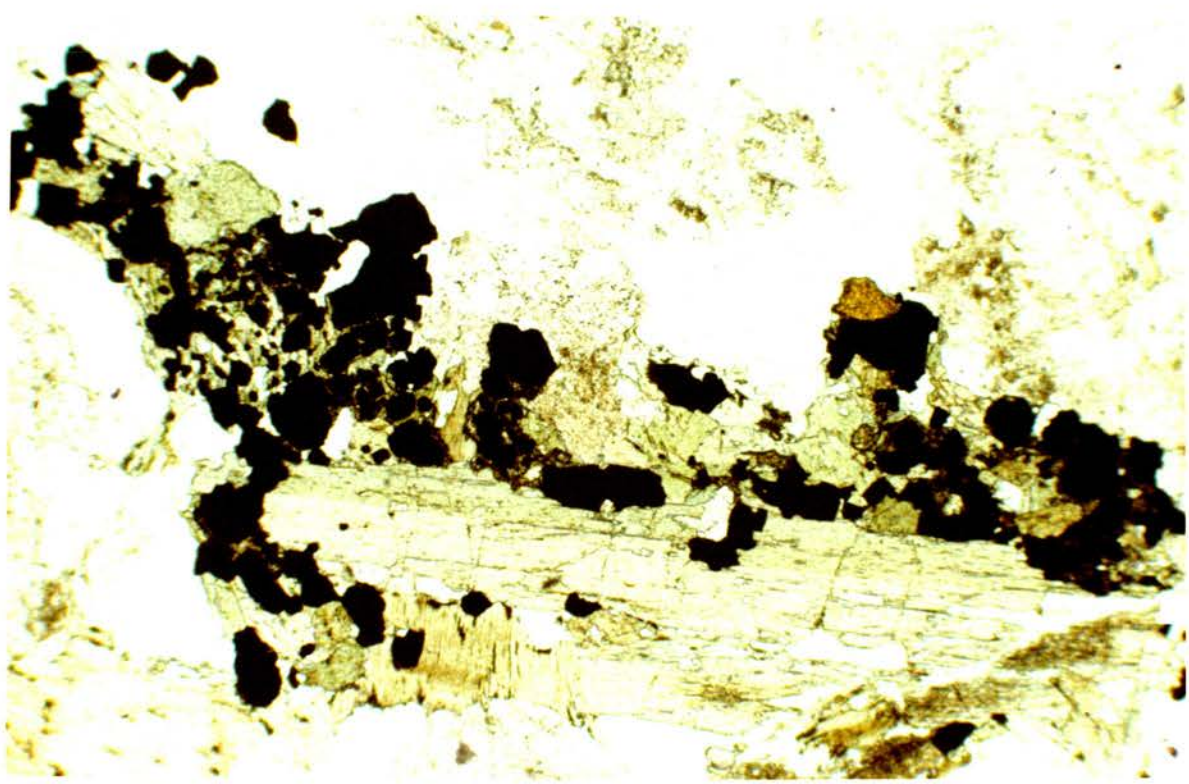

Plate 4.8 Actinolitic hornblende, with biotite and quartz inclusions mantled by secondary opaques. Secondary sphene is also seen in intimate association with opaque phases.
RM48. PPL. x50.

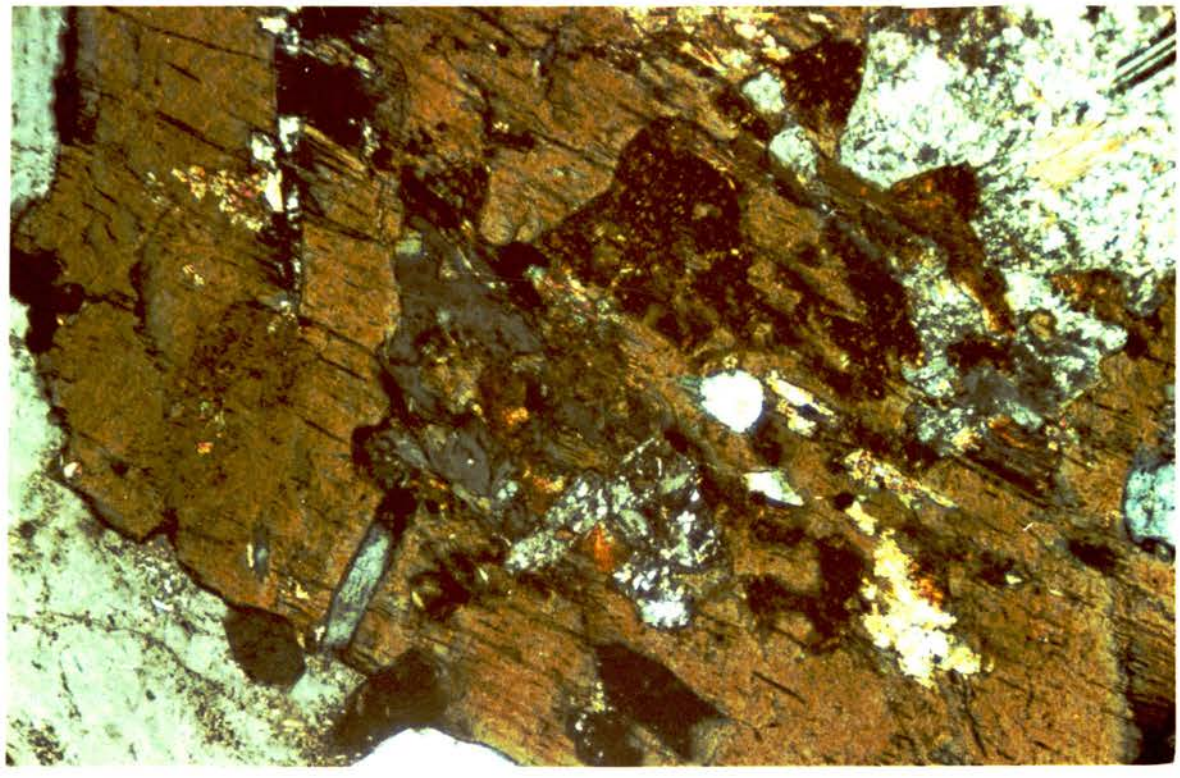

Plate 4.9 Quartz and plagioclase inclusions in amphibole and biotite RM100. XPL. x125

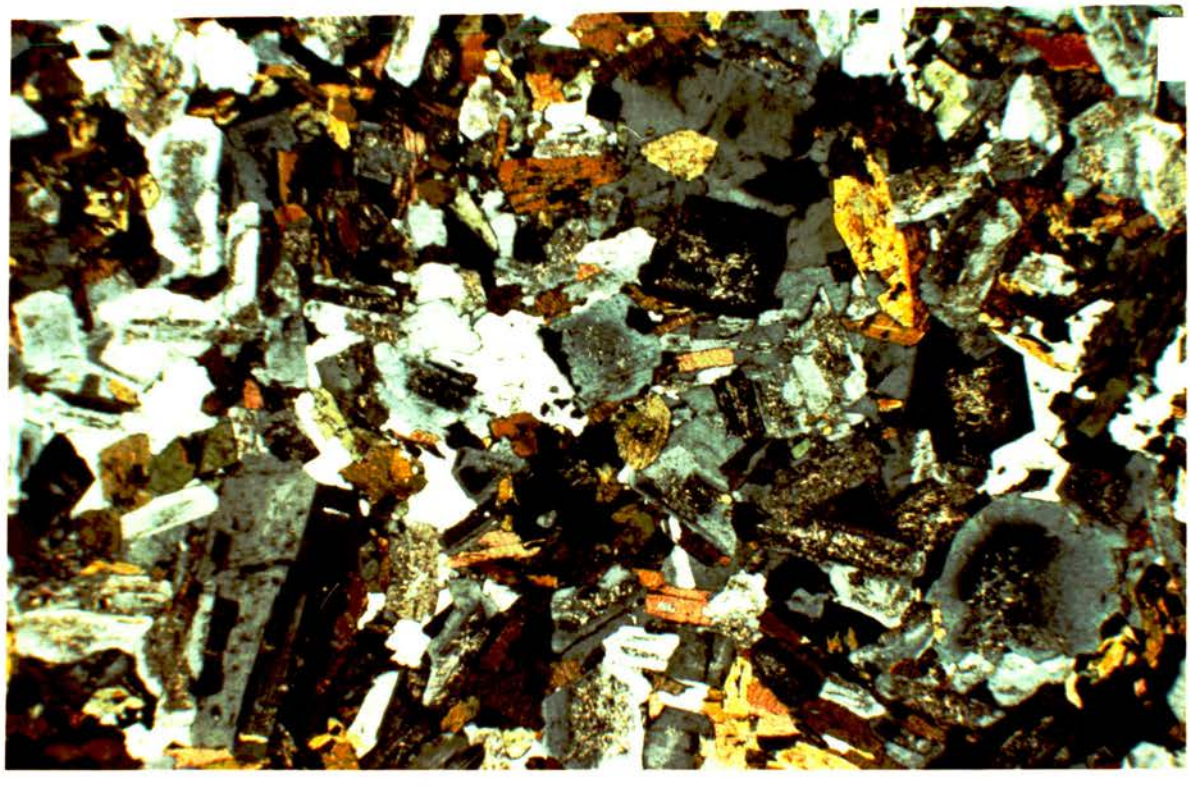

Plate 4.10 Texture of fine-grained, melanocratic quartz-monzodiorite showing zoned oligoclase, actinolitic hornblende with disequilibrium textures and lack of fabric.
RM89. XPL. x25.

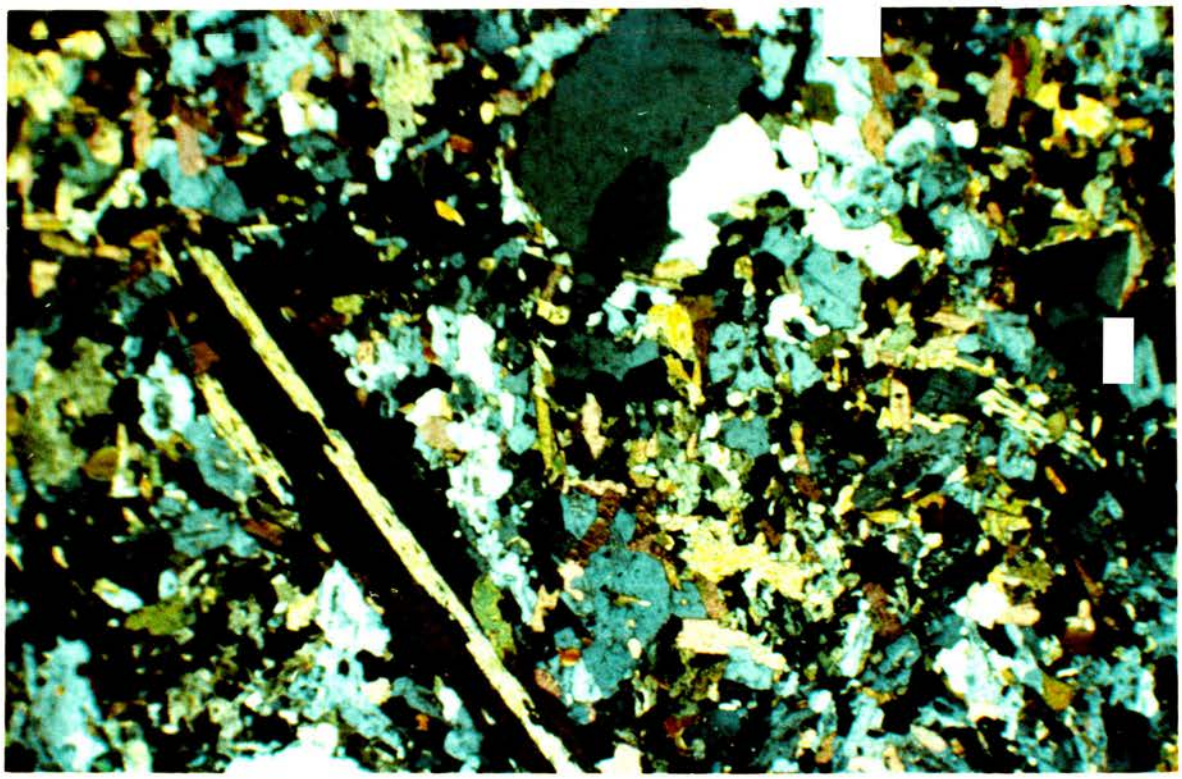

Plate 4.11 Hornblende and quartz phenocrysts in fine grained groundmass with interstitial orthoclase and quartz. RM117. XPL. x25.

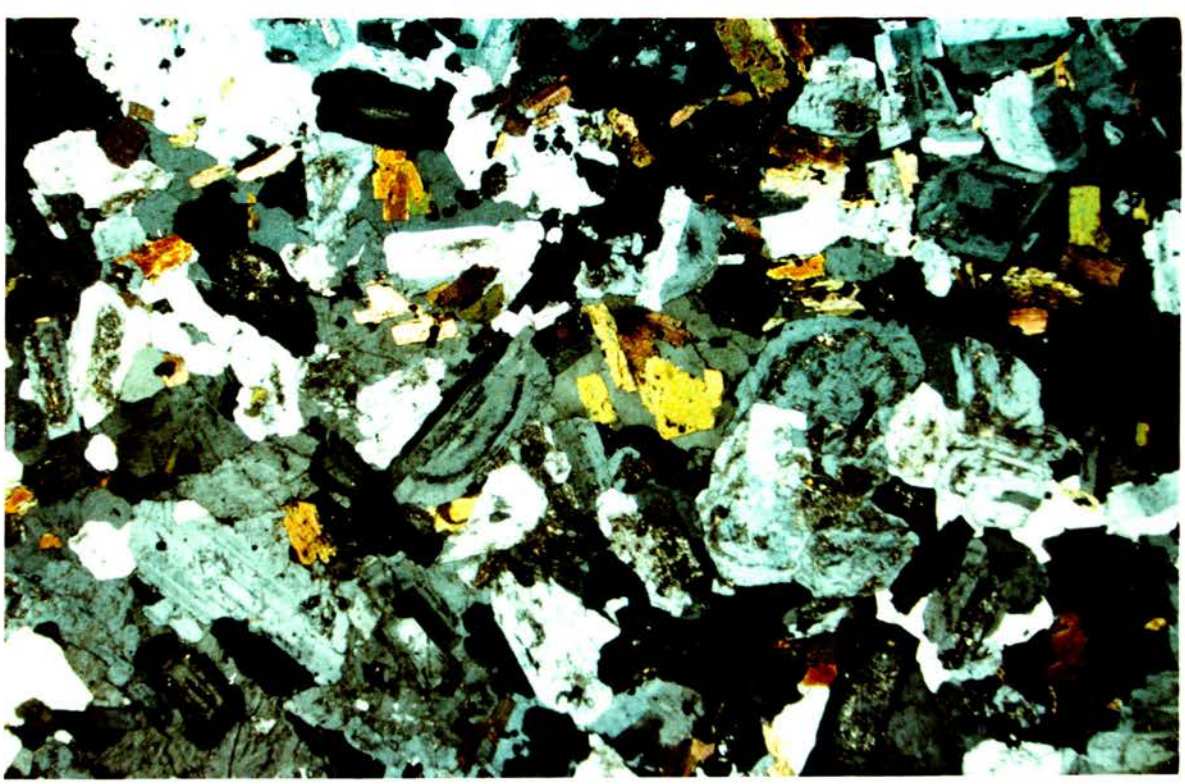

Plate 4.12 Texture of fine-grained, melanocratic quartz-monzogranite for comparison with Plate 4.10. Zoning within plagioclase is highlighted by selective sericitization. RM57A. XPL. x15.

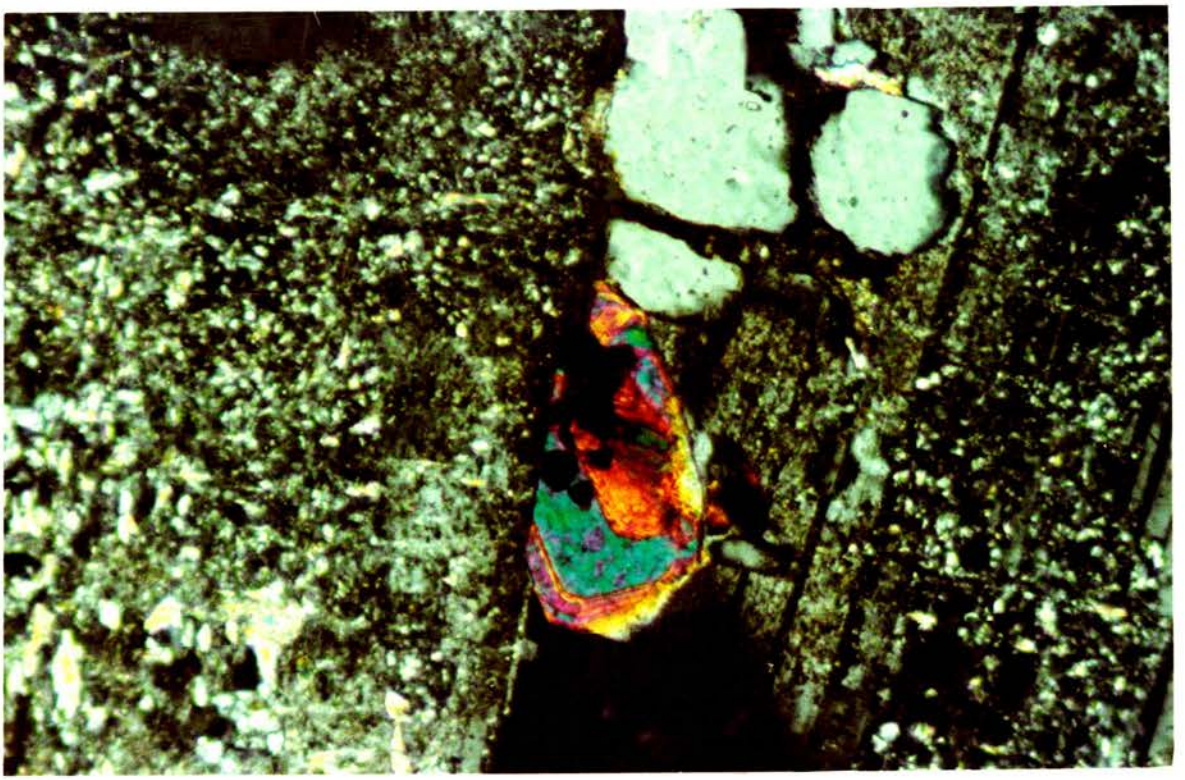

Plate 4.13 Zircon inclusion in plagioclase showing anhedral core and euhedral overgrowth with zoning. RM59. XPL. x250.

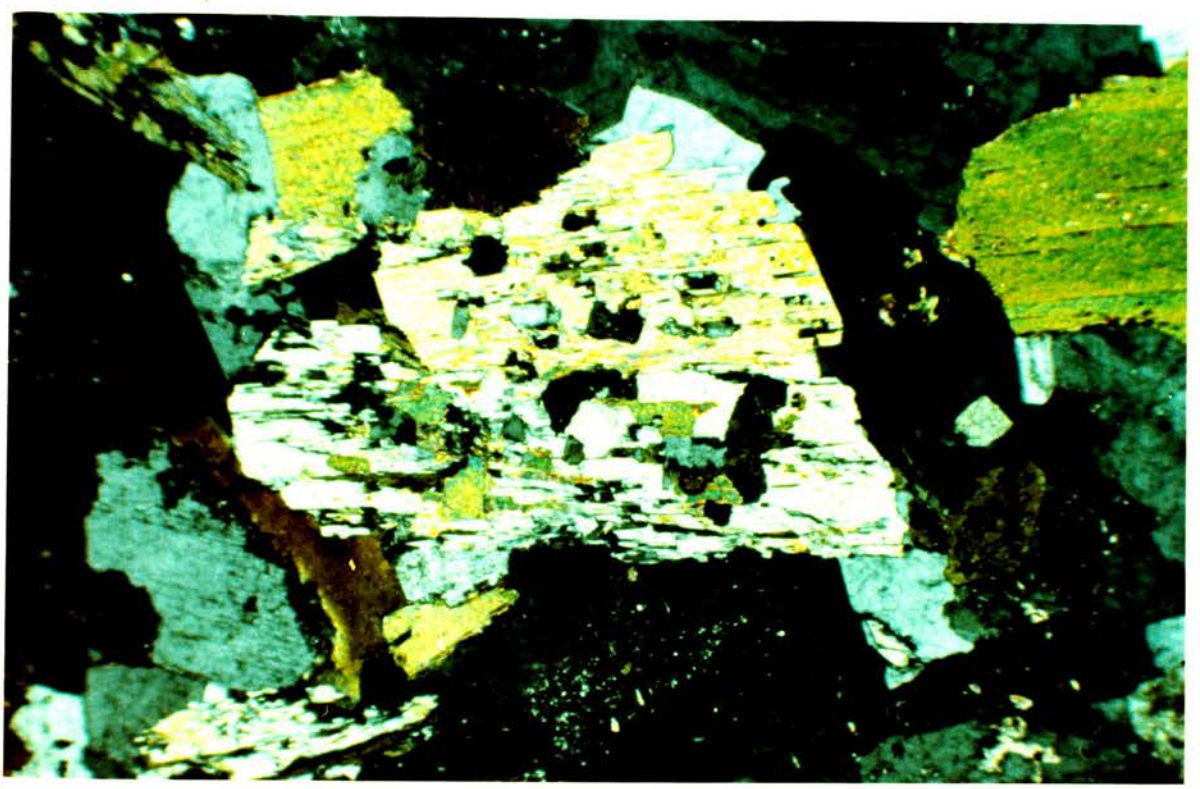

Plate 4.14 Quartz and biotite disequilibrium texture in amphibo. RM113. XPL. x50.

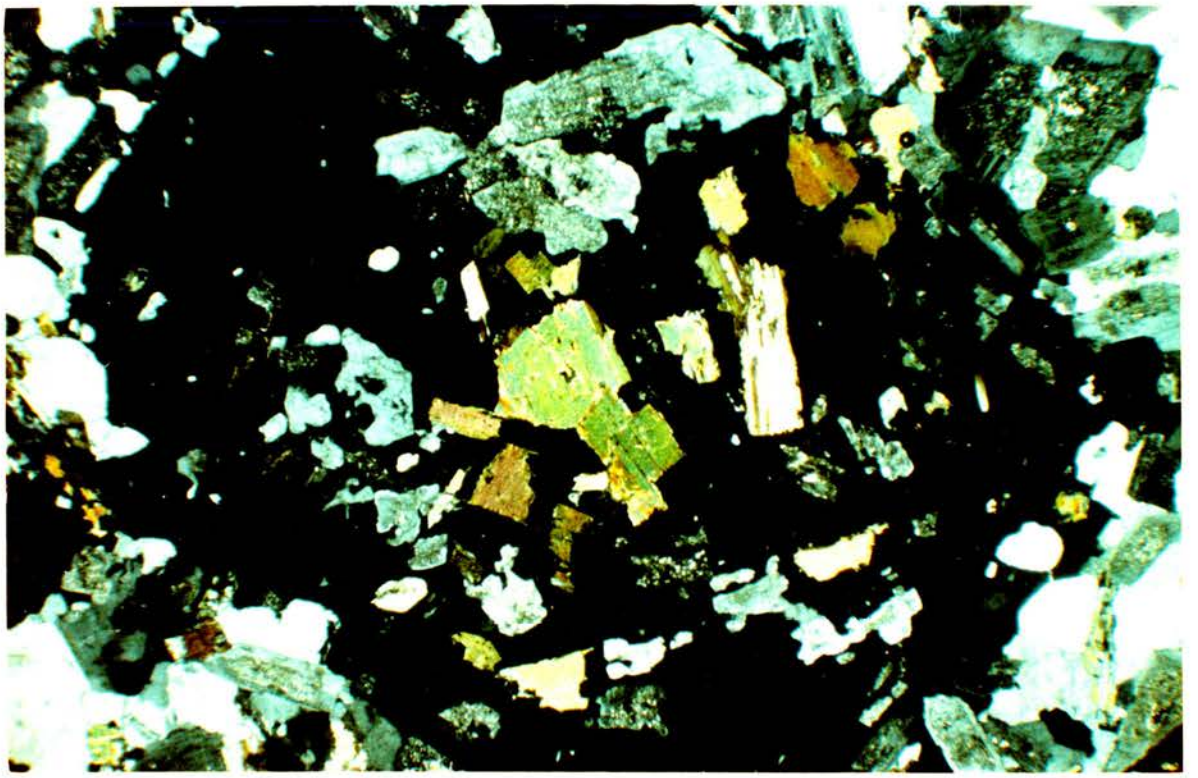

Plate 4.15 Poikilitic alkali feldspar in monzogranite. BM9. XPL. x25

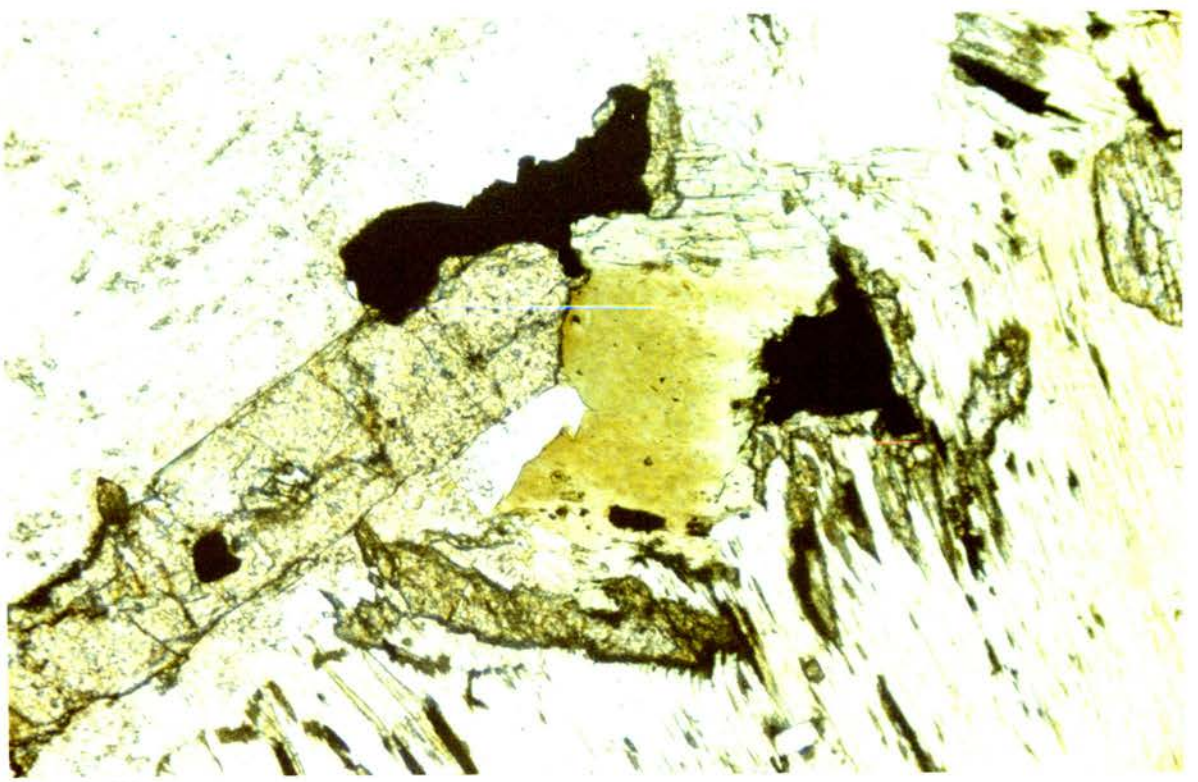

Plate 4.16 Secondary sphene, opaques and biotite mantling ragged, annitic biotite in granodiorite. BM76. PPL. x125.

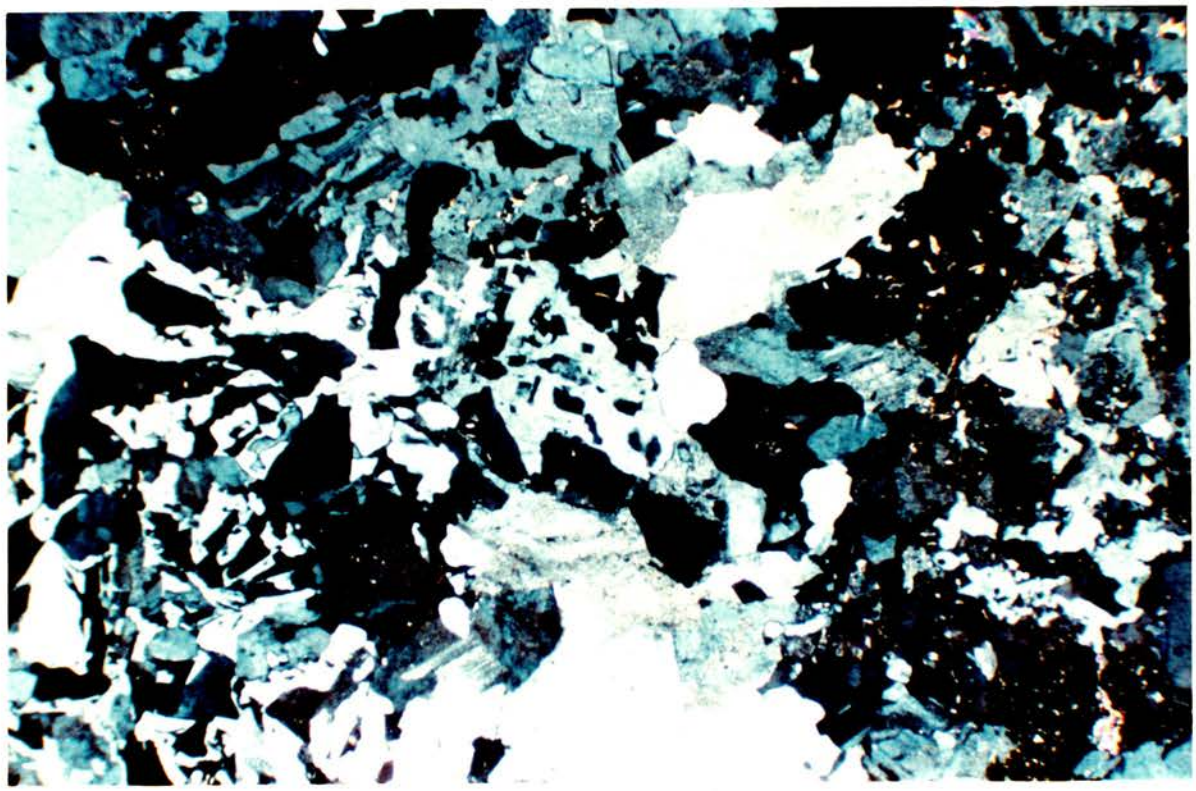

Plate 4.17 Consertal texture in granodiorite. This texture is seen only in granodiorite and is predominant in the western part of the pluton. RM47. XPL. x25.

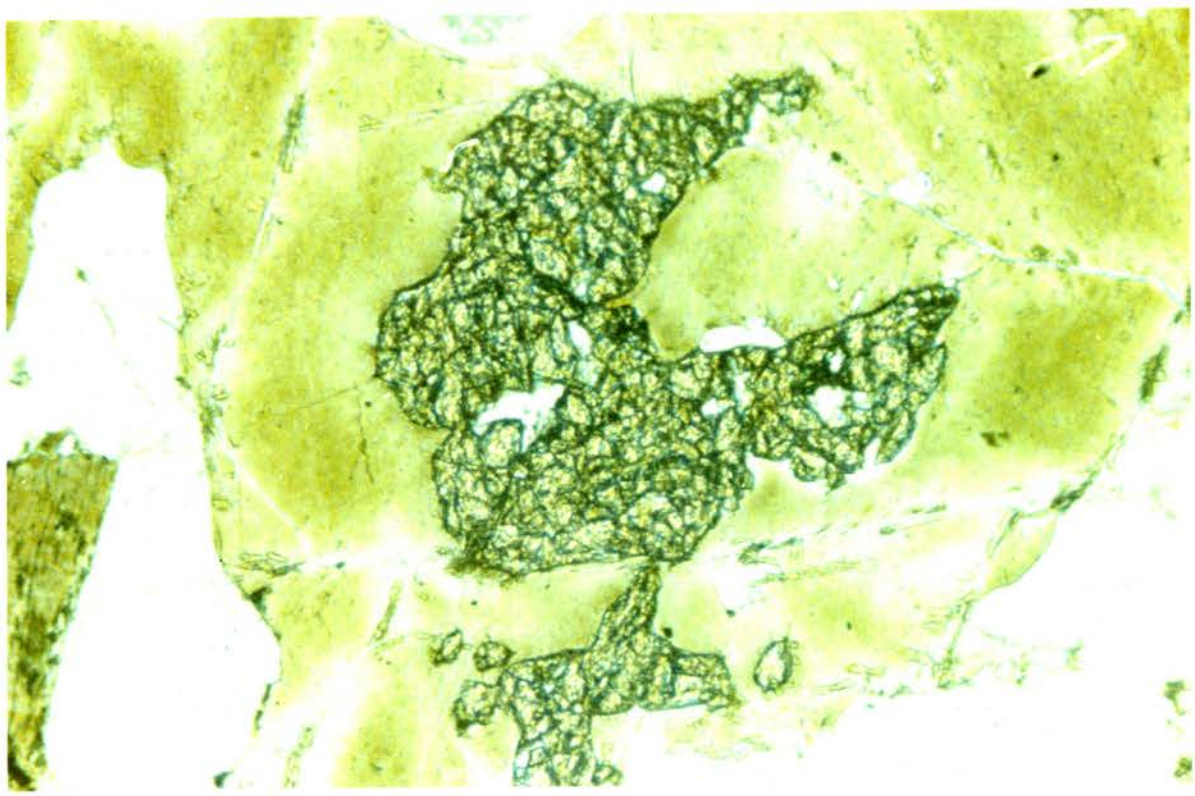

Plate 4.18 Allanite and apatite in biotite(secondary?). RM17. PPL. x125.

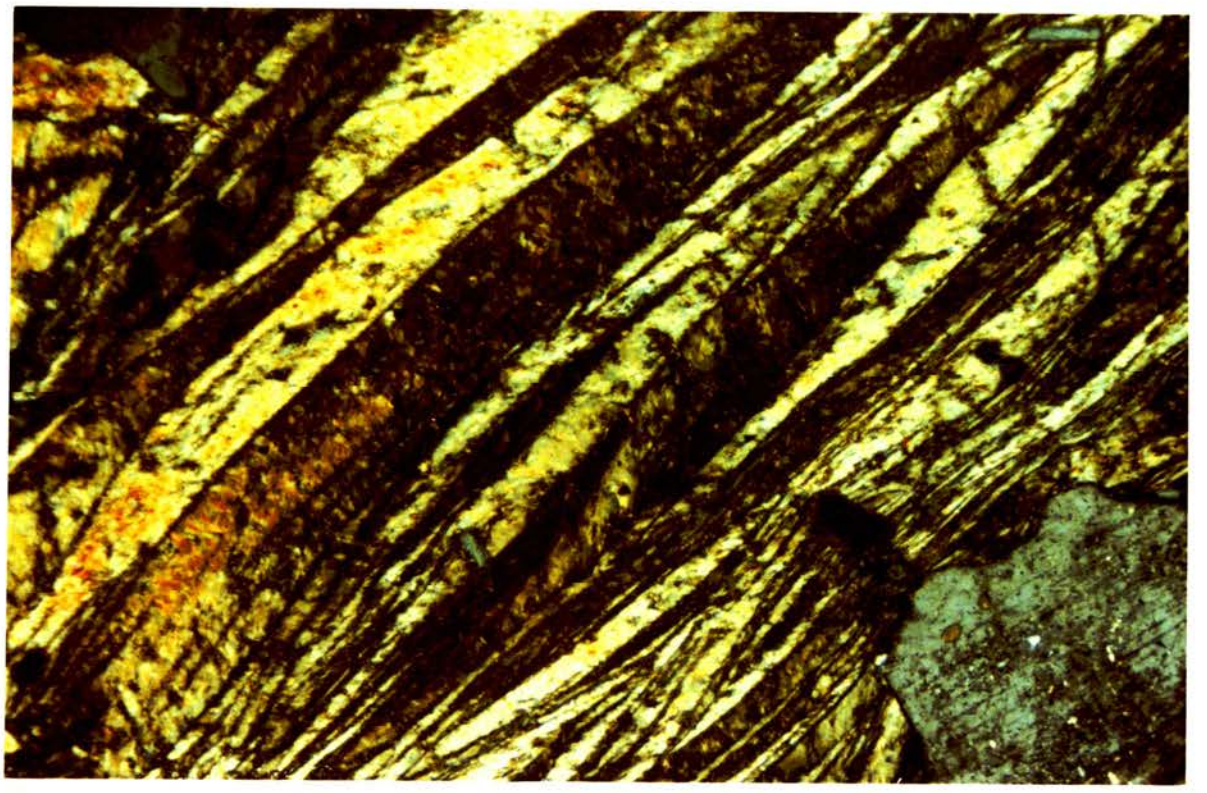

Plate 4.19 "Feather texture" in biotite from monzogranite. RM17A. XPL. x25.

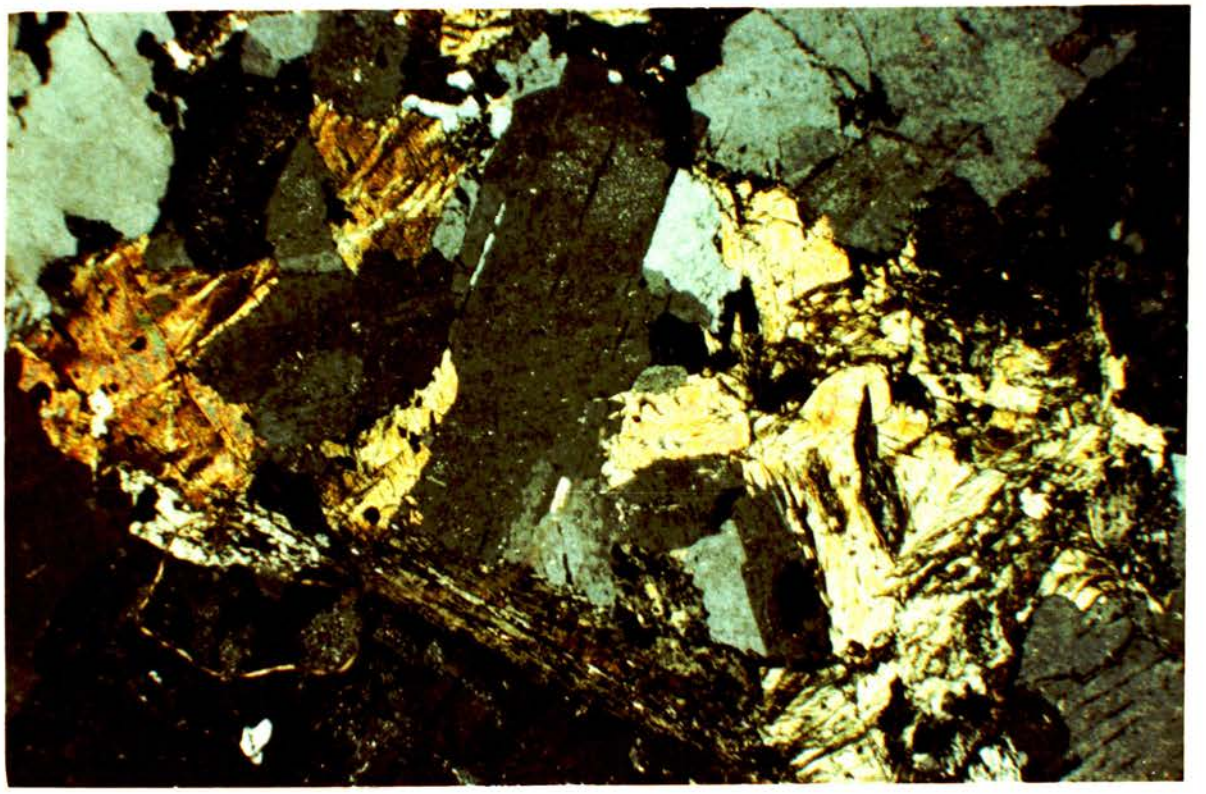

Plate 4.20 Texture of monzogranite, RM17A. XPL. x25

Plate 4.21 Texture of monzogranite, RM17. XPL. x25.

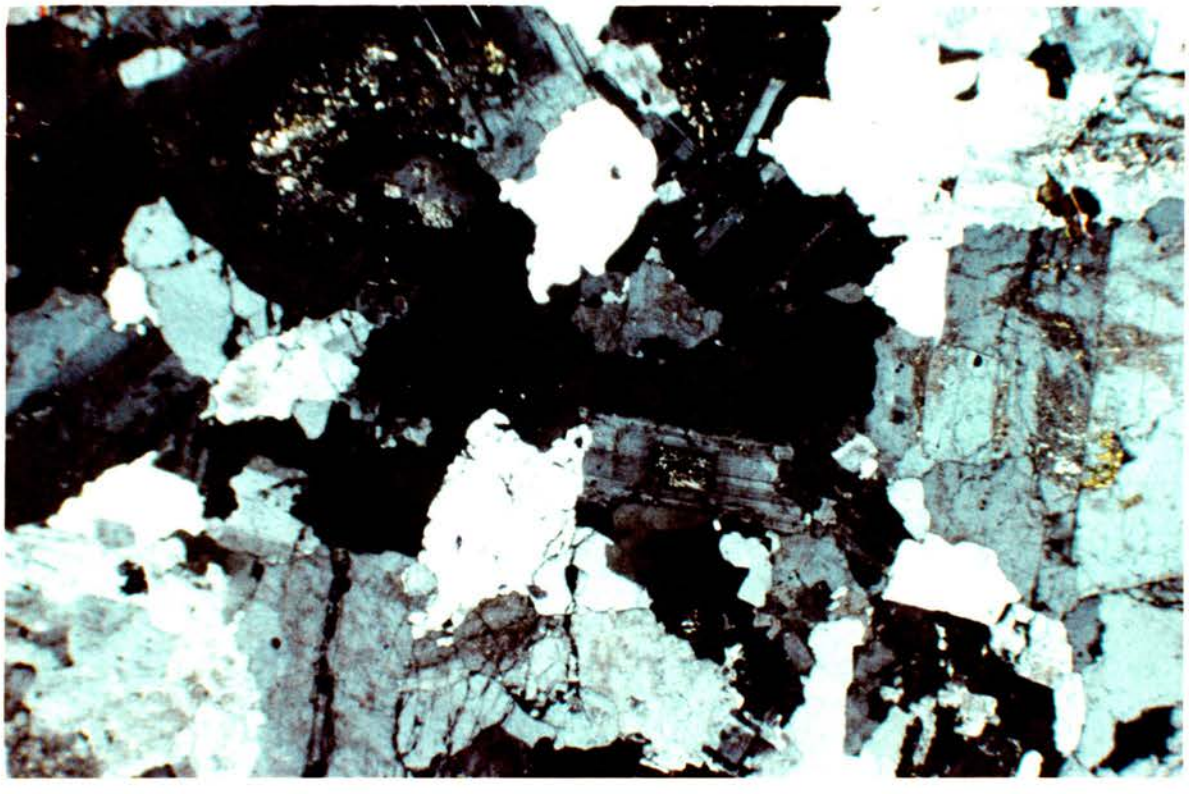

Plate 4.22 Texture of syenogranite from east of Laidon-Ericht fault. Absence of primary amphibole and scarcity of biotite is characteristic of this type. RM36. XPL. x50.

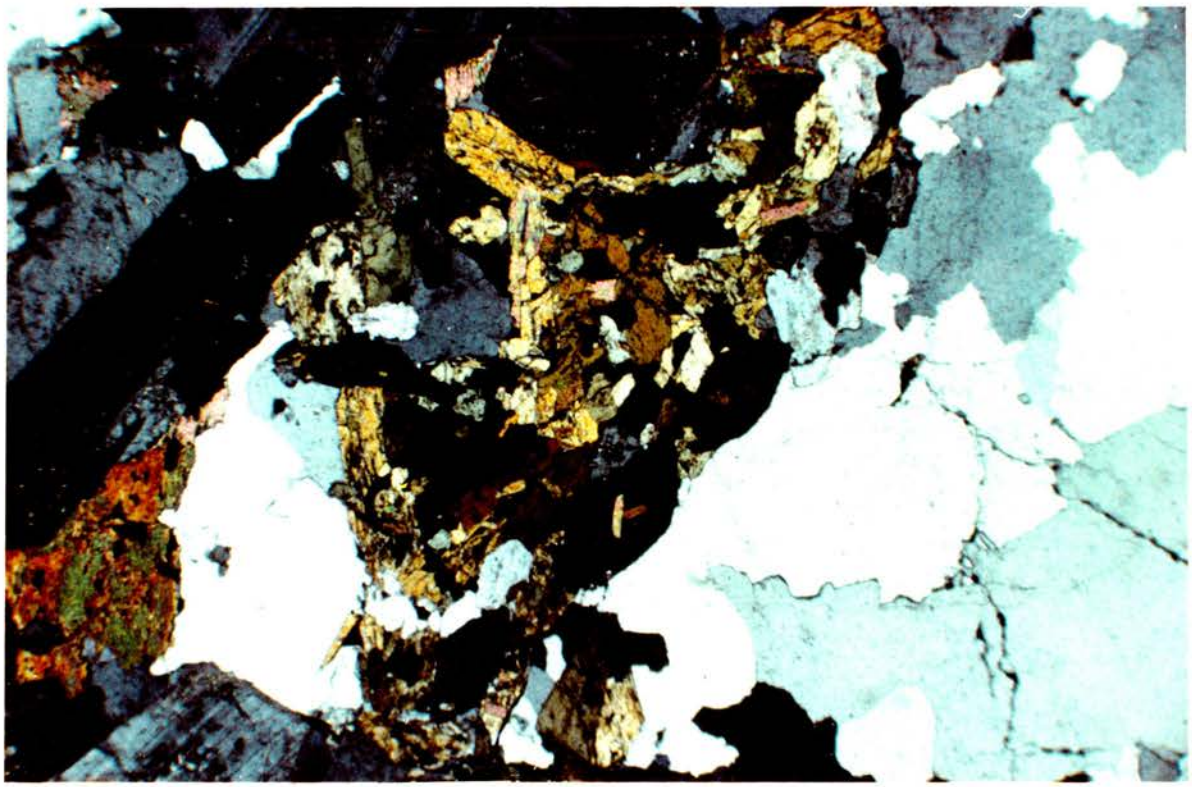

Plate 4.23 Granular texture of amphibole within mafic patch in granodiorite. RM50. XPL. x25.

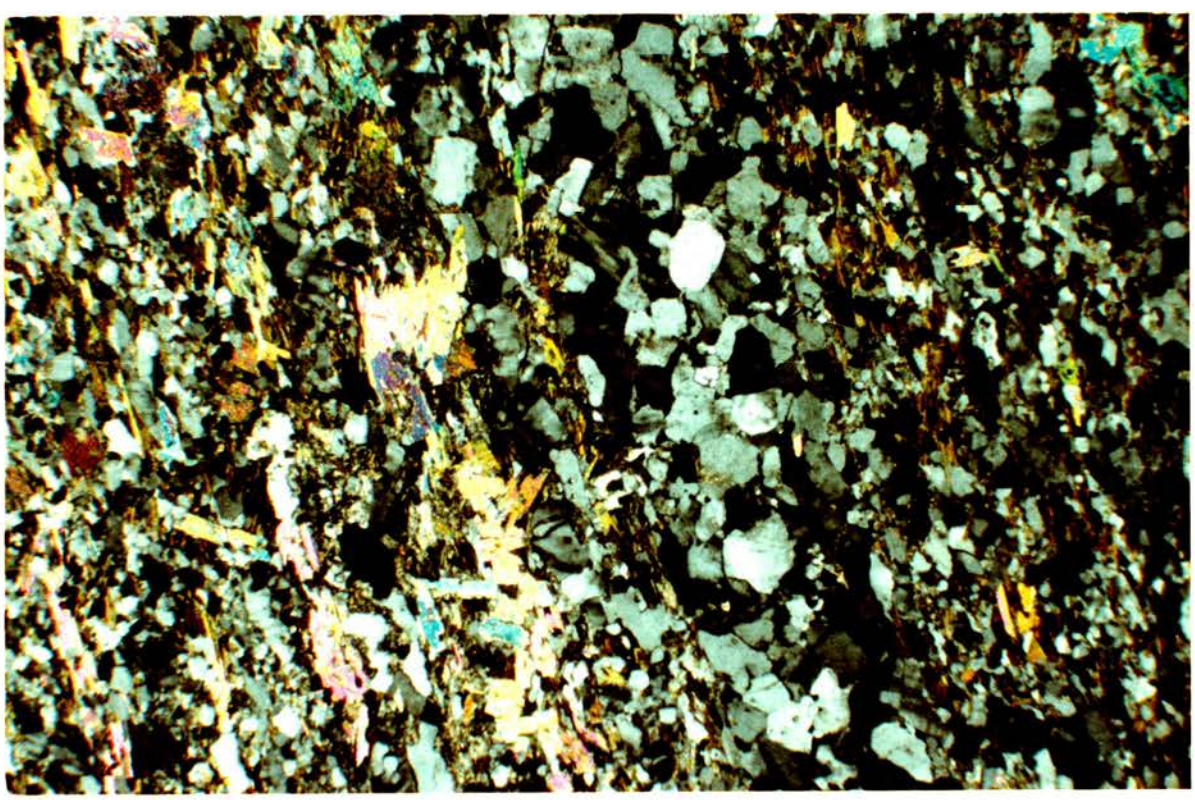

Plate 4.24 Texture of Lower Dalradian banded pelitic schist, showing alternate quartz and muscovite rich bands. RM74. XPL. x25

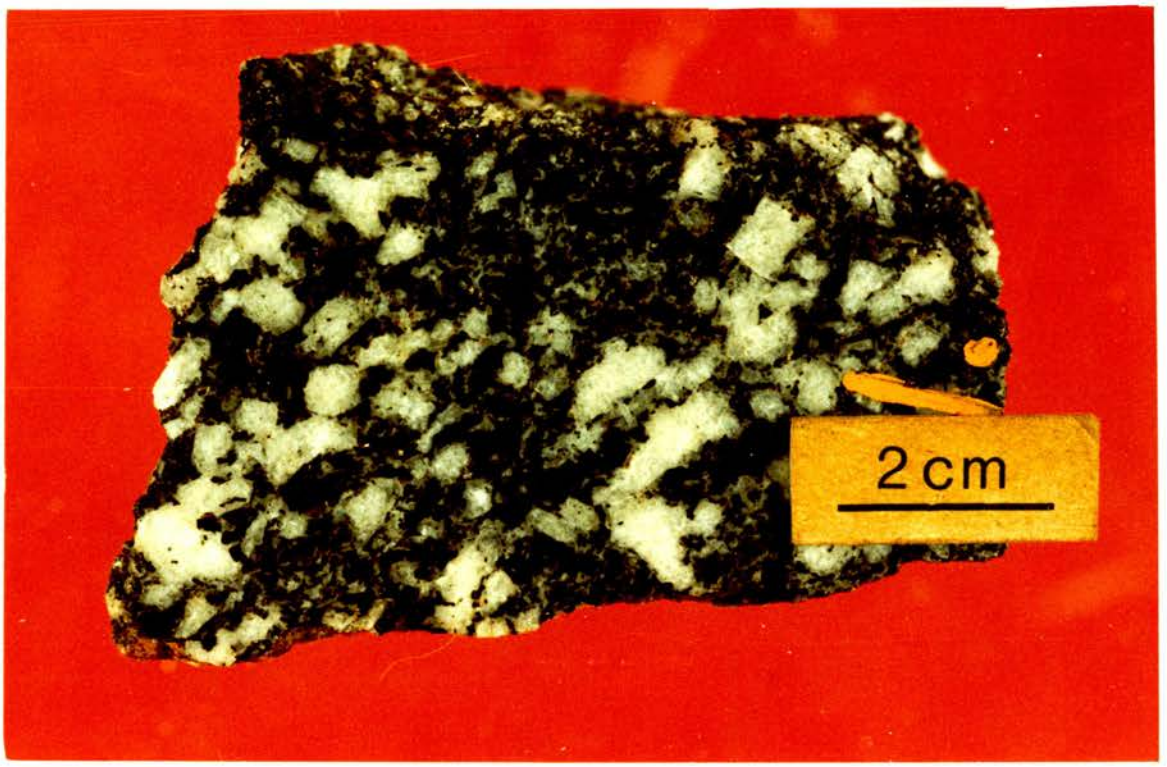

Plate 4.25 Hand specimen of monzodiorite, RM111.

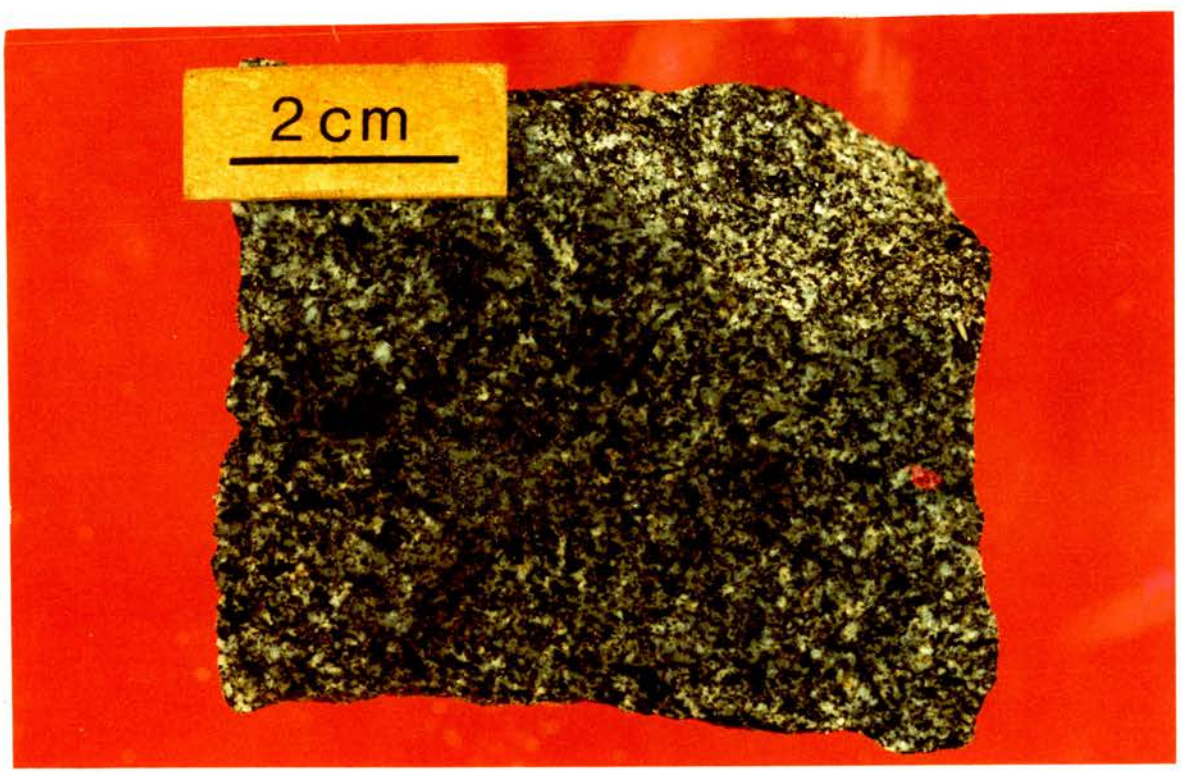

Plate 4.26 Hand specimen of melanocratic, fine-grained quartz-monzo diorite, RM89.

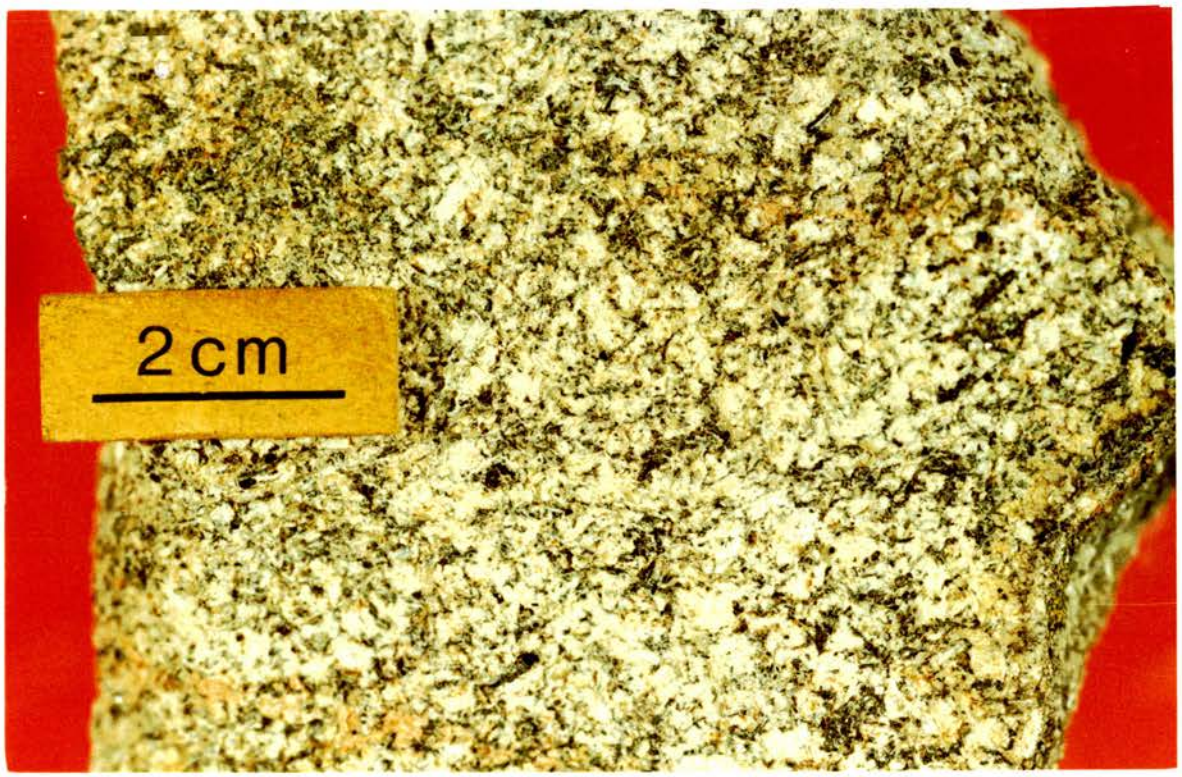

Plate 4.27 Hand specimen of leucocratic, fine-medium grained quartz monzodiorite, RM35.

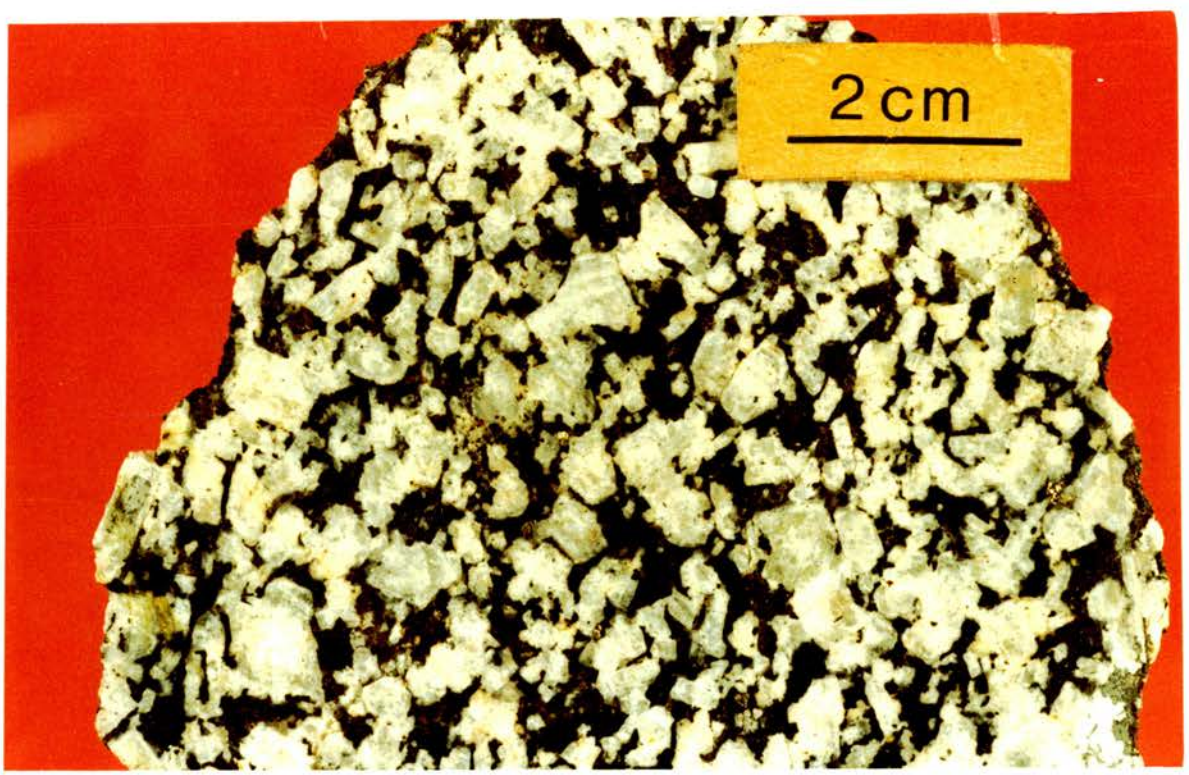

Plate 4.28 Hand specimen of melanocratic, medium-coarse grained quartz-monzodiorite, RM11.

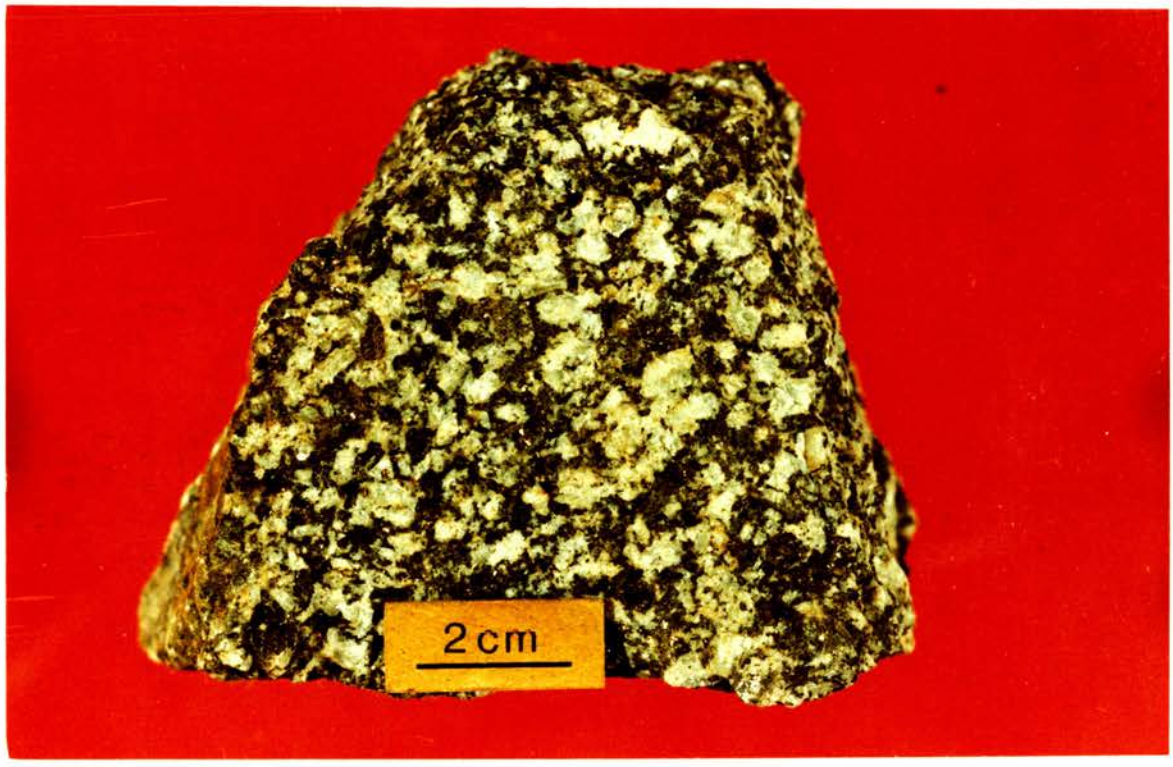

Plate 4.29 Hand specimen of mesocratic, medium-coarse grained quartz monzonite, RM66

Plate 4.30 Hand specimen of leucocratic medium-coarse grained granodiorite, RM51.

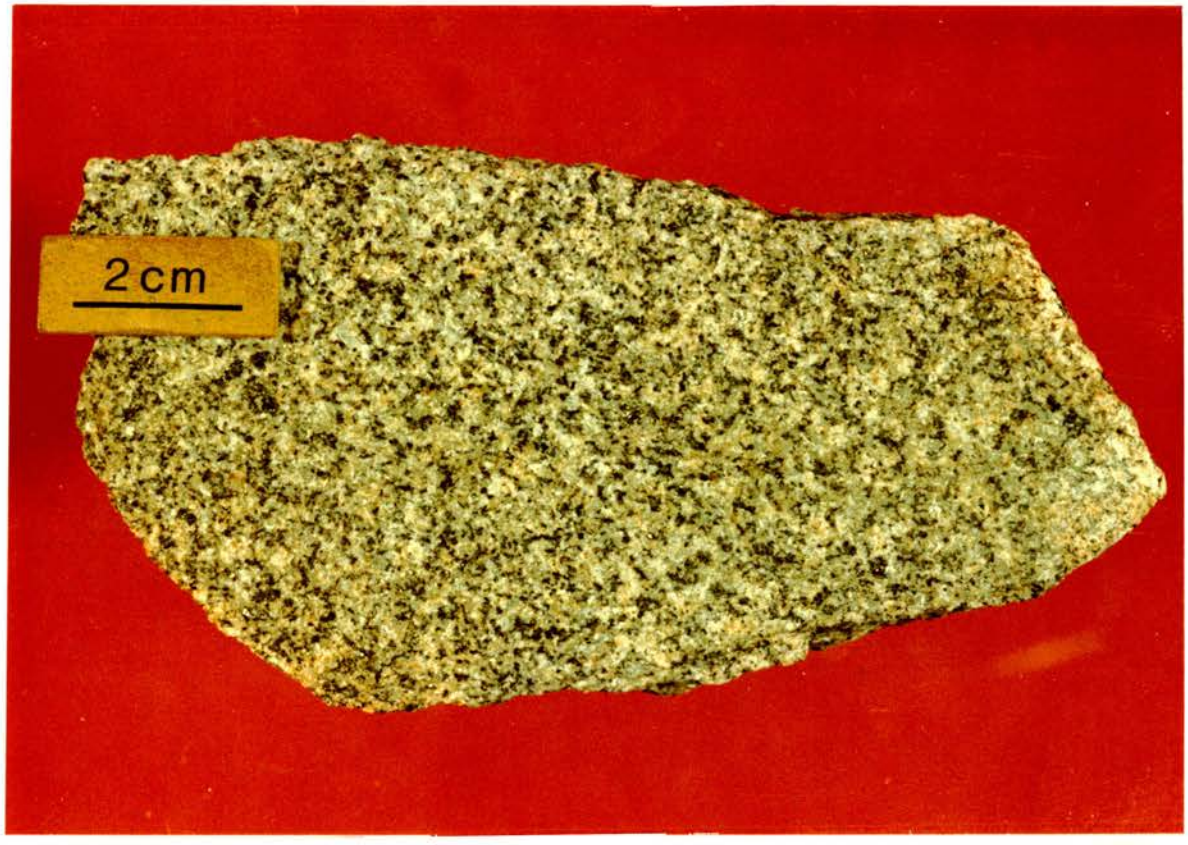

Plate 4.31 Hand specimen of mesocratic, fine grained monzogranite, RM112.

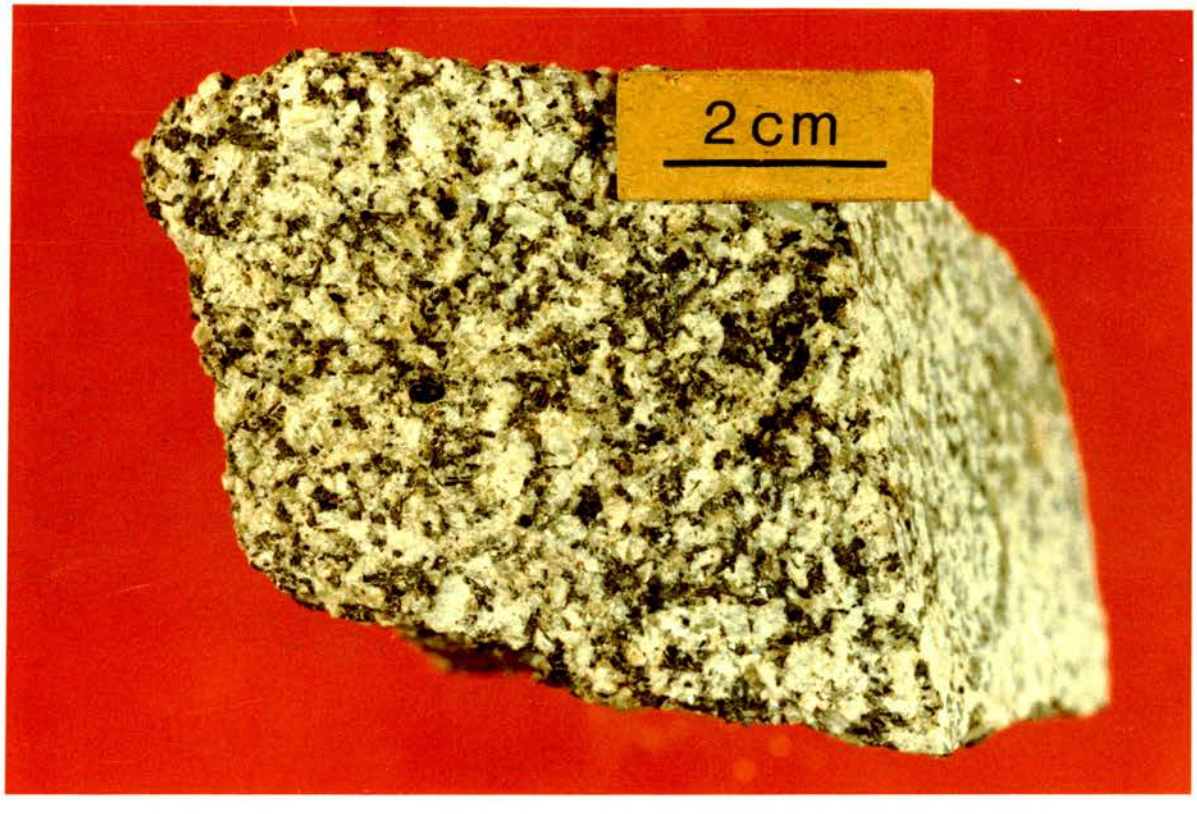

Plate 4.32 Hand specimen of mesocratic, medium-coarse grained monzogranite, RM120.

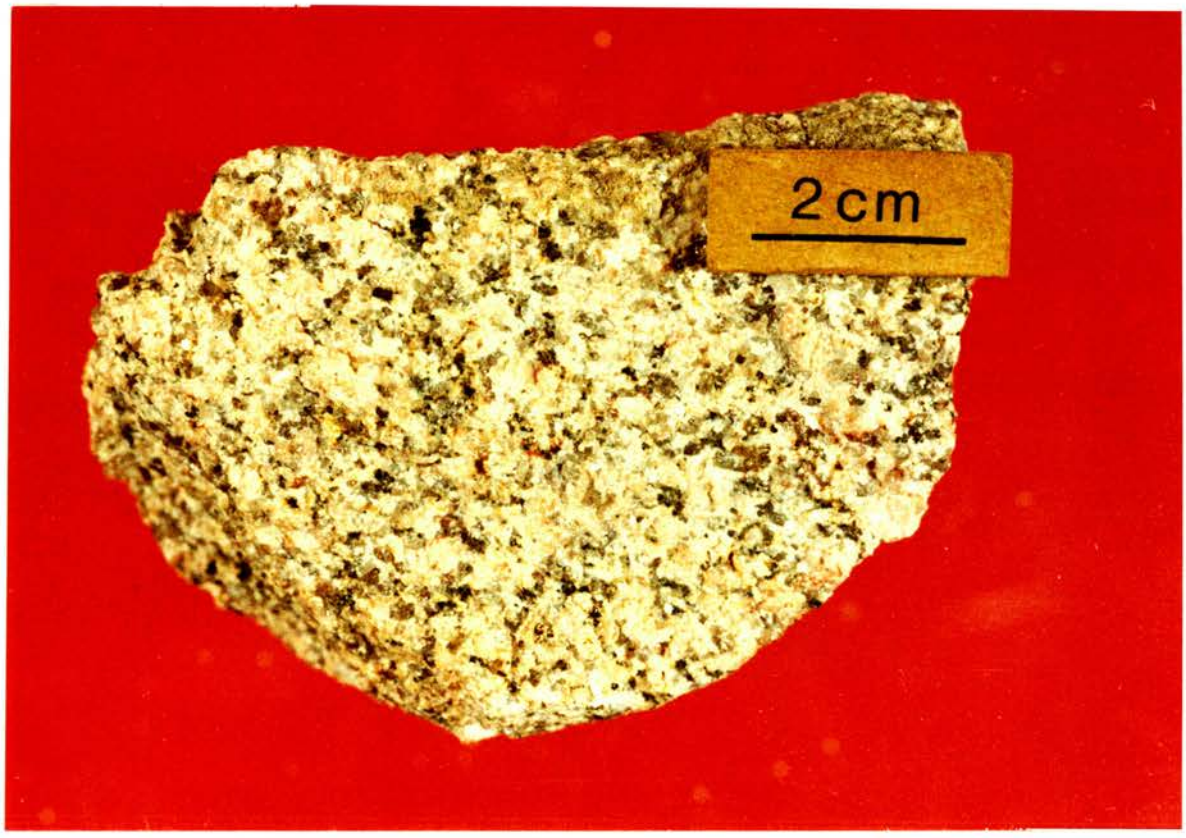

Plate 4.33 Hand specimen of leucocratic, medium grained monzogranite, RM86.

Plate 4.34 Hand specimen of leucocratic, fine-medium grained syeno-granite, RM38.

Geochemistry of the Moor of Rannoch pluton

5.0 Introduction

Sampling was initially based on a kilometer grid but modified as a result of exposure (Fig 5.0). Where exposure was sufficient to permit more extensive sampling, only representative examples of types found have been analysed. Inferences concerning chemical and mineralogical variation are made with reference to thin sections and hand specimens of analysed and non-analysed rocks.

Whole rock geochemical analysis was performed by X-ray fluorescence (XRF) spectrometry on fused discs for major oxides (except MnO) and on pressed powder pellets for trace elements and MnO. A description of methods, data processing and analytical error can be found in Appendix 1. A data table for major and trace elements, together with selected element ratios is presented for all samples analysed (Table 5.1).

5.1 Major element variation diagrams

A five-modal distribution for all major elements is obtained with the Harker diagrams as a result of a strong bias for silica to form distinct groups within the overall spread of analytical values. Error in the SiO2 analysis coupled with increased sample coverage may result in the gap between two of the intermediate range groups disappearing,

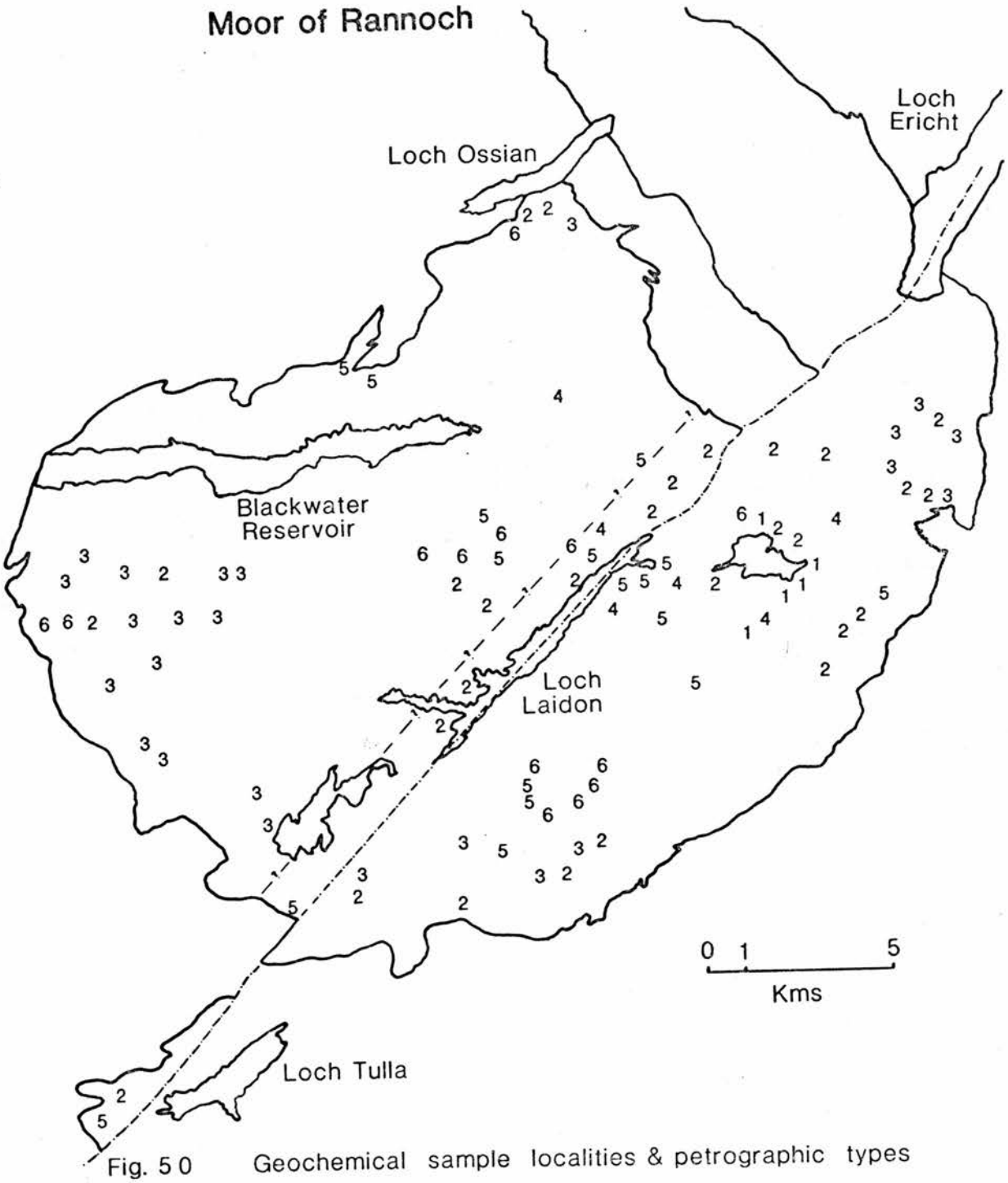

Fig. 5 0 Geochemical sample localities & petrographic types

but field evidence is strong for their separation as 2 distict types of intermediate monzodiorites and quartz monzodiorites. These groups have been allocated numbers I through V (Roman numerals) with increasing acidity.

5.2.0 Harker plots.

5.2.1 TiO2 - SiO2.(fig. 5.2.1)

TiO2 shows negative covariation with SiO2 and 5 major fields can be clearly separated. Together with a similar covariation of MgO v SiO2, this behaviour is consistent with micas or amphiboles being the dominant ferromagnesian minerals (Clemens and Wall, 1981). Sphene and /or titanomagnetite removal would also produce this type of plot for TiO2. The one sample (RM99) which is intermediate between the syenogranites and monzogranites has significantly higher TiO2 and lower SiO2 values despite geographical proximity to acidic members of the suite (eg RM36). Marginal samples (nos RM 22, RM30 & RM119) exhibit silica enrichment and possess slightly higher TiO2 values thus distinguishing them from the central syenogranitic members.

Two main fields are identified in the intermediate silica range 59-68 wt% SiO2. These fields have an east - west geographical bias in distribution with the more basic monzodiorites and quartz-monzodiorites, groups I,II & III, mainly to the east of the Laidon-Ericht fault. The more evolved monzogranites and granodiorites (group IV) are more common to the west with one granodiorite subgroup

found at the eastern margin by the Ericht river. The monzodioritic types form a distinct group and are predominantly found by Loch Eighach (excepting samples RM89 and RM102). Two samples, RM111 and RM117, within the group have anomalously high Ti values due to significant modal proportions of sphene and ferromagnesian minerals.

5.2.2 Al2O3 - SiO2.(fig. 5.2.2)

Al2O3 shows a negative correlation with SiO2 and follows a continuous trend from group II members through to group V. All group I members, (RM68, RM90 & RM109) are depleted in aluminium, (consistent with a deficiency in calcic amphibole, Table 4.1, except RM109) indicative of a significantly different mineralogy. Sample RM 117 from group II is also strongly Al depleted which coupled with Ti enrichment indicates that Ti-biotites were a major crystallising phase (Table 4.1).

5.2.3 MgO - SiO2.(fig. 5.2.3)

As expected, MgO has a negative covariation with SiO2 and shows good coherence with TiO2. Samples RM109 & RM111 are significantly Mg enriched and as diopside does not occur in Moor of Rannoch samples, Mg-rich amphibole may account for this feature. Amphiboles in groups I through IV show increasing Mg from core to rim (Table 6.1.1).Samples RM18 & RM22 show enrichment of Mg while RM119 is slightly depleted in Mg, placing both outwith the main cluster of group V. This indicates that they are not true granitic types but, depleted in ferromagnesians, are probably modified group IV 'granodiorites'.

5.2.4 FeO - SiO2.(fig. 5.2.4)

FeO shows negative covariation with scatter about the trend line more evident in groups II and III. Good separation of the acidic end members is seen with anomalous samples RM18, RM22 & RM119 showing slight to strong enrichment.

5.2.5 Fe2O3 - SiO2.(fig. 5.2.5)

This variation diagram shows scatter about a negative trend with silica. Samples from group IV within the northern and northern marginal areas to the west of the Laidon-Ericht fault exhibit consistently low values possibly as a result of local fO2 variations on emplacement.

5.2.6 CaO - SiO2.(fig. 5.2.6)

CaO, as with Al2O3, shows a negative covariation with SiO2 and with few exceptions they mimic the other (RM109, RM111 & RM117 have depleted Al2O3 and enriched CaO values). The linearity of the trend of CaO vs SiO2 through the groups suggests that calcic plagioclase and/or calcic pyroxene removal was a process operating throughout the evolution of the magma. Samples RM18, RM22 & RM119 have elevated Ca values consistent with silica enhancement of intermediate types, probably by assimilation of Moine quartzites. The Ca content would appear to be a primary magmatic feature as the surrounding quartzite country rocks with minor semi-pelites could not supply Ca.

5.2.7 Na2O - SiO2.(fig. 5.2.7)

A slight negative covariation with SiO2 is noted for the whole pluton excluding group I monzodiorite samples. Their significantly different modal mineralogy (Table 4.1) shows lower plagioclase content (RM109) or alkali feldspar content (RM68 & RM90). Within group V samples, a division of the granites as a function of geography (east or west of the Laidon-Ericht fault) can be made, with those samples from the western part being significantly Na depleted and K enriched. As a result of the spread of the data within each group, subdivisions can be identified (allowing for analytical error) which support observations in the trace element geochemistry. Those samples from the Western Black Corries (west of the Laidon-Ericht fault) are slightly Na (and K) depleted when compared to other group IV samples also from the west of the fault.

The above is consistent with continuous removal of sodic plagioclase from the magma as a function of time. Samples RM22 & RM119 appear affected by fluid phase chemical movements evidenced by extensive sericitisation of the feldspars and secondary muscovite development. These do show Na depletion (as well as K depletion) and this may indicate loss of alkalis. Silica-rich fluids percolating through an originally intermediate (group IV?) rock could also explain the observed variation.

5.2.8 K2O - SiO2.(fig. 5.2.8)

A positive trend of K20 with respect to silica is identified with either a straight line or slightly upward curving trend being applicable. The fields of Peccerillo and Taylor (1976) have been added to show the high K nature of the Moor of Rannoch data. Subdivision of group IV and V samples is possible and these mirror the subdivisions seen in the plot of Na20 vs Si02. The granites west of the Laidon-Ericht fault are K enriched and possibly form a subtrend when compared to those east of the fault. Geographical subdivision of the samples within group IV is also possible. Of the three group I samples, only RM68 displays marked K enrichment as well as enhanced Na values with respect to RM109. The samples from the northern margin, RM18, RM22 & RM119 all show depleted values for K20 compared to those values for the granitic types indicating a removal of potassic feldspar or extreme silica enrichment at the expense of biotite. The modal mineralogy of the samples tends to confirm the latter.

5.2.9 P205 - Si02.(fig. 5.2.9)

This diagram shows a negative covariation with silica. All marginal samples are P205 depleted while RM68 and RM111 have enhanced values which are confirmed by their higher modal content of apatite.

5.3.0 Major oxide variation diagrams.

5.3.1 Na20 - K20.(fig. 5.3.1)

The plot of wt% Na2O vs K2O shows the data lying between Na2O/K2O = 1 and Na2O/K2O = 2 with the granitic members clustering about the unity value at 4-4.5%. With the exception of sample RM107, the values are all within the field of Lachlan I-types but outwith the area given for Lachlan S - type granitoids.

5.3.2 CaO - MgO.(fig. 5.3.2)

A positive covariation is noted for this oxide pair with the overall trend suggesting a clinopyroxene or amphibole control over fractionation. Anomalous samples RM109 & RM117 show slight plagioclase deficiency while RM28 is markedly Ca depleted (also Sr and Rb depleted, see 5.6.2, 5.6.3).

5.3.3 CaO - Al2O3.(fig. 5.3.3)

Data are spread about a positive covariation on this plot. Varying amounts of biotite and amphibole or minor sphene removal, modifying a trend dominated by plagioclase removal, may account for the observed variation.

5.3.4 Na2O+K2O - SiO2.(fig. 5.3.4)

Plotting Na2O+K2O with respect to silica gives a trend which is appoximately constant or slightly positive. Within the major groups strongly positive subtrends can be identified, eg. RM36, RM37 & RM38 and RM91, RM92, RM93, RM94 & RM96. Sample RM109, which has a possible

appinitic affinity, lies off trend to the depleted side for Na2O+K2O which confirms the distinctive modal mineralogy, enrichment in MgO and depletion in Al2O3, i.e. relatively biotite and amphibole enhanced, plagioclase/alkali feldspar depleted. The foregoing diagrams suggest that the Moor of Rannoch complex is a composite of more than one intrusive phase or pluton, all with high K calc-alkaline characteristics.

5.3.5 $Fe^{2+}/Fe^{2+} + Mg^{2+}$ - SiO2.(fig. 5.3.5)

The overall covariation with silica is approximately constant. Possible subparallel subtrends within the groups are markedly different from the trend within group V granite types. Samples within groups II and III exhibit the most restricted range of ratio values; the range of values increases through group IV to group V which has the largest scatter. Together with the change in trends across the groupIV/V boundary, this could be the result of changes in biotite Fe and Mg content as a function of change in magma source, temperature of biotite crystallisation, fO2 or vapour pressure conditions.

5.4.0 Triangular variation plots.

5.4.1 Na2O+K2O - FeO+Fe2O3 - MgO.(fig. 5.4.1)

The trend shown by Moor of Rannoch rocks is of 'calc-alkaline' type or 'high K calc-alkaline' type (after Peccerillo and Taylor, 1976). The relatively Mg enriched samples, RM109 & RM117, clearly lie off trend and the enhanced modal content of amphibole (predominantly Mg-rich) explains these characteristics. Samples RM103 and RM29 show Mg depletion/Fe enichment and Mg enrichment/Fe depletion respectively and probably reflect significant local variations in original biotite composition and subsequent alteration.

5.4.2 Na20 - K20 - CaO.(fig. 5.4.2)

This diagram gives good separation of the acid members of the suite and indicates that those samples to the west of the Laidon-Ericht fault, RM86 & RM107, lie off trend and are K enriched with respect to those east of the fault. Samples RM68 & RM109 also lie outwith the main group indicating Na defieciency when compared to other group I & II rocks and this may be accounted for by their having more calcic plagioclase by mode (Table 4.1). The overall trend is of a decrease in Ca accompanied by an increase in Na and K, with K increasing slightly more relative to Na.

5.5.0 CIPW Normative minerals.

5.5.1 Quartz - Orthoclase - Albite.(fig. 5.5.1)

Analyses of Moor of Rannoch rocks with the sum of normative Q+Ab+Or>=80% (Thornton and Tuttle, 1960; Tuttle and Bowen, 1958) have been plotted with boundary curves corresponding to 1, 3 and 5 kilobars water vapour pressure superimposed. However, sample RM94 is the only analysis from the mafic rocks to exceed the 80% level and the cluster of points noted on the diagram (fig. 5.5.1) represents samples from mafic rocks whose sum normative Q+Ab+Or exceeded 77%. These samples are significantly different from remaining mafic types (Q+Ab+Or<70%).

Nonetheless, the following observations can be made, with due regard to resolving problems using 'calculated' mineralogy on the basis of geochemical data.

1) With one exception (RM107), the samples considered 'magmatic' appear to have crystallised at pressures over 3 kbars. However, the presence of K in biotite tends to shift the calculated values toward the orthoclase apex and thus plot close to the 1-3 kbar minimum. The group of points 4,5,6&7, although spread along the trend line, are considered part of the same intrusive pulse.

2) Those rocks from west of the Laidon-Ericht fault (samples RM86 & RM107) show enhanced normative orthoclase. This is consistent with their elevated K20 whole rock values and highlights a fundamental difference between them and rocks of similar composition and mineralogy east of the fault.

3) A more basic starting composition that did not fractionate

completely, or a magma with large amounts of restite could explain the feature that the sum of Q+Ab+Or does not exceed 80. The persistence of biotite into the syenogranites (>72 wt% SiO2) may also confirm this.

4) Those samples considered extensively contaminated with country rock material (eg. RM22A - inclusions of semi-pelitic and quartzite material) or having undergone metasomatic interaction with the host metasediments (refer to 5.2.7 & 5.2.8) are anomalous and do not plot coherently with the felsic or mafic rocks.

5.5.2 SiO2 - Normative corundum/diopside.(fig. 5.5.2)

This presentation of normative minerals is used to help to distinguish I-type from S-type granitoids (as defined by Chappell and White, 1974). Those analyses with >1% Corundum in the norm, may reflect an origin from aluminous metasedimentary material, i.e. S-type. Analyses which display diopside normative or mildly (<1%) corundum normative trends are thought to represent I-type material. Fractionation may account for this slight corundum normative trend.

The trend of Moor of Rannoch data suggests I-type affinity for the majority of the samples analysed. This is confirmed by the presence of primary hornblende, biotite and sphene. Contamination by assimilation of crustal material on or before intrusion may explain the behaviour of samples RM28, RM112, RM18 & RM119. Those samples which occur close to the internal contact between two magmatic pulses and are corundum normative remain enigmatic. The recognition of a

Key to symbols on Moor of Rannoch and Strath Ossian geochemical diagrams.

△ Monzodiorite

□ Quartz-Monzodiorite

▽ Quartz Monzonite

\+ Granodiorite

◇ Monzogranite

× Syenogranite

○ Marginal granite

All oxides quoted as percent(%)
All elements quoted as ppm

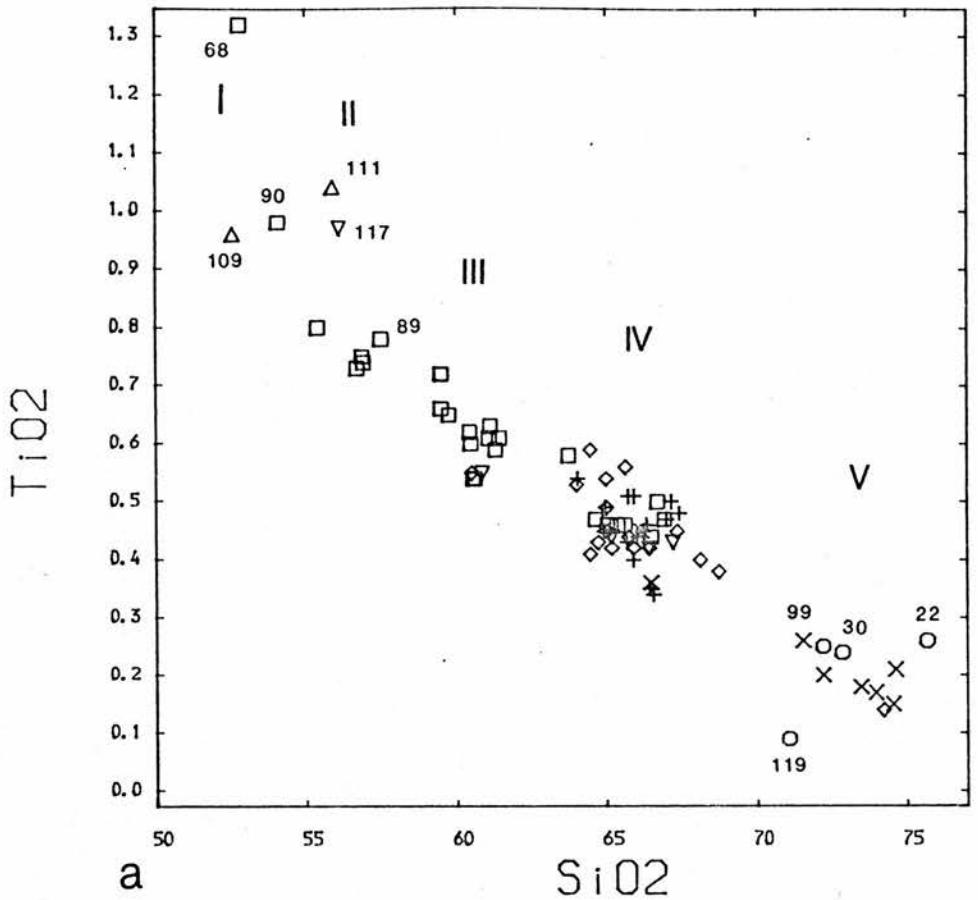

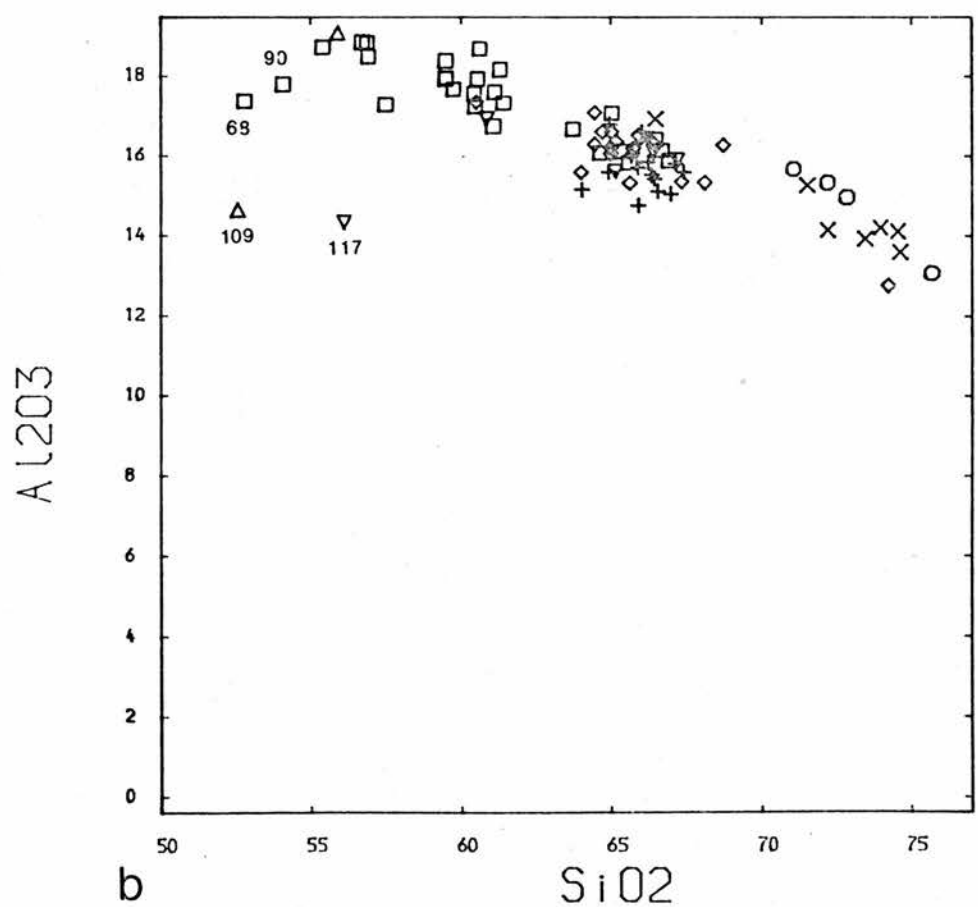

a) Figure 5.2.1, b) Figure 5.2.2

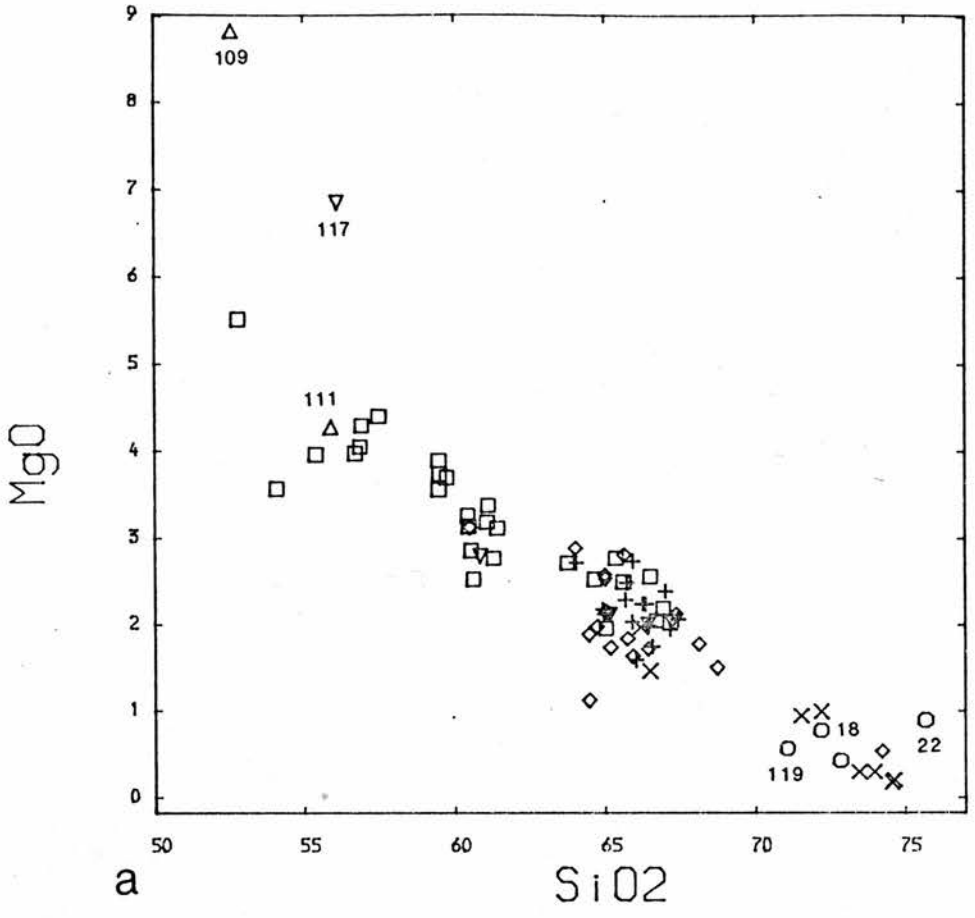

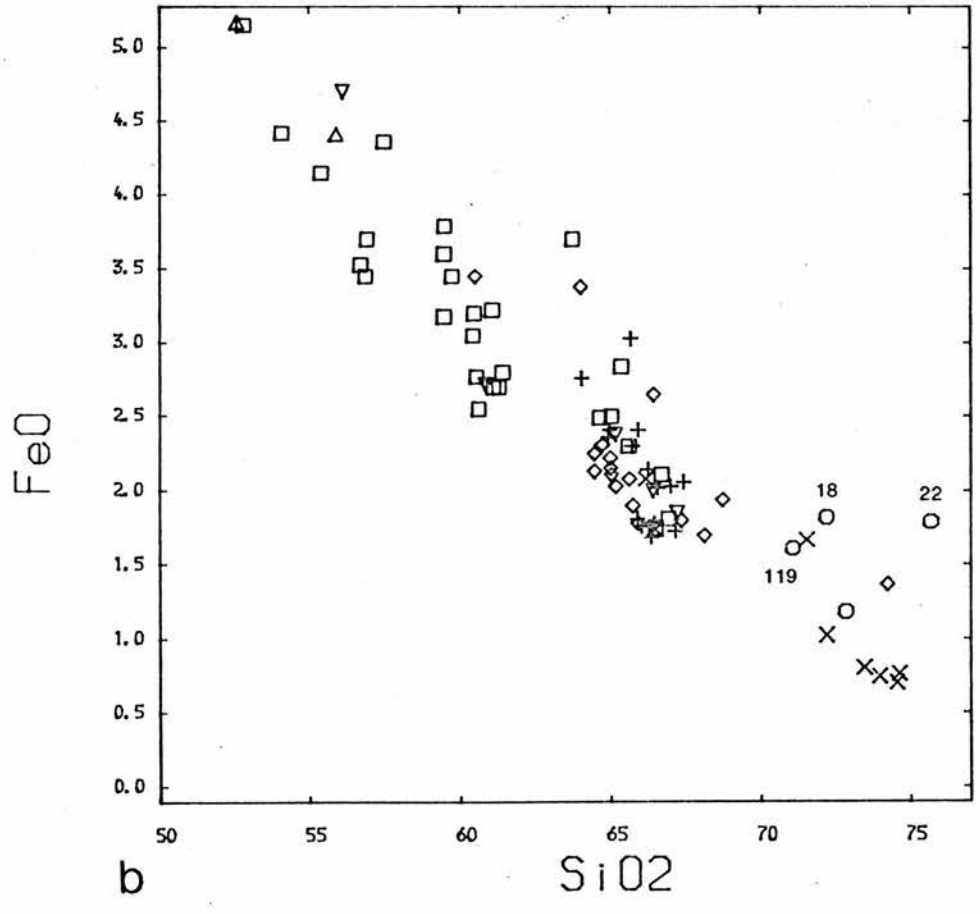

a) Figure 5.2.3, b) Figure 5.2.4

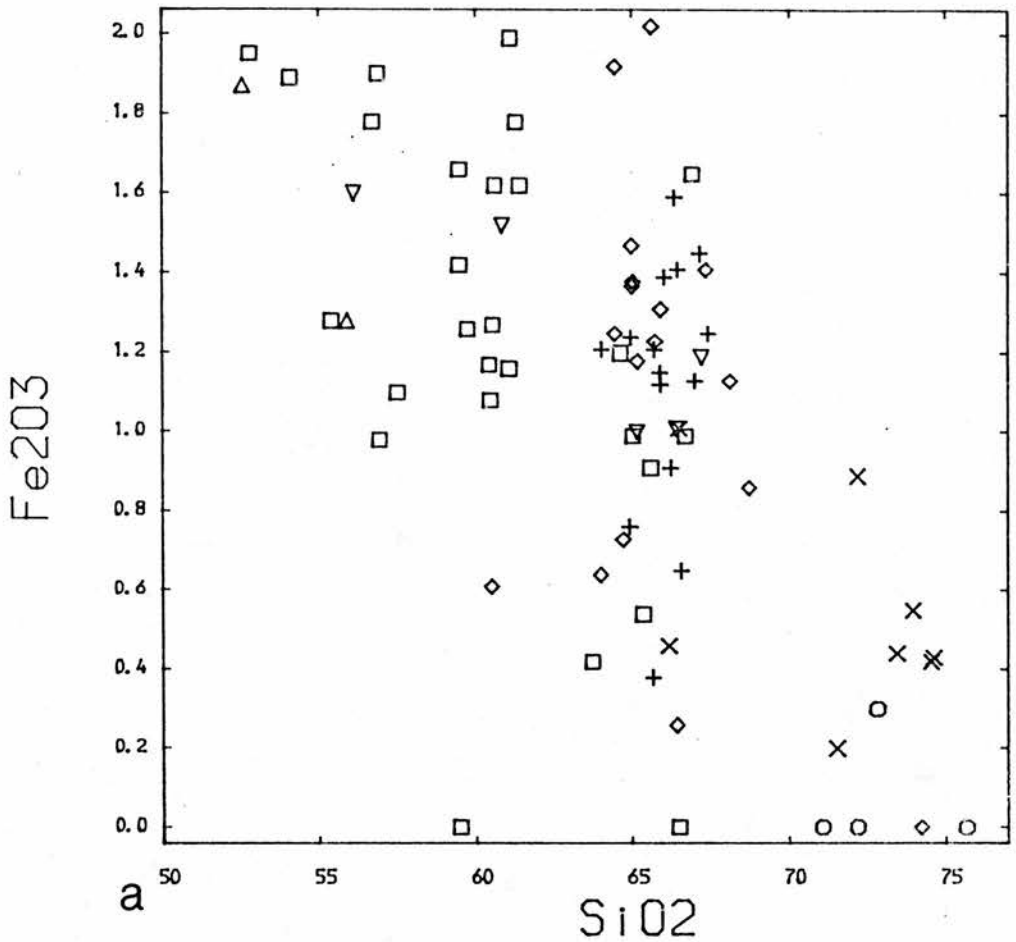

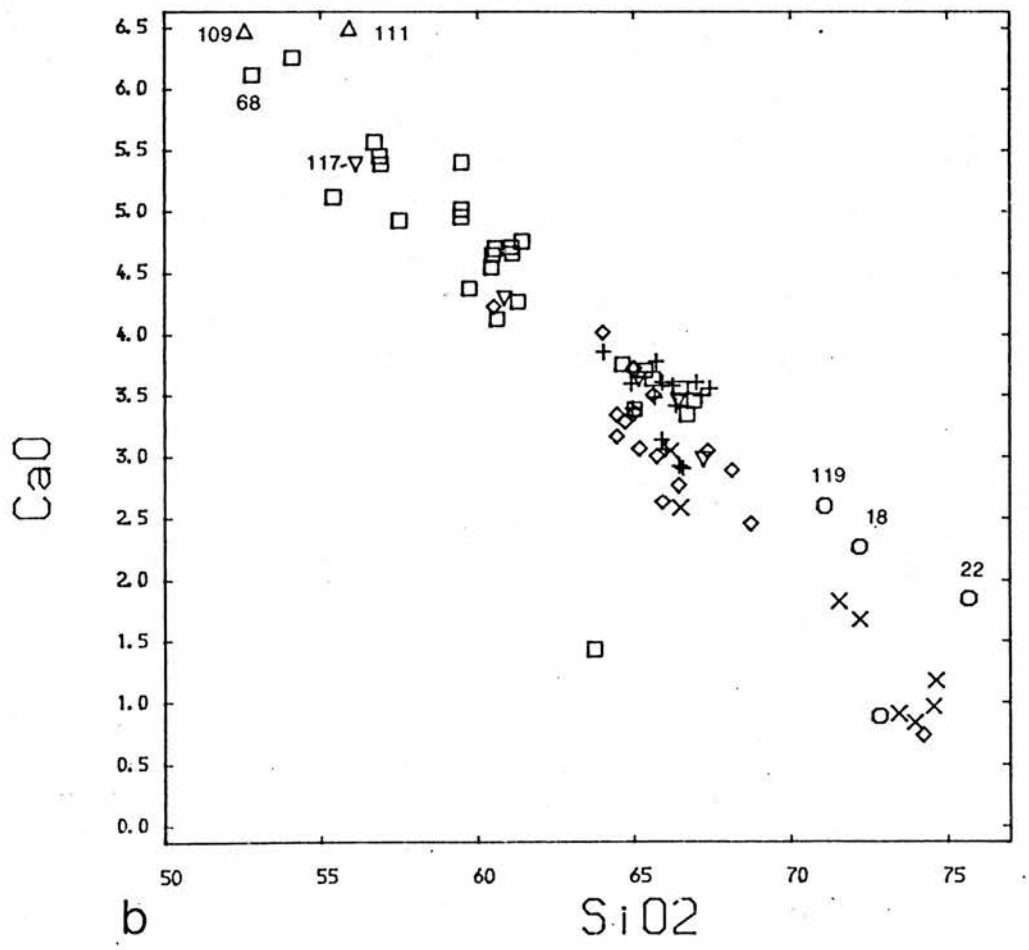

a) Figure 5.2.5, b) Figure 5.2.6

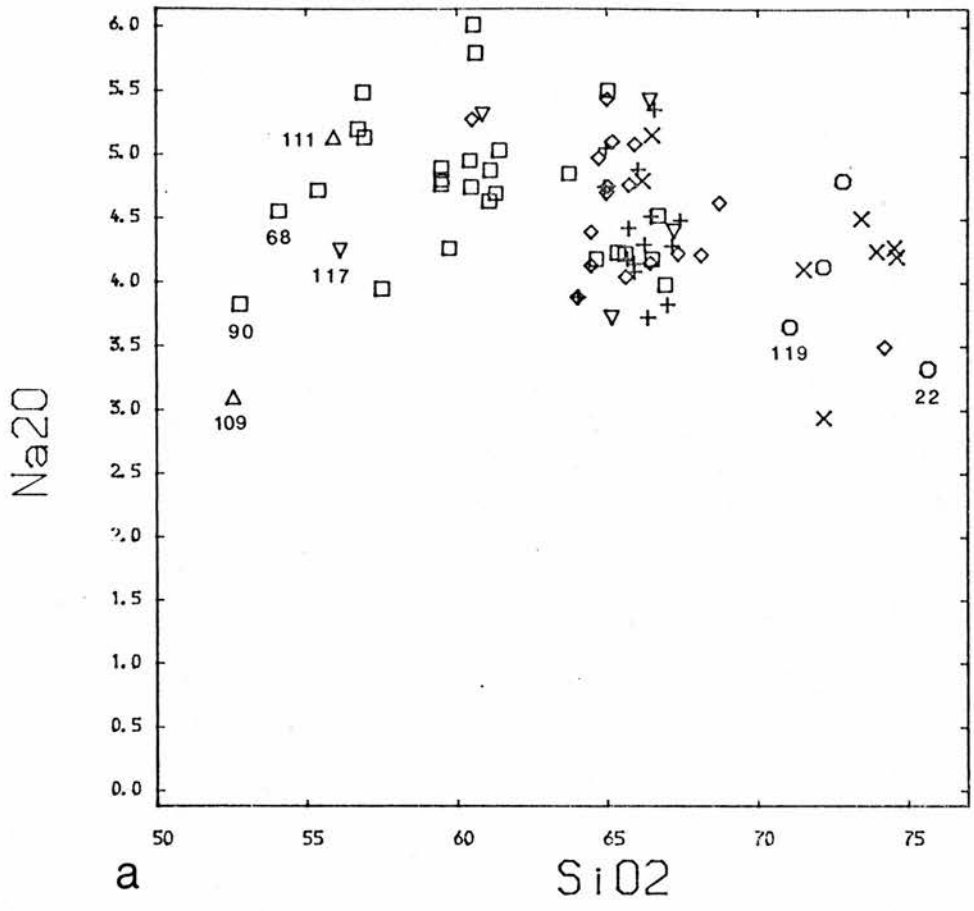

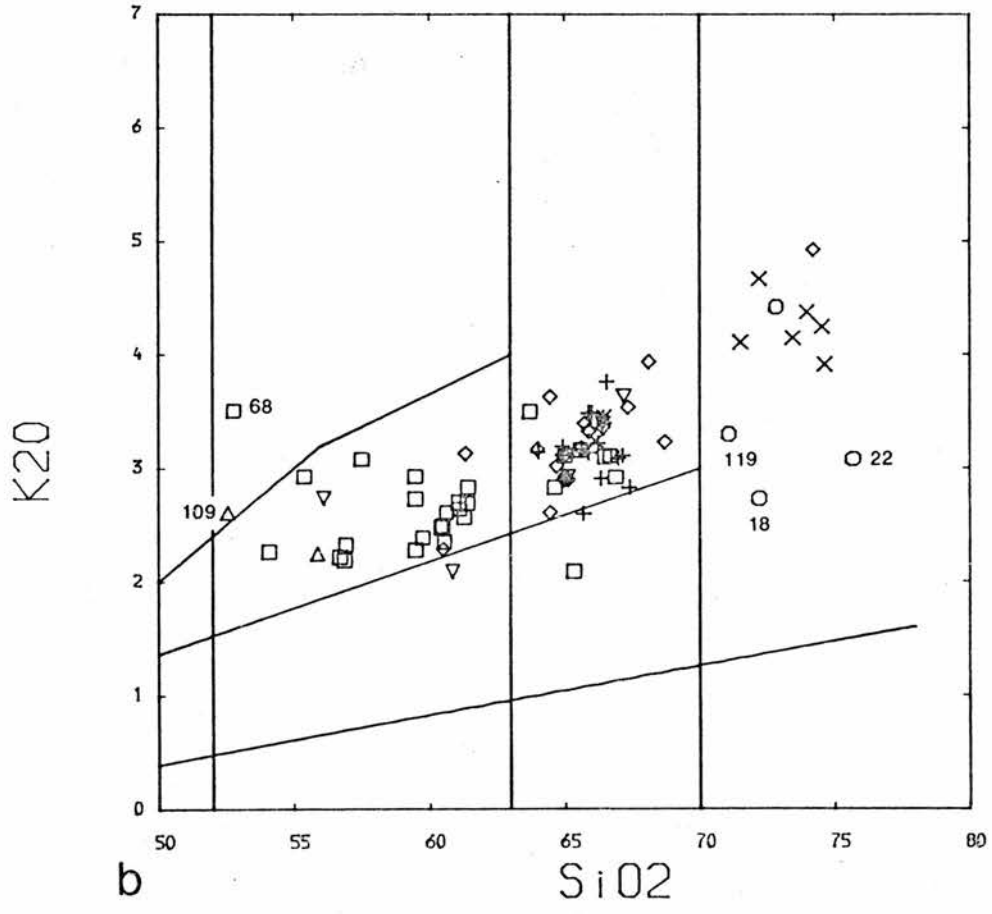

a) Figure 5.2.7, b) Figure 5.2.8

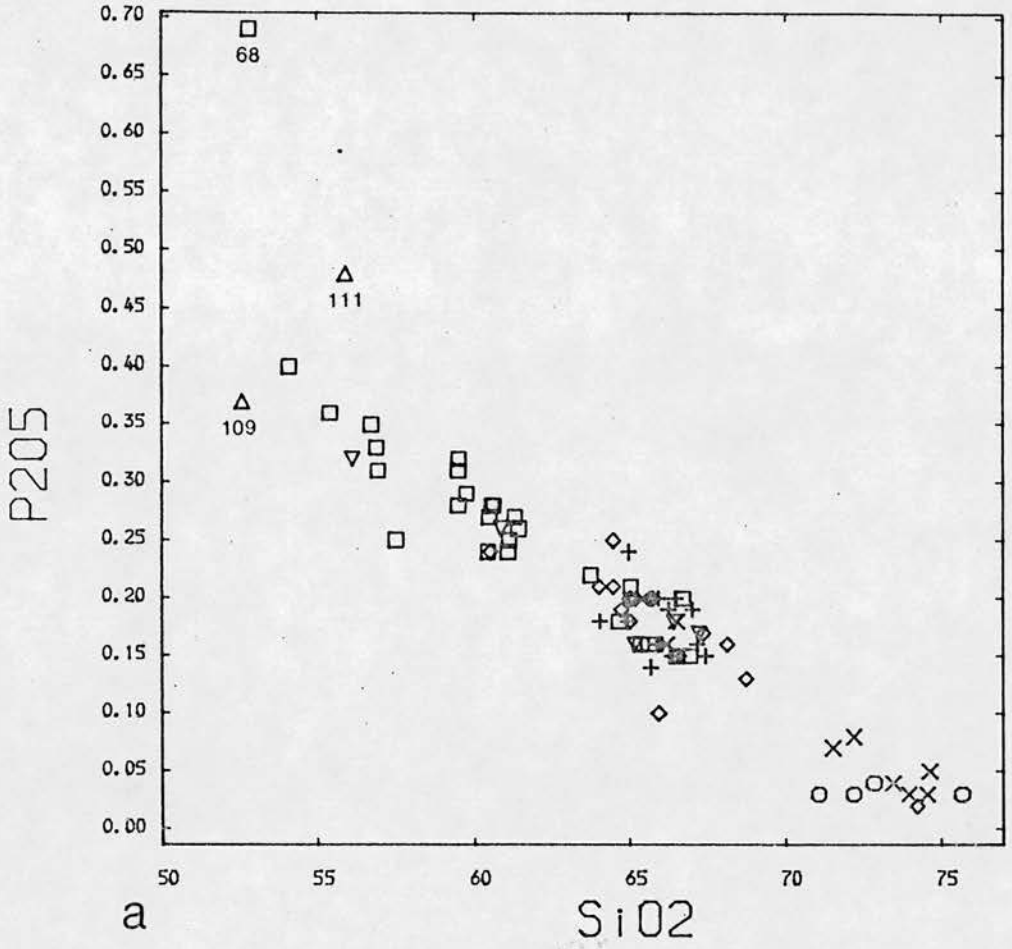

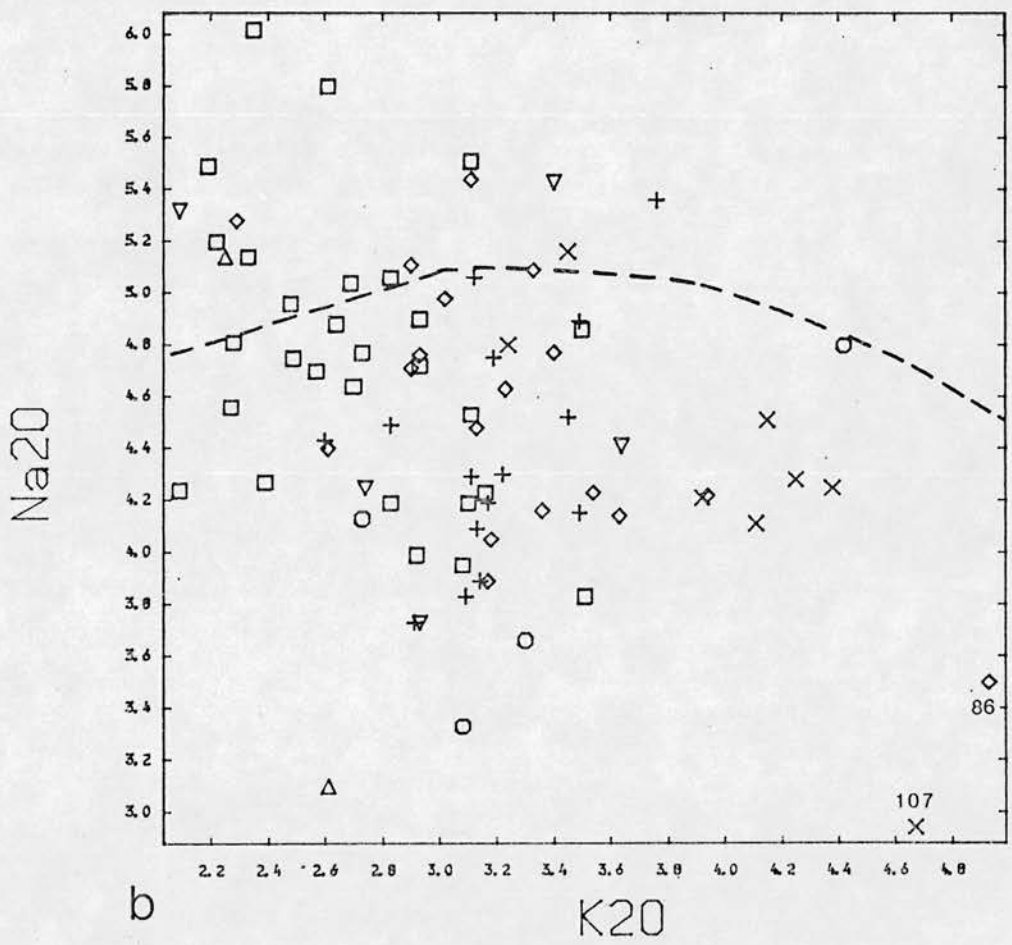

a) Figure 5.2.9, b) Figure 5.3.1, upper limit of field of Lachlan I-types shown by dashed line.

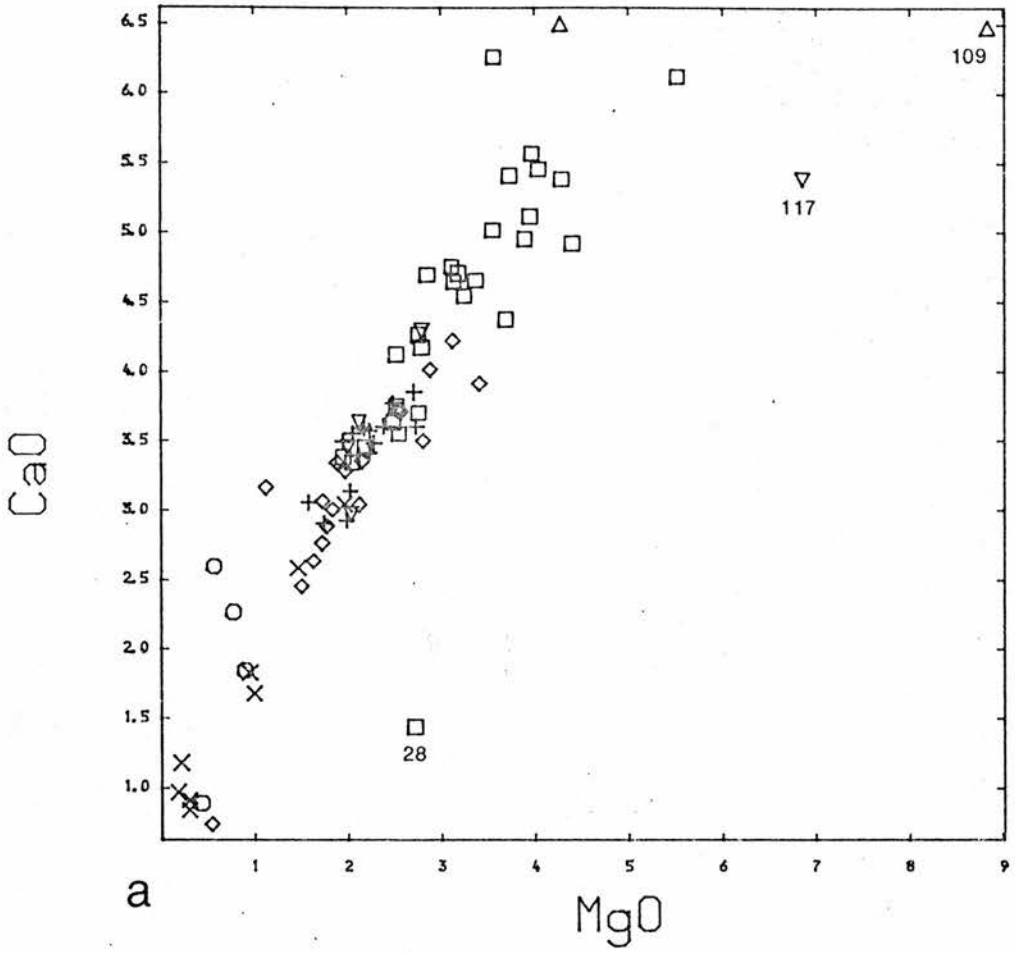

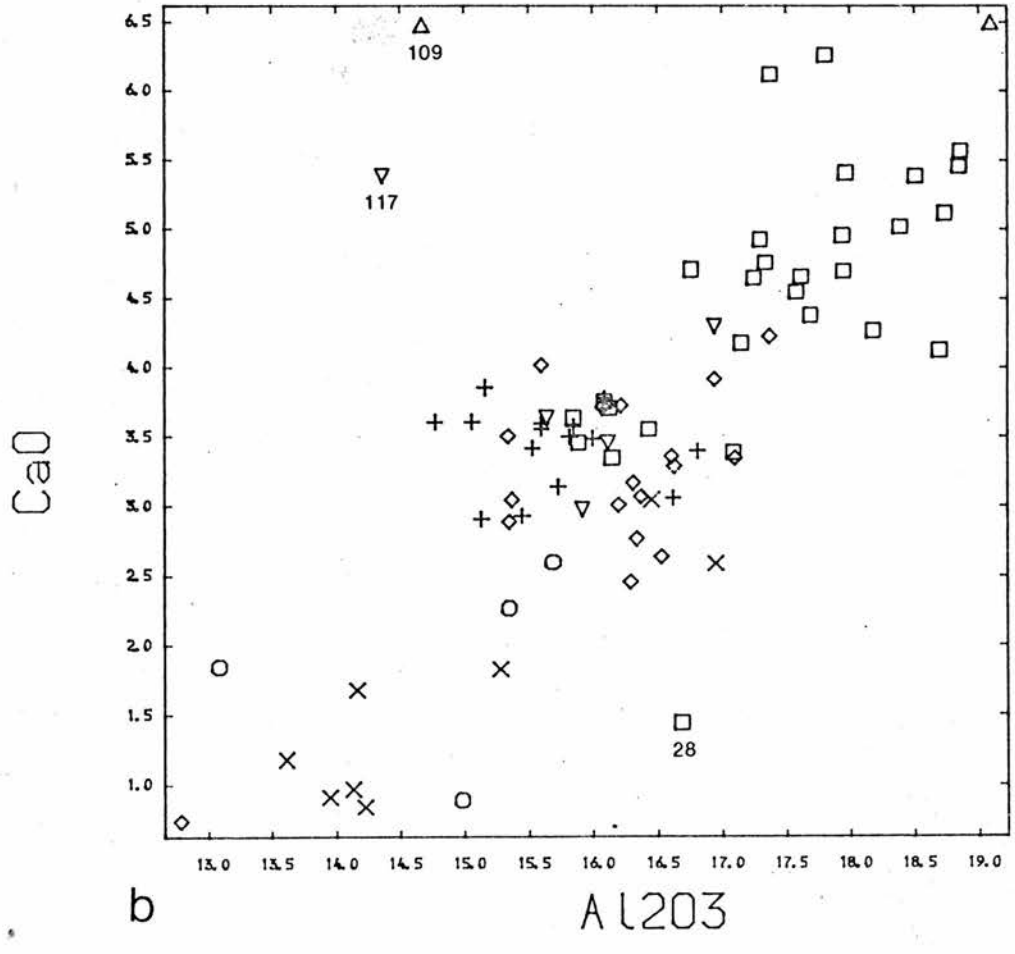

a) Figure 5.3.2, b) Figure 5.3.3

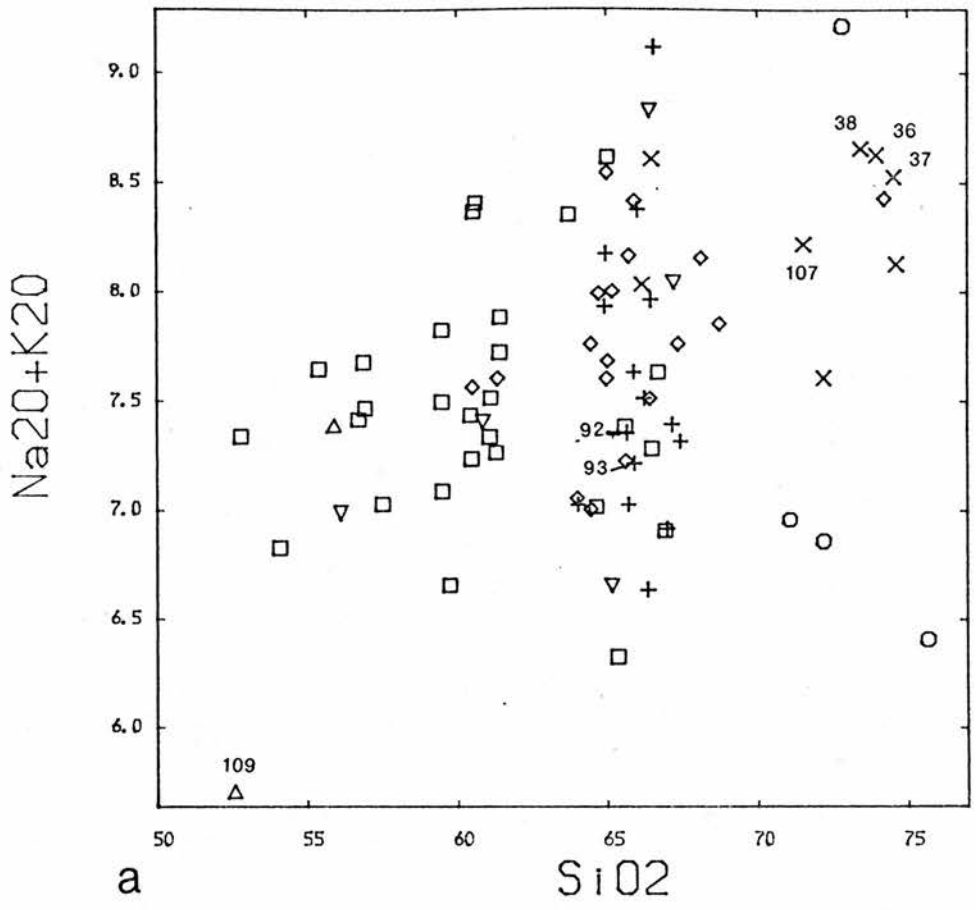

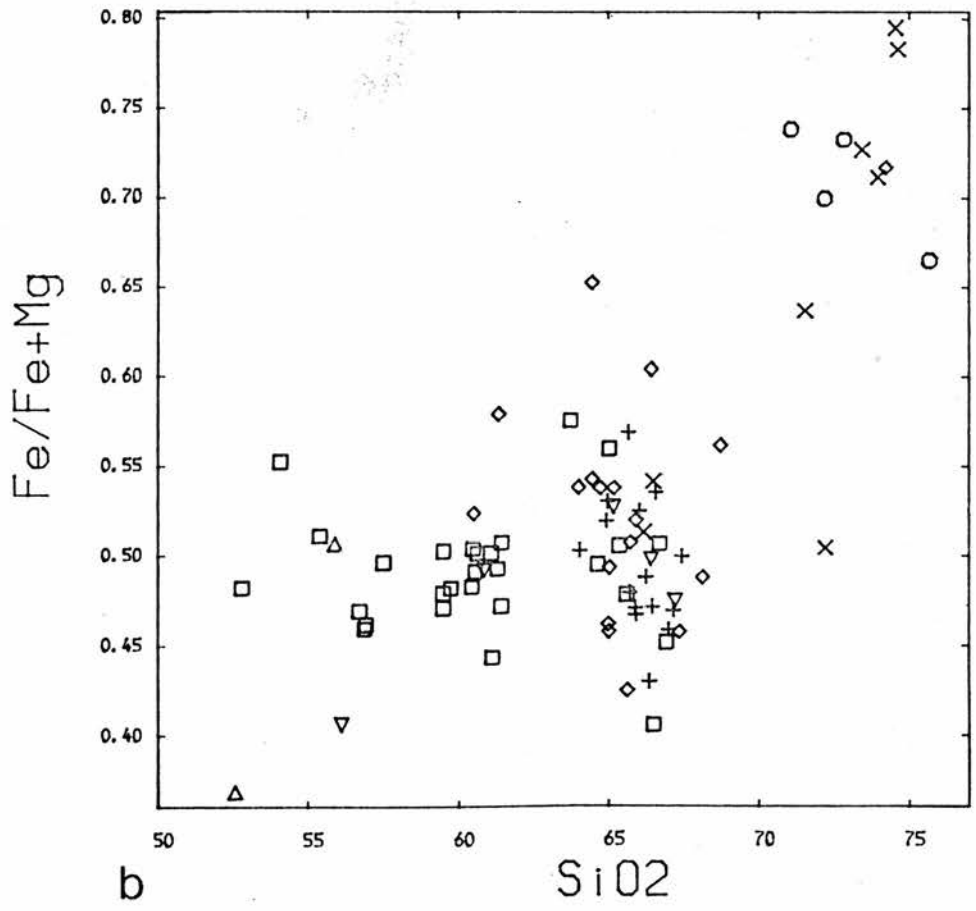

a) Figure 5.3.4, b) Figure 5.3.5

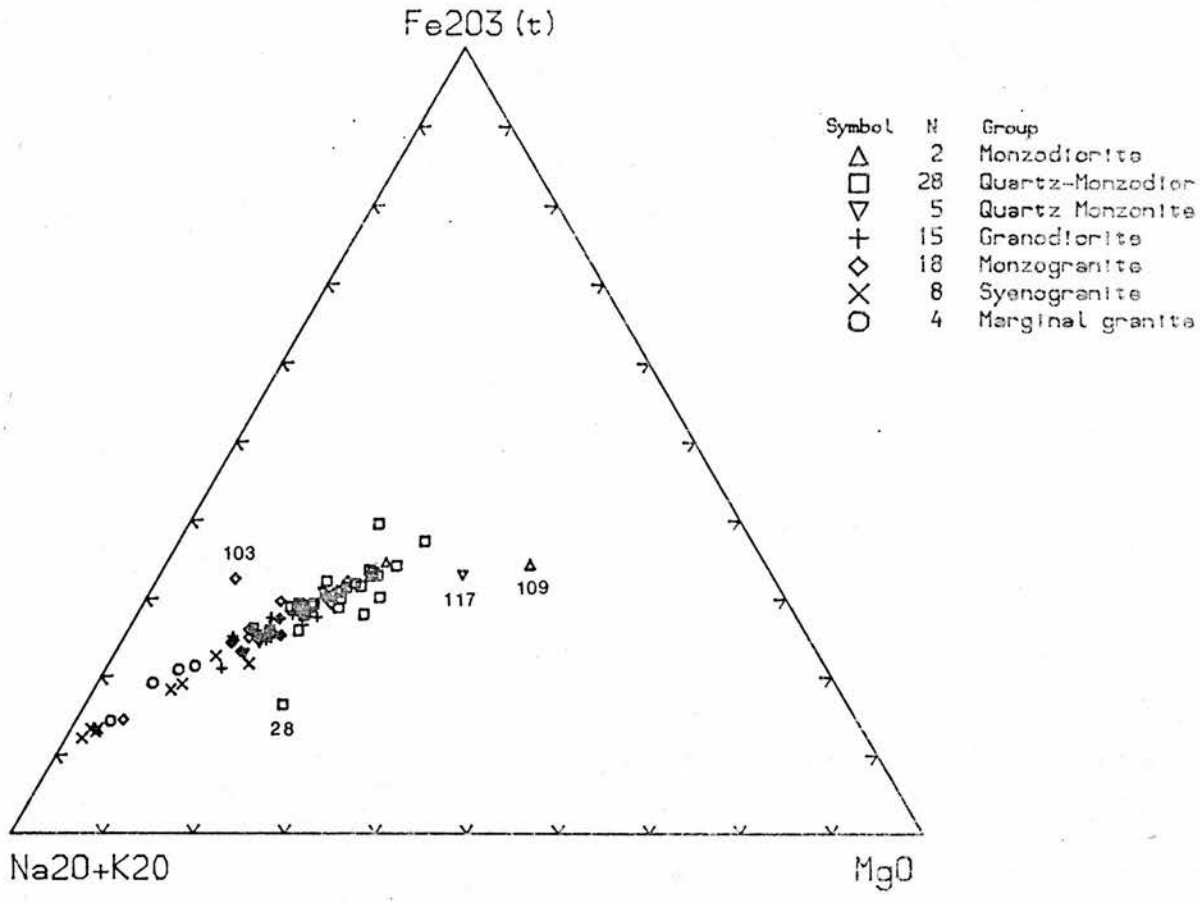

a

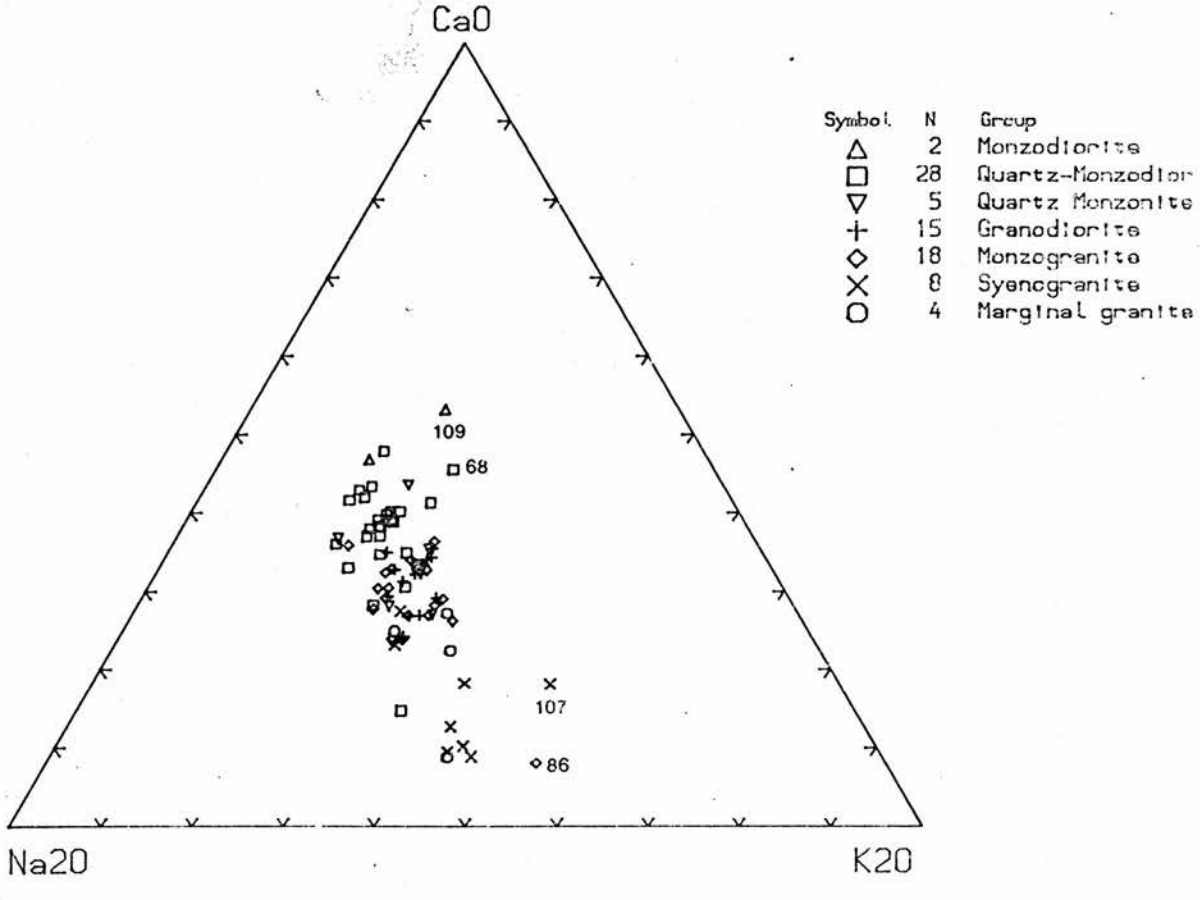

b

a) Figure 5.4.1, b) Figure 5.4.2

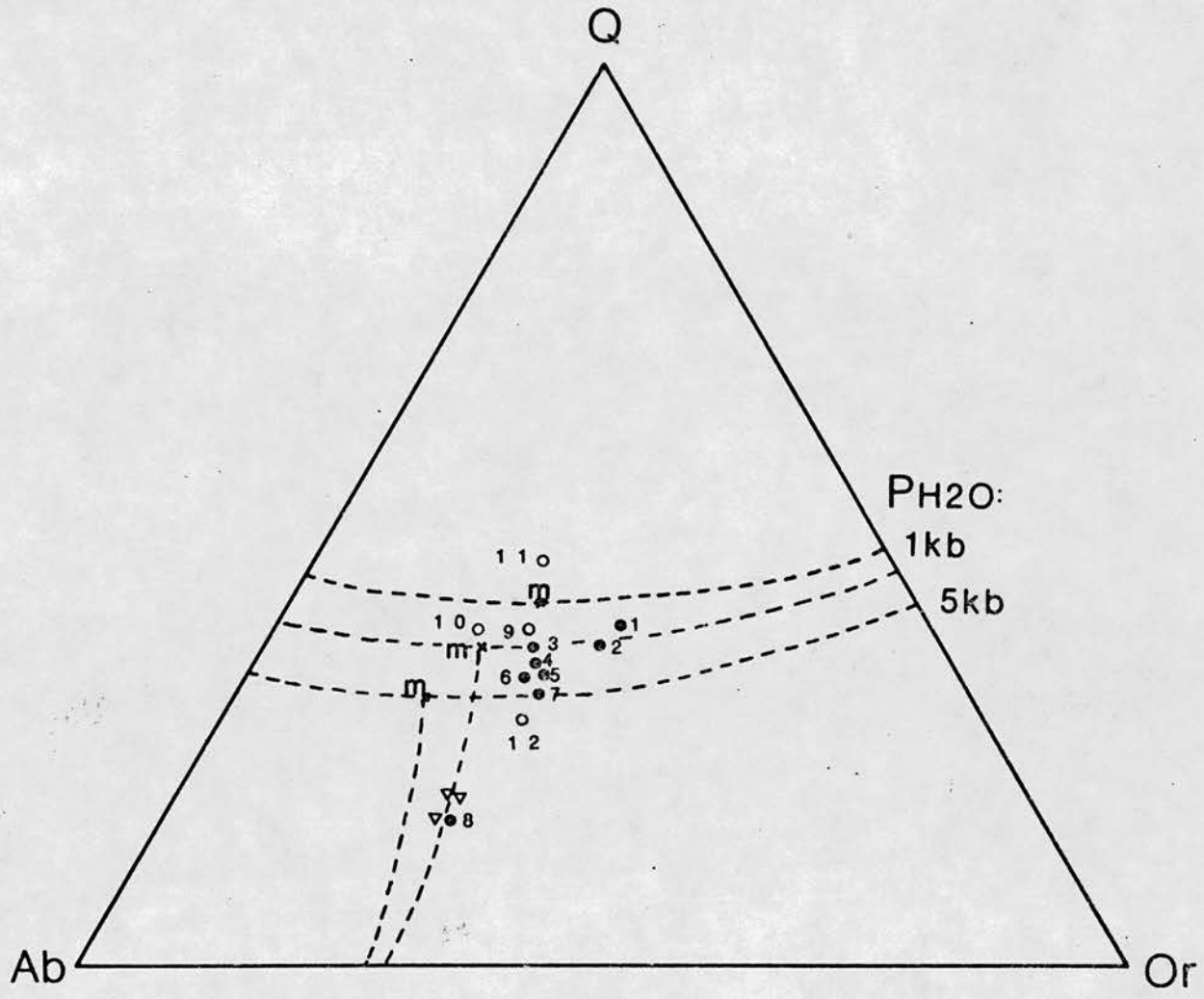

Figure 5.5.1 Numbers refer to samples as follows:

1 - RM107	5 - RM36	9 - RM119
2 - RM86	6 - RM38	10 - RM18
3 - RM30	7 - RM99	11 - RM22
4 - RM37	8 - RM94	12 - RM25

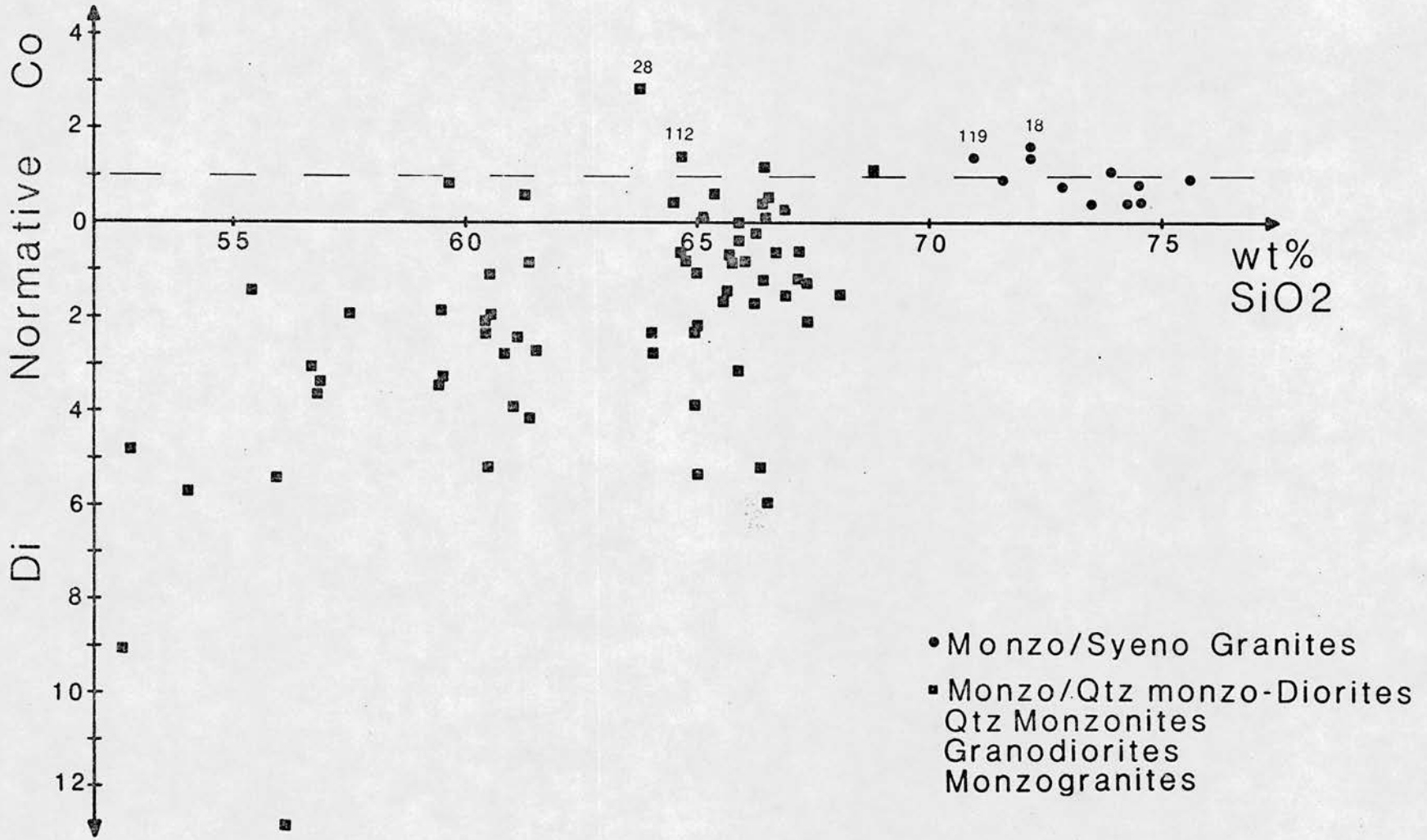

Figure 5.5.2 Point numbers refer to sample numbers.

restite component is considered in more detail in Chapter 7.

5.6 Trace elements.

5.6.0 Variation with major oxides.

5.6.1 Ba - SiO2.(fig. 5.6.1)

The plot of Ba against SiO2 shows scatter, with high (>1000ppm) Ba values persisting into siliceous members of the suite with low Ni and Cr values. It appears to be a primary feature, present in both pimitive and evolved magmas and is considered by Stephens and Halliday (1984) to be a regional feature throughout their 'Argyll' suite regardless of whether a mantle or crustal source is invoked.

Electron microprobe analyses of both potassic feldspar and biotites indicates that the biotites are rich in Ba (see table 6.1) and this may explain the isolated extreme analyses, eg. RM37, RM40. Ba values increase to the southern and eastern part of the pluton.

5.6.2 Sr - SiO2.(fig. 5.6.2)

A negative trend against silica is noted with samples RM109, RM89, RM117 & RM86 being strongly Sr depleted. As these samples are relatively plagioclase poor (modal analysis), removal of calcic plagioclase from the fractionating magma could explain this. One sample, RM28 from the outlier at Loch Tulla, lies consistently off the

main trend of points and is similar to the Etive intusive complex with low Sr concentration, eg Cruachan monzogranite (Batchelor, pers. com.). It may thus represent an offshoot of that complex.

5.6.3 Rb - SiO2.(fig. 5.6.3)

A weak positive trend of Rb against silica is noted. There is scatter of points for all rock types - quartzmonzodiorites through to monzogranites (especially groups III & IV) and sub-parallel positive trends in geographically coherent data points can be identified. There is an increase in Rb values from east to west within group IV samples while the reverse holds true for group III samples which are restricted to a zone c.2.5km west of the Laidon-Ericht fault and in the eastern part of the pluton.

The syenogranites are Rb depleted due to either a change in source for these types or as a result of changing fractionating minerals in the parental magma. High Rb values for the marginal types (eg. RM18, RM119) indicate a link with the northern group IV type granodiorites. The sample from Loch Tulla shows extreme Rb enrichment consistent with that outlier being an offshoot of Etive (Batchelor, 1984).

5.6.4 Zr - SiO2.(fig. 5.6.4)

Zr shows negative covariation with SiO2 and sub-parallel negative trends within the groups can be identified. Those samples from west of the Laidon-Ericht fault are Zr enriched with respect to those east of the fault. Scatter of the data is evident with certain samples (RM70, RM76, RM90 & RM109) lying off trend. Zr depletion is noted in RM86 - syeno/monzogranite - while a traverse of three samples (RM99-100-101) across a concealed contact between monzogranite and syenogranite (Chapter 3.8) shows a distinct break between the types. The anomalous enrichment of samples RM25 and RM76 is not easily accounted for in terms of their mineralogies other than by abnormal Zr content of spheneas zircon crystals are very rare.

5.6.5 Y - SiO2.(fig. 5.6.5)

Yttrium has negative covariation with SiO2 and subdivisions within the major groups confirms this overall trend (monzogranite - group IV - samples RM57, RM112, RM60, RM63, RM64 & RM110 from the eastern part of the pluton are the exception). Syenogranites from west of the Laidon-Ericht fault are Y depleted when compared to those east of the fault. Group IV samples exhibit the opposite effect, being Y enhanced in the western part of the pluton. This may indicate a change in source material for the granite members or be due to a fundamental difference in source material across the fault. Sample RM76 has anomalously high Y but this is not reflected in significantly different modal concentration of accessory phases, although monazite and sphene in biotite are present.

5.6.6 V - SiO2.(fig. 5.6.6)

Vanadium decreases with increasing silica, with very little scatter about the trend except in group II (quartz monzodiorite) samples. Sample RM68 is V depleted reflecting the low modal percentage of Fe-Ti oxides. The extreme enrichment of RM76 cannot solely be ascribed to oxide minerals and amphibole is the only significant V-rich mineral present. Enrichment in Zr, Y, La and Ce is also noted. There are no microprobe data available to test this.

5.6.7 Cr - SiO2.(fig. 5.6.7)

Cr displays negative covariation with silica, decreasing to zero at approximately 71 wt% SiO2. This could represent a minimum melt point and imply that the syenogranites are not directly related to the remainder of the suite. There is some scatter about the trend in groups II through V with none of the group I samples plotting on trend - RM109 is strongly Cr enhanced while RM68 & RM90 are Cr depleted.

The presence of 3.6% by mode Fe-Ti oxides in RM109 can account for the observed variation, while the lower than expected modal percentages of opaques and ferromagnesian minerals in the other two samples would explain their relative Cr depletion. Enhanced values for Cr in RM117 may be similarily explained. Observed Cr values for the marginal samples, (RM18, RM22 & RM119), appear to link them with the group IV samples of intermediate composition.

5.6.8 Ni - SiO2.(fig. 5.6.8)

The plot of Ni mimics that of Cr with the exception that the values do not fall to zero within the SiO2 range but the observations made for the preceding diagram hold good.

5.6.9 Cu - SiO2.(fig. 5.6.9)

Copper decreases with increasing silica. Anomalous substitution of Cu for Fe in biotite may be the cause of enhaced values in samples RM89 & RM118.

5.6.10 Zn - SiO2.(fig.5.6.10)

There is negative covariation of Zn with SiO2. Relative depletion of Zn can be seen in samples RM68, RM69 & RM113 while RM117 and RM103 show enhanced Zn values. Granite samples from east of the Laidon-Ericht fault are slightly Zn depleted compared to those west of the fault.

5.6.11 Pb - SiO2.(fig. 5.6.11)

A positive trend with scatter about the line through groups I through IV characterises Pb against silica. The granite samples lie markedly off-trend to the depleted side while the marginal samples (RM18 & RM22) show Pb values consistent with a group IV original composition.

5.6.12 Nb - SiO2.(fig. 5.6.12)

Nb shows scatter about an approximately constant trend value and the variability is due to sporadic distibution of accessory phases.

5.6.13 Th - SiO2.(fig. 5.6.13)

The plot of Th against silica shows scatter about a positive trend with a wide range of Th values in the monzogranites and granodiorites of group IV. The syenogranites are slightly Th depleted, especially those in traverses across the contacts between the intermediate and granite types (RM99 & RM107).

5.6.14 La - SiO2.(fig. 5.6.14)

Lanthanum shows scatter and no significant covariation with SiO2. There is a possible negative covariation in the syenogranite members while those from west of the Laidon-Ericht fault have enhanced values with respect to samples from the eastern part of the pluton. Monazite is present in samples RM34, RM35 & RM76, while the lack of accessory phases in RM89 (see Table 4.1) may explain its relative La, Ce & Y depletion.

5.6.15 Ce - SiO2.(fig. 5.6.15)

There is a negative covariation of Ce against silica with scatter of data points about the trend line. A significant modal percentage of apatite in RM109 may account for the enhanced Ce values shown, while the presence of sphene in RM111 and to a lesser extent in RM76 may

explain their Ce levels. The syenogranites of the eastern part of the pluton are significantly Ce depleted when compared across the Laidon-Ericht fault, though this may only reflect local changes in accessory phase crystallising conditions.

5.6.16 Hf - SiO2.(fig. 5.6.16)

Due to the range of Hf values little can be said about their distribution on the diagram except to note a broadly negative covariation. RM76, a granodiorite, displays Hf enhancement possibly as a function of entry of Hf into the Zr phases although no zircon has been noted in a thin section of the sample.

5.6.17 Ba - K2O.(fig. 5.6.17)

Ba shows poor covariation with K2O, those syenogranites from west of the Laidon-Ericht fault showing slightly enhanced K2O and slightly depleted Ba values. Ba remains constant for the group I types.

5.6.18 Rb - K2O.(fig. 5.6.18)

The plot of Rb against K2O shows good separation of the syenogranitic samples on the Rb depleted side of a steep positive trend. With one exception (RM25), the marginal granitic types all plot within the fields of the intermediate monzogranites and granodiorites. The granodiorites plot as a more coherent group than do the monzogranites and there is a wide range of values noted for the quartzmonzodiorites. The high K/low Rb of the monzo/syenogranitic

sample RM86 is consistent with that of the syenogranites in general but shows the K enhanced values typical from west of the Laidon-Ericht fault.

5.6.19 V - Ti.(fig.5.6.19)

At high fO2, V behaves as an incompatible element and V increases as sphene is crystallised, while at low fO2 fractionation of amphibole and ilmenite will decrease the V/Ti. Thus, anomalously high V values will indicate the possible fractionation of sphene and low V values the fractionation of Fe/Ti oxides or amphibole. A positive correlation of V and Ti with little scatter implies that fractionation of amphibole +/- biotite at low-intermediate fO2 conditions operated through groups I to IV. The gap between data points in groups III and IV is closed indicating a strong chemical/physical relationship despite field evidence showing they exist as separate magma pulses (eg. samples RM17 & RM17A which are taken across an internal contact between two pulses). Samples RM99 & RM107 show V values intermediate between group IV granodiorites/monzogranites and group V syeno granites.

5.6.20 V - MgO.(fig. 5.6.20)

A positive covariation of V with MgO may infer that a common source links the groups with an offsetting of the trend within the syenogranites suggesting a separate source or pulse for them. RM90 is thought to represent restite material while RM109, with its unique mineral textures (Plate 4.3), may be a product of magma mixing or have

an anomalously high proportion of restitic material in the rock.

5.6.21 Cr,Ni - MgO.(figs. 5.6.21 & 5.6.21b)

Both Cr and Ni show positive covariation with MgO and the same anomalous features. Enrichment of Cr and Ni in RM109 and RM117 (by a factor of 2) is attributable to Fe/Ti oxides (RM109) and amphibole and biotite (RM117). The depletion of these elements in RM68 and RM90 may be due to removal of greater proportions of oxides and clinopyroxene minerals from the parental magma which would indicate a unique restite mineralogy.

5.6.22 Ce - P2O5.(fig. 5.6.22)

Ce shows a positive covariation with P2O5 suggesting apatite as the host mineral (Table 4.1). The monzogranites west of the Laidon-Ericht fault show enhanced Ce values with respect to samples in the eastern part.

5.6.23 Chondrite normalised plot.(figs. 5.6.23 & 5.6.24)

To highlight variation in selected trace and major data, the values are normalised to chondrite abundances. The abundances used here are taken from Sun et.al. (1979). Two diagrams were plotted; overall variation within the Moor of Rannoch pluton displayed using selected samples from each major group identified (fig. 5.6.23) and within-group variation displayed for group IV selected values only (fig. 5.6.24).

Considering fig 5.6.23, the most notable features are Nb depletion and high Ba, K and Sr values with a pronounced 'spike' of Sr, especially at lower SiO2 levels. This Sr enrichment is a characteristic of the SW Highlands granitoids and thought to be a primary feature of the suite (Stephens and Halliday, 1984). Enrichment of Sr is not consistent with plagioclase fractionation from a common source magma, while the enhanced Ba values in biotite and alkali feldspar (Chapter 6.2, 6.4) may be due to a high restitic component in the magma. Ba preferentially goes into biotite and alkali feldspar in earlier melts. The Moor of Rannoch complex (especially the Ba enriched eastern part) may thus represent the first partial melts of the region. When other nearby Caledonian plutons are considered, both Ba and Sr show regionally enhanced values.

Removal of apatite (Y) or ilmenite (Th) could account for the depleted values for RM86 (Y) and RM68 & RM69 (Th). Overall low values of Y could be the result of amphibole, clinopyroxene (and apatite) fractionation from the source magma or garnet fractionation at the source. The common Ba and Sr, together with intermediate Th, Rb and Nb values, of the basic rocks (monzodiorites and quartz-monzodiorites) suggests a common characteristic of sources for the suite analysed.

5.7.0 Other trace element variation diagrams.

5.7.1 Sr - CaO.(fig. 5.7.1)

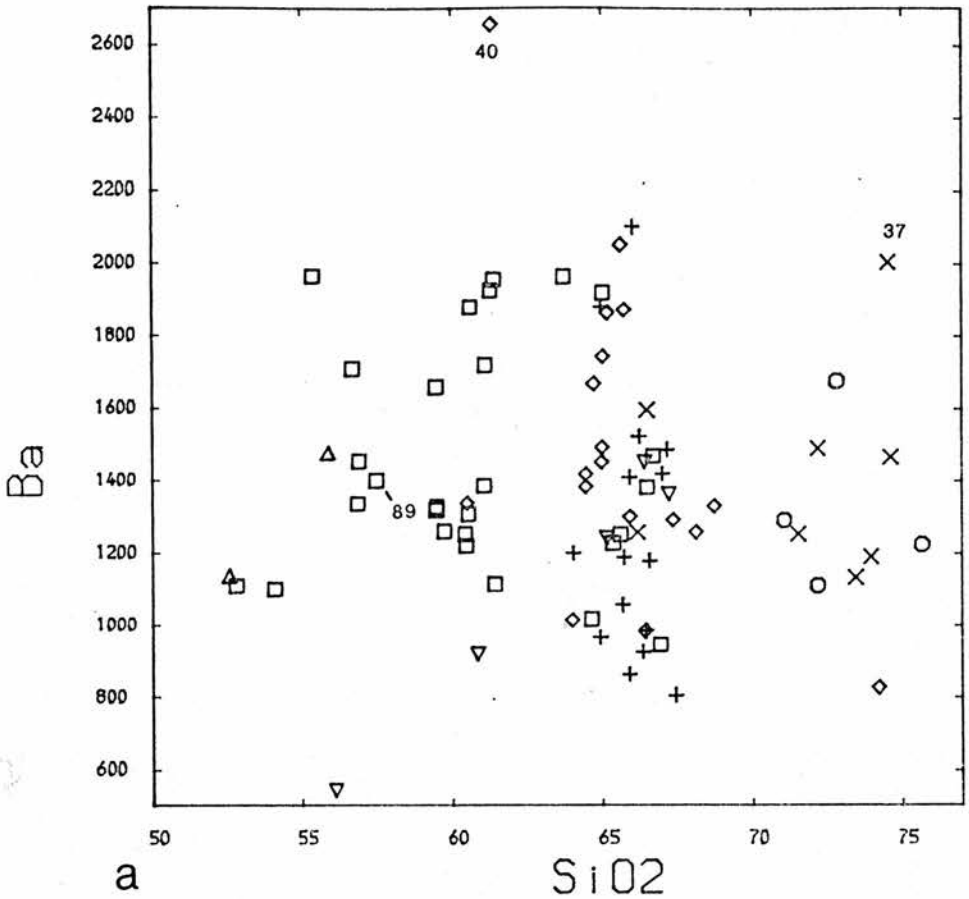

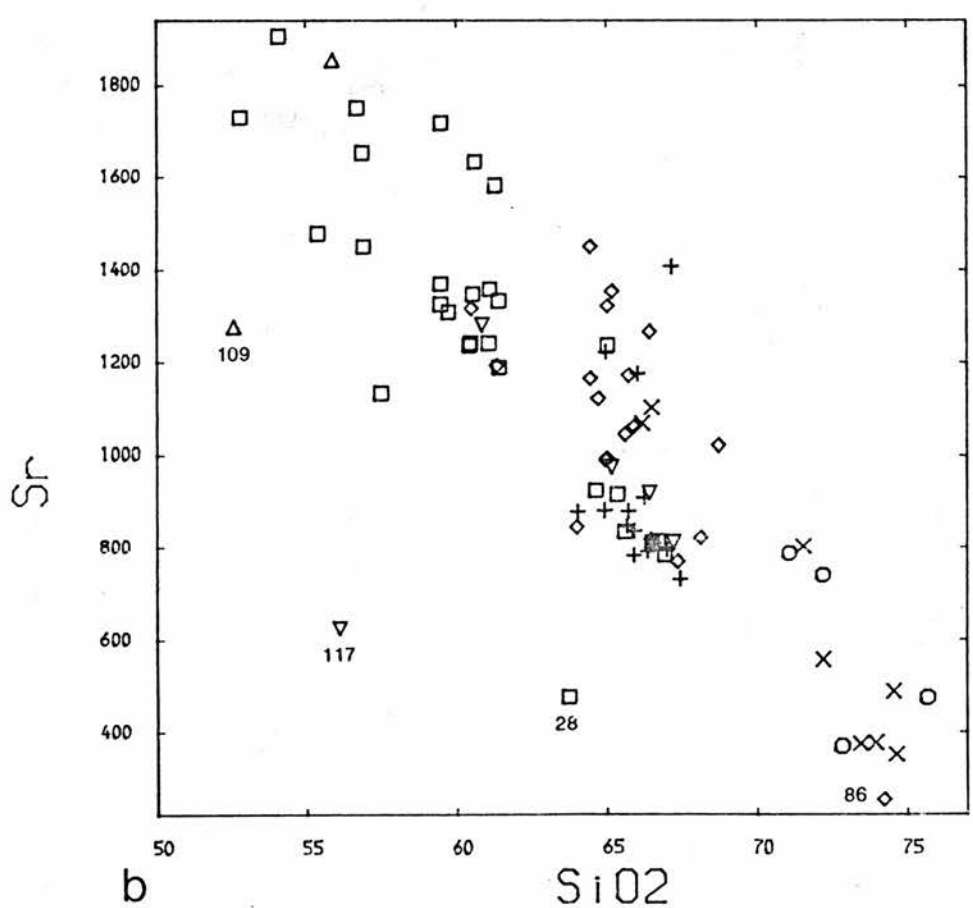

a) Figure 5.6.1, b) Figure 5.6.2

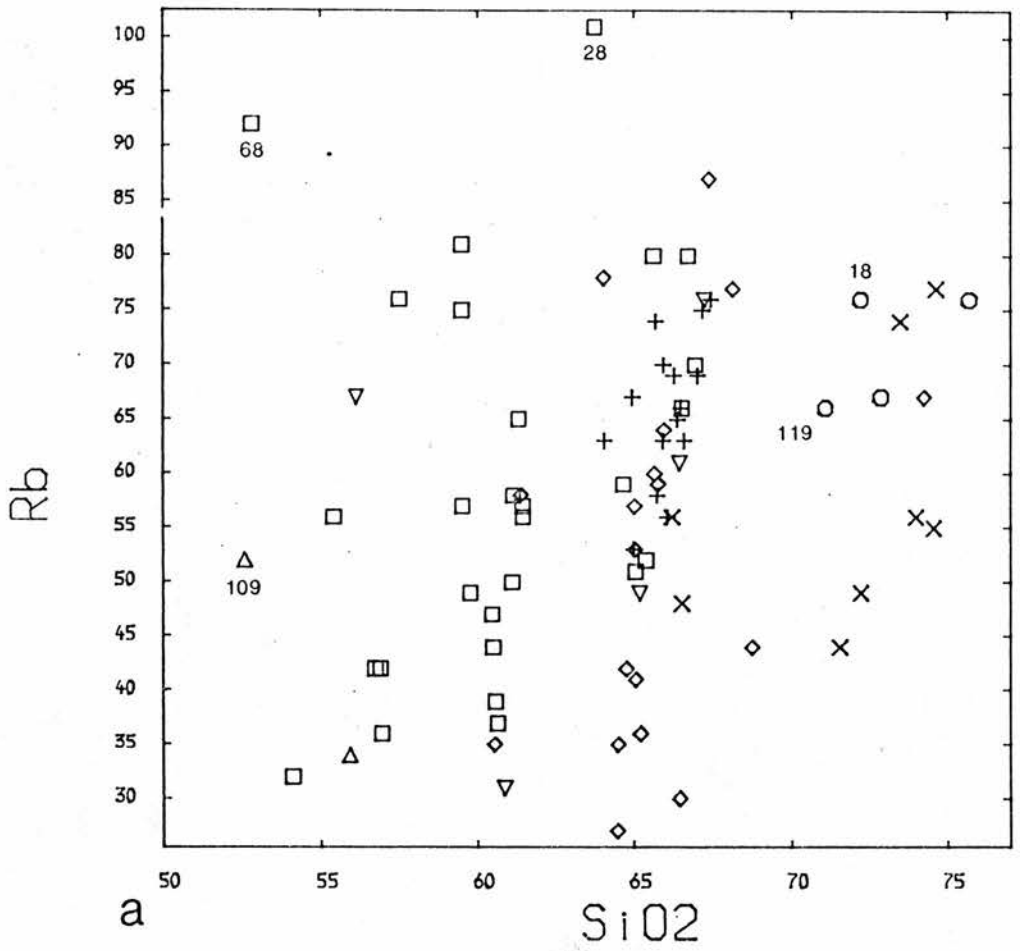

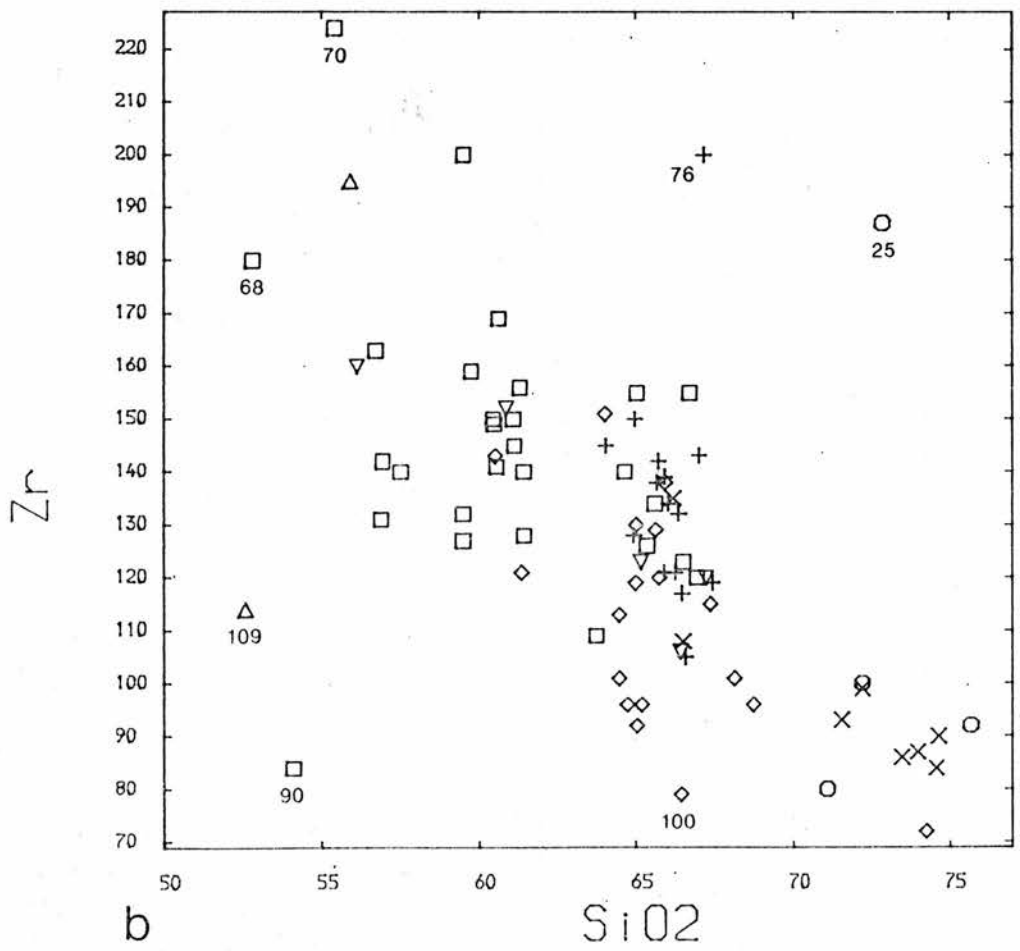

a) Figure 5.6.3, b) Figure 5.6.4

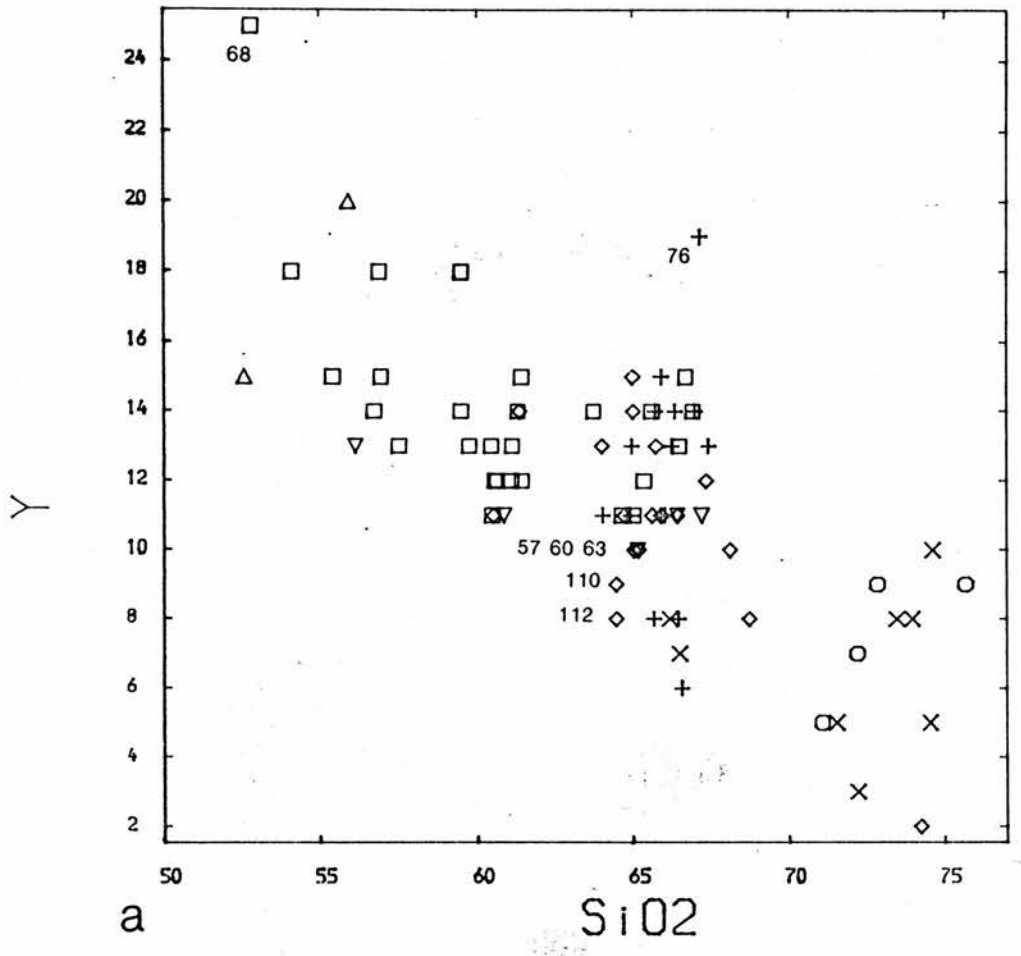

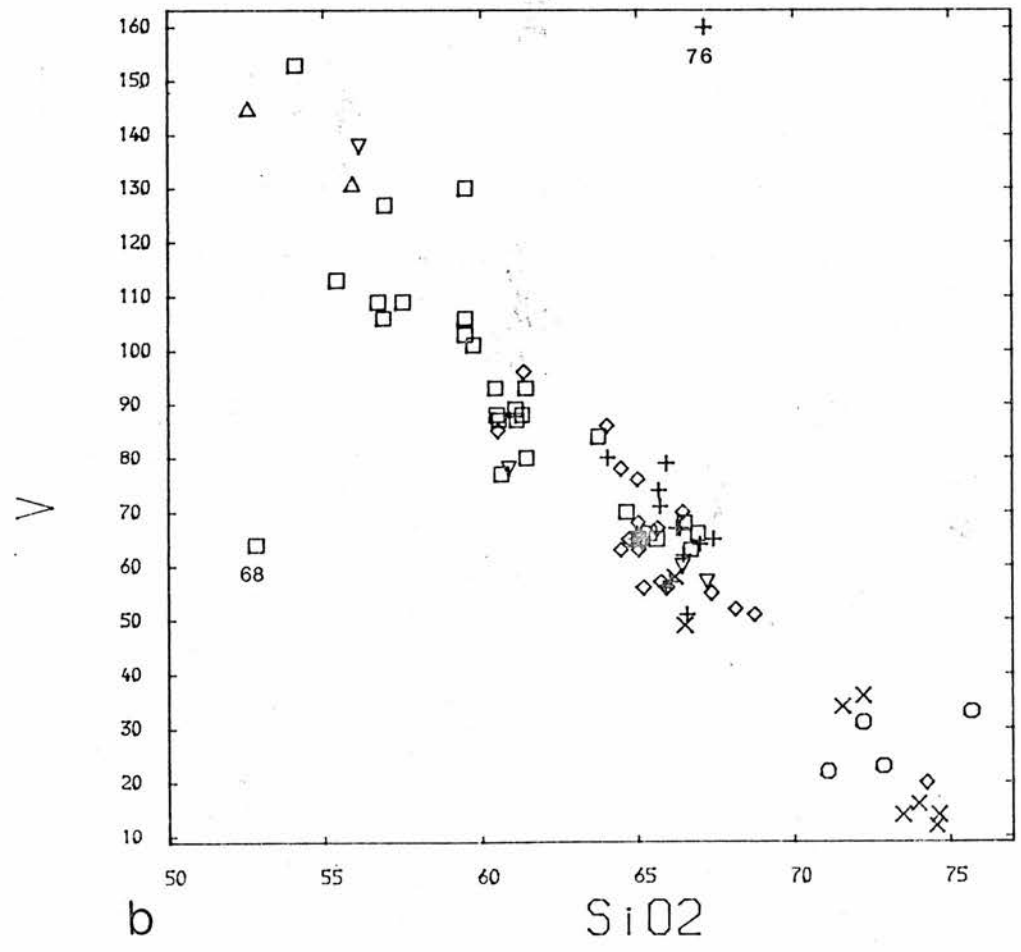

a) Figure 5.6.5, b) Figure 5.6.6

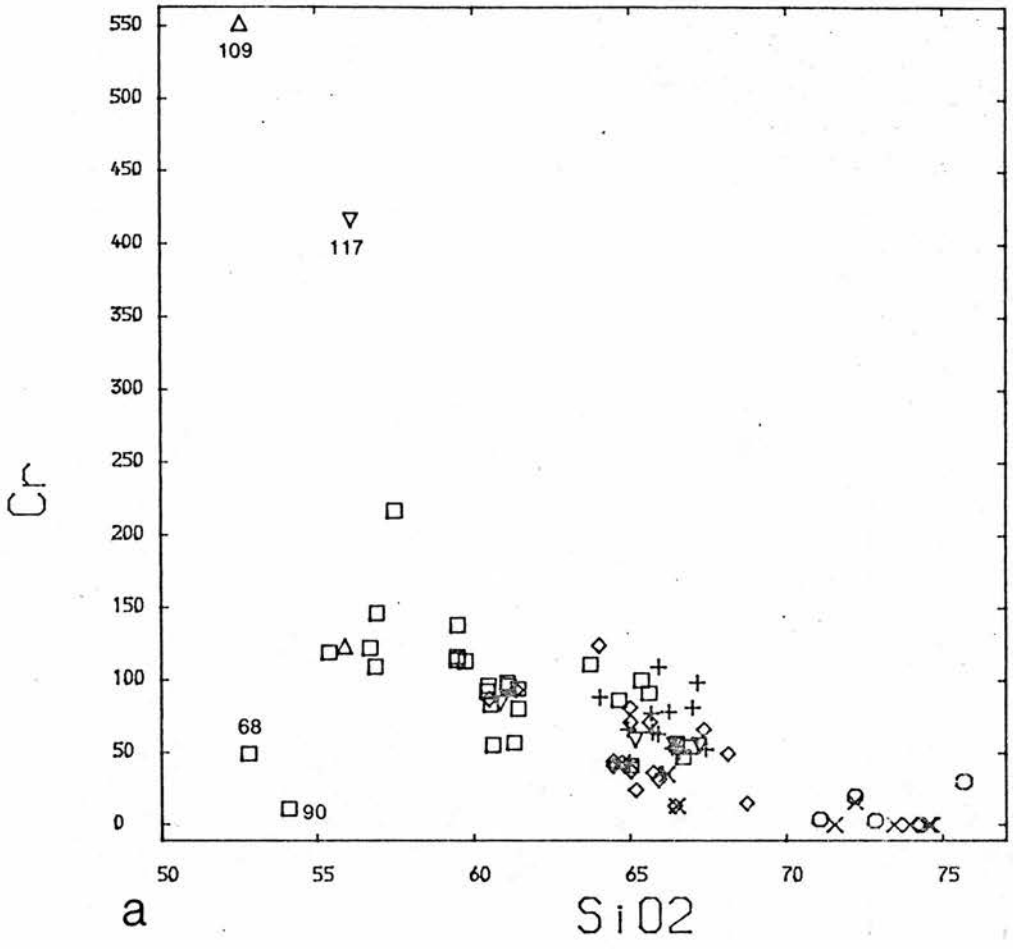

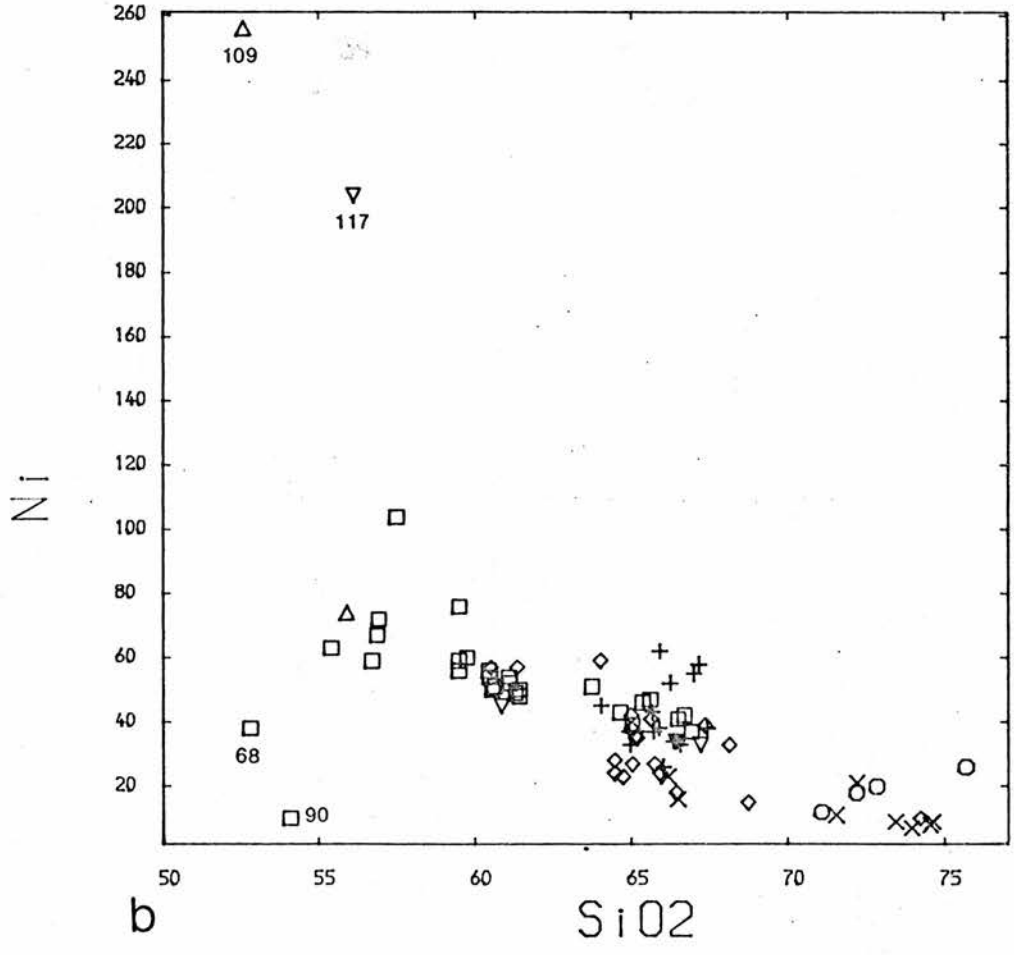

a) Figure 5.6.7, b) Figure 5.6.8

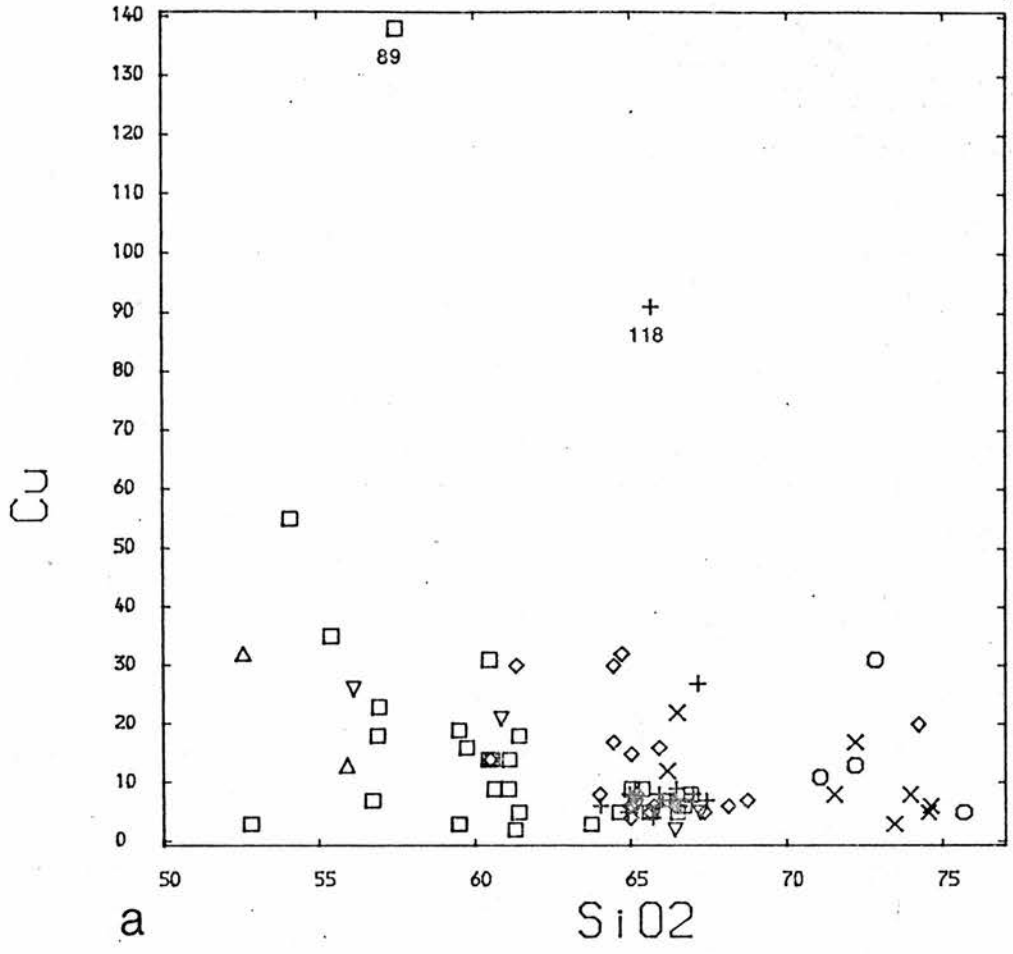

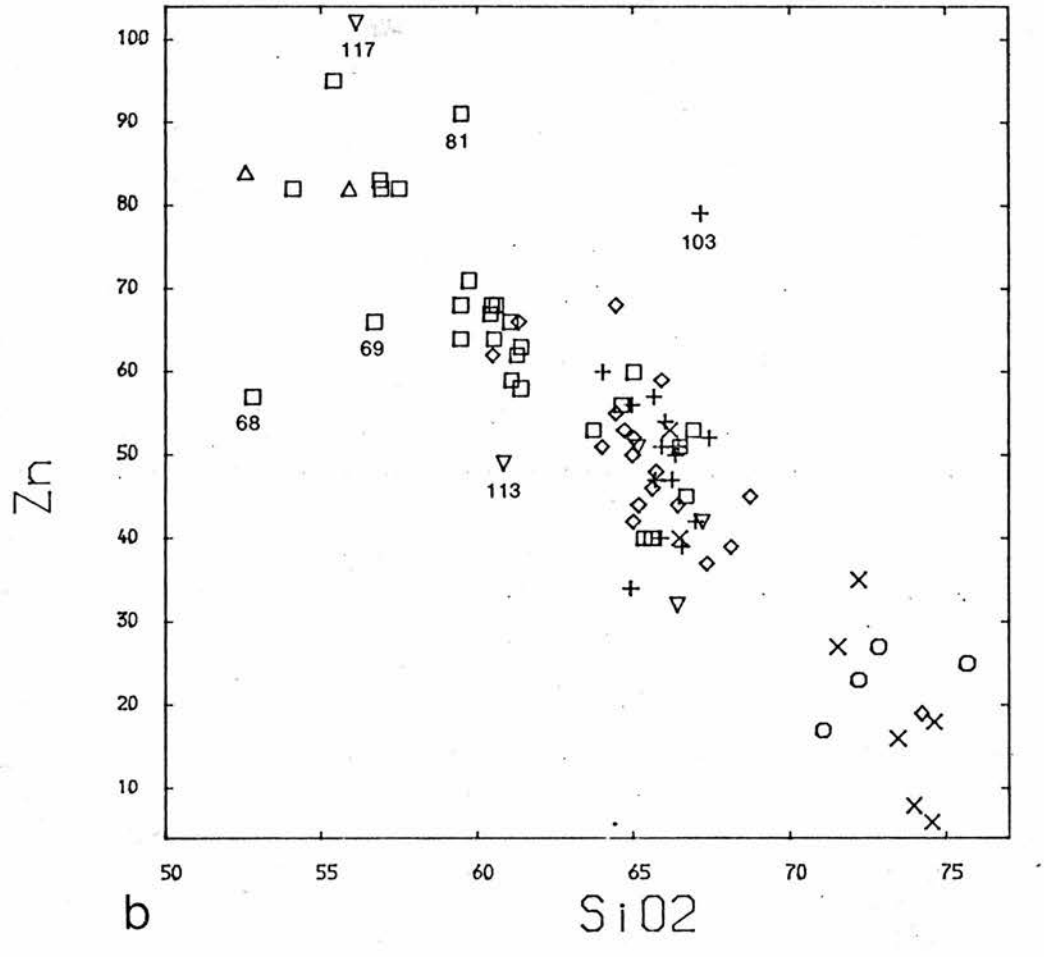

a) Figure 5.6.9, b) Figure 5.6.10

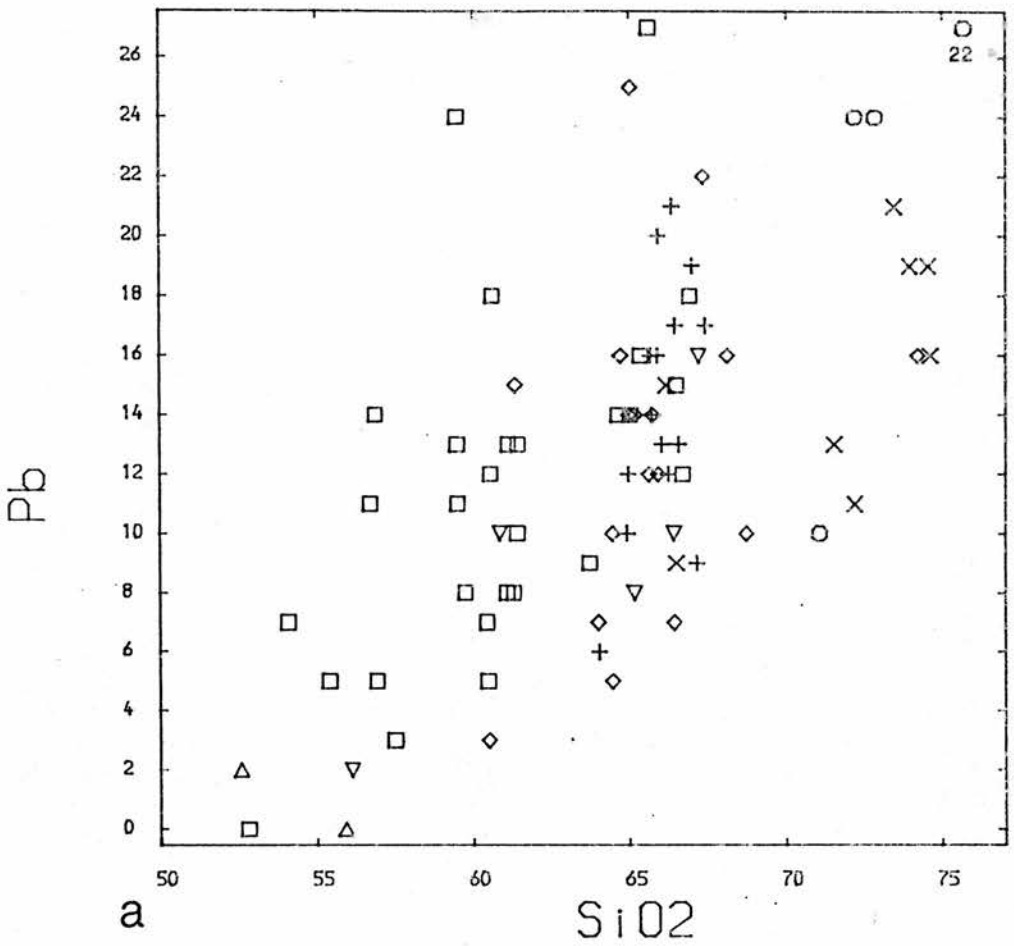

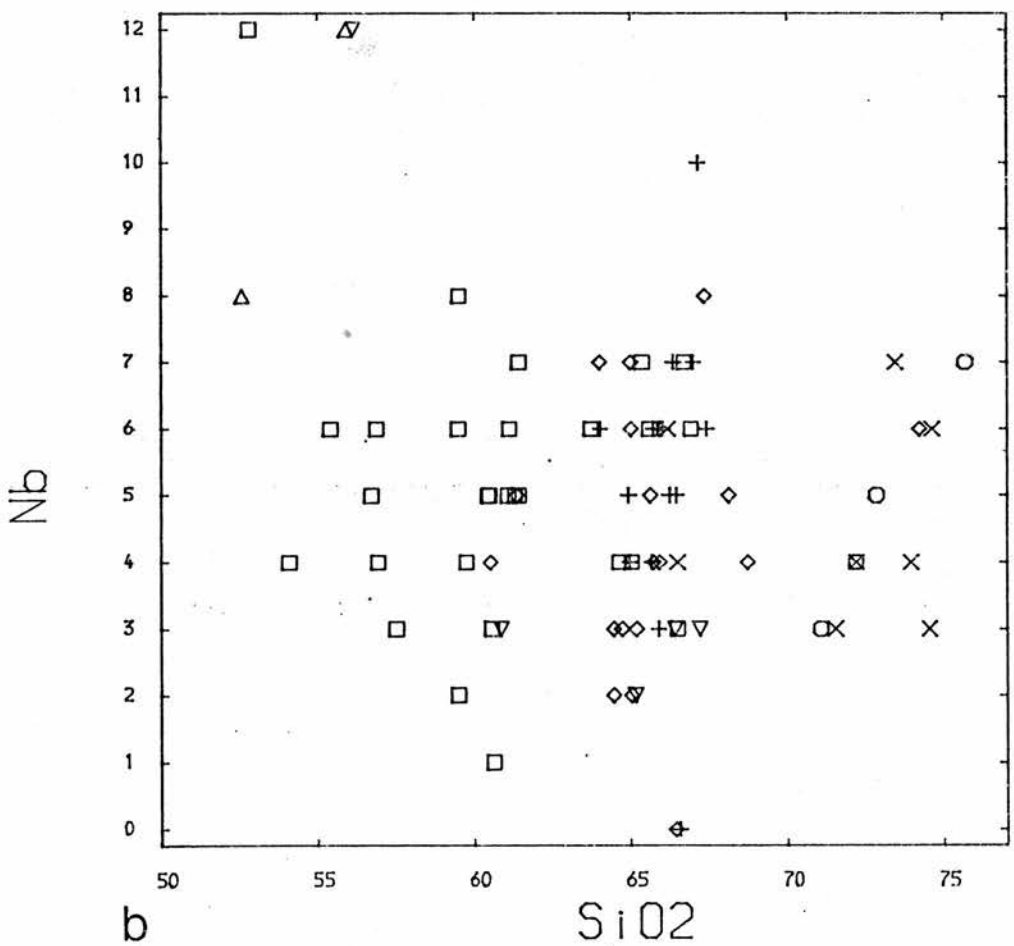

a) Figure 5.6.11, b) Figure 5.6.12

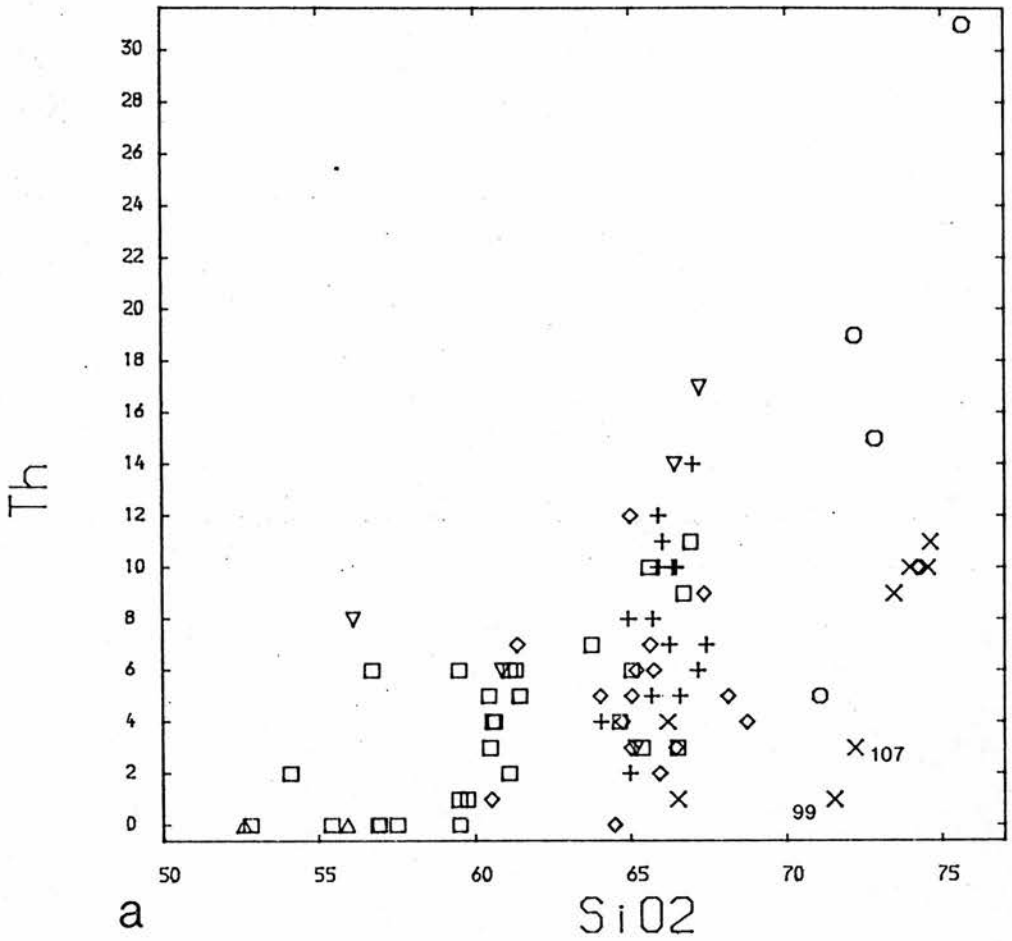

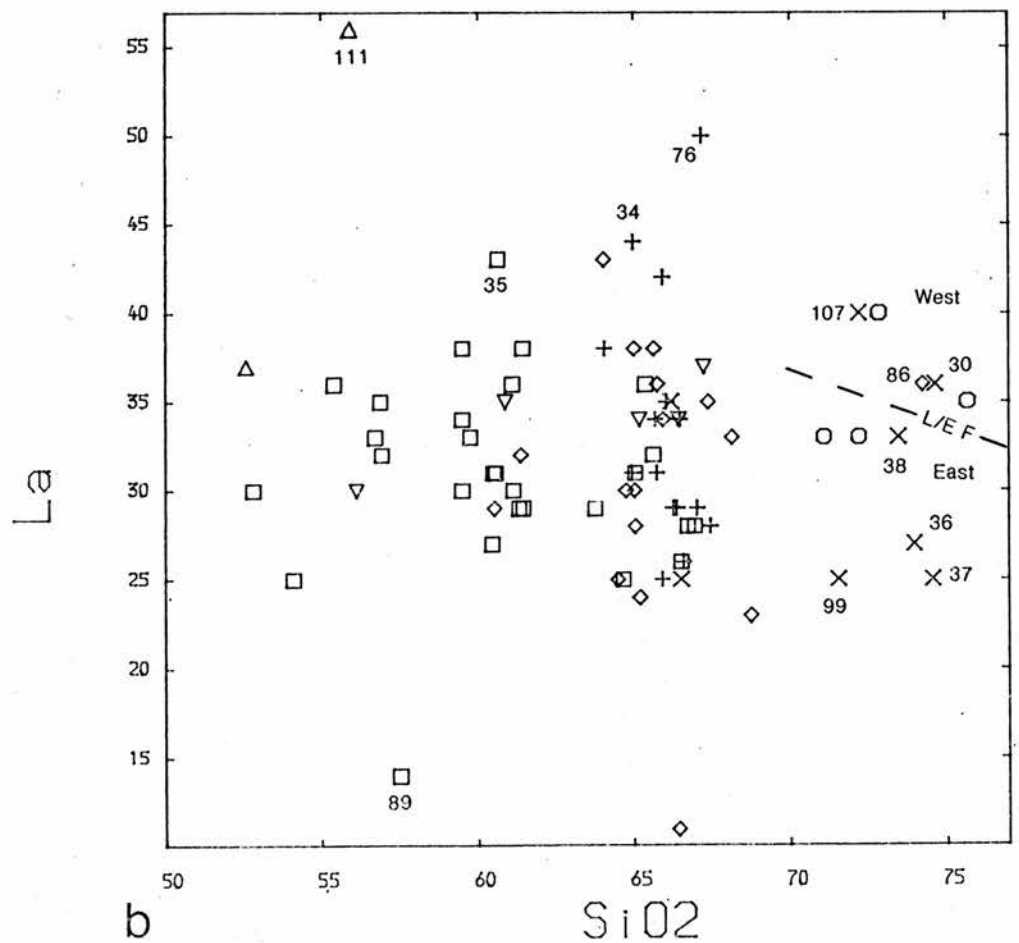

a) Figure 5.6.13, b) Figure 5.6.14

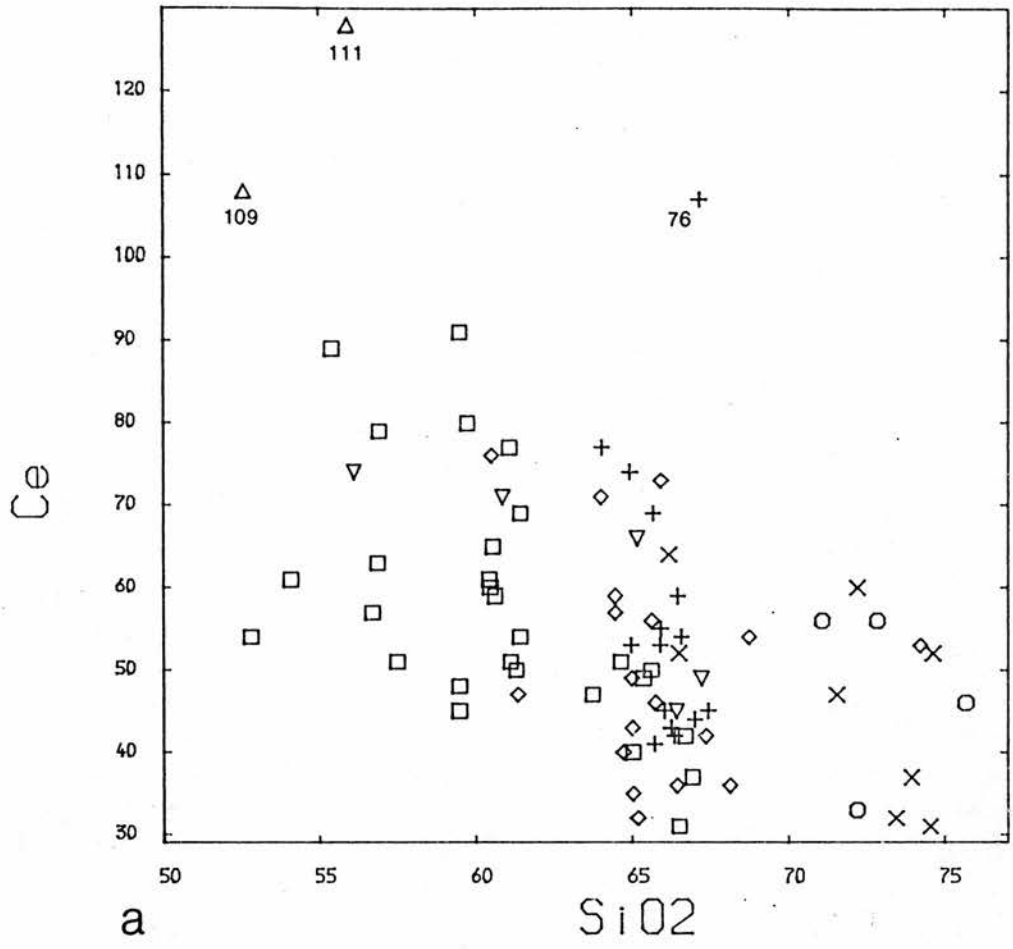

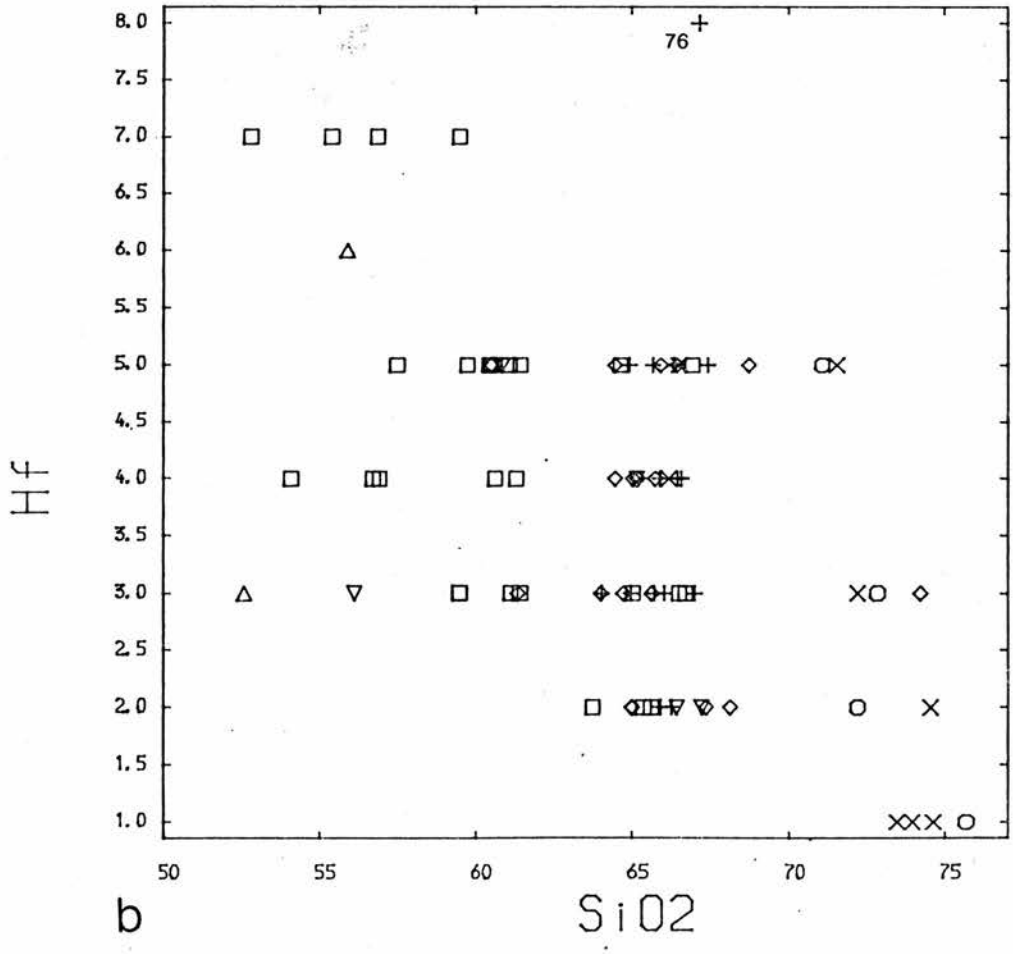

a) Figure 5.6.15, b) Figure 5.6.16

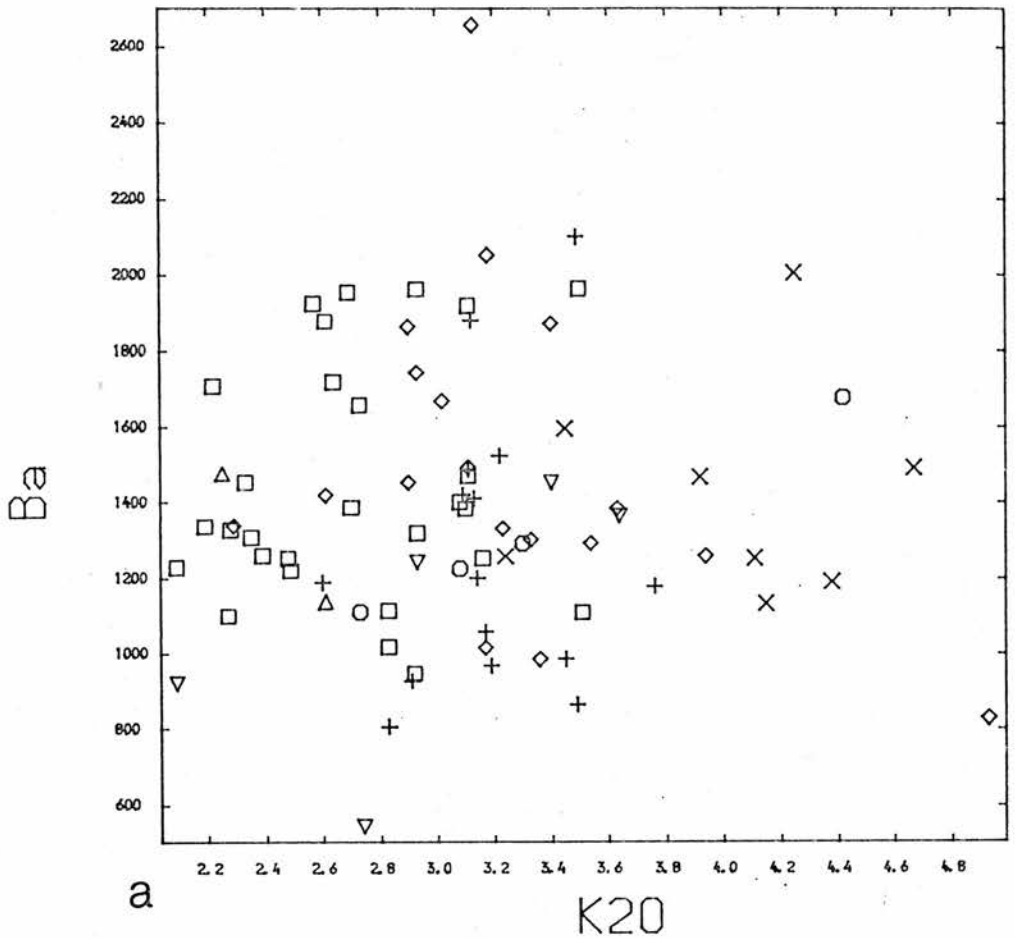

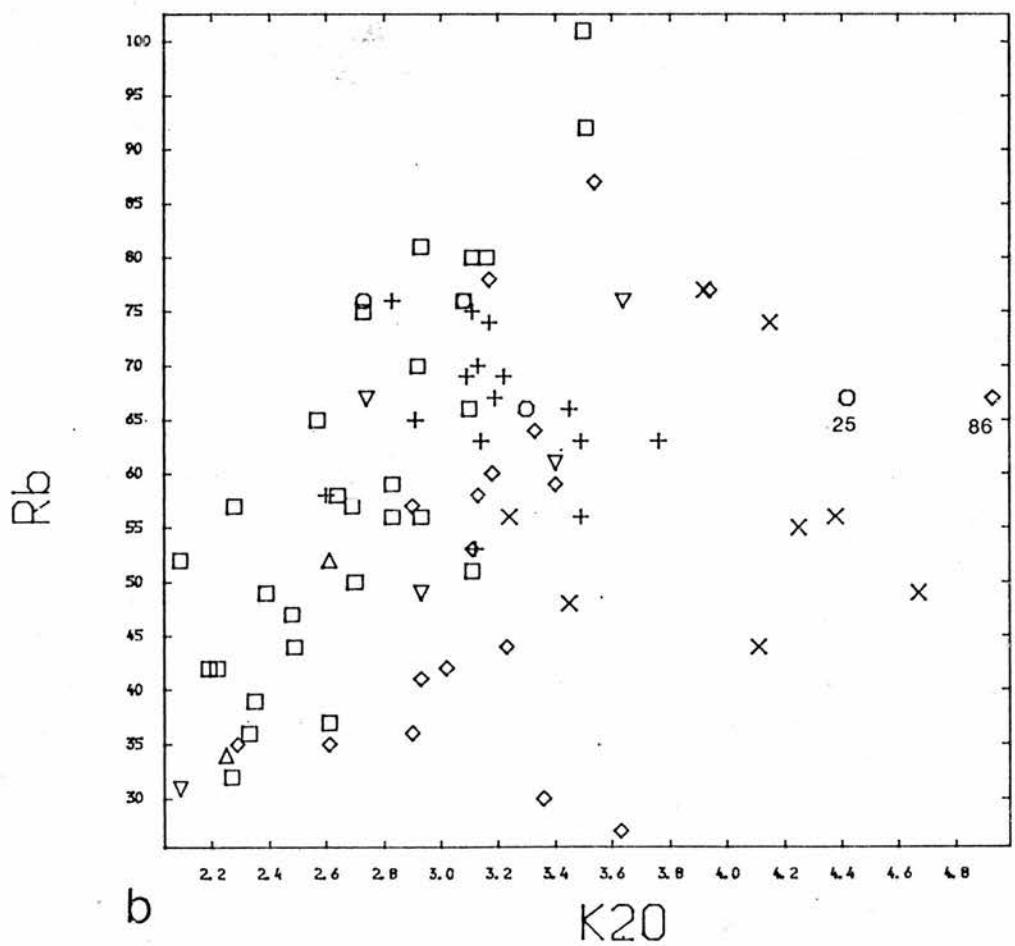

a) Figure 5.6.17, b) Figure 5.6.18

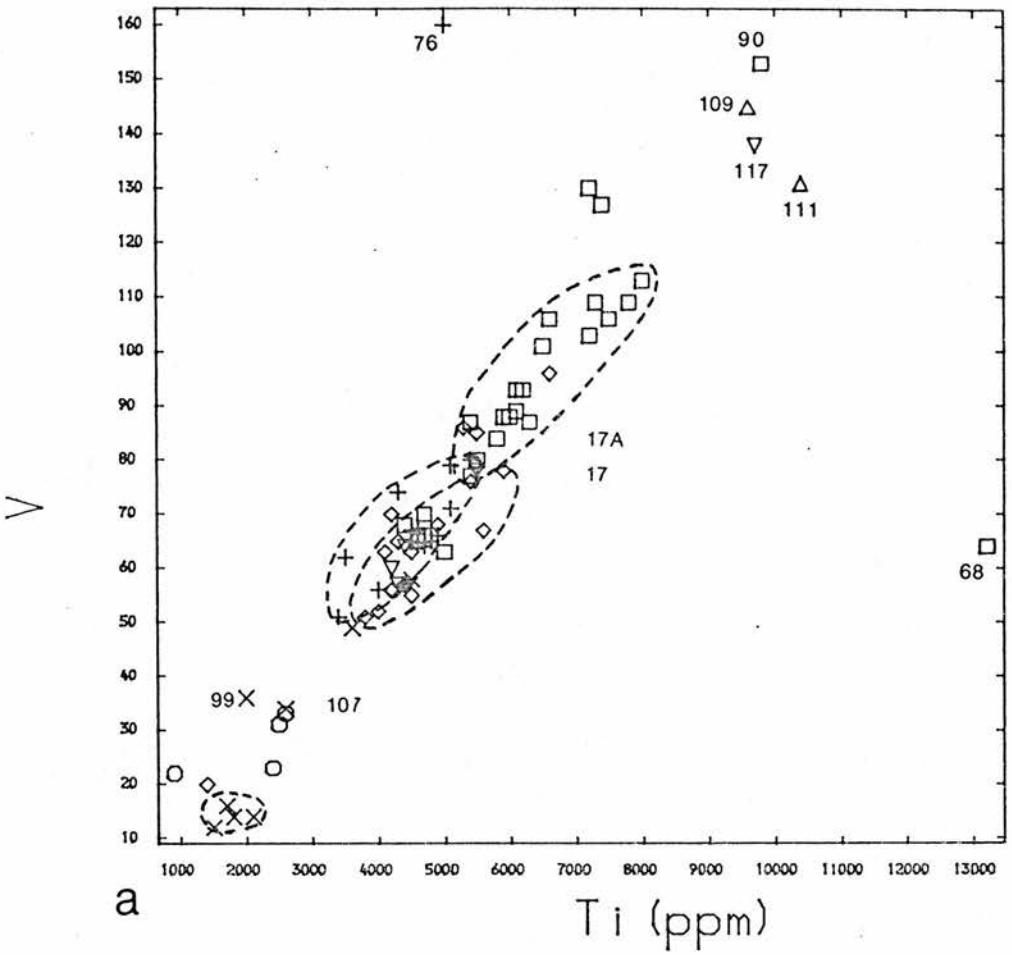

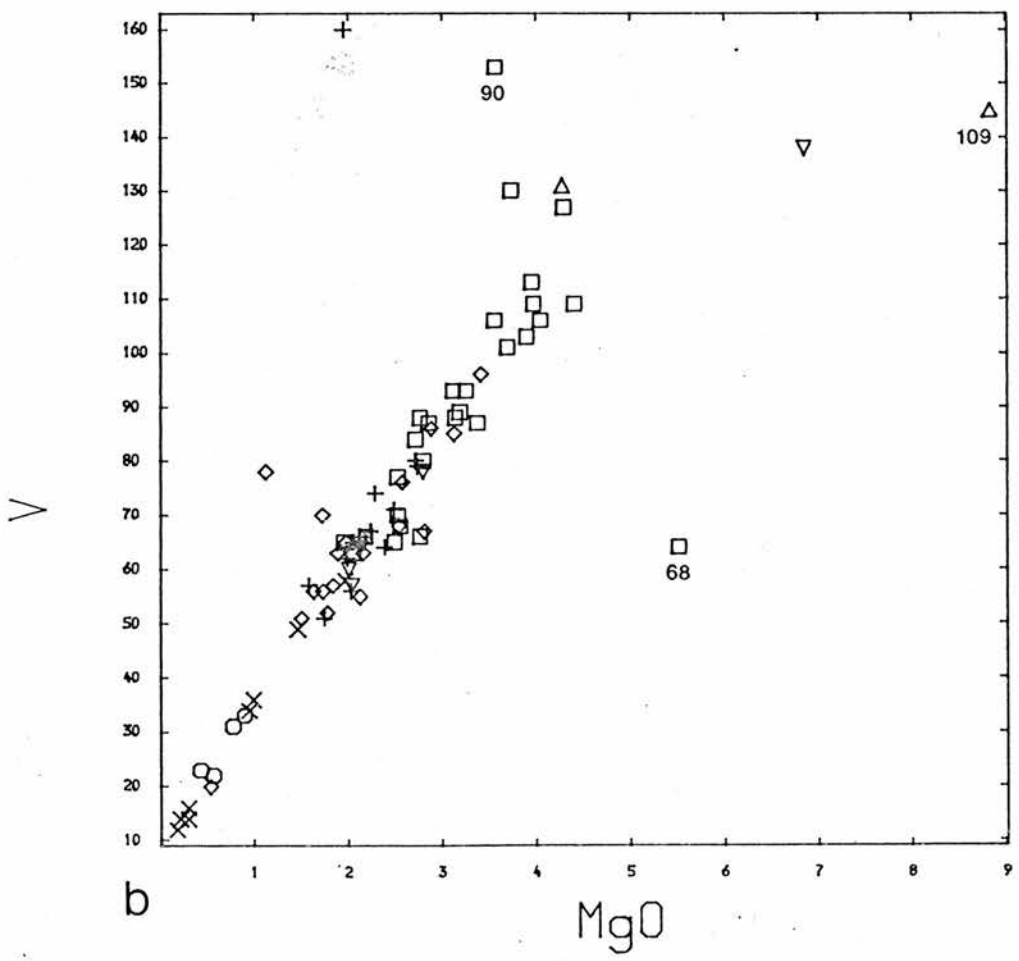

a) Figure 5.6.19, b) Figure 5.6.20

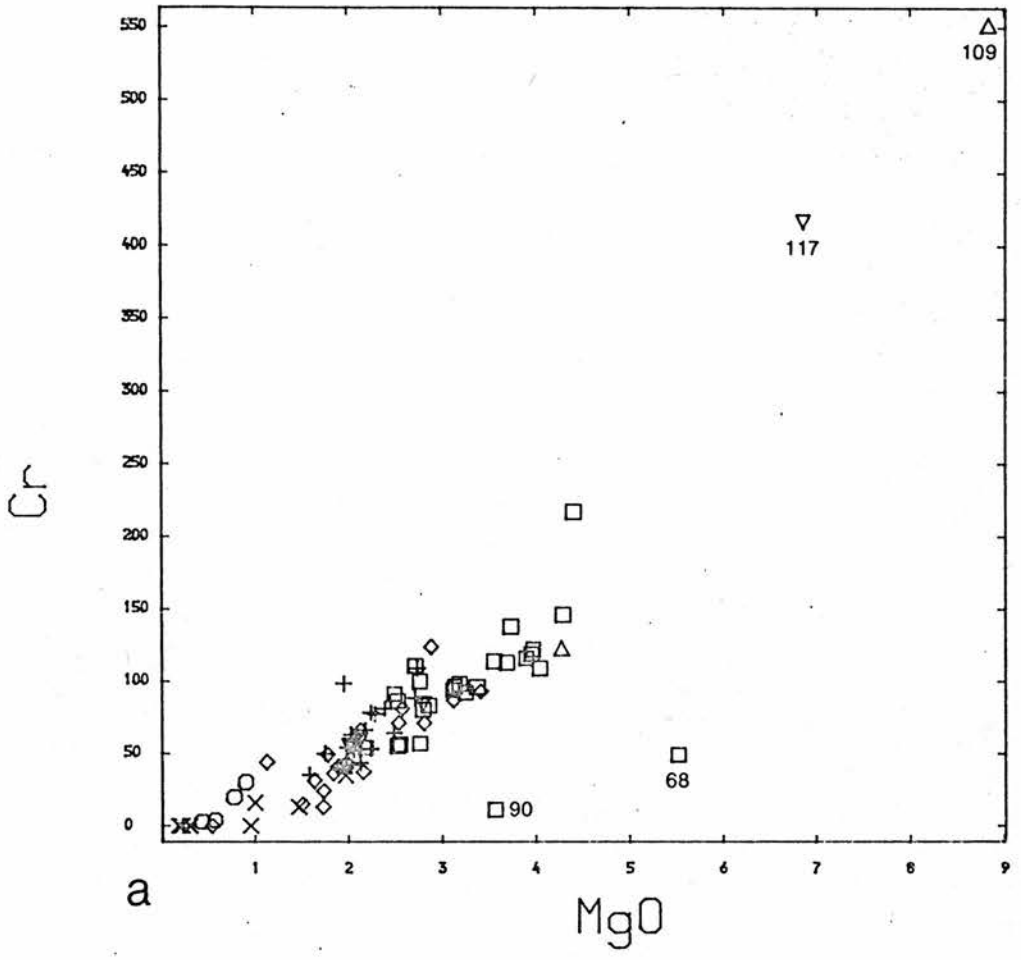

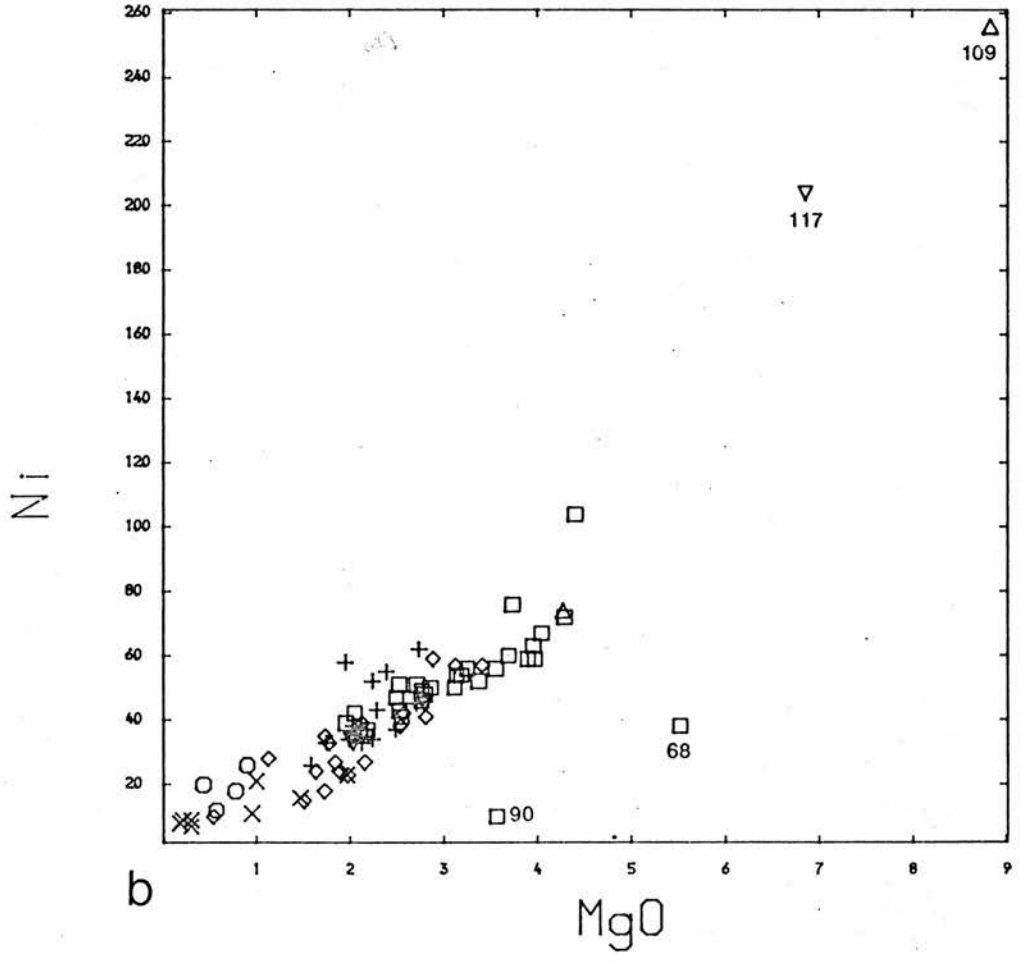

Figure 5.6.21 a & b

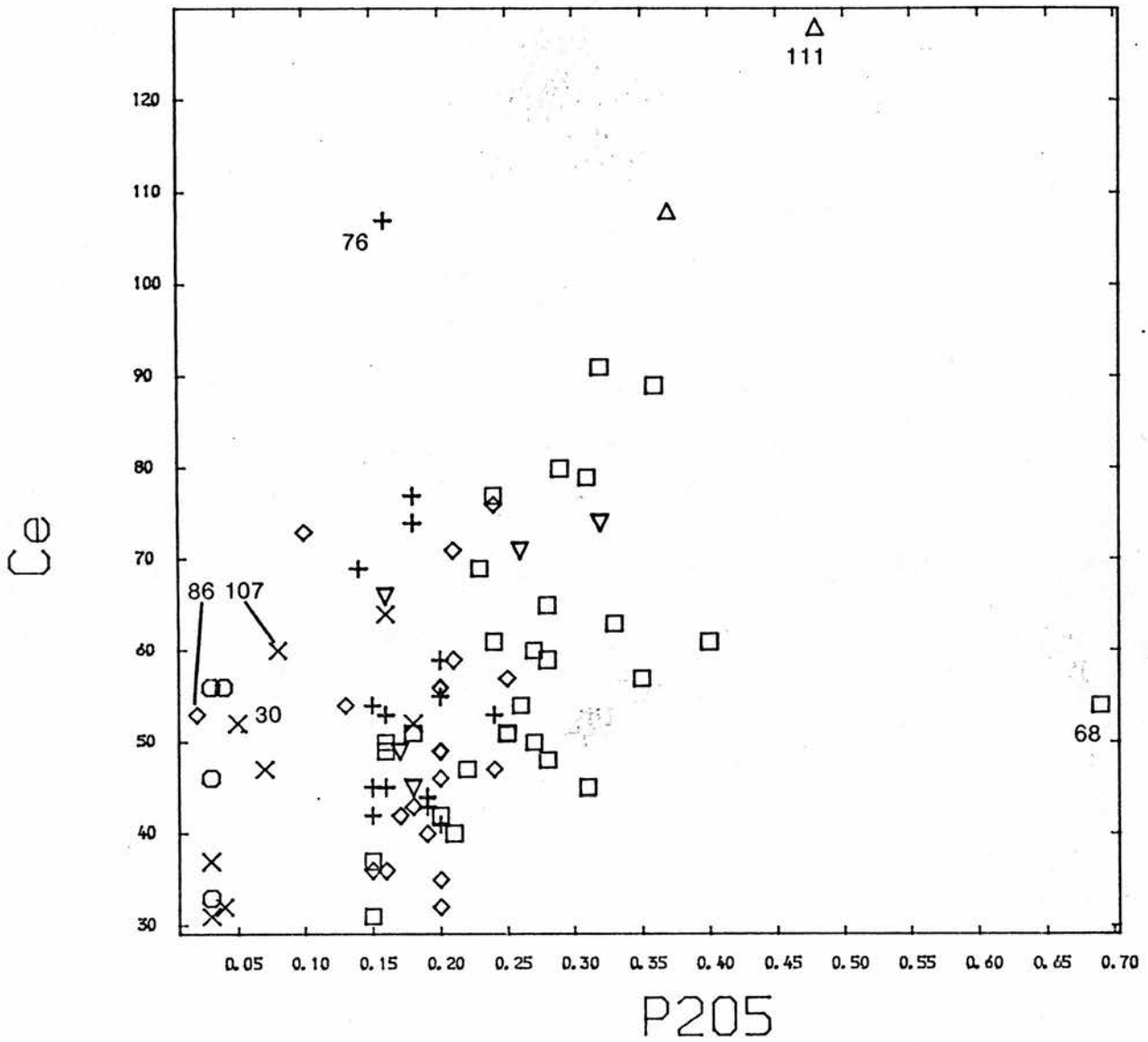
111
76
86
107
30
68
120
110
100
90
80
70
60
50
40
30
0.05
0.10
0.15
0.20
0.25
0.30
0.35
0.40
0.45
0.50
0.55
0.60
0.65
0.70
P205

Figure 5.6.22

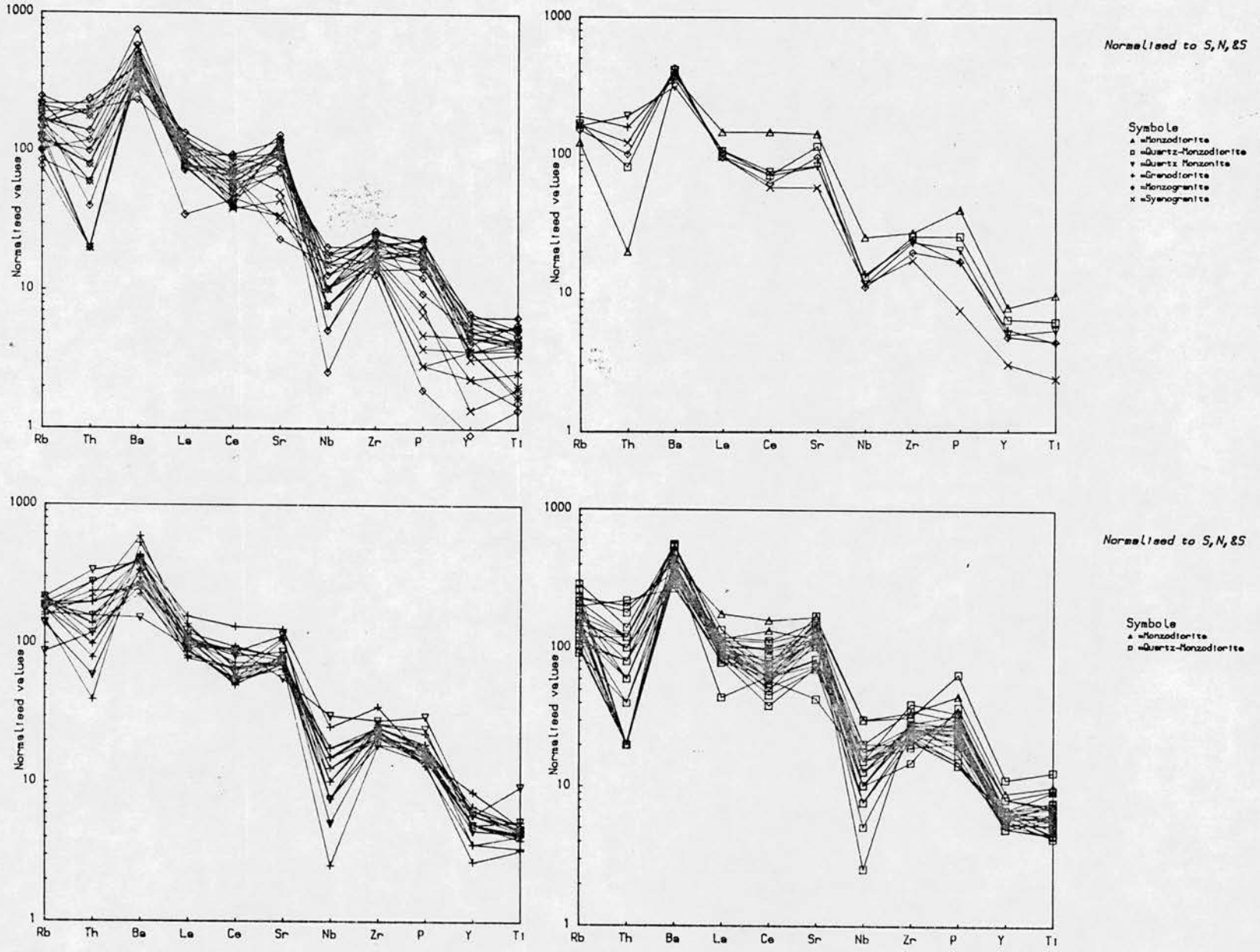

Figure 5.6.23 Data normalised to Sun, S-S, Nesbitt, R.W. and Sharaskin, A. Ya (S,N & S), (1979).

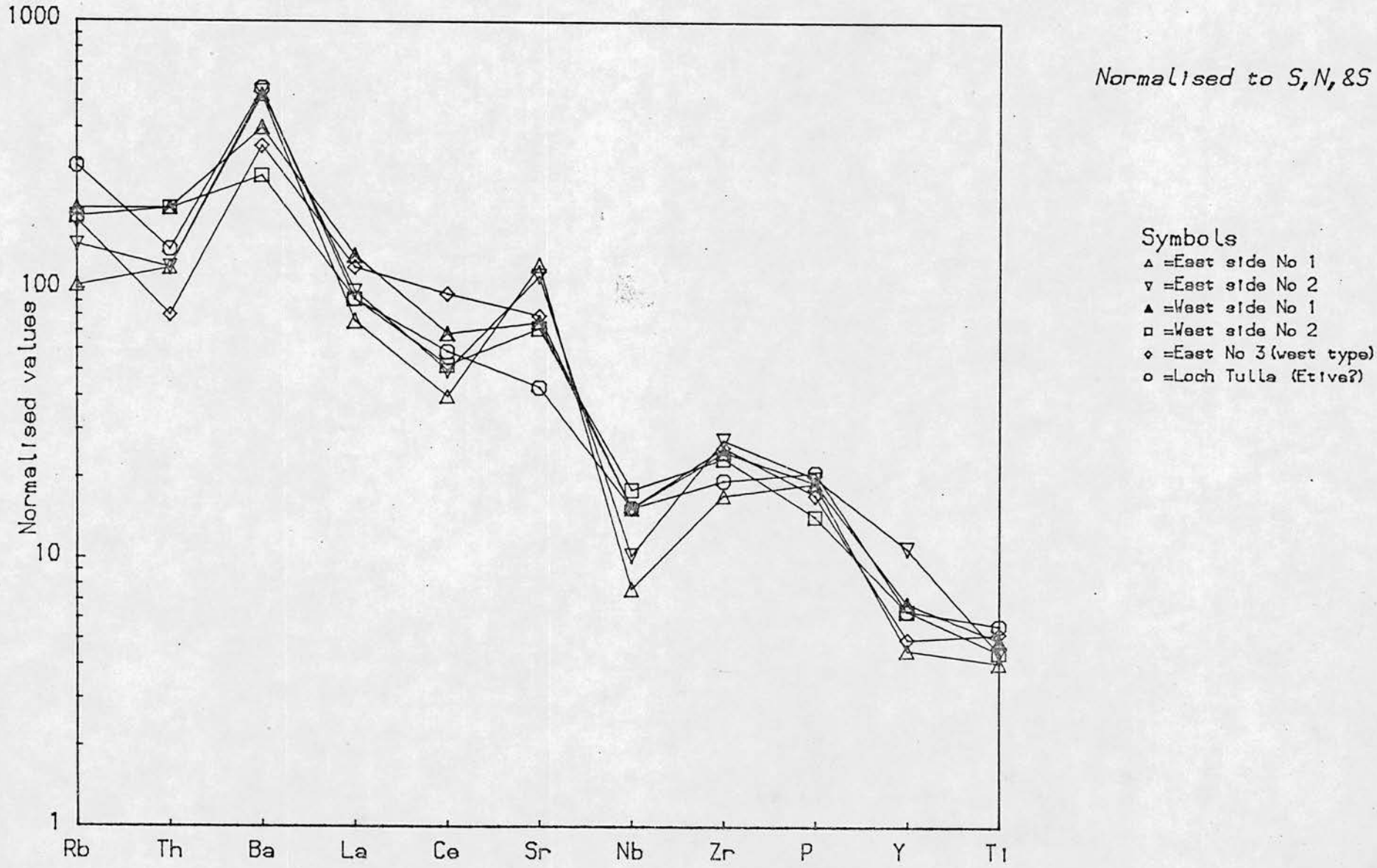

Figure 5.6.24 Data normalised to Sun, S-S, Nesbitt, R.W. and Sharaskin, A. Ya (S,N & S), (1979).

Sr against CaO shows a positive covariation with slight scatter about the trend line. The feature of enhanced Sr values to the east of the Laidon-Ericht fault and increasing to the southeast is noted. Separation of the quartz monzodiorites, granodiorites and monzogranites is good showing the granodiorites to be relatively Sr depleted with respect to monzogranites despite having modally higher plagioclase content. The Sr depletion in sample RM117 is due to the relative deficiency in plagioclase with respect to petrographically similar rocks and is mirrored by a depleted Ca value.

5.7.2 log Sr - log Rb.(fig. 5.7.2)

The evolution of the different sample groups can be identified by the overlapping trends of the data. Granodiorites from the western part of the complex are Rb enriched compared to those east of the Laidon-Ericht fault, while it is noted that there is a large variation of Rb in group III quartzmonzodiorites. Fractionation in the pulses could account for these observed features.

The monzo/syenogranites (group V) are Rb depleted, lying off the trend. This anomaly cannot be easily accounted for as the modal percentages of biotite and alkali feldspar do not relate to the observed Rb values. A distinct fall in Sr with no concomitant drop in Rb may represent a change in fractionating mineral ,possibly from plagioclase and biotite to plagioclase only.

5.7.3 log Sr - log Ce.(fig. 5.7.3)

Ce shows a weak positive correlation against Sr with good subdivision of group IV samples on a geographical basis. Those east of the Laidon-Ericht fault are Sr-enriched with the exception of the 'western' type Ce-enriched, Sr depleted granodiorite. This bias of Ce enrichment to the western part of the complex is most clearly seen in the monzogranites RM86 and RM107. Ce enrichment in sample RM76 can be related to the presence of monazite.

5.7.4 log Sr - log Ba.(fig. 5.7.4)

A plot of Sr - Ba will reflect plagioclase (Sr) and alkali feldspar and biotite (Ba) behaviour within the suite. The identification of geographically and petrographically coherent sample subtrends within the overall spread of data is thought by Fourcade and Allegre (1981) to represent separate pulses or intrusions of magma. Within group IV samples, there is an evolution to Ba and Sr depletion and subdivision of this group is possible on the basis of geographical location relative to the Laidon-Ericht fault. The subtrends noted would be consistent with biotite and calcic plagioclase fractionation at source.

The monzo/syenogranites are Ba enriched and lie off the overall trend for the basic and intermediate types, suggesting that they represent separate, more acid pulses than the last of the Ba depleted group IV granodiorites. A change of source material or source inhomogeneity could also explain the observed differences.

5.7.4 Sr - Ni,Cr.(figs. 5.7.5 & 5.7.5a)

There is little enrichment of Ni or Cr at low Sr levels but a positive overall correllation is noted. Geographical separation of group IV samples into two distinct groups, trending to zero Ni and Cr, suggesting that two pulses of magm within group IV occurred, resetting the trend of Ni and Cr values.

5.7.6 Ca/Sr - SiO2.(fig.5.7.6)

The most notable feature of this plot is the subdivision of groups IV and V samples on the basis of geographical locality in relation to the Laidon-Ericht fault. Samples from these two groups which lie to the east of the fault show lower Ca/Sr ratios to petrographically equivalent samples from west of the fault. This tendency to lower ratio values is also noted in group III samples from the southeastern part of the pluton (RM35,RM40 & RM44) close to group IV localities and is thus thought to be a primary feature. Since the group I,II & III types do not occur west of a c.2.5km zone along the western side of the fault, the above subdivisions do not apply excepting the noted example.

The Ca/Sr values of the granodiorite group IV samples found at the eastern margin indicate that they may represent a later pulse, related to the granodiorites found predominantly west of the fault. Both samples from the Loch Tulla outlier (RM25 & RM28) plot in the lower region of the groups V and IV respectively, confirming their Ca-poor, Sr-poor nature and further suggesting their similarity to the

Etive complex.

5.7.7 Ba/Rb - SiO2.(fig.5.7.7)

The variability of Ba previously noted introduces scatter on the diagram but the eastern intermediate group IV types all have ratio values 1.5 - 2 times that of the western type and the inferred later eastern granodiorite type. A distinct fall in the Ba/Rb ratio is noted between these and the syenogranites (RM36, RM37 & RM38).

The anomalously high Ba in RM37 is attributed to increased modal potassic feldspar which have up to 2.5 wt% Ba (Table 6.4) and cause the point to lie off trend. Subvertical positive trends are noted with increasing silica through groups IV and V. The marginal samples from west of the Laidon-Ericht fault show depletion in Ba/Rb values consistent with geographically similar group IV samples.

5.7.8 Rb/Sr - SiO2.(fig. 5.7.8)

The spread of data increases through the range of increasing silica and shows decreasing Sr in two possibly diverging trends. Rb enhancement/Sr depletion of the Loch Tulla outlier is noted as is the Rb depletion of the syenogranites from the eastern part of the complex. The granodiorites appear to have distinctly higher Rb/Sr values than the monzogranites and this may indicate fractionation of the different magmas at source prior to emplacement.

5.8 REE and RE-like elements.

5.8.1 Ce/Y - SiO2.(fig. 5.8.1).

The significantly enhanced Ce/Y ratios for the syenogranites RM86, RM107 may indicate a change in source for the granitic material across the Laidon-Ericht fault. Granodiorites from the eastern part of the complex by the River Ericht also show elevated Ce/Y values which would be consistent with a change in magma source material through time.

5.8.2 La - Y.(fig. 5.8.2)

This plot shows sample RM28 to be Y enriched and samples RM76 & RM109 to be La enriched. There is some separation of the petrographic types on this plot and the granodiorites appear to be intermediate between the monzogranites and quartzmonzodiorites. RM86 is significantly Y depleted giving rise to an anomalously high Ce/Y ratio (fig. 5.7.2).

5.8.3 Ce - Y.(fig. 5.8.3)

The plot of Ce against Y shows positive covariation with the syenogranitic types being both Ce and Y depleted. The monzogranites appear to be Ce depleted relative to the other intermediate types and the monzodiorites and granodiorite sample (RM76) are Ce enriched. The low Ce/highY value for the Loch Tulla quartz monzodiorite (RM28) is readily apparent.

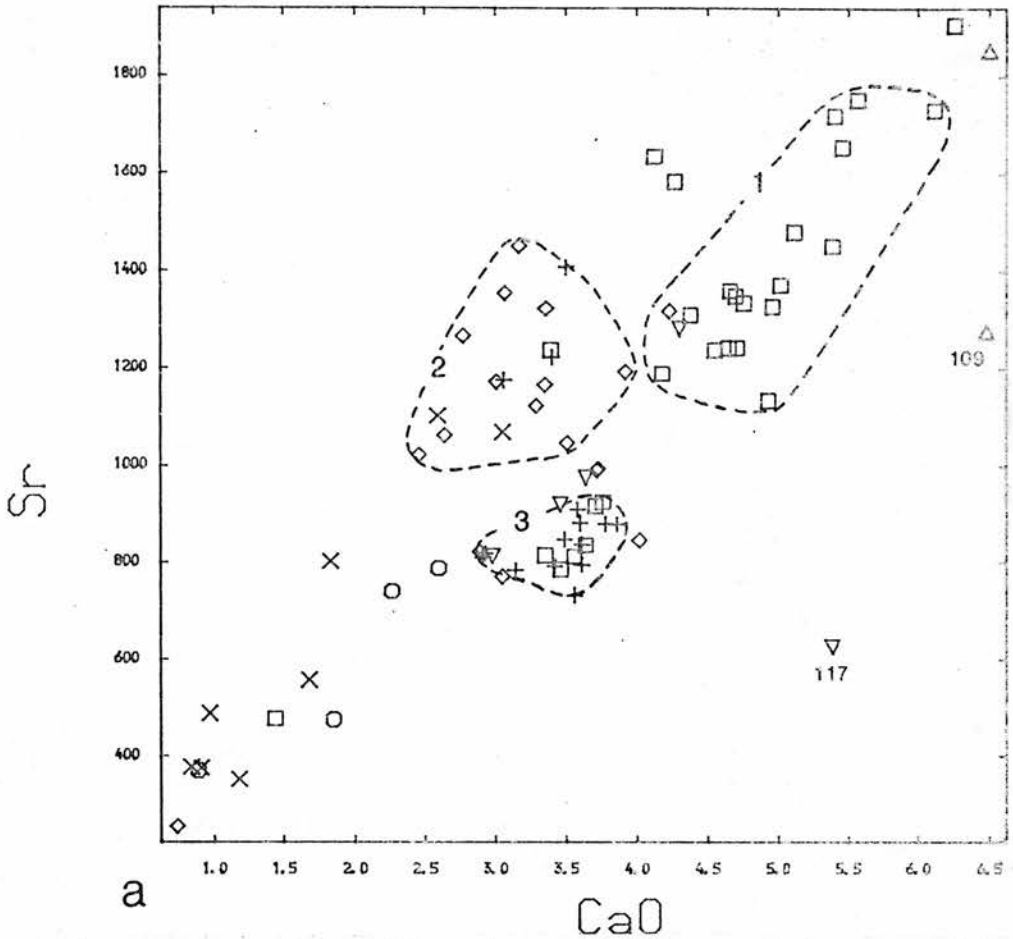

a) Figure 5.7.1, field numbers refer to rock types as follows: 1- Quartz-Monzodiorites, 2- Monzogranites, 3- Granodiorites

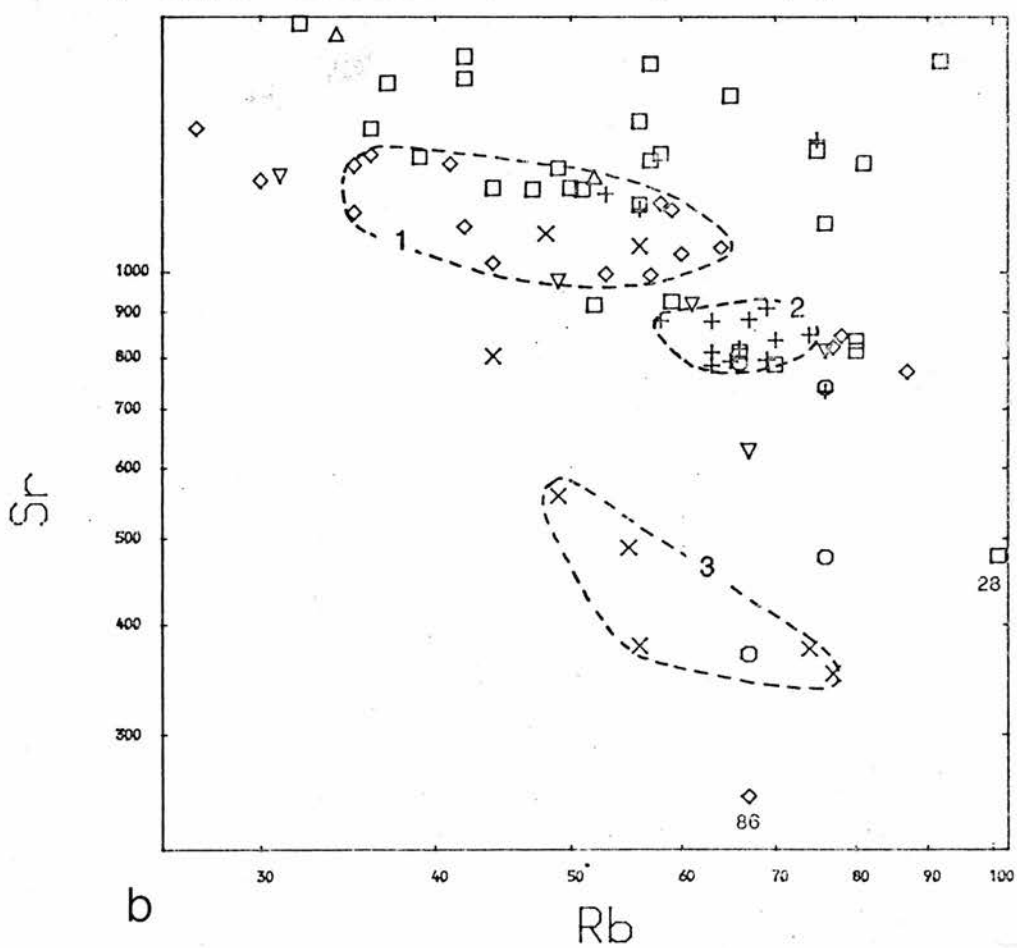

b) Figure 5.7.2, field numbers refer to rock types as follows: 1- Monzogranites, 2- Granodiorites (west and east of Laidon Ericht fault), 3- Syenogranites (group V)

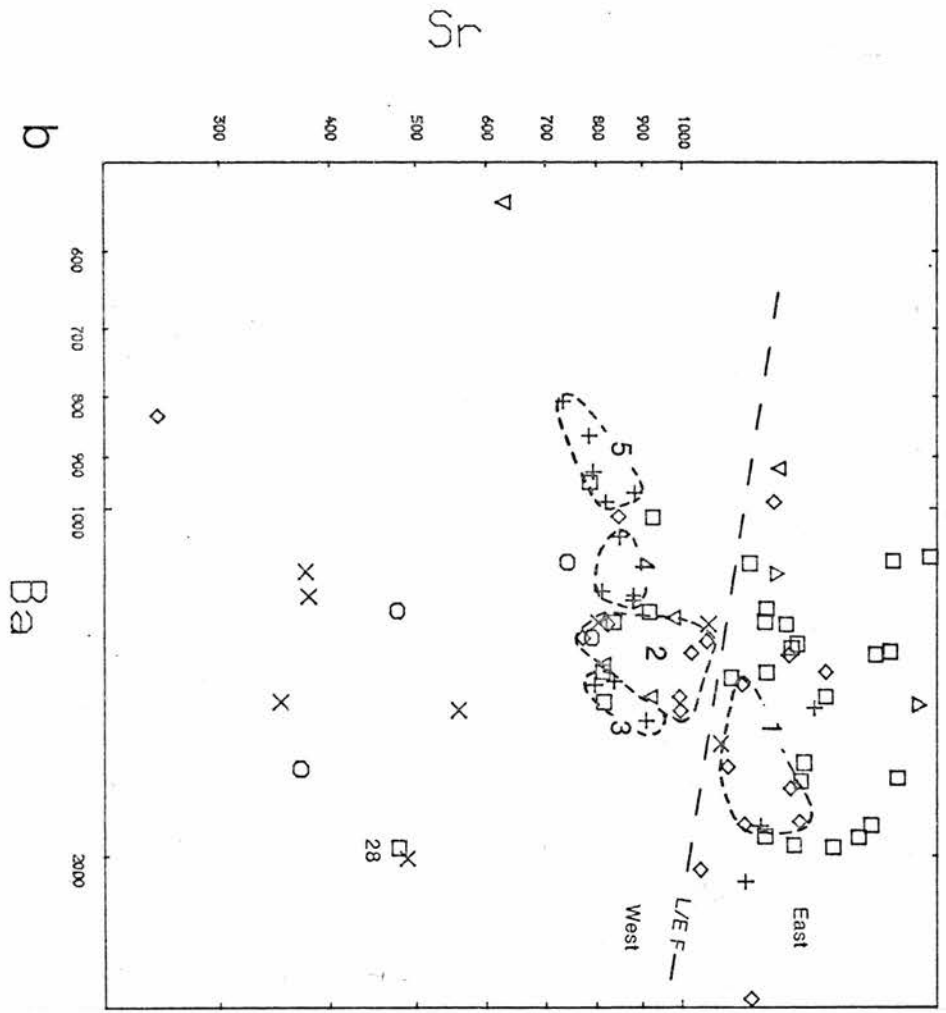

b) Figure 5.7.4, field numbers refer to rock types as follows: 1 & 2- Monzogranites, 3,4 & 5- Granodiorites. Dashed line represents division of samples by location relative to the Laidon-Ericht fault (L/E F).

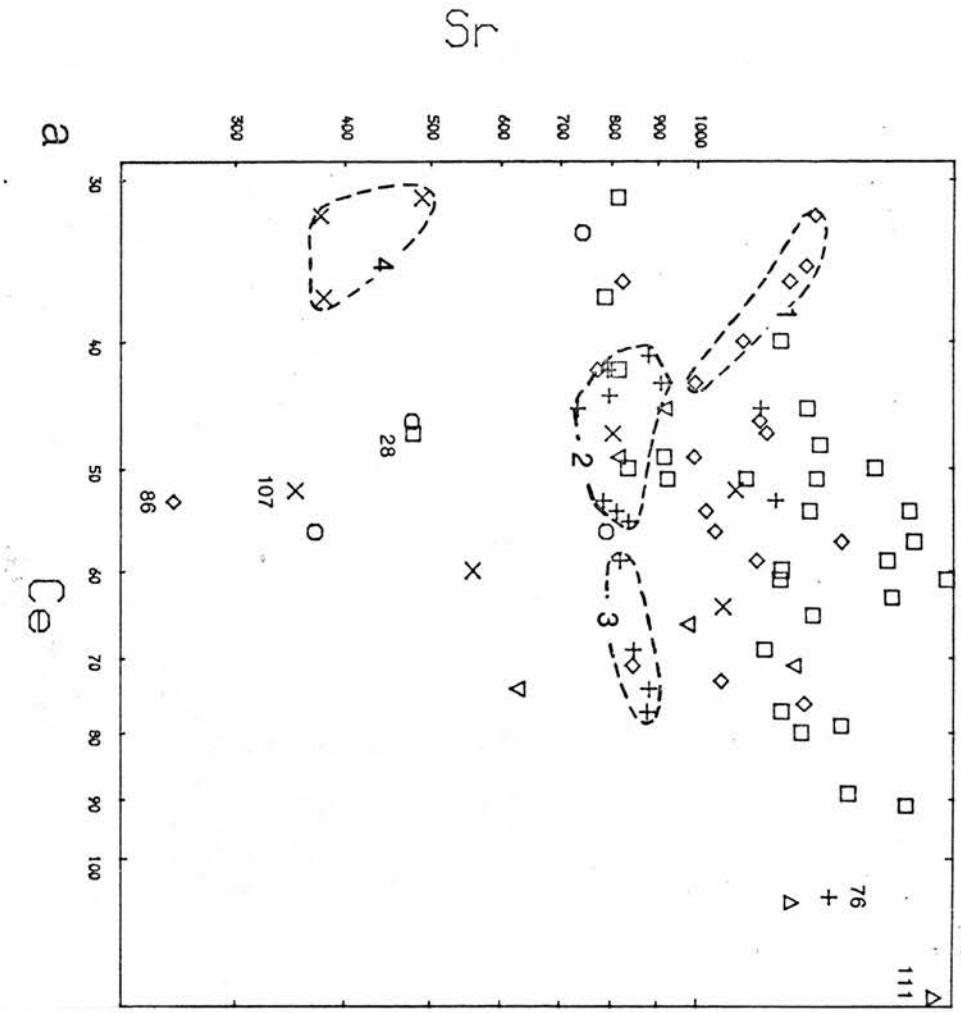

a) Figure 5.7.3, field numbers refer to rock types as follows:
1- Monzogranites from east of the Laidon-Ericht fault,
2- Granodiorites from west of the Laidon-Ericht fault,
3- Granodiorites from east of the Laidon-Ericht fault,
4- Syenogranites from east of the Laidon-Ericht fault.

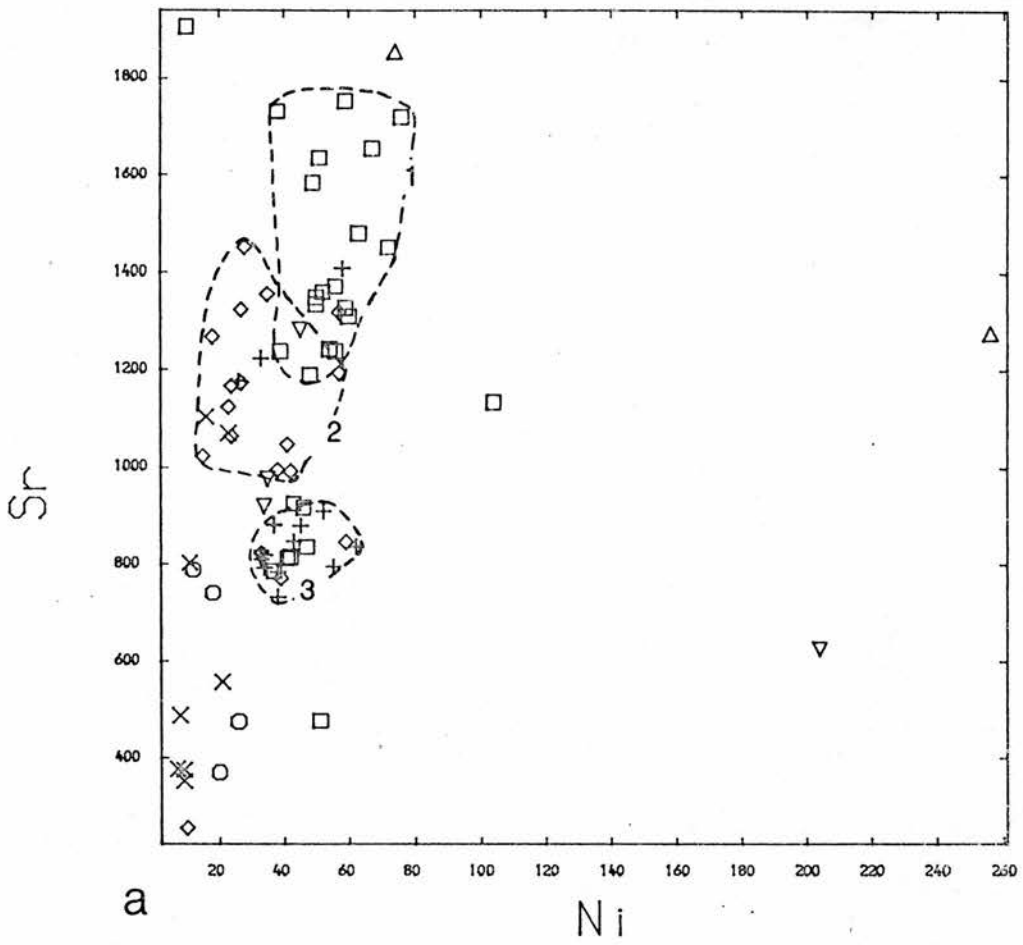

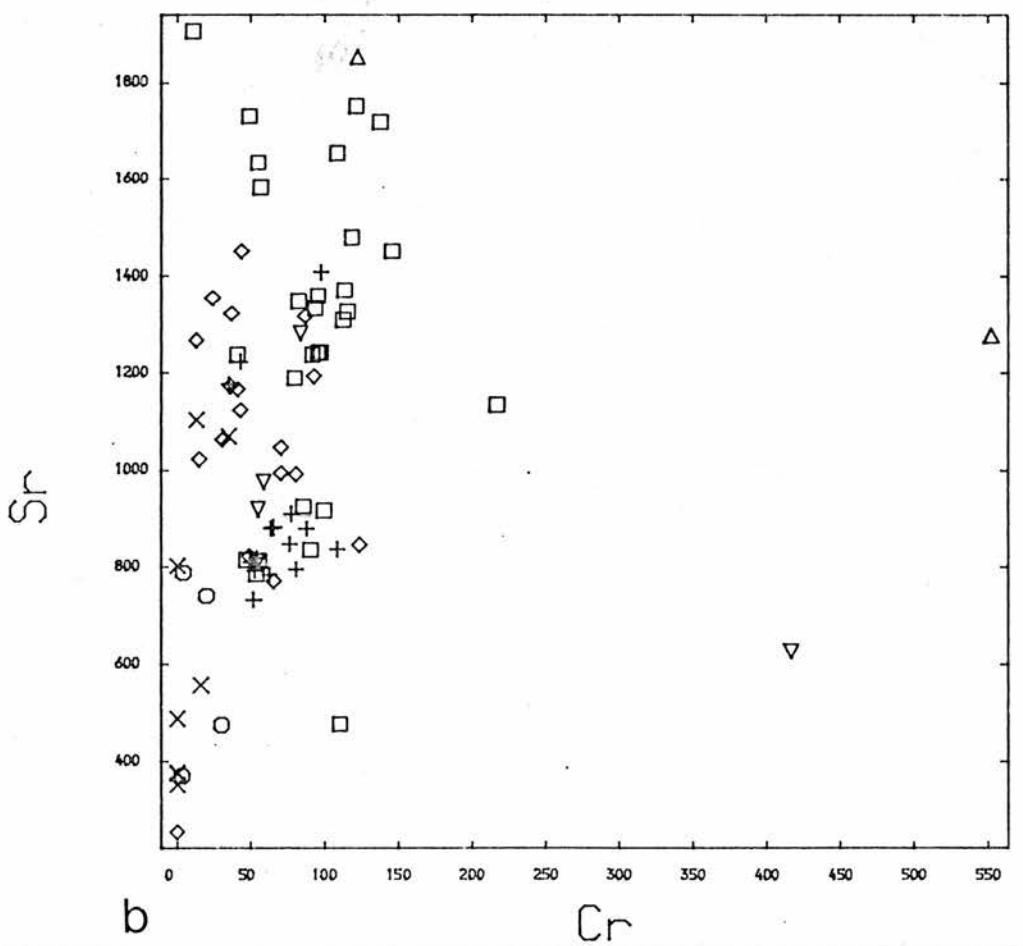

Figure 5.7.5 a & b, field numbers refer to rock types as below:
1- Quartz-Monzodiorites, 2- Monzogranites, 3- Granodiorites

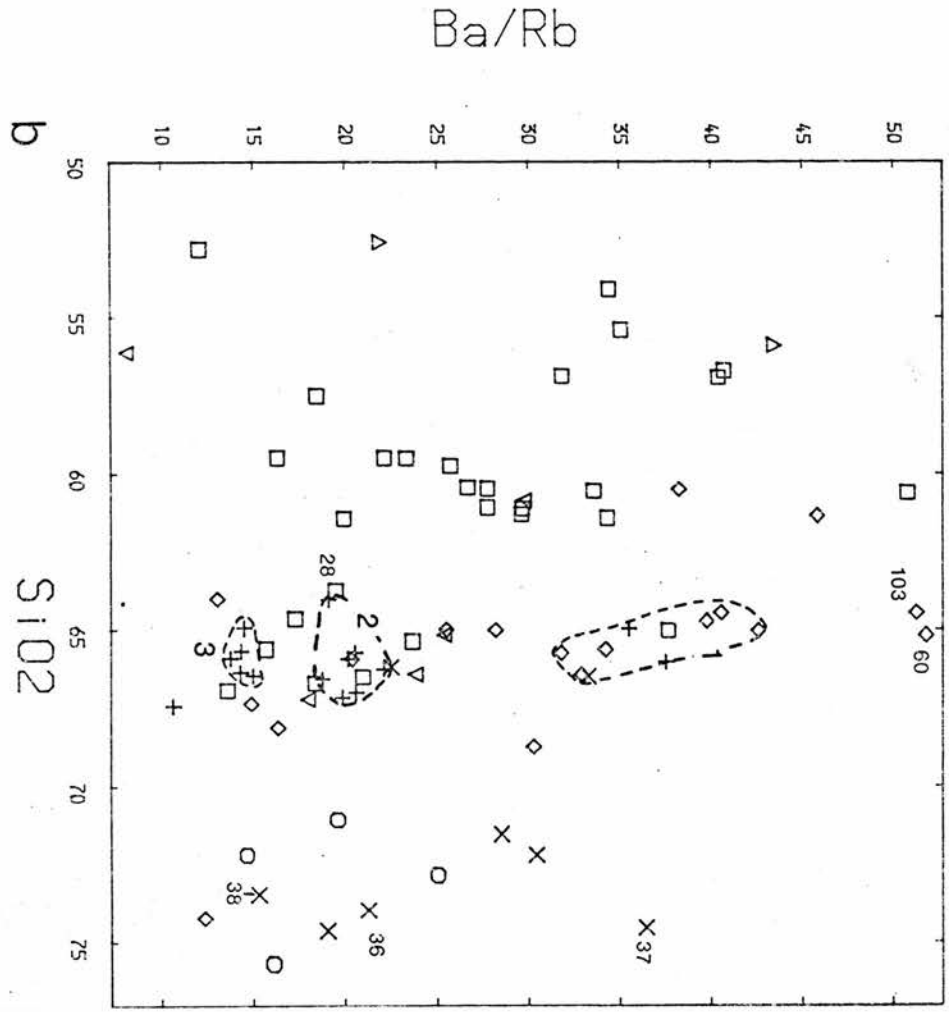

b) Figure 5.7.7, field numbers refer to rock types as follows:
1- Monzogranites from east of Laidon-Ericht fault,
2- Granodiorites from west of Laidon-Ericht fault,
3- Granodiorites from east of Laidon-Ericht fault.

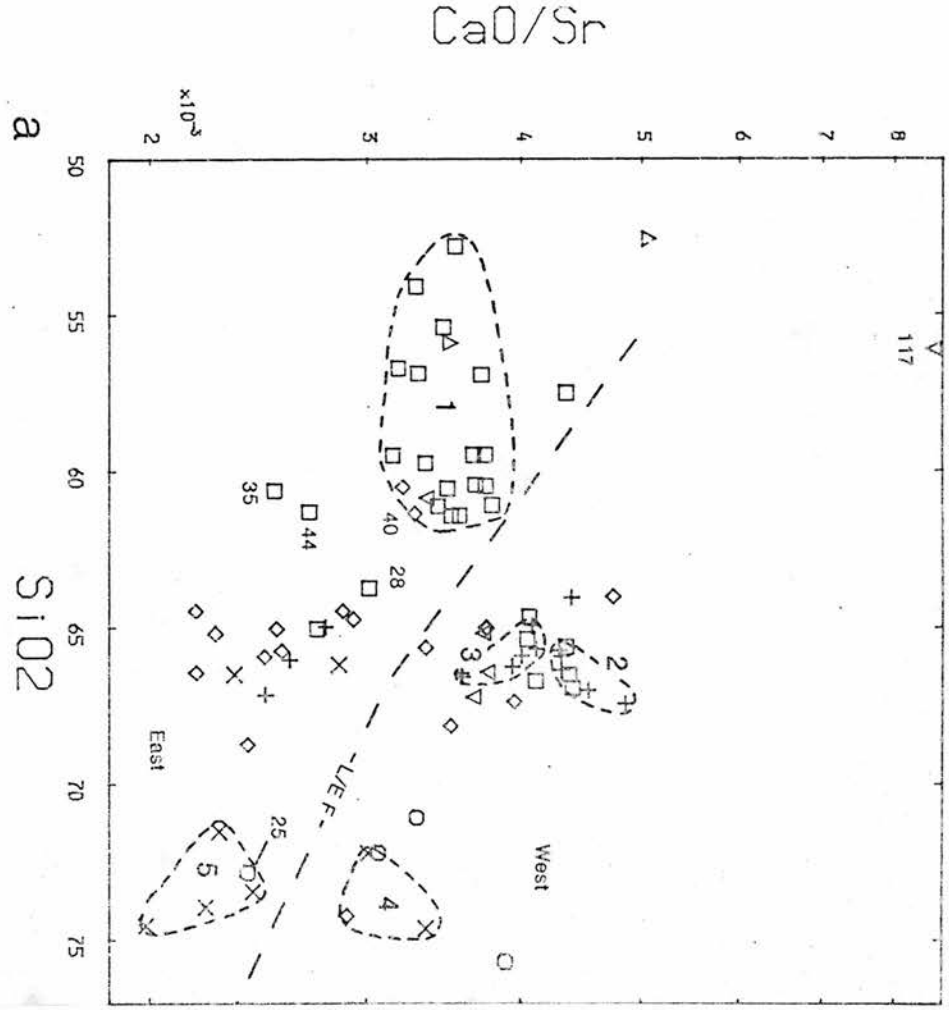

a) Figure 5.7.6, field numbers refer to rock types as follows:
1-Quartz-Monzodiorites, 2 & 3- Granodiorites
4 & 5- Monzo/syencgranites (group V). Dashed line (L/E F) represents division of samples by location relative to the Laidon-Ericht fault

a) Figure 5.7.8, field numbers refer to rock types as follows:
1- Granodiorites, 2- Monzogranites

b) Figure 5.8.1, 1- field of granodiorites.

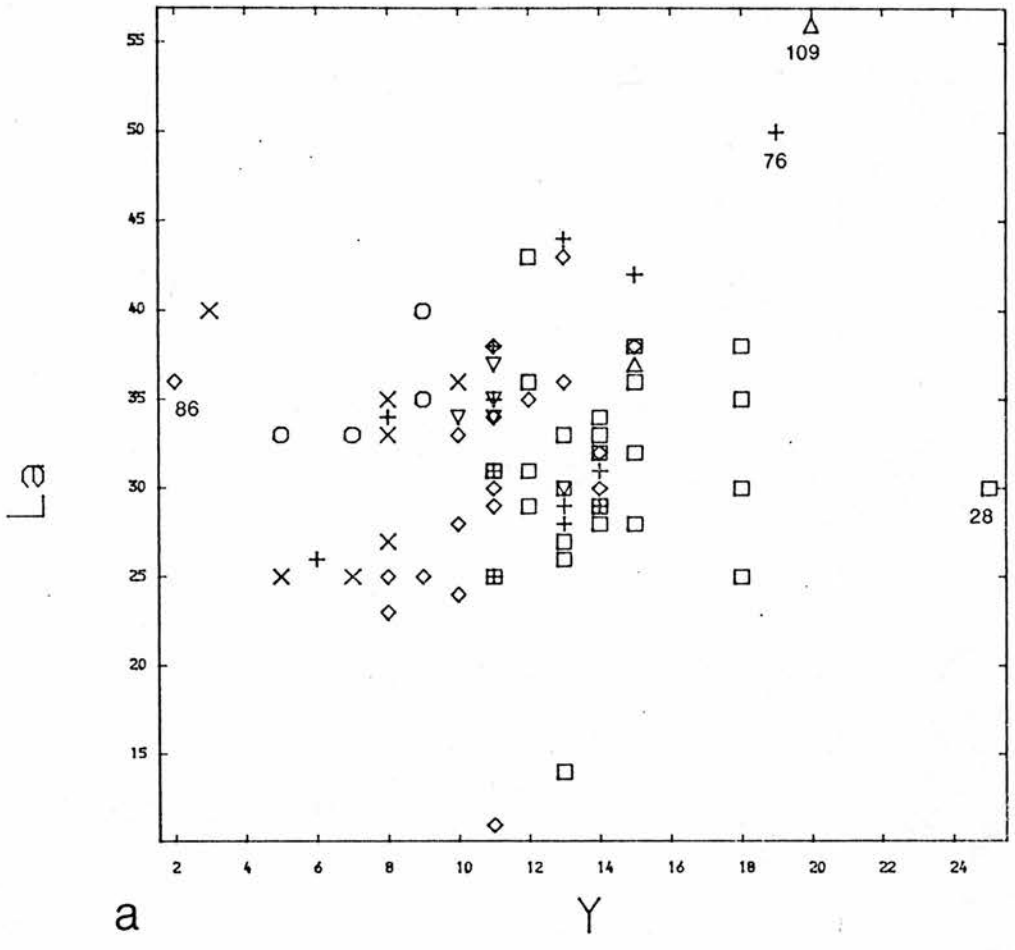

a

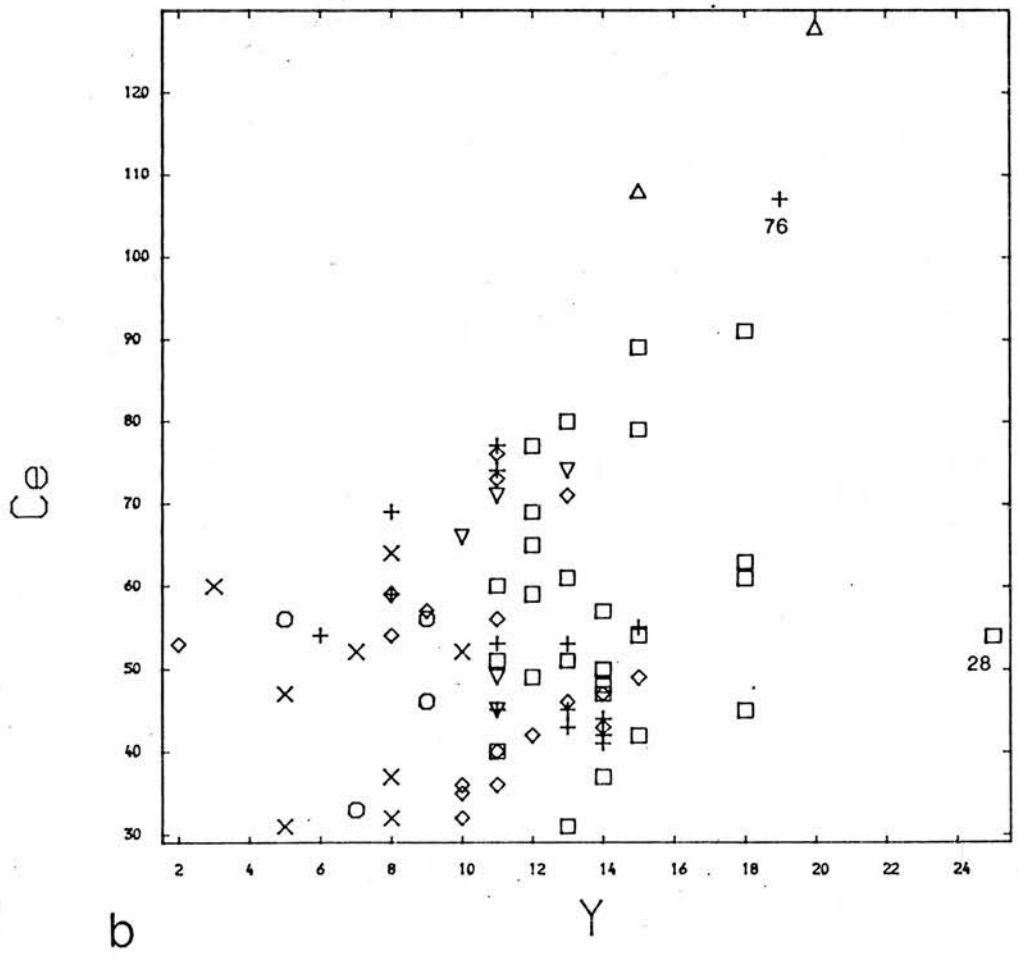

b

a) Figure 5.8.2, b) Figure 5.8.3

5.9 High field strength (HFS) elements.

5.9.1 Zr/Ti - SiO2.(fig. 5.9.1)

The increasing Zr/Ti ratio with increasing SiO2 indicates TiO2 removal before Zr implying biotite or titanomagnetite removal is the controlling mechanism. As the syenogranites lie off the trend a separate source or modified evolution of the magma is necessary to account for the displacement. The control of Ti removal from the melt is inferred to be similar as the slope of the trend is still positive.

5.9.2 Zr/Hf - TiO2.(fig. 5.9.2).

A poor negative covariation results from this ratio plot. The Zr depletion in sample RM68 is the result of a modally Fe-Ti oxide-poor mineralogy, while the trend is consistent with biotite removal as the fractionating control. The granodiorites and monzogranites can be subdivided with relation to the Laidon-Ericht fault, those samples with higher Zr/Hf ratios (usually >35) occurring west of the fault.

5.9.3 Zr - Hf.(fig. 5.9.3)

Zr shows a vague covariation with Hf but the range of absolute values for Hf makes interpretation difficult. Sample RM76 shows Hf enrichment relative to the other granodiorites and the syenogranites from east of the Laidon-Ericht fault appear to be Hf depleted relative

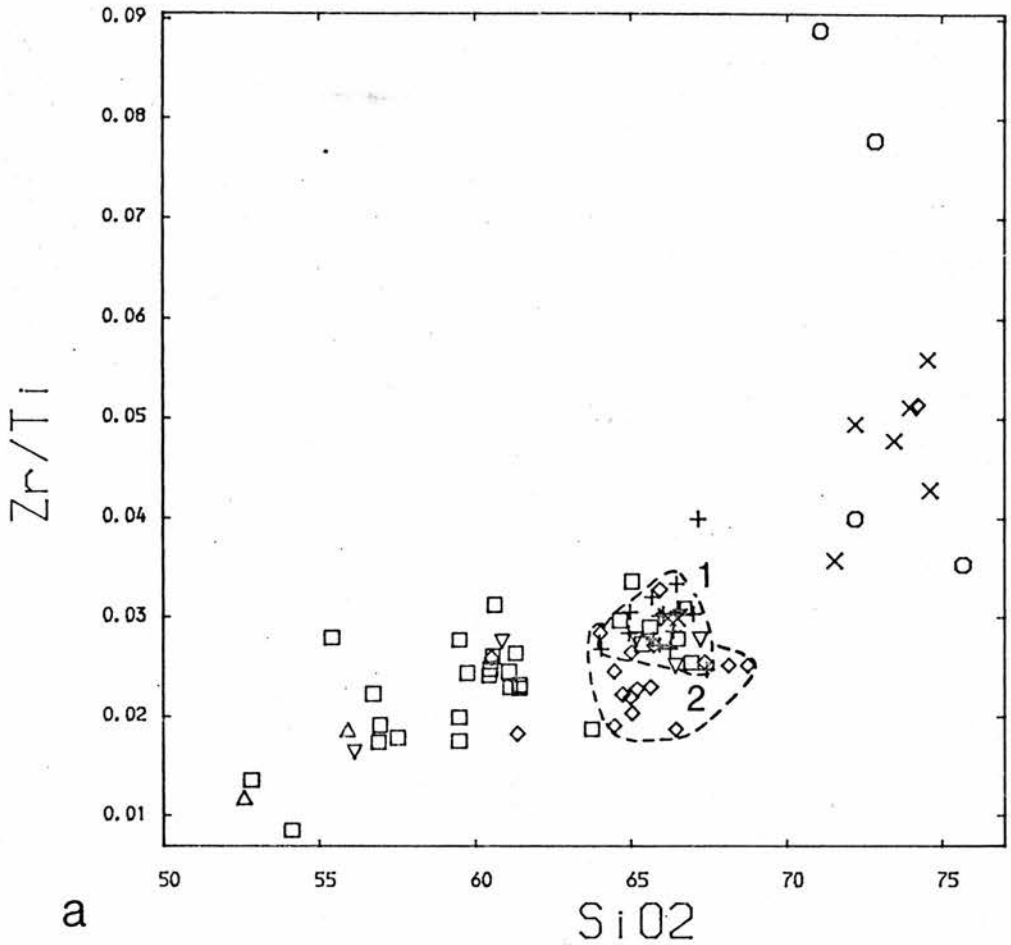

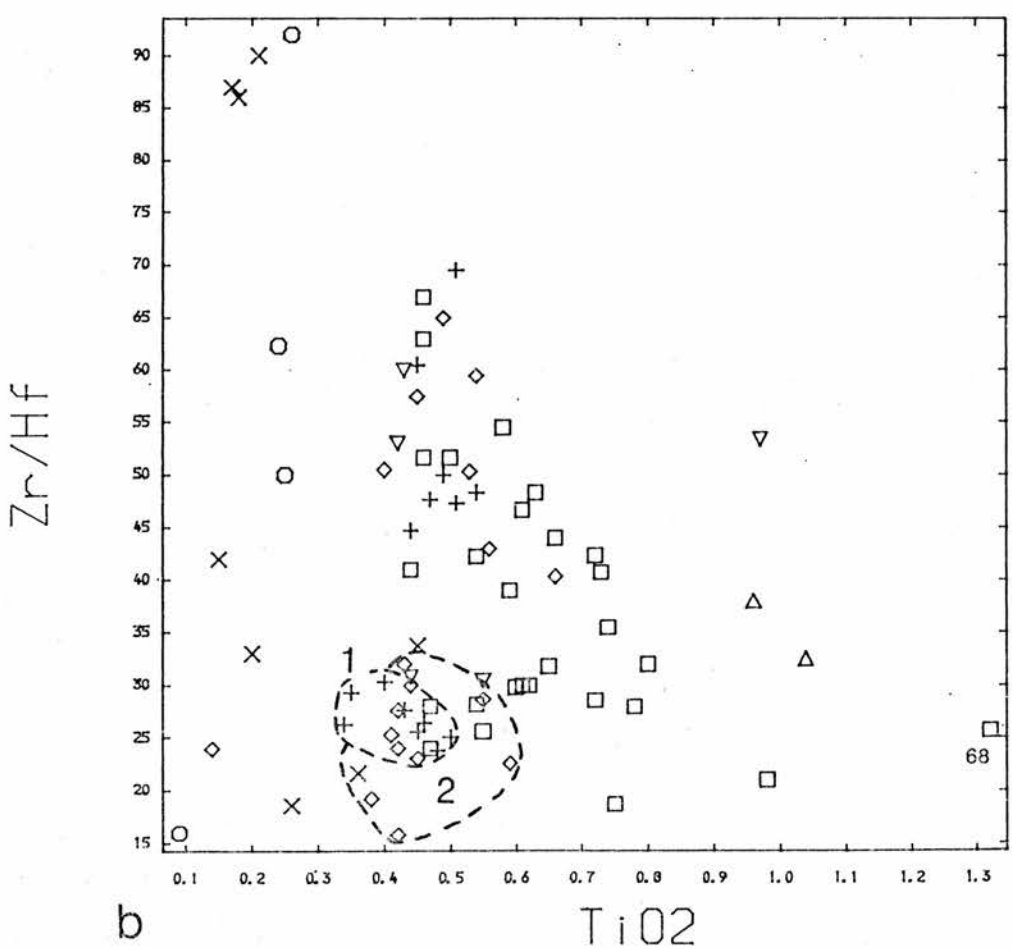

a) Figure 5.9.1, b) Figure 5.9.2, field numbers refer to rock types as follows: 1- Granodiorites, 2- Monzogranites

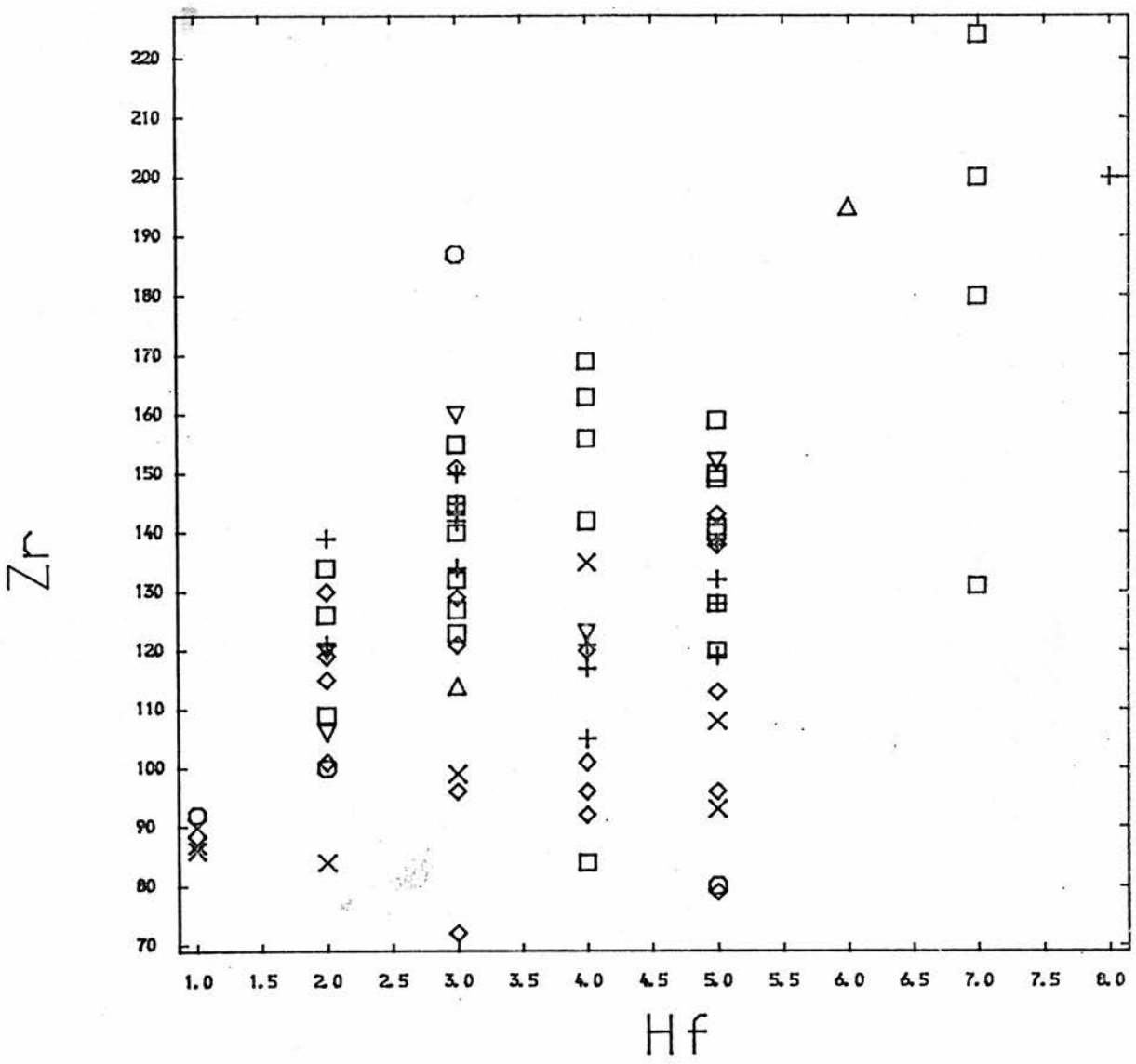
Zr
220
210
200
190
180
170
160
150
140
130
120
110
100
90
80
70
1.0
1.5
2.0
2.5
3.0
3.5
4.0
4.5
5.0
5.5
6.0
6.5
7.0
7.5
8.0
Hf

Figure 5.9.3

to those west of the fault.

SUMMARY

The overall interpretation of the major element geochemistry is that the Moor of Rannoch pluton is a high K, calc-alkaline complex which does not fit into a simple scheme involving a single intrusive pulse of magma fractionally crystallising in situ. The range of compositions presented has not been previously recorded in the literature. A strong bias to increased chemical (and petrographic) variation in the part of the complex to the east of the Laidon-Ericht fault is discussed later in Chapter 7. This bias is not thought to be a function of sampling scheme and the variations noted do represent genuine differences in origin or intrusive history between the two parts of the complex. Good correspondence between major element groups identified and modal mineralogy is noted.

Trace element geochemistry has proved useful for sudivision of the major-element groups identified, especially those in the intermediate (group IV) 64-70 wt % SiO2 range. Differences in trace element concentrations across the Laidon-Ericht fault may represent either changes in source composition or differing fractionation histories on intrusion. The possibility that the two parts of the complex may represent two different plutons juxtaposed as a result of movements along the fault is further considered in Chapter 7.

The possibility that the major and trace element variation diagrams describe an essentially continuous trend followed by a later(?), more evolved separate acidic phase is considered and more a more detailed treatment of this can be found in Chapter 7.2.

Table 6.1

Sample	RM2	RM3	RM4	RM5	RM6	RM7	RM8	RM10
SiO2	59.49	59.49	65.00	61.42	61.13	65.62	67.36	67.20
TiO2	0.72	0.66	0.54	0.61	0.63	0.56	0.45	0.43
Al2O3	17.94	18.39	16.08	17.34	17.62	15.34	15.37	15.92
Fe2O3	1.42	1.66	1.47	1.62	1.99	2.02	1.41	1.19
FeO	3.60	3.18	2.22	2.80	2.70	2.08	1.80	1.85
MnO	0.09	0.09	0.07	0.07	0.08	0.06	0.06	0.06
MgO	3.90	3.56	2.58	3.12	3.38	2.81	2.13	2.04
CaO	4.96	5.02	3.72	4.76	4.66	3.51	3.05	2.98
Na2O	4.90	4.77	4.71	5.04	4.88	4.05	4.23	4.41
K2O	2.93	2.73	2.90	2.69	2.64	3.18	3.54	3.64
P2O5	0.31	0.28	0.20	0.26	0.25	0.20	0.17	0.17
Loss	0.00	0.20	0.80	0.20	0.20	0.40	0.00	0.00
TOTAL	100.59	100.40	100.59	100.32	100.53	100.20	99.83	100.16
Nb	6	2	7	7	6	5	8	3
Zr	127	132	119	140	145	129	115	120
Y	18	14	15	15	13	11	12	11
Sr	1327	1372	992	1335	1360	1047	772	814
Rb	81	75	57	57	58	60	87	76
Th	1	6	12	5	6	7	9	17
Pb	13	24	14	10	13	12	22	16
Zn	68	64	50	58	59	46	37	42
Cu	3	3	6	5	14	5	5	5
Ni	59	56	42	50	52	41	39	33
Cr	116	114	81	94	96	71	66	55
V	103	106	76	93	87	67	55	57
Ba	1320	1660	1454	1957	1721	2054	1294	1365
Hf	3	3	2	3	3	3	2	2
Ce	45	48	49	54	51	56	42	49
La	30	34	38	38	30	38	35	37

Sample	RM11	RM13	RM16	RM17	RM17A	RM18	RM19	RM20
SiO2	56.71	68.12	66.21	65.01	60.51	72.20	65.60	65.35
TiO2	0.73	0.40	0.42	0.49	0.55	0.25	0.46	0.46
Al2O3	18.86	15.35	16.12	16.22	17.37	15.35	15.85	16.13
Fe2O3	1.78	1.13	0.95	1.37	0.61	0.00	0.91	0.54
FeO	3.53	1.70	1.90	2.15	3.45	1.82	2.30	2.84
MnO	0.09	0.06	0.05	0.07	0.08	0.04	0.06	0.07
MgO	3.98	1.78	2.01	2.54	3.13	0.78	2.50	2.77
CaO	5.57	2.89	3.46	3.73	4.23	2.27	3.64	3.71
Na2O	5.20	4.22	5.43	5.44	5.28	4.13	4.23	4.24
K2O	2.22	3.94	3.40	3.11	2.29	2.73	3.16	2.09
P2O5	0.35	0.16	0.18	0.18	0.24	0.03	0.16	0.16
Loss	0.60	0.40	0.40	0.20	2.60	0.60	0.60	0.80
TOTAL	100.04	100.40	100.81	100.81	100.67	100.43	99.74	99.43
Nb	5	5	3	6	4	4	6	7
Zr	163	101	106	130	143	100	134	126
Y	14	10	11	14	11	7	14	12
Sr	1752	823	920	994	1319	741	836	917
Rb	42	77	61	53	35	76	80	52
Th	6	5	14	3	1	19	10	3
Pb	11	16	10	14	3	24	27	16
Zn	66	39	32	42	62	23	40	40
Cu	7	6	2	4	14	13	5	9
Ni	59	33	34	38	57	18	47	46
Cr	122	49	55	71	87	20	91	100
V	109	52	60	68	85	31	65	66
Ba	1710	1260	1454	1495	1339	1113	1255	1230
Hf	4	2	2	2	5	2	2	2
Ce	57	36	45	43	76	33	50	49
La	33	33	34	30	29	33	32	36

Sample	RM22	RM25	RM28	RM29	RM30	RM32	RM33	RM34
SiO2	75.69	72.85	63.73	66.49	74.62	66.02	65.02	64.96
TiO2	0.26	0.24	0.58	0.44	0.21	0.44	0.46	0.49
Al2O3	13.09	14.98	16.69	16.43	13.61	16.62	17.09	16.81
Fe2O3	0.00	0.30	0.42	0.00	0.43	1.39	0.99	1.24
FeO	1.79	1.18	3.70	1.75	0.76	1.76	2.50	2.41
MnO	0.02	0.03	0.08	0.06	0.04	0.06	0.06	0.07
MgO	0.90	0.43	2.72	2.56	0.21	1.59	1.96	2.13
CaO	1.85	0.89	1.44	3.56	1.18	3.06	3.39	3.40
Na2O	3.33	4.80	4.86	4.19	4.21	4.89	5.51	5.06
K2O	3.08	4.42	3.50	3.10	3.92	3.49	3.11	3.12
P2O5	0.03	0.04	0.22	0.15	0.05	0.16	0.21	0.24
Loss	0.20	0.20	2.00	1.40	0.60	0.60	0.20	0.40
TOTAL	100.45	100.62	100.25	100.40	100.06	100.46	100.87	100.69
Nb	7	5	6	3	6	6	4	4
Zr	92	187	109	123	90	134	155	150
Y	9	9	14	13	10	11	11	13
Sr	476	370	478	813	352	1177	1239	1224
Rb	76	67	101	66	77	56	51	53
Th	31	15	7	3	11	11	6	2
Pb	27	24	9	15	16	13	14	12
Zn	25	27	53	51	18	54	60	56
Cu	5	31	3	5	6	7	9	8
Ni	26	20	51	41	9	26	39	33
Cr	30	3	111	56	0	35	41	43
V	33	23	84	68	14	57	65	66
Ba	1226	1679	1966	1384	1468	2102	1922	1882
Hf	1	3	2	3	1	3	3	3
Ce	46	56	47	31	52	45	40	53
La	35	40	29	26	36	35	31	44

Sample	RM35	RM36	RM37	RM38	RM40	RM43	RM44	RM51
SiO2	60.63	73.97	74.54	73.46	61.35	66.70	61.30	65.90
TiO2	0.54	0.17	0.15	0.18	0.66	0.50	0.59	0.51
Al2O3	18.70	14.22	14.13	13.95	16.94	16.15	18.18	14.77
Fe2O3	1.62	0.55	0.42	0.44	0.00	0.99	1.78	1.12
FeO	2.55	0.74	0.70	0.80	4.72	2.11	2.70	2.41
MnO	0.07	0.01	0.01	0.03	0.08	0.07	0.07	0.07
MgO	2.53	0.30	0.18	0.30	3.42	2.05	2.77	2.74
CaO	4.13	0.84	0.97	0.91	3.92	3.35	4.27	3.61
Na2O	5.80	4.25	4.28	4.51	4.48	4.53	4.70	4.09
K2O	2.61	4.38	4.25	4.15	3.13	3.11	2.57	3.13
P2O5	0.28	0.03	0.03	0.04	0.24	0.20	0.27	0.20
Loss	0.60	0.20	0.40	0.60	1.20	0.60	0.60	1.40
TOTAL	100.47	99.85	100.34	99.55	100.59	100.64	100.21	100.24
Nb	1	4	3	7	5	7	5	6
Zr	169	87	84	86	121	155	156	139
Y	12	8	5	8	14	15	14	15
Sr	1635	378	488	375	1194	815	1584	837
Rb	37	56	55	74	58	80	65	70
Th	4	10	10	9	7	9	6	10
Pb	18	19	19	21	15	12	8	20
Zn	68	8	6	16	66	45	62	51
Cu	9	8	5	3	30	6	2	8
Ni	51	7	8	9	57	42	49	62
Cr	55	0	0	0	93	47	57	109
V	77	16	12	14	96	63	88	79
Ba	1880	1191	2007	1134	2659	1470	1927	1411
Hf	4	1	2	1	3	3	4	2
Ce	59	37	31	32	47	42	50	55

Sample	RM52	RM54	RM55	RM57	RM60	RM63	RM64	RM68
SiO2	66.24	65.71	66.99	64.72	65.17	65.03	65.74	52.82
TiO2	0.45	0.51	0.47	0.43	0.42	0.45	0.44	1.32
Al2O3	15.85	16.09	15.06	16.63	16.37	16.61	16.20	17.38
Fe2O3	0.91	1.21	1.13	0.73	1.18	1.38	1.23	1.95
FeO	2.14	2.30	2.03	2.31	2.03	2.11	1.90	5.15
MnO	0.06	0.07	0.06	0.06	0.06	0.07	0.06	0.07
MgO	2.24	2.49	2.39	1.98	1.74	2.16	1.84	5.52
CaO	3.58	3.78	3.61	3.29	3.07	3.36	3.01	6.12
Na2O	4.30	4.43	3.83	4.98	5.11	4.76	4.77	3.83
K2O	3.22	2.60	3.09	3.02	2.90	2.93	3.40	3.51
P2O5	0.19	0.20	0.19	0.19	0.20	0.20	0.20	0.69
Loss	0.40	0.60	0.60	1.20	1.40	1.20	0.40	1.00
TOTAL	99.88	100.25	99.73	99.87	100.01	100.61	99.54	99.71
Nb	5	6	7	3	3	2	4	12
Zr	121	142	143	96	96	92	120	180
Y	13	14	14	11	10	10	13	25
Sr	910	880	796	1124	1356	1324	1174	1731
Rb	69	58	69	42	36	41	59	92
Th	7	8	14	4	6	5	6	0
Pb	12	14	19	16	14	25	14	0
Zn	47	47	42	53	44	52	48	57
Cu	7	4	8	32	8	15	6	3
Ni	52	37	55	23	35	27	27	38
Cr	78	64	81	43	24	37	36	49
V	67	71	64	65	56	63	57	64
Ba	1525	1190	1420	1671	1866	1746	1875	1111
Hf	2	3	3	3	4	4	4	7
Ce	43	41	44	40	32	35	46	54
La	29	31	29	30	24	28	36	30

Sample	RM69	RM70	RM71	RM76	RM77	RM78	RM79	RM81
SiO2	56.88	55.41	67.42	67.14	66.34	66.92	60.48	59.50
TiO2	0.75	0.80	0.48	0.50	0.46	0.47	0.60	0.72
Al2O3	18.85	18.74	15.60	15.82	15.53	15.89	17.25	17.97
Fe2O3	1.90	1.28	1.25	1.45	1.59	1.65	1.08	0.00
FeO	3.45	4.15	2.06	1.73	1.69	1.81	3.20	3.79
MnO	0.09	0.10	0.06	0.11	0.07	0.06	0.07	0.10
MgO	4.05	3.96	2.06	1.95	2.24	2.19	3.14	3.74
CaO	5.46	5.12	3.56	3.50	3.42	3.46	4.65	5.41
Na2O	5.49	4.72	4.49	4.29	3.73	3.99	4.75	4.81
K2O	2.19	2.93	2.83	3.11	2.91	2.92	2.49	2.28
P2O5	0.33	0.36	0.15	0.16	0.15	0.15	0.27	0.32
Loss	0.60	1.20	0.00	0.60	1.40	0.80	0.80	0.60
TOTAL	100.41	99.20	100.17	100.74	99.76	100.54	99.09	99.63
Nb	6	6	6	10	7	6	5	8
Zr	131	224	119	200	132	120	149	200
Y	18	15	13	19	14	14	11	18
Sr	1654	1480	733	1408	793	786	1243	1719
Rb	42	56	76	75	65	70	44	57
Th	0	0	7	6	10	11	3	0
Pb	14	5	17	9	21	18	5	11
Zn	83	95	52	79	50	53	68	91
Cu	18	35	7	27	7	8	31	19
Ni	67	63	38	58	34	37	54	76
Cr	109	119	52	98	53	54	96	138
V	106	113	65	160	67	66	88	130
Ba	1338	1965	807	1488	929	949	1222	1330
Hf	7	7	5	8	5	5	5	7
Ce	63	89	45	107	42	37	60	91
La	35	36	28	50	29	28	31	38

Sample	RM85	RM86	RM89	RM90	RM91	RM92	RM93	RM94
SiO2	61.44	74.23	57.51	54.30	65.46	64.93	64.04	66.56
TiO2	0.55	0.14	0.78	1.04	0.44	0.45	0.54	0.34
Al2O3	17.15	12.79	17.30	17.81	15.64	15.60	15.16	15.13
Fe2O3	1.17	0.00	1.10	1.89	1.00	0.76	1.21	0.65
FeO	2.89	1.37	4.36	4.42	2.38	2.36	2.76	2.02
MnO	0.07	0.01	0.11	0.10	0.06	0.05	0.07	0.05
MgO	2.80	0.54	4.41	3.57	2.63	2.18	2.72	1.75
CaO	4.18	0.74	4.93	6.26	3.74	3.60	3.86	2.91
Na2O	5.06	3.50	3.95	4.56	3.73	4.75	3.89	5.36
K2O	2.83	4.93	3.08	2.27	2.93	3.19	3.14	3.76
P2O5	0.23	0.02	0.25	0.40	0.16	0.18	0.18	0.15
Loss	1.00	0.80	1.00	1.20	0.60	1.20	1.40	0.60
TOTAL	99.66	99.21	99.13	98.18	99.04	99.49	99.24	99.52
Nb	5	6	3	4	2	5	6	0
Zr	128	72	140	84	123	128	145	105
Y	12	2	13	18	10	11	11	6
Sr	1190	256	1135	1906	976	882	879	811
Rb	56	67	76	32	49	67	63	63
Th	5	10	0	2	3	8	4	5
Pb	13	16	3	7	8	10	6	13
Zn	63	19	82	82	51	34	60	39
Cu	18	20	138	55	6	5	6	6
Ni	48	10	104	10	35	37	45	33
Cr	80	0	217	11	59	66	88	50
V	80	20	109	153	64	65	80	51
Ba	1116	830	1402	1102	1244	970	1202	1180
Hf	5	3	5	4	4	5	3	4
Ce	69	53	51	61	66	74	77	54
La	29	36	14	25	34	31	38	26

Sample	RM95	RM96	RM97	RM98	RM99	RM100	RM101	RM102
SiO2	61.09	65.88	59.86	64.65	71.53	66.43	68.72	56.93
TiO2	0.61	0.40	0.65	0.47	0.26	0.42	0.38	0.74
Al2O3	16.76	15.73	17.74	16.09	15.28	16.34	16.29	18.51
Fe2O3	1.16	1.15	1.26	1.20	0.20	0.26	0.86	0.98
FeO	3.22	1.81	3.45	2.49	1.67	2.65	1.94	3.70
MnO	0.07	0.05	0.09	0.07	0.03	0.06	0.05	0.10
MgO	3.19	2.03	3.70	2.53	0.95	1.73	1.51	4.30
CaO	4.71	3.14	4.38	3.76	1.83	2.77	2.46	5.39
Na2O	4.64	4.15	4.27	4.19	4.11	4.16	4.63	5.14
K2O	2.70	3.49	2.39	2.83	4.11	3.36	3.23	2.33
P2O5	0.24	0.16	0.29	0.18	0.07	0.15	0.13	0.31
Loss	0.60	0.60	0.80	1.20	0.40	0.60	0.40	1.00
TOTAL	99.32	98.81	99.21	99.91	100.68	99.19	100.87	99.80
Nb	5	3	4	4	3	0	4	4
Zr	150	121	159	140	93	79	96	142
Y	12	11	13	11	5	11	8	15
Sr	1243	784	1310	926	803	1268	1023	1452
Rb	50	63	49	59	44	30	44	36
Th	2	12	1	4	1	3	4	0
Pb	8	16	8	14	13	7	10	5
Zn	66	40	71	56	27	44	45	82
Cu	9	6	16	5	8	6	7	23
Ni	54	38	60	43	11	18	15	72
Cr	98	63	113	86	0	13	15	146
V	89	56	101	70	34	70	51	127
Ba	1388	865	1261	1019	1255	987	1333	1455
Hf	5	4	5	5	5	5	5	4
Ce	77	53	80	51	47	36	54	79
La	36	25	33	25	25	11	23	32

Sample	RM103	RM104	RM106	RM107	RM109	RM110	RM111	RM112
SiO2	64.47	60.44	66.16	72.20	52.58	66.48	55.80	64.47
TiO2	0.59	0.62	0.45	0.20	0.96	0.36	1.04	0.41
Al2O3	16.31	17.58	16.45	14.16	14.87	16.95	18.99	17.10
Fe2O3	1.92	1.17	0.46	0.89	1.87	1.01	1.28	1.25
FeO	2.13	3.05	2.08	1.02	5.17	1.74	4.41	2.25
MnO	0.08	0.07	0.06	0.02	0.12	0.04	0.09	0.06
MgO	1.13	3.26	1.97	1.00	8.83	1.47	4.28	1.89
CaO	3.17	4.55	3.05	1.68	6.48	2.59	6.50	3.35
Na2O	4.14	4.96	4.80	2.94	3.43	5.16	5.14	4.40
K2O	3.63	2.48	3.24	4.67	2.61	3.45	2.25	2.61
P2O5	0.25	0.24	0.16	0.08	0.37	0.18	0.48	0.21
Loss	1.00	1.20	0.40	0.40	1.40	0.40	0.40	1.20
TOTAL	99.15	99.93	99.56	99.50	99.07	100.14	101.08	99.50
Nb	2	5	6	4	8	4	12	3
Zr	113	150	135	99	114	108	195	101
Y	9	13	8	3	15	7	20	8
Sr	1452	1239	1070	558	1279	1104	1854	1167
Rb	27	47	56	49	52	48	34	35
Th	0	5	4	3	0	1	0	0
Pb	5	7	15	11	2	9	0	10
Zn	68	67	53	35	84	40	82	55
Cu	30	14	12	17	32	22	13	17
Ni	28	56	23	21	256	16	74	24
Cr	44	92	35	16	552	13	123	41
V	78	93	58	36	145	49	131	63
Ba	1385	1254	1259	1492	1140	1598	1479	1420
Hf	5	5	4	3	3	5	6	4
Ce	57	61	64	60	108	52	128	59
La	25	27	35	40	37	25	56	25

Sample	RM113	RM114	RM115	RM116	RM117	RM118	RM119	RM120
SiO2	60.86	65.91	66.44	60.56	56.26	65.65	71.08	64.01
TiO2	0.55	0.42	0.35	0.54	0.97	0.43	0.09	0.53
Al2O3	16.94	16.53	15.45	17.95	14.36	16.00	15.69	15.60
Fe2O3	1.52	1.31	1.41	1.27	1.60	0.38	0.00	0.64
FeO	2.72	1.78	1.78	2.77	4.70	3.03	1.61	3.38
MnO	0.07	0.07	0.06	0.07	0.14	0.06	0.01	0.08
MgO	2.80	1.64	1.99	2.86	6.86	2.29	0.57	2.89
CaO	4.30	2.64	2.93	4.70	5.39	3.49	2.60	4.02
Na2O	5.32	5.09	4.52	6.02	4.25	4.19	3.66	3.89
K2O	2.09	3.33	3.45	2.35	2.74	3.17	3.30	3.17
P2O5	0.26	0.10	0.20	0.28	0.32	0.14	0.03	0.21
Loss	1.60	1.20	1.00	1.00	1.20	0.60	1.00	1.00
TOTAL	99.31	100.31	99.81	100.70	99.03	99.69	99.88	99.68
Nb	3	4	5	3	12	4	3	7
Zr	152	138	117	141	160	138	80	151
Y	11	11	8	12	13	8	5	13
Sr	1283	1064	819	1349	627	848	789	847
Rb	31	64	66	39	67	74	66	78
Th	6	2	10	4	8	5	5	5
Pb	10	12	17	12	2	16	10	7
Zn	49	59	51	64	102	57	17	51
Cu	21	16	9	14	26	91	11	8
Ni	45	24	34	50	204	43	12	59
Cr	84	31	54	83	417	77	4	124
V	78	56	62	87	138	74	22	86
Ba	923	1303	987	1310	545	1059	1293	1017
Hf	5	5	4	5	3	5	5	3
Ce	71	73	59	65	74	69	56	71
La	35	34	34	31	30	34	33	43

Sample	SOG1	SOG2	SOG2A	SOG3	SOG4	SOG5
SiO2	71.20	63.92	60.40	66.38	51.67	52.83
TiO2	0.41	0.58	0.73	0.36	1.16	1.51
Al2O3	13.81	16.80	16.80	15.79	16.17	17.87
Fe2O3	1.00	1.69	1.00	1.05	1.63	2.50
FeO	1.81	2.51	3.75	1.81	4.95	5.52
MnO	0.05	0.08	0.08	0.60	0.11	0.11
MgO	1.82	2.57	3.50	1.92	7.45	5.08
CaO	2.69	4.00	4.17	3.19	9.86	7.42
Na2O	3.06	4.26	4.11	4.15	2.47	3.18
K2O	3.04	2.50	2.94	3.15	1.46	1.93
P2O5	0.16	0.21	0.31	0.13	0.30	0.55
Loss	0.60	0.40	1.20	1.00	1.60	1.00
TOTAL	99.85	99.75	99.31	99.77	99.04	99.75
Nb	10	5	6	6	5	8
Zr	145	149	153	122	91	139
Y	17	13	10	9	16	27
Sr	562	855	1147	709	718	1086
Rb	80	78	40	70	35	50
Th	12	6	1	1	4	0
Pb	13	7	3	11	5	7
Zn	40	56	53	44	55	83
Cu	6	5	10	5	60	19
Ni	30	44	58	30	105	27
Cr	37	80	103	49	325	84
V	56	79	93	54	172	242
Ba	896	853	1379	1173	475	658
Hf	4	4	6	3	2	4
Ce	54	57	86	46	45	86
La	32	30	39	27	14	26

Sample	SOG6	SOG7	SOG8	SOG9	SOG10
SiO2	61.30	63.37	59.58	65.77	66.96
TiO2	0.72	0.69	0.70	0.62	0.96
Al2O3	16.41	16.33	17.03	15.74	16.51
Fe2O3	1.70	0.61	2.36	1.38	5.06
FeO	2.79	3.70	2.89	2.28	1.80
MnO	0.07	0.08	0.08	0.07	0.05
MgO	3.22	2.83	4.53	2.36	1.94
CaO	4.45	4.09	5.42	3.41	1.45
Na2O	4.28	3.73	4.01	4.01	1.85
K2O	2.73	3.34	2.34	3.27	3.35
P2O5	0.23	0.20	0.24	0.22	0.15
Loss	1.00	0.40	0.40	0.40	0.20
TOTAL	99.15	99.63	99.82	99.75	100.48
Nb	13	7	12	12	10
Zr	264	143	253	173	172
Y	21	14	22	21	20
Sr	757	950	674	617	624
Rb	78	57	108	94	120
Th	7	2	11	16	18
Pb	12	5	10	15	16
Zn	59	66	61	52	45
Cu	24	11	15	7	6
Ni	44	81	35	34	30
Cr	104	215	78	75	48
V	96	111	93	77	57
Ba	864	854	945	845	689
Hf	6	3	5	6	4
Ce	83	68	87	70	71
La	42	29	39	38	30

Mineral Chemistry

6.0 Introduction.

Polished thin sections representative of the geochemical and petrographic range found within the Moor of Rannoch pluton were selected and their major constituent minerals analysed using an electron microprobe (see Appendix B). The objective was to establish and explain any chemical variation found within the major crystallising phases. Although the total number of mineral analyses is small, compositional variation is evident and tentatively correlatable with bulk rock chemical variation.

6.1 AMPHIBOLES

The amphiboles from the Moor of Rannoch show limited chemical variation and are predominantly magnesio hornblendes. Average analyses from 34 analyses are presented in Table 6.1. The various substitution schemes possible within amphiboles are briefly reviewed in an attempt to explain such variation found.

6.1.1 Substitutions within amphibole.

Amphiboles possess complex crystal chemistry which permits a number of cation substitutions to be made. These substitutions are not mutually exclusive and so, to simplify interpretation, they are thought of as a series of end member interactions. An accepted definition of the amphibole structure is: $A_{0-1}\ B_2\ C_5\ T_8\ O_{22}\ (OH,F,Cl)_2$

(after Leake, 1978; Hawthorne, 1981).

where A = Na, K; B = Na, Li, Ca, Mn, Fe^{3+}, Mg; C = Mg, Fe^{2+}, Mn, Al, Fe^{3+}, Ti; T = Si, Al, Fe^{3+}.

The nomenclature of Leake (1978) is based on cation occupancy of the B-site as this is a dominant factor in amphibole crystal structure and chemistry. However, amphibole compositions are the product of coupled, as well as simple substitutions (e.g. Mg^{2+} - Fe^{2+}), (Czamanske and Wones (1973), Leake (1978) and Hawthorne (1981)). Amphibole compositions from Moor of Rannoch are plotted in Figs. 6.1.1 - 6.1.8 in an attempt to identify the substitution schemes operating.

From Fig. 6.1.1, it can be seen that the majority of the data points are of magnesio-hornblende composition with significant core to rim changes in composition towards actinolitic-tremolitic hornblende. Cation site occupancy (ie. tetrahedral/octahedral) for Al, displayed in Fig. 6.1.2 shows analyses clustered around values between common hornblende and edenite. A trend within the data suggests a line extending towards tremolite and pargasite. Analyses of magmatic amphibole rims and secondary amphibole cores tend toward the tremolite join while analyses of amphiboles within a xenolithic inclusion in quartz-monzodiorite suggests a tendency to the pargasite join. The majority of the analyses could be classified as edenitic-hornblende.

From Table 6.1, the variation in composition from core to rim in magmatic amphiboles can be summarised as increasing Si, Mg, and F with concomitant decreasing Ti, Al, Fe(t), Na, K. Both Mn and Ca remain approximately constant. Comparing magmatic amphibole rim compositions with secondary amphiboles (identified optically), Si can be seen to increase slightly, Ti and Mg decrease slightly with all other elements remaining approximately constant. Thus a strong correspondence between magmatic amphibole rim compositions and post-magmatic (secondary) amphibole compositions is noted.

The core - rim variation in magmatic amphiboles can also be related to changes involving Ti, Mg, Al, Na and K. Ti vs Al^{IV} (Fig.6.1.3) shows good positive correlation with little scatter. A residual component of approximately 0.15 cation Al^{IV} at zero Ti, together with the trend of the data, indicates that Ti-tschermakite substitution is dominant. Ti substitution is poorly understood but Doolan et. al. (1978) consider that Ti is equivalent to two trivalent cations. The increase in the C-site charge is given by $(Al^{VI}+Fe^{3+}+Cr+2Ti)$ which gives a measure of tschermakite and glaucophane substitution involved with $Al^{IV}+Na_B$. On this plot (Fig. 6.1.4), data clusters about a median area between edenite and hornblende (cf. Fig. 6.1.2), but is extended along a line towards pargasite.

As both Figs. 6.1.2 & 6.1.4 show analyses to lie between edenite and hornblende, it is useful to show the contributions of coupled substitutions involving Si, Al, Fe, Mg and Ti. Edenite substitution involves Al coupled substitution and appears to be the predominant, but not the only, control over composition. By considering $(Na + K)_A$ vs Al^{IV}, a 1:1 ratio for the slope of the trend line would be expected if this were the case. In Fig. 6.1.5, the data falls about a line with a ratio of 2:1 (with little scatter). indicating that Al^{IV} substitution is occurring in other substitutions in addition to the edenitic scheme. Residual Al^{IV} at zero (Na + K)A indicates edenite substitution is less important in more basic rocks (eg. RM3, RM69), rim compositions of magmatic amphiboles and core compositions of secondary amphibole.

Other coupled substitutions involving Al, namely Al-tschermakite and Ti-tschermakite (Figs. 6.1.3 & 6.1.4) must also be considered. Both Al^{IV} and Fe^{3+} may be involved in Al-tschermakite substitution and Fig. 6.1.6 shows their relative contributions. A 1:1 slope would indicate a minor role for Al^{VI} or that Fe^{3+} was the dominant variable cation in the trivalent C-site. The data lies on a trend between 1.2:1 & 1.5:1, suggesting a moderate excess of Al^{IV} over Al^{VI}. Thus both Fe^{3+} and Al^{IV} participate in Al-tschermakite substitution. Considering edenite and Al-tschermakite substitutions further, data plotted in Fig. 6.1.7 (Al^{VI} vs Al^{IV}) indicates that there is more Al^{IV} (>2:1) than required by these two substitutions. Ti-tschermakite (Fig. 6.1.3) could account for this.

From the above, Ti-tschermakite and edenite are considered to be the two dominant substitution schemes with minor, variable Al-tschermakite involved. If this were the case, considering $(Na + K)_A + Al^{VI} + Fe^{3+} + 2Ti$ vs Al^{IV} a 1:1 ratio should result. As can be seen from Fig. 6.1.8, this holds true but post-magmatic, secondary amphiboles have a residual $A + Al^{VI} + Fe^{3+} + 2Ti$ component and lie off the line of 1:1. This occurs only with Na occupancy in the B-site and is a function of the Fe2O3/FeO calculation or is an indirect indicator of variable Fe-Mg simple substitution.

Substitution of Fe^{2+} for Mg^{2+} gives a range of amphibole compostitions between magnesio-hornblende (Mg/(Mg+Fe)>0.5) and ferro-hornblende (Mg/(Mg+Fe)<0.5). This ratio is not a simple reflection of the bulk rock composition as Fe-oxide and biotite crystallisation must also be considered (Leake, 1978). The Fe - Mg substitution is also a function of other, more complex coupled substitutions in the amphibole structure. Magmatic amphibole rim compositions show enhanced Mg values with resect to their cores, but remain approximately constant or are slightly lower when compared to post-magmatic amphiboles.

6.1.2 Secondary/post-magmatic amphiboles.

Secondary amphiboles have been identified optically and are thought to be actinolitic-hornblende in composition, based on optical properties. Their analyses are Si, Mg, F enhanced and Ti, Al, Fe, Na and K depleted relative to magmatic amphibole cores, while Mn and Ca

remain approximately constant. These concentrations mimic that of magmatic amphibole core-rim variation. Comparison of magmatic crystal rim values with secondary crystal core values indicates that in the latter only Ti and Mg show depletion. Figs. 6.1.2 through 6.1.8 show possible gradation between primary and secondary amphiboles, but by averaging analyses (Fig. 6.1.1) it would appear a compositional gap is present.

The ratio Mg/Mg+Fe is higher for secondary amphibole cores in comparison to primary crystal cores but is lower with respect to magmatic rims, indicating slight Fe enhancement in the secondary minerals. This compositional gap is dependent on temperature and Fe/Mg ratio and may be the result of inequilibrium or a miscibility gap (Tagiri, 1977). Petrographic evidence for disequilibrium crytallisation has been noted (Chapter 4, Plate 4.14).

The decrease in Ti & Mg may be the result of concommitant biotite crystallisation (a magmatic origin) or due to retrogressive alteration of biotite to sphene, chlorite & oxides with associated amphibole formation. The development of opaque oxides and chlorite is well documented - Chapter 4, Plate 4.8 - while the occurrence of sphene, both in cleavage fractures and mantling biotite within amphibole, is noted.

Two separate processes, which temporally overlap, may have operated. The first is a late stage magmatic phase in which pre-existing amphiboles are rimmed by a more Si, Mg & F amphibole . The second is probably a subsolidus phase in which an amphibole of

similar composition crystallises. Optically, there is no abrupt change evident from core to rim in this type.

6.1.3 Discussion.

The amphiboles analysed are primarily magnesio-hornblende with secondary actinolitic hornblende found in all rocks. All are calcic class A (after the classification of Leake, 1978) with the exception of those analysed from the inclusion (RM69), which were calcic class B. The composition of secondary amphiboles generally lies outwith the limit $Al^{IV}:Al^{VI}$ >3.3:1 (Fig. 6.1.7) and are thus more typical of metamorphic amphiboles (Fleet & Barnett, 1978).

The decrease in Ti, Al, Na and K from core to rim in magmatic amphiboles may be due to a decrease in magma temperature (Leake, 1965). There is a marked shift to the lower Ti side of the trend $Al^{IV}:Ti$ = 3:1 and this is thought by Moyes (in prep.) to represent possible isobaric cooling of an intercumulus amphibole.

The simple substitution of Fe-Mg in granitic amphiboles has been found to be influenced by fO2 conditions (Kanisawa, 1975). At high fO2 values, Fe^{3+} is favoured in magnetite, increasing the Mg/Mg+Fe ratio, ie. towards magnesio-hornblende. At low fO2 ilmenite crystallises and the Mg/Mg+Fe ratio is lowered towards ferro-hornblende. Biotite contains significant Ti and analyses of biotite within Camphibole suggests that the amphibole is significantly Ti-depleted at the junction of the minerals. Higher Ti in the core of the biotite, decreasing to the rim of the amphiboles may confirm this (Table 6.1).

TABLE 6.1 MOOR OF RANNOCH AVERAGE AMPHIBOLE COMPOSITONS

	QUARTZ-MONZODIORITE RM3		RM33			RM69b		GRANODIORITE RM54			MONZOGRANITE RM8		
	PRIMARY	SECONDARY	CORE	RIM	SECONDARY	HOST CORES	XENOLITH	CORE	RIM	SECONDARY	CORE	RIM	SECONDARY
SiO_2	48.09	49.46	47.66	49.80	49.83	47.55	45.46	47.02	49.23	50.10	48.17	50.39	50.54
TiO_2	1.17	1.15	1.38	1.14	0.71	1.13	1.59	1.23	0.74	0.52	1.06	0.62	0.59
Al_2O_3	6.42	5.97	6.56	4.96	4.53	6.41	7.95	6.60	5.36	5.26	5.82	3.90	3.93
$FeO_{(t)}$	14.11	13.66	12.96	12.27	12.53	14.33	15.68	14.17	13.23	13.05	12.93	11.49	11.40
MnO	0.37	0.38	0.47	0.46	0.48	0.33	0.33	0.45	0.45	0.45	0.45	0.46	0.45
MgO	13.53	13.82	13.97	15.12	14.96	13.37	12.07	13.34	14.45	14.61	14.40	16.07	15.77
CaO	11.61	11.62	11.56	11.49	11.71	11.75	11.69	11.71	11.79	11.95	11.65	11.68	11.57
Na_2O	1.18	1.14	1.40	1.18	0.97	1.18	1.40	1.20	0.99	0.98	1.34	0.95	0.97
K_2O	0.15	0.12	0.15	0.20	0.21	0.11	0.11	0.59	0.46	0.41	0.57	0.36	0.35
F	0.15	0.12	0.15	0.20	0.21	0.11	0.11	0.05	0.22	0.14	0.19	0.15	0.14
TOTAL	97.22	97.83	96.63	97.00	96.30	96.74	97.07	96.36	96.92	97.47	96.58	96.04	95.71
Si	7.112	7.226	7.066	7.297	7.364	7.080	6.823	7.026	7.260	7.322	7.147	7.416	7.456
Al^{IV}	0.888	0.774	0.934	0.703	0.636	0.920	1.177	0.974	0.740	0.678	0.853	0.584	0.544
Σ_{TET}	8.000	8.000	8.000	8.000	8.000	8.000	8.000	8.000	8.000	8.000	8.000	8.000	8.000
Al^{VI}	0.231	0.254	0.213	0.154	0.153	0.206	0.230	0.189	0.192	0.229	0.165	0.093	0.140
Ti	0.130	0.126	0.154	0.126	0.079	0.127	0.180	0.138	0.082	0.057	0.118	0.069	0.066
Fe^{3+}	0.000	0.000	0.000	0.000	0.000	0.010	0.029	0.049	0.015	0.000	0.000	0.015	0.000
Mg	2.982	3.009	3.087	3.302	3.295	2.967	2.700	2.971	3.175	3.182	3.184	3.525	3.467
Fe^{2+}	1.745	1.669	1.607	1.504	1.549	1.775	1.940	1.722	1.617	1.595	1.604	1.400	1.407
Mn	0.046	0.047	0.059	0.057	0.060	0.042	0.042	0.057	0.056	0.057	0.057	0.057	0.056
Σ_{OCT}	5.134	5.105	5.120	5.143	5.136	5.127	5.121	5.126	5.138	5.119	5.128	5.159	5.136
Ca	1.840	0.819	1.837	1.804	1.854	1.875	1.880	1.875	1.836	1.871	1.852	1.842	1.829
Na	0.338	0.323	0.403	0.335	0.278	0.341	0.407	0.348	0.283	0.278	0.386	0.271	0.278
K	0.111	0.095	0.098	0.071	0.070	0.110	0.152	0.113	0.087	0.076	0.108	0.068	0.066
Na_B	0.026	0.075	0.044	0.054	0.011	0.000	0.000	0.000	0.000	0.010	0.021	0.000	0.035
$(Ca+Na)_B$	1.866	1.894	1.880	1.858	1.865	1.875	1.880	1.875	1.863	1.881	11872	1.842	1.864
$(Na+K)_A$	0.424	0.343	0.457	0.352	0.337	0.451	0.559	0.461	0.370	0.345	0.473	0.339	0.308

NUMBER OF IONS ON BASIS OF 23(O)

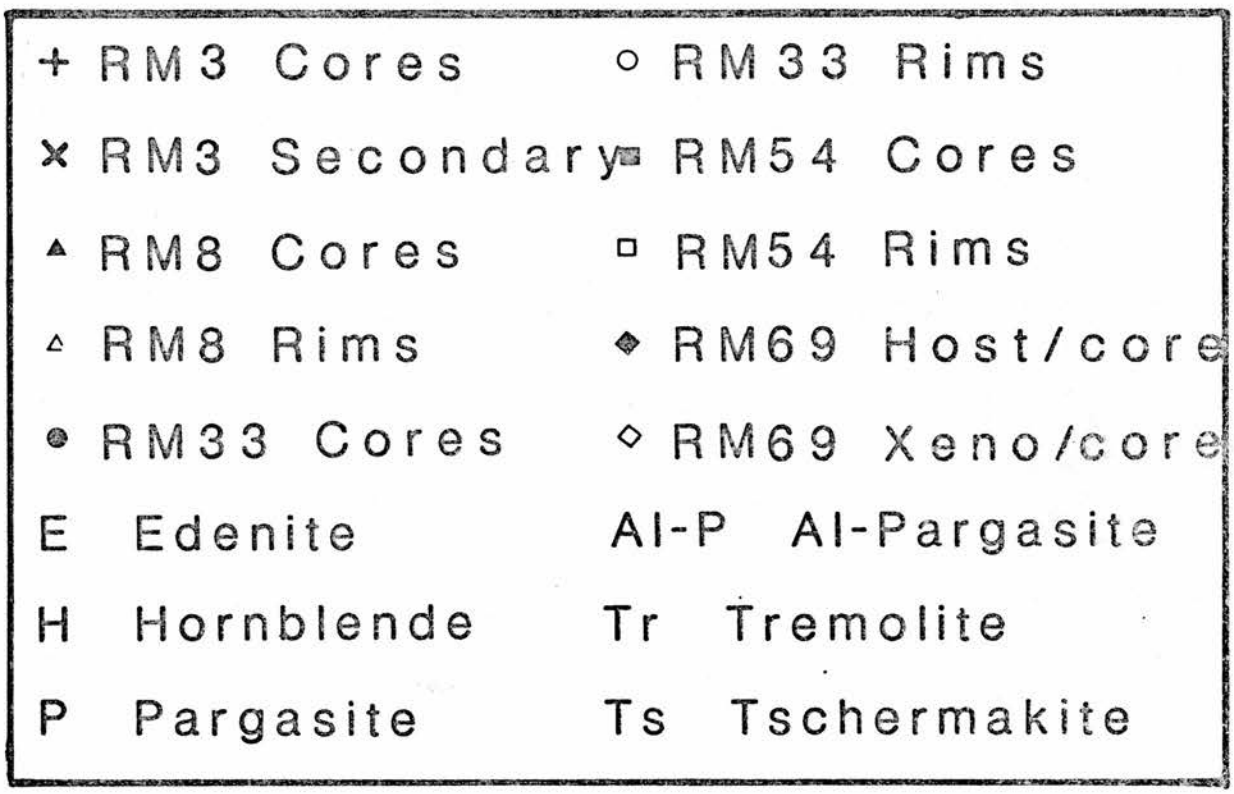
+ RM3 Cores
× RM3 Secondary
▲ RM8 Cores
△ RM8 Rims
● RM33 Cores
E Edenite
H Hornblende
P Pargasite
○ RM33 Rims
▪ RM54 Cores
□ RM54 Rims
◆ RM69 Host/core
◇ RM69 Xeno/core
Al-P Al-Pargasite
Tr Tremolite
Ts Tschermakite

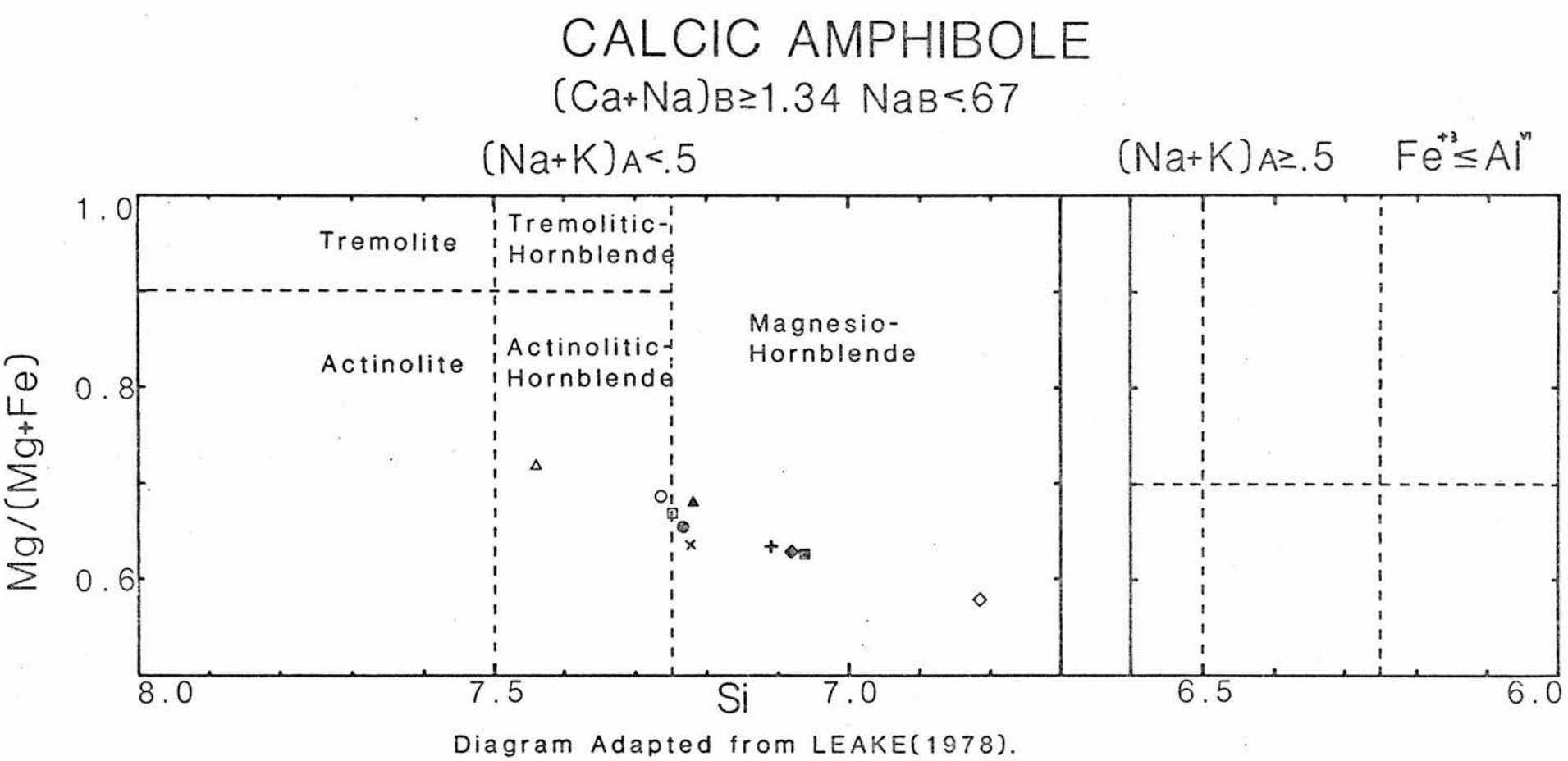

Figure 6.1.1 Amphibole compositions on basis of cations per unit formula, O=23. Symbols as per key.

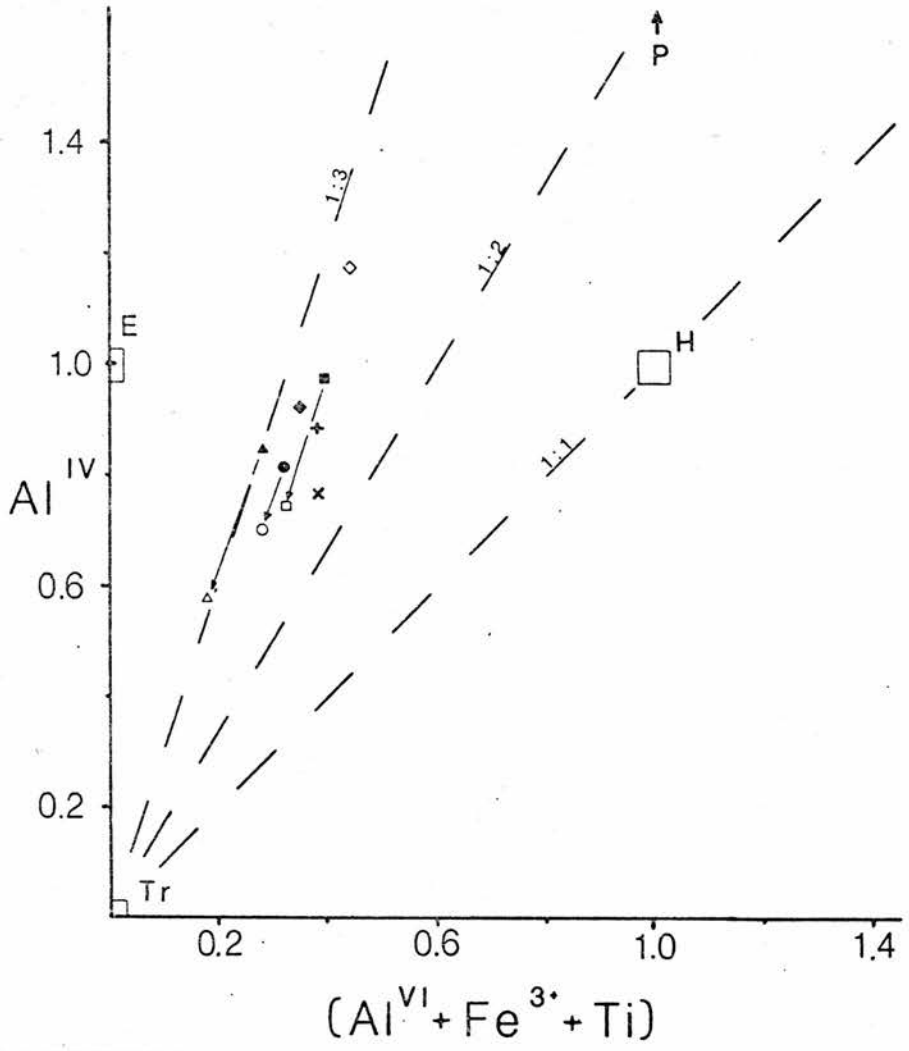

Figure 6.1.2 Plot of amphibole analyses with end-member fields as defined in key. Tie lines indicate core to rim variation for each type. Dashed lines indicate ratios of ordinate and abscissa componenents.

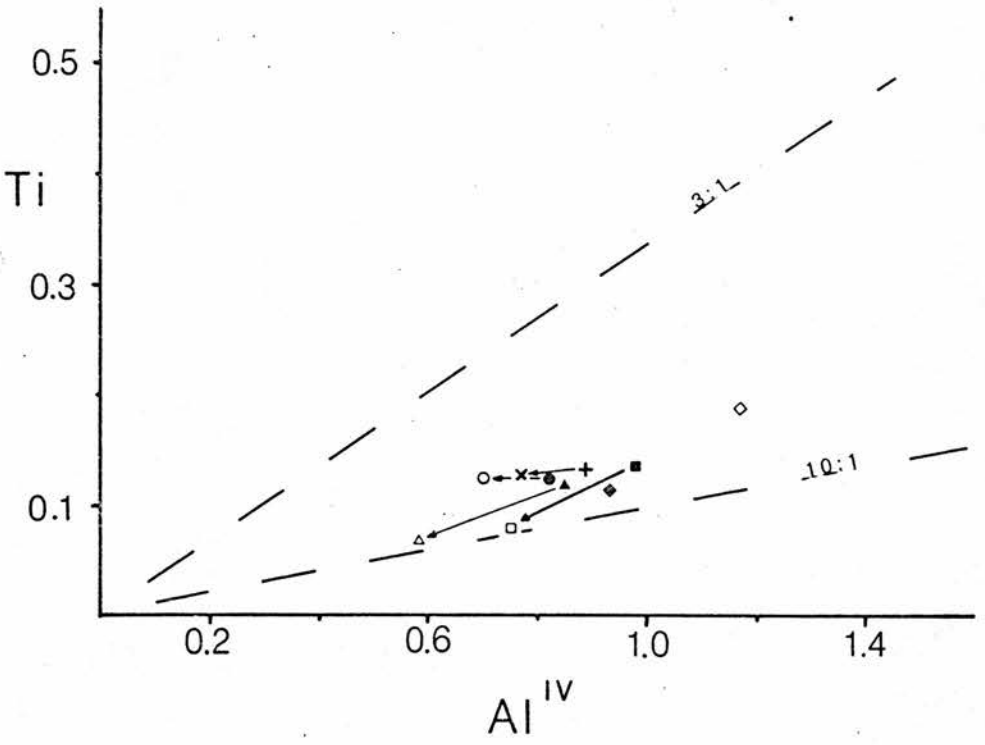

Figure 6.1.3 Plot of amphibole analyses with tie lines to denote core - rim variation. Dashed lines indicate component ratio values to define bounding fields.

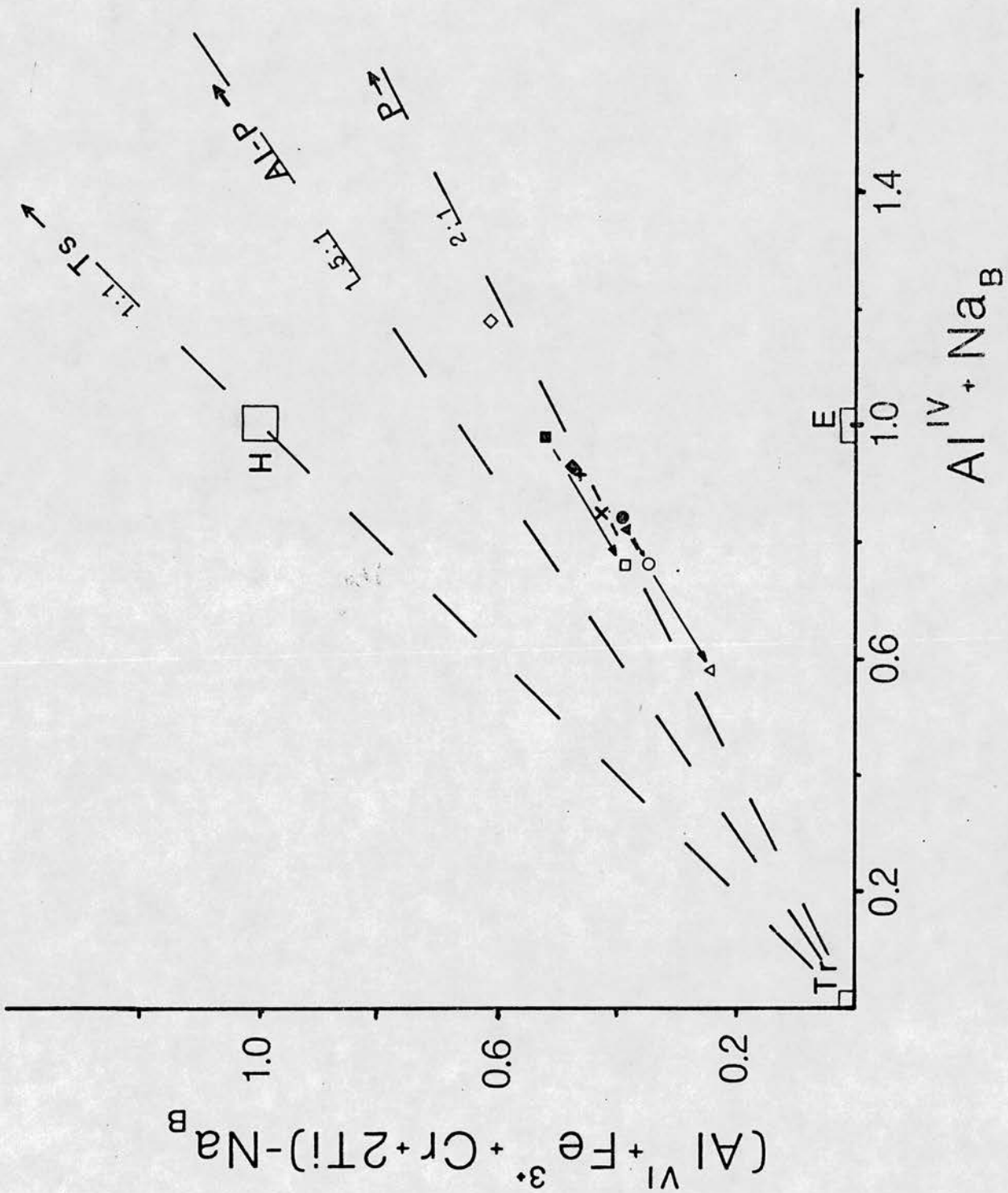

Figure 6.1.4 Plot of amphibole analyses with tie lines to denote core - rim variation. Dashed lines indicate ratio values of ordinate and abscissa components.

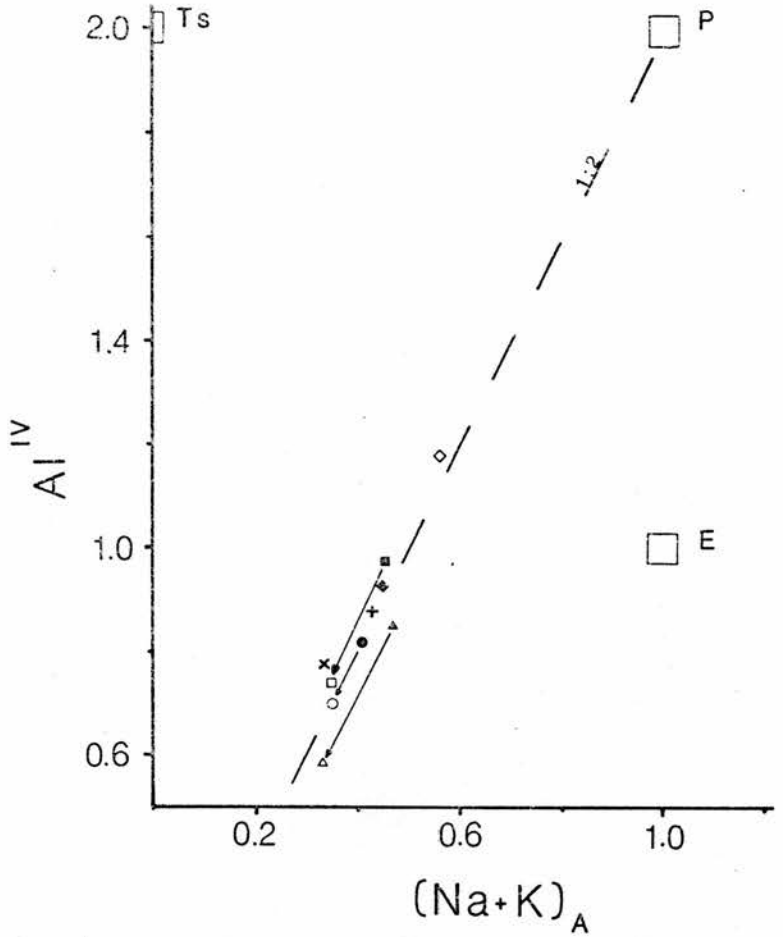

Figure 6.1.5 Plot of amphibole analyses with tie lines to denote core - rim variation. Dashed lines indicate ratio values of ordinate and abscissa components.

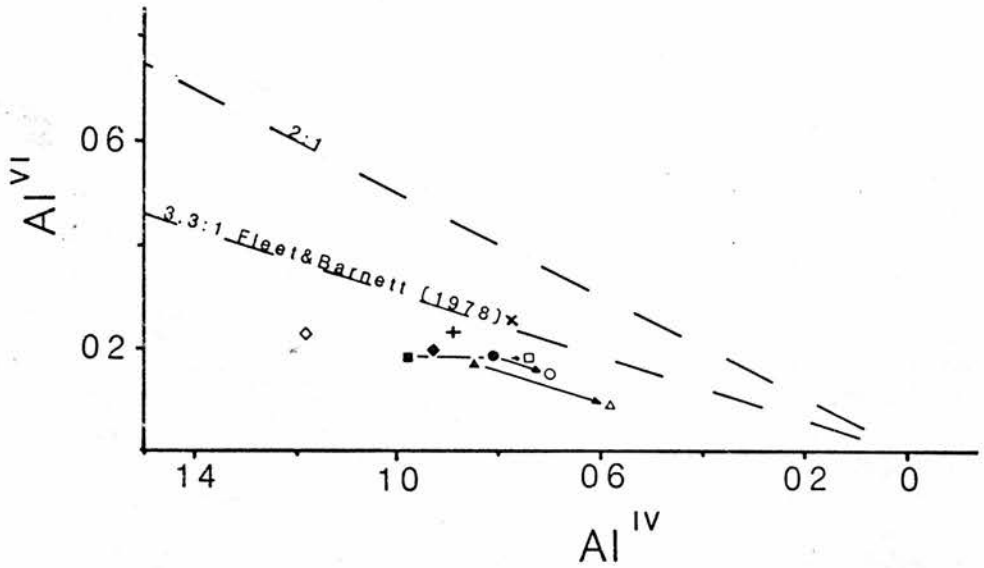

Figure 6.1.7 Plot of amphibole analyses with limit of metamorphic amphiboles of Fleet and Barnett (1978) superimposed. Tie lines show core - rim variation.

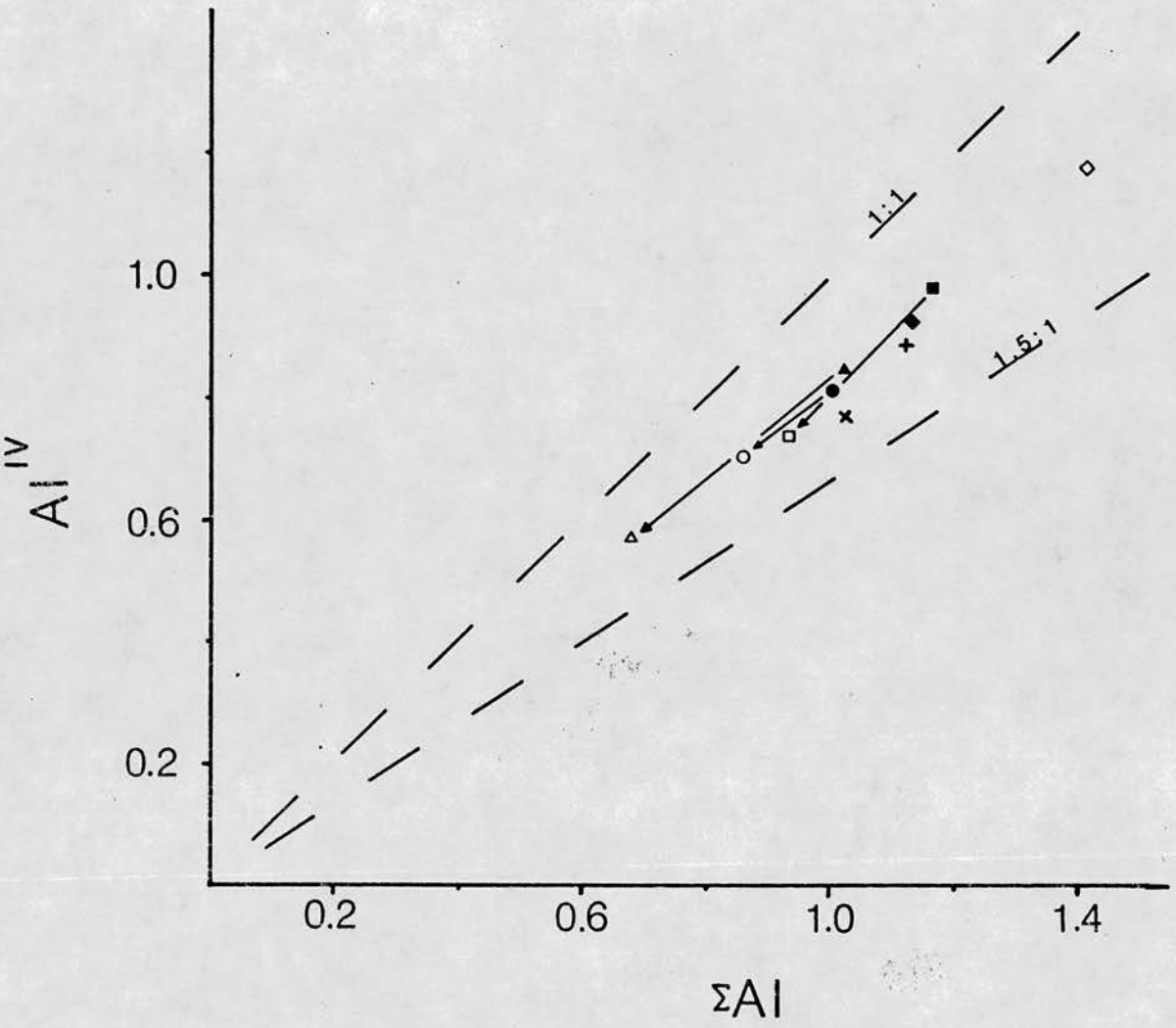

Figure 6.1.6 Plot of sum octahedral and tetrahedral Al against tetrahedral Al for amphibole analyses. Tie lines indicate core - rim variation with dashed line representing ordinate and abscissa component ratios.

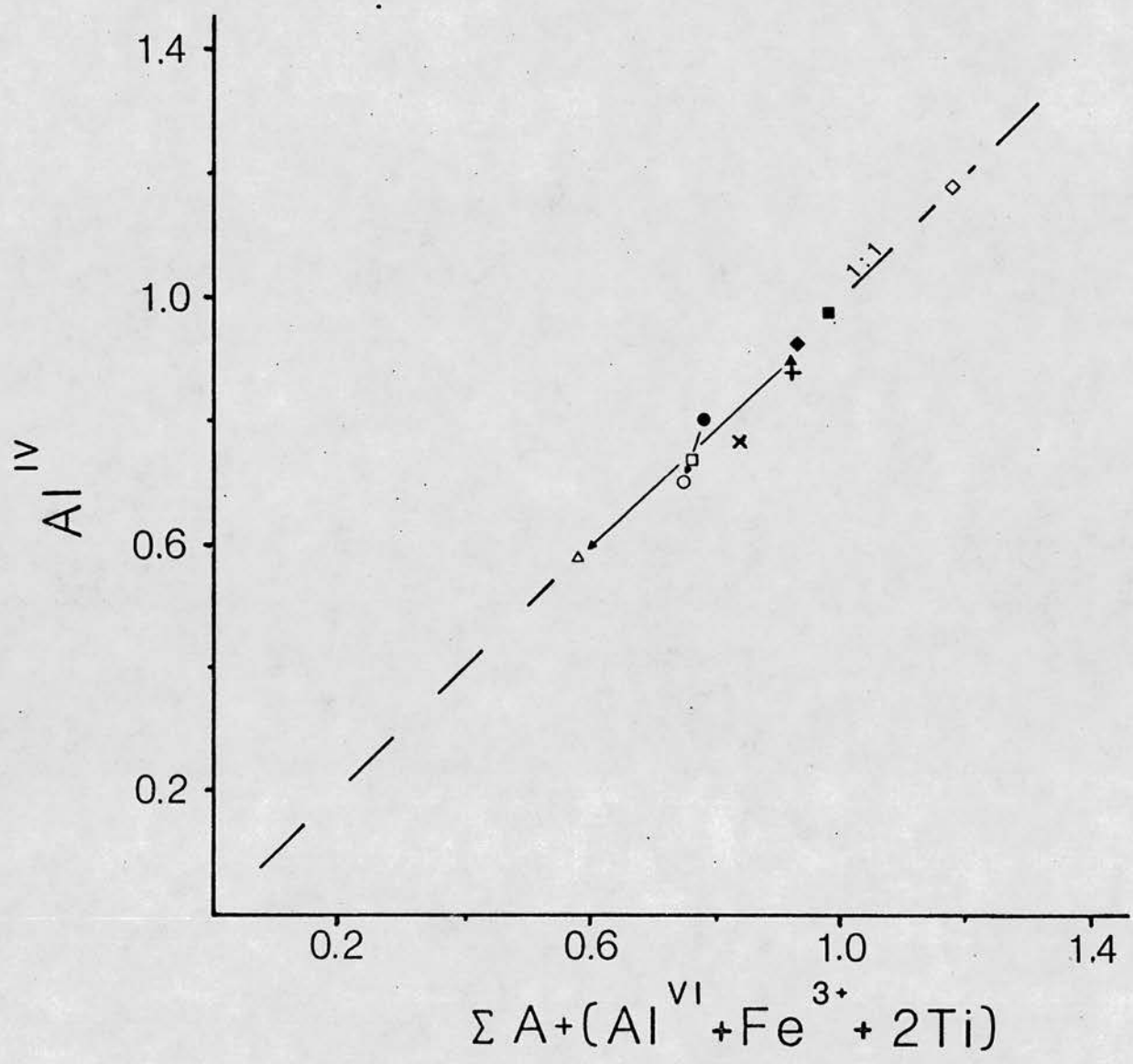

Figure 6.1.8 Plot of amphibole analyses with some tie lines of core - rim variation omitted for clarity.

From Table 6.4, the opaque phases are noted as predominantly magnetite with minor Cr and Mn. There is little Ti present in the magnetite as the element is concentrated in biotite and sphene. This evidence suggests that moderate fO2 conditions existed for the quartz-monzodiorites. The lack of Ti and Mg in the magnetite of the syenogranite sample (RM36) is a function of their low initial concentration in the magma.

6.2 BIOTITE

6.2.0 Introduction.

Biotite is found throughout the range of rock types within the Moor of Rannoch pluton. It is the dominant mafic constituent of the intermediate types, occurring as both unaltered and chloritised aggregates or as discrete mineral grains of both primary and secondary origin.

6.2.1 Biotite chemistry and substitution schemes.

Representative analyses from a total of 41 are shown in Table 6.2 and are grouped on the basis of modal mineralogy of the host rock. Biotite has a crystal chemistry which enables a number of cation substitutions to be made. An accepted general formula is: $A_2\ B_{6-4}\ C_{0-2}\ T_8\ O_{22}\ (OH,F)_4$ (Deer, Howie & Zussman)

where A = K, Na; C = Fe^{3+}, Al, Ti; B = Mg, Fe^{2+}; T = Si, Al.

From Fig. 6.2.1, it is noted that the analysed biotites have a range restricted to the magnesium side of the annite - phlogopite join with little extension towards more Al-rich varieties. This tendency to a more magnesian end member mirrors the overall variation within magmatic amphiboles discussed earlier while the Al^{IV} site occupancy is only weakly correlatable with bulk rock geochemistry. A weak trend of decreasing Al^{IV} from core to margin is noted and as the Fe/Fe+Mg ratio remains constant, Si substitution is considered most likely. Total Al is negatively correlated with Si (Fig. 6.2.2).

A weak geographic distibution of Fe-enhanced samples in the eastern part of the pluton is noted, indicating either that fO2 conditions were variable throughout different parts of the pluton, a more Mg-rich parental magma was involved, or that the micas crystallised at lower temperatures. It must be stated that the inability of the microprobe to differentiate between the oxidation states of Fe, along with very variable H2O and F contents, makes interpretation of substitutions in biotite involving Fe (and Ti and Mg) tentative.

Figure 6.2.4 shows the relationship between Ti and Fe/Fe+Mg and a weak trend of higher Ti with an increasing Fe-ratio suggests that Ti replaces Mg in the octahedral site. There is inter-sample variation and this may reflect the differing oxidation states or a bulk rock variation. Comparing octahedral Ti with Al^{VI} (Fig. 6.2.5) and

octahedral Mg with Al^{VI} (Fig. 6.2.6), Mg and to a lesser extent Ti substitute for Al in this site. Both Fe and Ti are variable within samples leading to variable Al^{IV} site occupancy.

There appears to be a correlation between Al^{VI} and Mn with increasing Mn coupled to decreasing Al^{VI} (Fig. 6.2.8a). This variation is more readily comparable with bulk rock variation than cationic Si or Al^{IV} but it is noted that there are no other easily identified trends of Mn, ie. Mn vs Fe(t) or Mn vs Mg. Ba within the samples shows negative covariation with cationic Si (Fig. 6.2.7). With one exception (RM54), Ba decreases from core to rim and has an approximately constant covariation with Al^{VI}. This suggests that Ba is replacing K, with charge imbalance being accomodated by coupled Al^{VI} substitution.

The plot F v Mg (Fig. 6.2.9) indicates positive covariation of F with Mg which suggests the F content of biotite is systematically related to Mg content (Munoz & Luddington, 1974). Gilbert and Troll (1974) note this as a feature of I-type granite biotites and suggest that biotite is able to concentrate F more effectively than amphibole. As the F content between altered and unaltered biotites remains approximately constant, F values appear little affected by alteration. Thus the significantly different F content of biotite in the syenogranite sample (RM36) could reflect a fundamental difference in the parental magma volatile content or subsequent magma evolution.

Biotites in a traverse across the contact between a mesocratic, medium-coarse grained quartz-monzodiorite and a melanocratic, fine grained xenolith of igneous(?) origin were analysed (sample RM69). Relative to the host rock biotite analyses, those of the xenolith have similar Fe/Fe+Mg raios, slightly higher $Al^{IV\ \&\ VI}$ occupancy and lower Si. Both Ti and Ba are enhanced in the xenolith biotites while Mg and Mn are depleted. Core to rim variations follow that of the host rock biotites. Analyses of the contact between host and xenolith plot consistently intermediate to the other analyses (Figs. 6.2.1 - 6.2.9). This suggests that the xenolith represents included material that was equilibrating, at its margins, with the host.

6.2.3 Discussion.

The analyses presented show that the biotites are not simple phlogopite - annite solid solutions but contain excess Al and that the siderophyllite component increases in the basic rocks. Together with Fe, the main variable elements are Ti, Mg, Ba and Al although positively identifying an Fe-enrichment east of the Laidon-Ericht fault would require further analyses to be made.

Bowen's (1928) discontinuous reaction series involving amphibole and biotite is observed in the granodiorites and granites, but the order has been noted reversed in calc-alkaline intrusions (Bateman & Wones, 1972; Beams, 1980). The occurrence of biotite within amphibole is common in the Moor of Rannoch suite.

TABLE 6.2 MOOR OF RANNOCH, AVERAGE BIOTITE COMPOSITION

	QUARTZ-MONZODIORITE								GRANO-DIORITE	MONZOGRANITE		SYENO-GRANITE
	RM33 CORE	RIM	RM69b CORE HOST	RIM HOST	CORE CONTACT	RIM CONTACT	CORE XENOLITH	RIM XENOLITH	RM54 CORE	RM8 CORE	RIM	RM36 CORE
SiO_2	36.45	36.44	36.46	36.48	36.53	36.34	36.24	36.25	36.87	36.60	36.24	37.20
TiO_2	4.14	4.11	4.03	3.80	3.98	4.38	4.07	4.14	3.67	3.85	3.43	3.86
Al_2O_3	13.44	13.71	13.93	13.86	14.04	13.87	14.00	13.88	13.97	13.49	13.91	13.11
$FeO_{(t)}$	17.10	16.95	18.09	17.82	18.20	17.75	18.02	17.85	16.54	16.09	16.05	17.24
MnO	0.29	0.26	0.21	0.19	0.21	0.21	0.20	0.21	0.30	0.29	0.28	0.37
MgO	13.23	13.17	12.52	12.62	12.47	12.28	12.41	12.67	13.14	13.87	13.99	13.42
CaO	0.00	0.02	0.01	0.01	0.02	0.02	0.01	0.04	0.01	0.01	0.02	0.02
Na_2O	0.11	0.12	0.11	0.10	0.13	0.13	0.10	0.11	0.10	0.09	0.08	0.08
K_2O	9.34	9.29	9.36	9.44	9.34	9.34	9.34	8.93	9.54	9.61	9.69	8.98
F	0.25	0.20	0.23	0.27	0.23	0.28	0.22	0.18	0.26	0.30	0.34	0.47
Ba	0.65	0.58	0.67	0.44	0.74	0.75	0.79	0.65	0.27	0.19	0.10	0.38
TOTAL	95.00	94.85	95.62	95.03	95.89	95.35	95.40	94.91	94.67	94.39	94.13	95.13
Si	5.830	5.836	5.825	5.852	5.823	5.823	5.809	5.815	5.891	5.866	5.836	5.937
Al^{IV}	2.170	2.164	2.175	2.148	2.177	2.177	2.191	2.185	2.109	2.134	2.164	2.063
Σ_{TET}	8.000	8.000	8.000	8.000	8.000	8.000	8.000	8.000	8.000	8.000	8.000	8.000
Al^{VI}	0.396	0.424	0.449	0.473	0.461	0.443	0.454	0.440	0.523	0.327	0.458	0.404
Ti	0.450	0.495	0.485	0.458	0.478	0.528	0.491	0.499	0.441	0.464	0.415	0.463
Fe	2.287	2.270	2.444	2.391	2.426	2.379	2.415	2.395	2.210	2157	2.162	2.344
Mg	3.154	3.142	2.981	3.017	2.963	2.932	2.966	3.029	3.130	3.312	3.357	3.192
Mn	0.039	0.035	0.029	0.026	0.028	0.029	0.027	0.029	0.041	0.039	0.038	0.050
Σ_{OCT}	6.326	6.366	6.388	6.365	6.356	6.311	6.353	6.392	6.345	6.299	6.430	6.453
Ca	0.000	0.004	0.002	0.002	0.003	0.003	0.002	0.007	0.001	0.003	0.004	0.003
Na	0.034	0.036	0.034	0.031	0.040	0.040	0.031	0.034	0.031	0.029	0.025	0.026
K	1.905	1.898	1.908	1.932	1.905	1.909	1.909	1.827	1.945	1.956	1.970	1.827
Σ	1.939	1.938	1.944	1.965	1.948	1.952	1.942	1.868	1.977	1.988	1.999	1.856
F	0.127	0.101	0.109	0.136	0.115	0.142	0.111	0.092	0.131	0.153	0.175	0.237
Ba	0.045	0.041	0.047	0.031	0.051	0.052	0.055	0.045	0.019	0.013	0.007	0.027

NUMBER OF IONS ON BASIS OF 23(O)

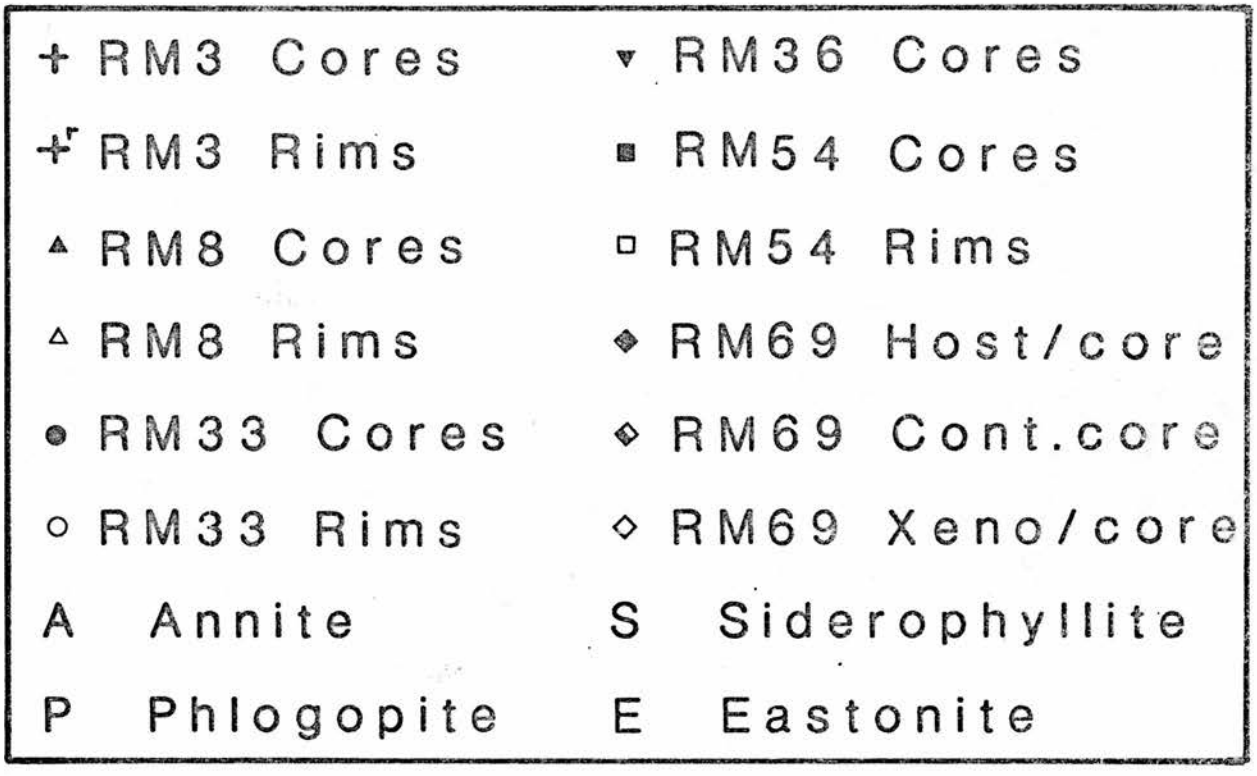
+ RM3 Cores
RM3 Rims
▲ RM8 Cores
△ RM8 Rims
● RM33 Cores
○ RM33 Rims
A Annite
P Phlogopite
▼ RM36 Cores
■ RM54 Cores
□ RM54 Rims
◆ RM69 Host/core
◈ RM69 Cont.core
◇ RM69 Xeno/core
S Siderophyllite
E Eastonite

Figure 6.2.1 Plot of biotite analyses with enlarged inset to clarify compositional variation. All biotite plots are calculated on basis of cations per unit formula O=23. Symbols as per key.

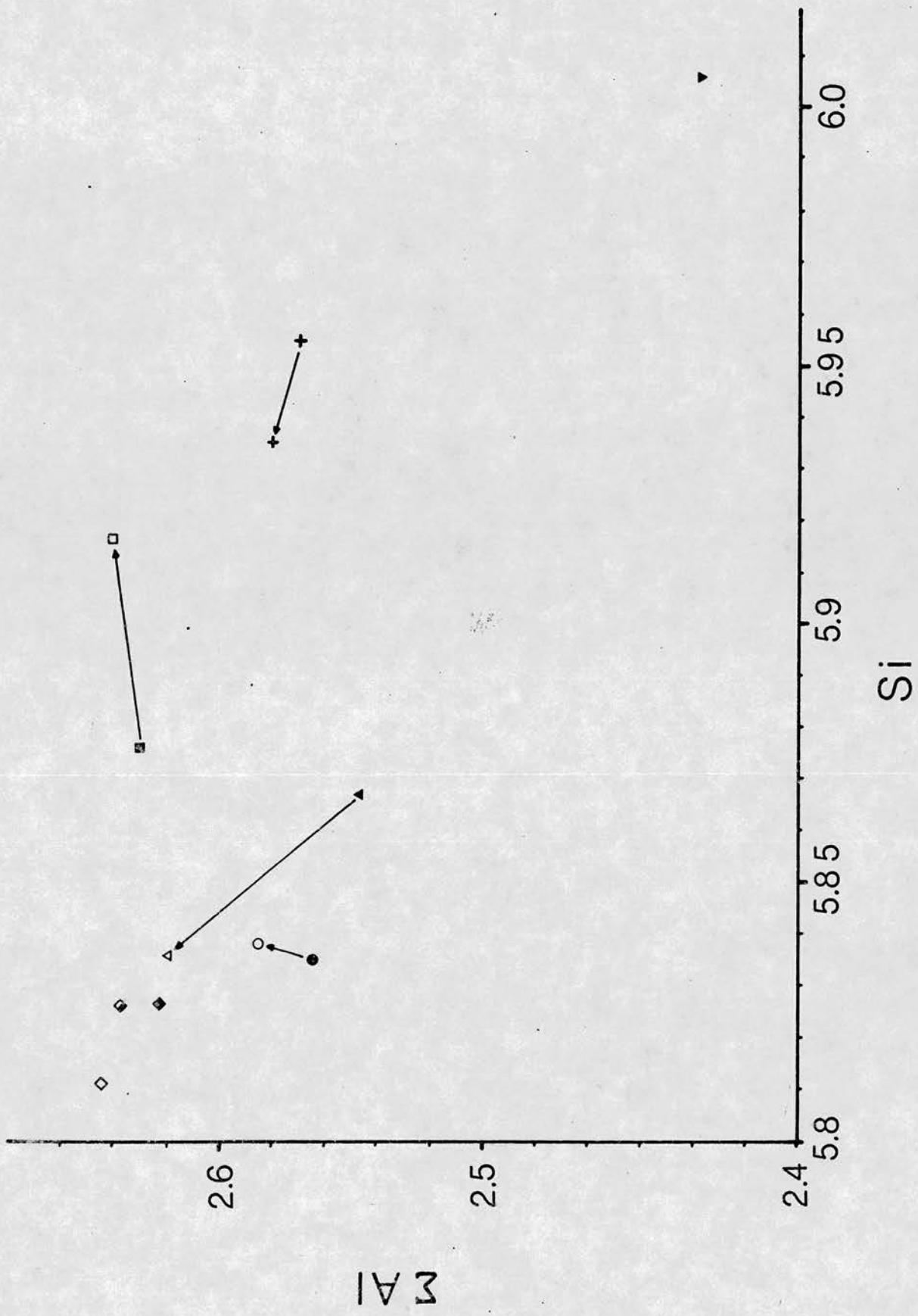

Figure 6.2.2 Plot of biotite analyses with tie lines indicating core - rim variation. Symbols as per key.

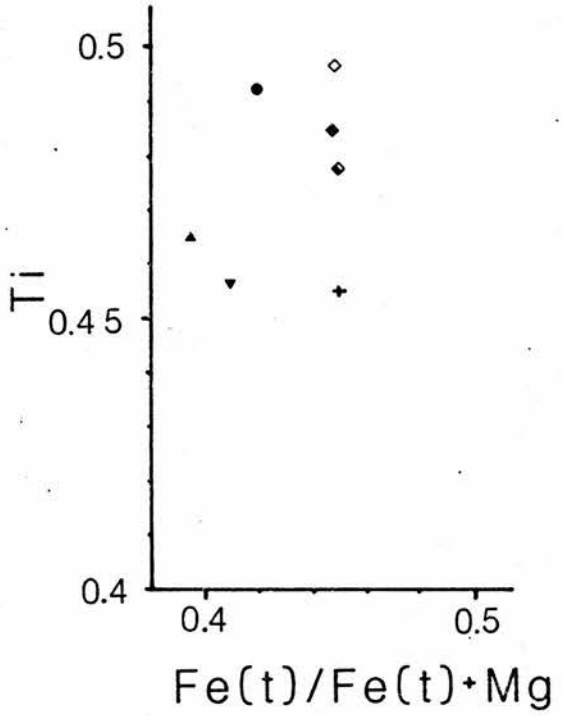

Figure 6.2.4

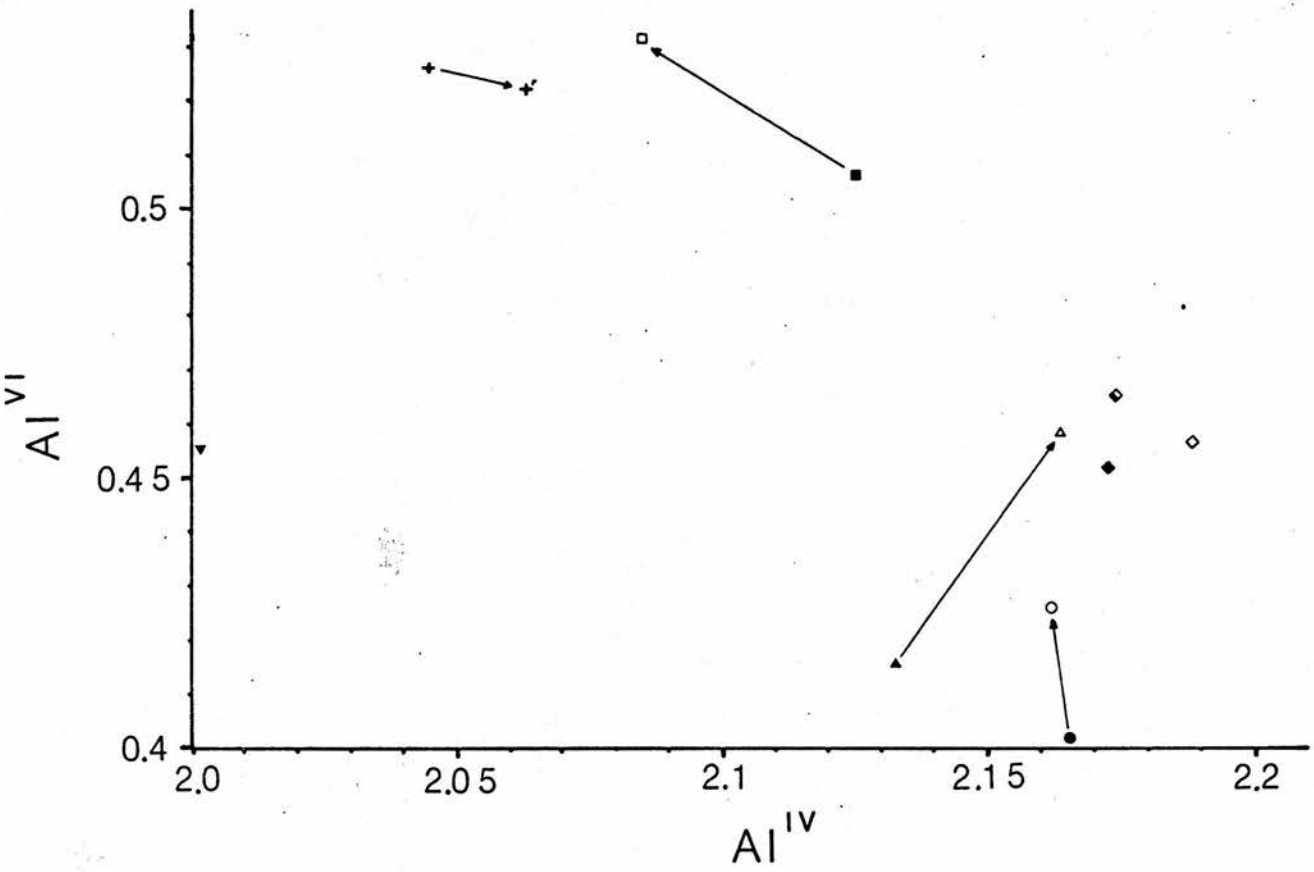

Figure 6.2.3 Plot of biotite analyses with tie lines indicating core - rim variation. Symbols as per key.

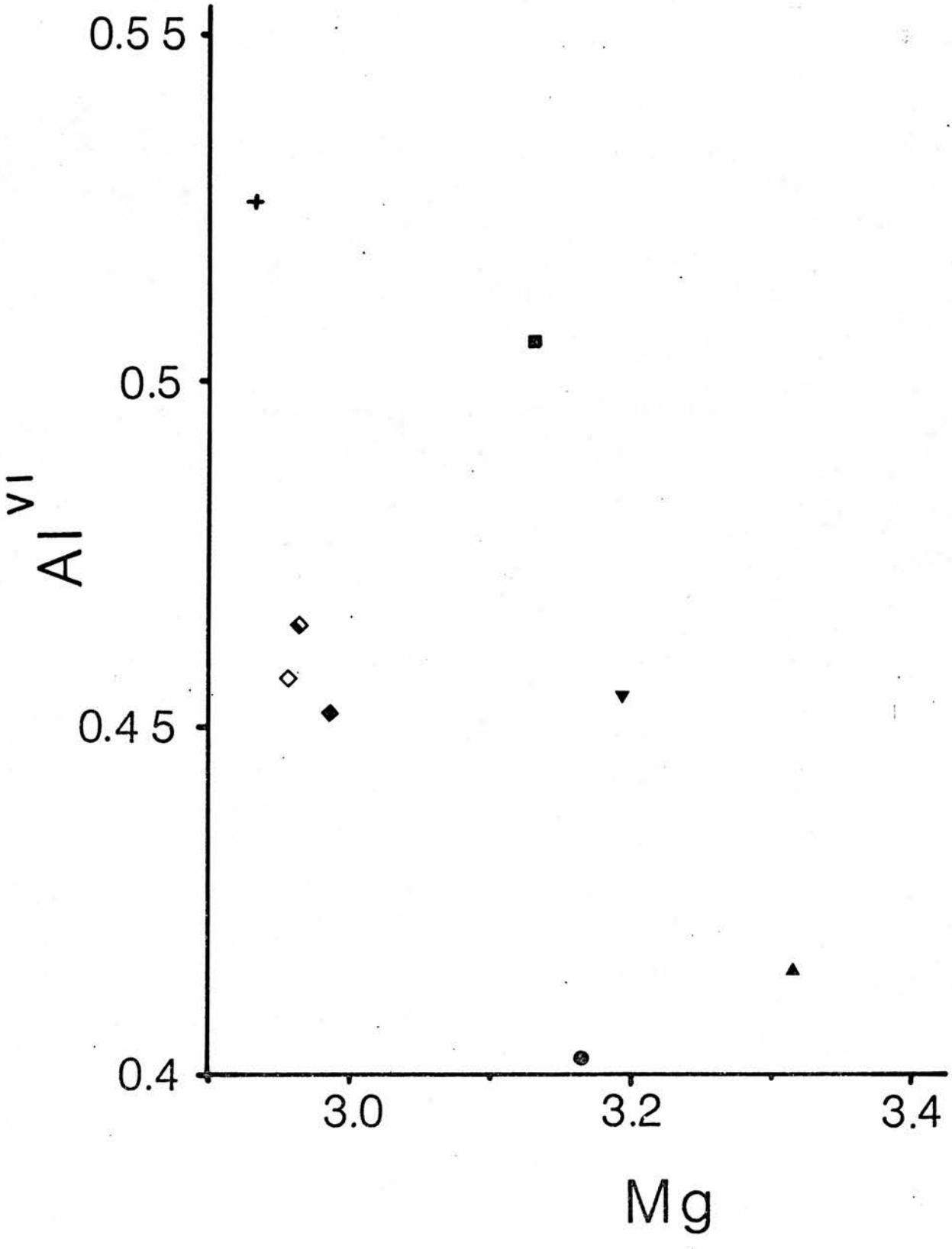

Figure 6.2.6

Figure 6.2.7 Plot of biotite analyses with tie lines indicating core - rim variation. Symbols as per key.

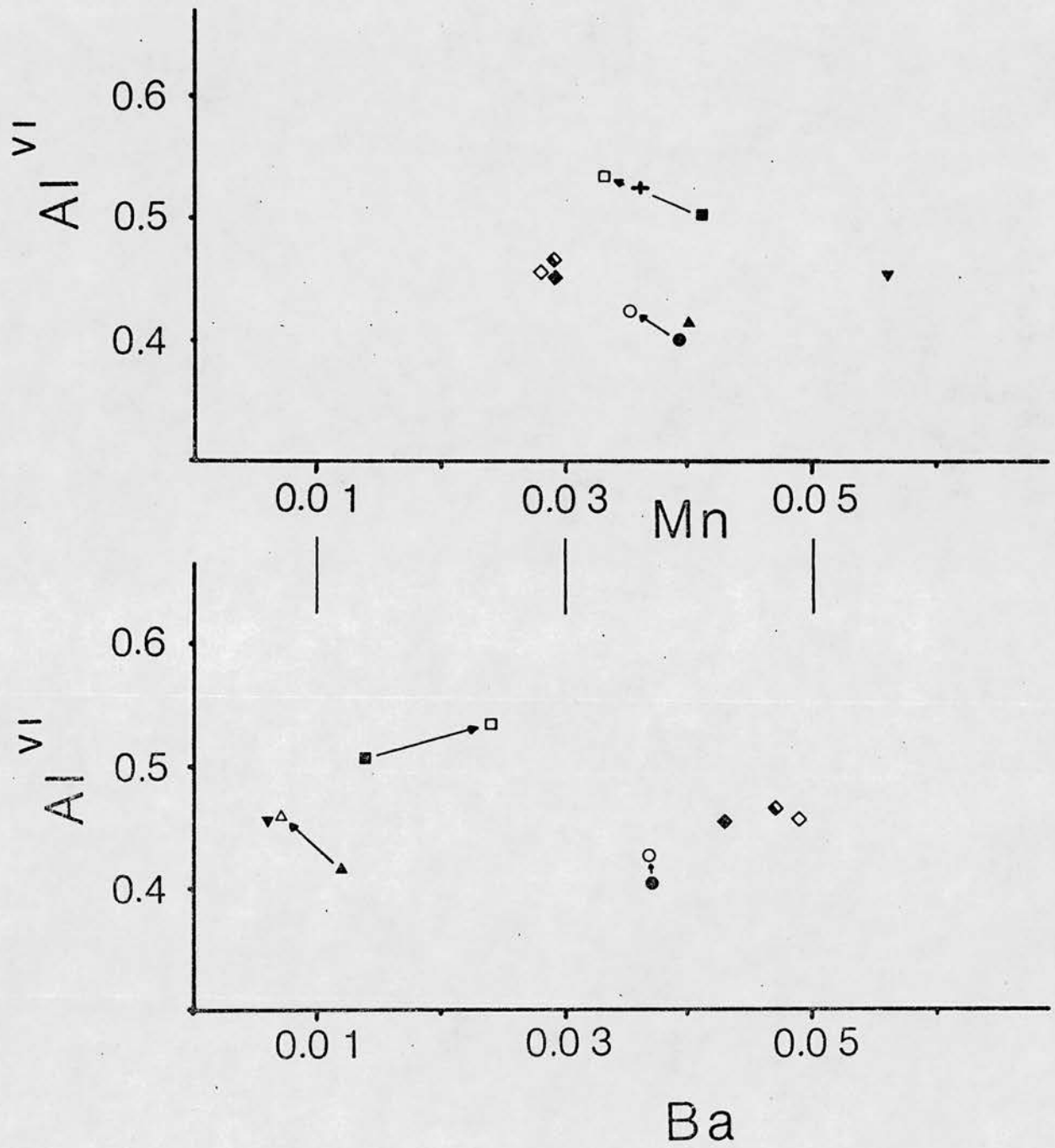

Figure 6.2.8a/b Plots of biotite analyses with tie lines indicating core - rim variation. Symbols as per key.

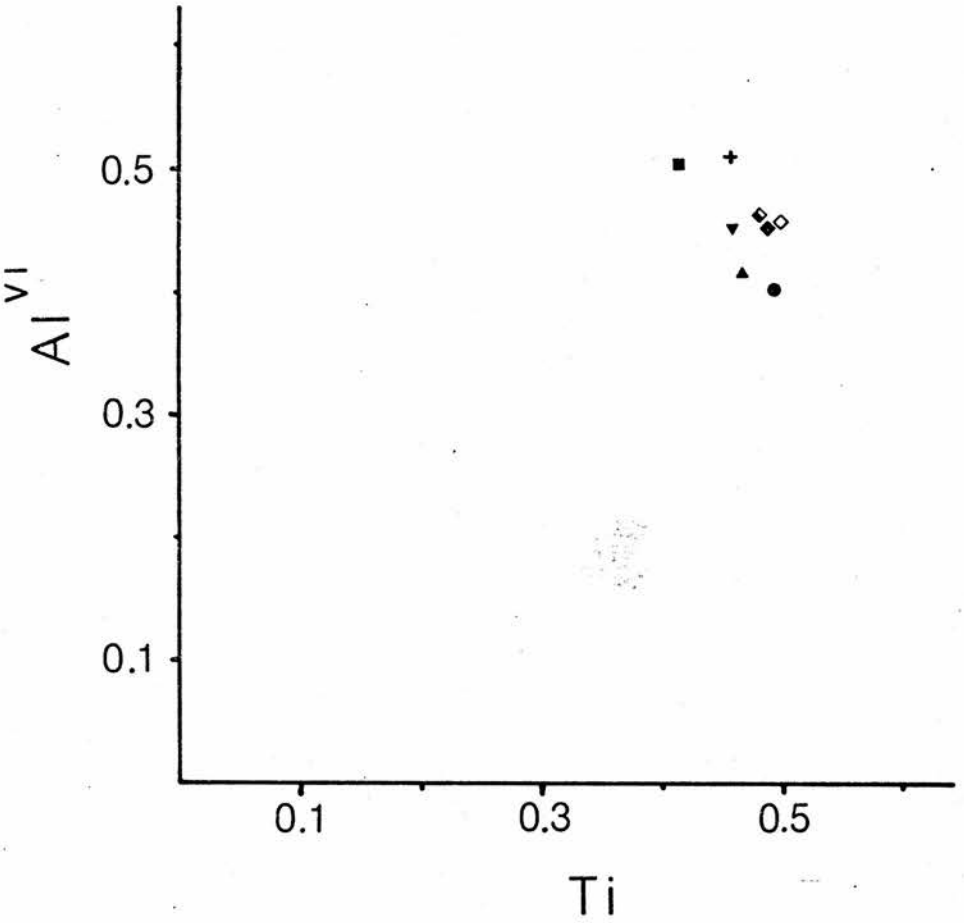

Figure 6.2.5 .

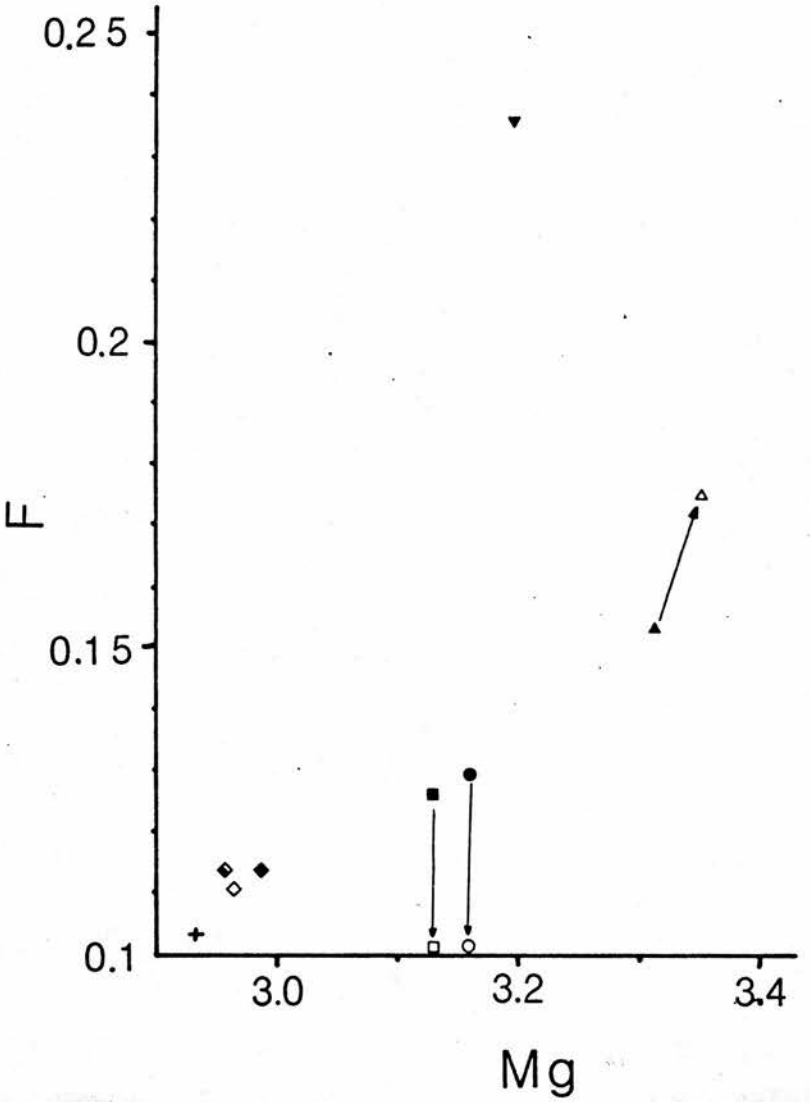

Figure 6.2.9 Plot of biotite analyses with tie lines indicating core - rim variation. Symbols as per key.

As most tonalites and granodiorites have low SiO2 and KAlSi3O8 activity until late stages of crystallisation, amphibole crystallises early and biotite is the late stage mineral (Wones, 1981). Where a magma has low fH2O, fO2 and moderate - high K2O values, the order of crystallisation may be reversed. Naney and Swanson (1980) also considered that silicate melts close to alkali feldspar saturation which were hypersthene normative would crystallise biotite before amphibole. From Chapter 5, Fig. 5.5.2, it can be seen that the Moor of Rannoch intrusive complex is predominantly hypersthene normative.

6.3 PLAGIOCLASE

6.3.0 Introduction.

A total of 31 analyses were obtained and the average values for each sample are given in Table 6.3. A close correspondence between probe and optical composition determinations was noted.

6.3.1 Plagioclase chemistry.

The range in anorthite composition is from An 11 to An 34, i.e. from sodic oligoclase to sodic andesine. SiO2 varies from 60.61 to 67.62 wt% and Al2O3 antipathetically from 21.89 to 24.06 wt%. K is always present in amounts from 0.69 wt% K2O (RM36) to 0.19 wt% K2O (RM33) with an average value of 0.37 wt% in core and 0.22 wt% in rim analyses. The consistent presence of K2O would appear to be a function of the bulk rock chemistry, the Moor of Rannoch pluton fits

high K calc alkaline criteria (Peccerillo & Taylor), with significant K20 levels persisting into the more basic members of the suite (monzodiorites) (Fig. 5.2.8).

Fe is always present and exhibits marked variation sympathetic with anorthite content (Fig. 6.3.1,a&b). Fe varies from 0.23 wt% (RM8) down to 0.08 wt% (RM33). There is no obvious correlation with bulk rock chemical variations. Ti has been detected and this may be due to sub-microscopic inclusions in analysed crystals.

The analyses show that in the granodiorite, plagioclase core compositions are calcic oligoclase/sodic andesine (An27-34) while rim compositions are sodic oligoclase (An11-18). Samples from quartz-monzodiorites have oligoclase cores and sodic oligoclase rims while monzogranites have variable oligoclase/andesine core and rim compositions (combined probe and optical determinations).

6.3.2 Compositional zoning.

From optical determinations, zoning appears to be ubiquitously developed in plagioclase throughout the suite. Much work has been carried out by various authors (Vance, 1962; Smith, 1974; Allegre, 1981) to account for the features exhibited by the different zoning schemes. These zoning schemes have been summarised by Smith (1974). Normal, reverse and complex zoning types are noted in plagioclases of the Moor of Rannoch suite.

Zoning is regarded as a disequilibrium effect and the outward progression may be continuous or discontinuous. Examples of this type are noted from samples RM33 and RM36.

Fe decreases from core to rim (Fig. 6.3.1,a&b) as does Ti and K, eg. RM33. In sample RM36, Fe shows anomalous behaviour by initially decreasing outward from the core, but then reversing to higher values in the rim. This may indicate the cessation of annitic biotite crystallisation in favour of a more phlogopitic composition. The crystal-melt Kd of Fe is higher for plagioclase than alkali feldspar and the Fe would enter that lattice in preference.

Complex zoning is present in some samples and two examples are presented to illustrate the combination of reverse and normal within a crystal. An initial increase in An content out from the core is followed by a decrease to the rim. From Fig. 6.3.1, it should be noted that both Fe and Mg tend to mimic this compositional change, small differences in the scheme are probably due to inter sample variation.

Discontinuities in plagioclase composition of > 5% An may result from pressure reduction effects on crystallisation in the anorthite-albite solid solution system. Thus, discontinuous or reverse zoning may reflect the uplift or intrusion of a body of magma at an approximately constant temperature (Jorgensen, 1971; Allegre, 1981). The build-up of volatiles as a result of anhydrous mineral crystallisation together with uplift (pressure decrease) was advocated

TABLE 6.3 MOOR OF RANNOCH AVERAGE PLAGIOCLASE COMPOSITIONS

	QUARTZ-MONZODIORITE					GRANODIORITE		MONZO-GRANUITE	SYENOGRANITE	
	RM3 CORE	RM33 CORE	RIM	RM69b CORE HOST	CORE XENOLITH	RM54 CORE	RIM	RM8 CORE	RM36 CORE	RIM
SiO_2	62.70	62.28	64.13	61.26	61.07	61.32	63.75	61.23	66.02	65.47
TiO_2	0.02	0.03	0.03	0.01	0.00	0.01	0.01	0.01	0.00	0.00
Al_2O_3	23.54	23.27	22.20	23.76	23.88	23.90	22.60	23.88	21.21	21.30
$FeO_{(t)}$	0.19	0.17	0.08	0.20	0.15	0.15	0.12	0.23	0.19	0.18
MnO	0.00	0.00	0.00	0.00	0.00	0.00	0.00	0.00	0.00	0.00
MgO	0.01	0.03	0.02	0.02	0.01	0.02	0.01	0.02	0.01	0.01
CaO	5.15	4.67	3.41	5.54	5.57	5.81	3.93	5.50	2.29	2.30
Na_2O	8.27	8.72	9.73	8.33	8.24	8.22	9.41	8.20	9.84	10.27
K_2O	0.43	0.44	0.20	0.40	0.36	0.38	0.35	0.51	0.38	0.48
TOTAL	100.35	99.61	99.80	99.52	99.28	99.81	100.18	99.58	99.94	100.01
Si	11.081	11.092	11.347	10.951	10.936	10.932	11.262	10.941	11.595	11.555
Al	4.904	4.885	4.632	5.008	5.042	5.024	4.721	5.032	4.392	4.410
Ti	0.002	0.004	0.003	0.001	0.000	0.001	0.001	0.001	0.000	0.000
Fe^{3+}	0.000	0.000	0.000	0.000	0.000	0.000	0.000	0.000	0.000	0.000
Mg	0.003	0.008	0.004	0.005	0.004	0.004	0.003	0.004	0.003	0.003
Fe^{2+}	0.028	0.025	0.012	0.028	0.023	0.002	0.017	0.034	0.028	0.026
Na	2.833	3.134	3.336	2.887	2.861	2.840	3.224	1.053	0.435	3.495
Ca	0.983	0.891	0.647	1.062	1.069	1.109	0.743	2.842	2.444	0.433
K	0.097	0.101	0.044	0.090	0.081	0.087	0.079	0.115	0.087	0.108
Ba	-	-	-					-		-
Z	16.018	16.014	15.998	15.993	16.005	15.983	16.004	15.978	16.018	15.994
X	3.913	4.126	4.027	4.039	4.011	4.036	4.046	4.010	3.966	4.036

NUMBER OF IONS ON BASIS OF 32 (O)

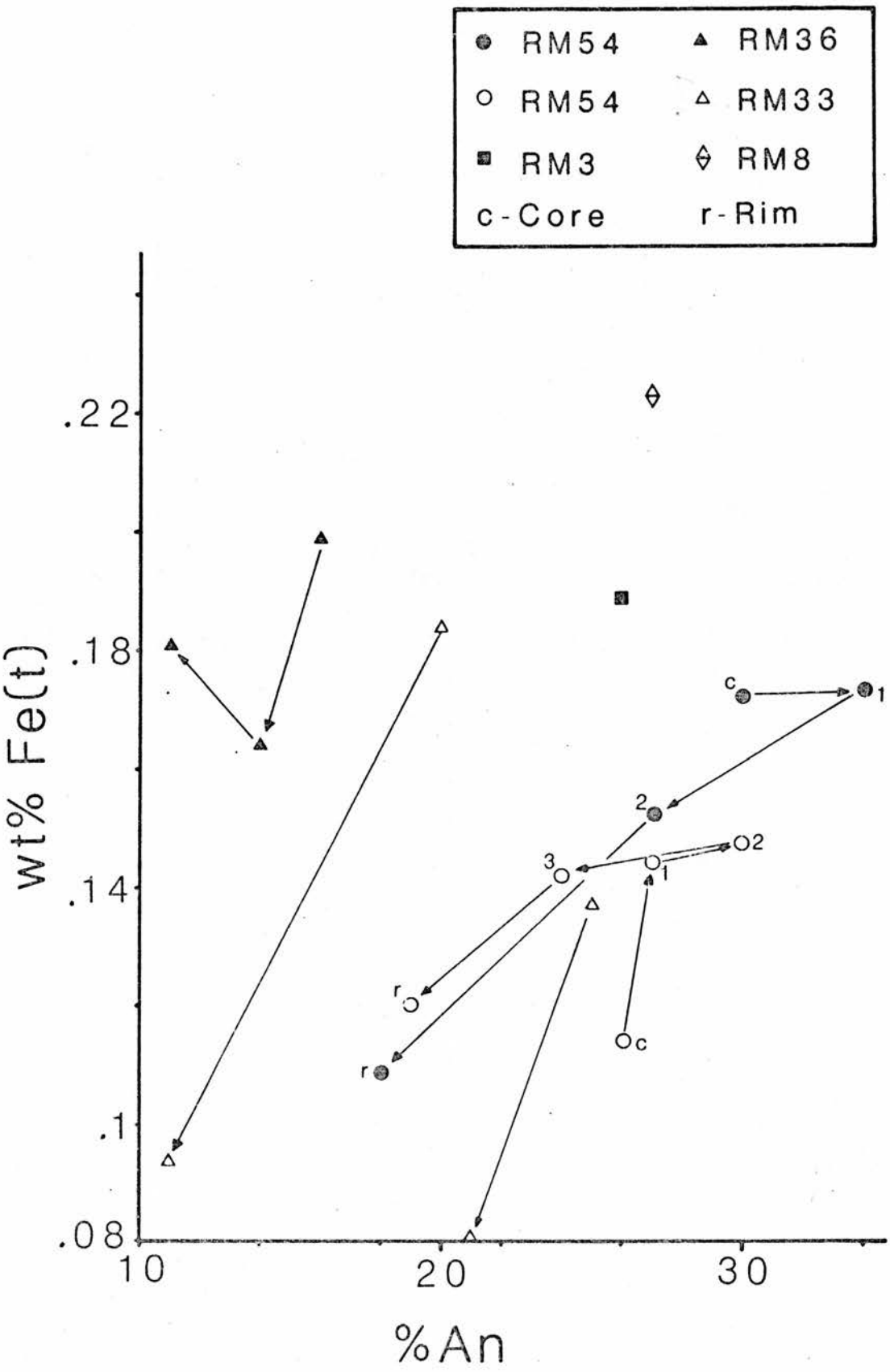

Figure 6.3.1 Plot of plagioclase analyses with tie lines to denote core - rim variation. Numbers on diagram, where present, refer to traverse step number from core(c) to rim(r). Ordinate axis values in weight percent.

by Vance (1962) to account for the rapid decrease in An content towards the rims of plagioclase crystals. The persistence of both biotite and amphibole (primary and secondary) throughout the suite is indicative of a 'wet' magma at Moor of Rannoch in contrast to that reqiured by Vance's scheme.

Sibley et.al. (1975) proposed a constitutional supercooling model to explain compositional differences <5% An. This postulated concentration gradients in the melt at crystal-melt interfaces as a result of supersaturation. The interaction of diffusion rates and crystal growth with supersaturation is considered responsible for chemical zoning which may be normal, reversed or oscillatory. The abruptly more albitic rims suggest that a change in external conditions occurred, with the resultant plagioclase composition augmented by sodic metasomatic fluids.

6.4 ALKALI FELSPAR

6.4.0 Introduction.

A total of 13 analyses of alkali feldspars were made and these are shown in Table 6.4. The range of values is from Or74.5 (RM33) to Or89 (RM54) with significant core to rim variation in samples RM33 & RM36. Ca content does not exceed An0.6 but up to 2.4 wt% Ba is recorded, this variation in Ba correlating with bulk rock values.

6.4.1 Alkali feldspar chemistry.

TABLE 6.4 MOOR OF RANNOCH AVERAGE ALKALI FELDSPAR COMPOSITIONS

	QUARTZ-MONZODIORITE			GRANO-DIORITE	MONZO-GRANITE	SYENOGRANITE	
	RM3 CORE	RM33 CORE	RIM	RM54 CORE	RM8 CORE	RM36 CORE	RIM
SiO_2	63.42	63.07	63.52	64.20	63.33	64.42	64.98
TiO_2	0.00	0.00	0.00	0.00	0.00	0.00	0.00
Al_2O_3	18.82	19.03	18.79	18.36	18.93	18.65	18.58
$FeO_{(t)}$	0.08	0.12	0.11	0.05	0.08	0.11	0.11
MnO	0.00	0.00	0.00	0.00	0.00	0.00	0.00
MgO	0.01	0.00	0.00	0.00	0.02	0.01	0.00
CaO	0.08	0.06	0.04	0.00	0.11	0.03	0.02
Na_2O	1.95	2.74	2.38	1.19	2.62	1.29	1.79
K_2O	13.16	12.57	13.59	14.97	12.61	14.54	14.14
BaO	1.71	1.97	0.80	0.51	1.53	0.70	0.22
TOTAL	99.23	99.56	99.23	99.28	99.23	99.75	99.84
Si	11.848	11.791	11.862	11.956	11.810	11.932	11.967
Al	4.144	4.194	4.121	4.031	4.162	4.073	4.033
Fe^{3+}	0.000	0.000	0.000	0.000	0.000	0.000	0.000
Mg	0.003	0.000	0.000	0.000	0.006	0.009	0.000
Fe^{2+}	0.012	0.019	0.017	0.008	0.013	0.016	0.016
Na	0.705	0.993	0.791	0.430	0.947	0.462	0.639
Ca	0.015	0.012	0.008	0.000	0.022	0.005	0.004
K	3.135	2.879	3.219	3.557	3.000	3.435	3.321
Ba	0.139	0.160	0.065	0.041	0.124	0.055	0.018
Z	16.007	16.004	16.000	15.995	15.991	16.030	15.986
X	3.994	4.044	4.083	4.028	4.093	3.957	3.982

NUMBER OF IONS BASIS OF 32(O)

Figure 6.4.1 Plot of alkali feldspar analyses with tie lines to indicate core - rim variation. Symbols as per key.

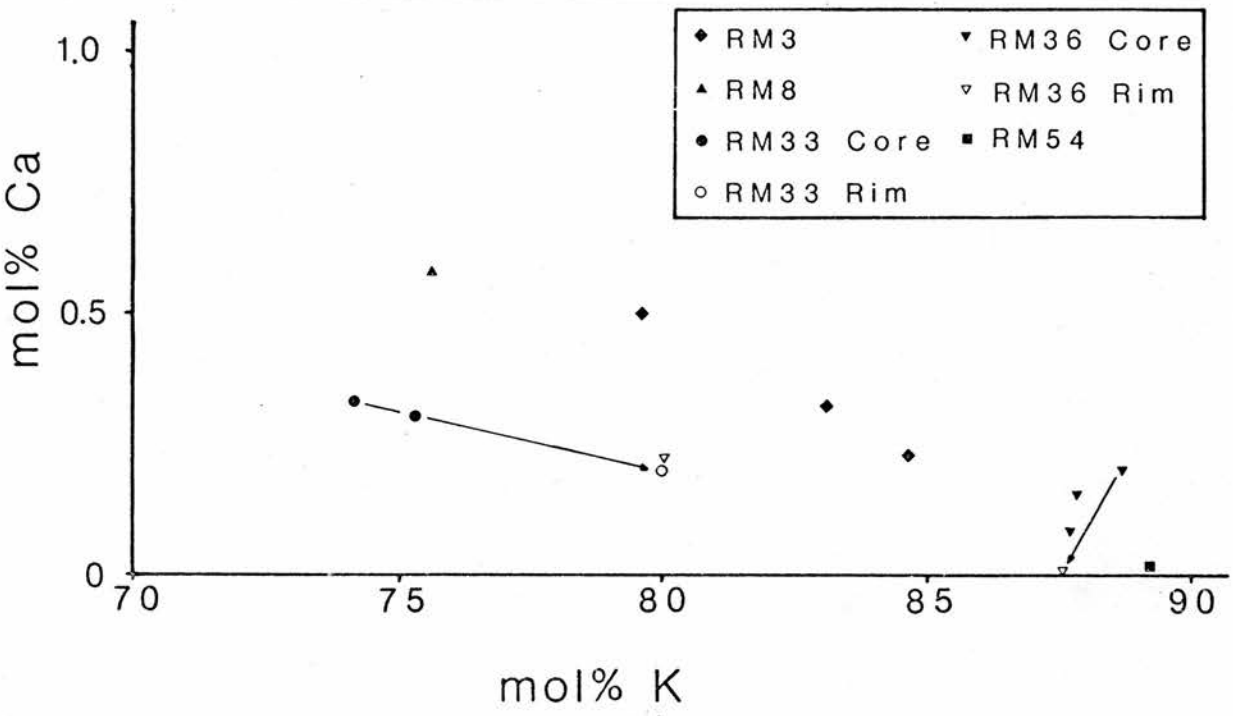

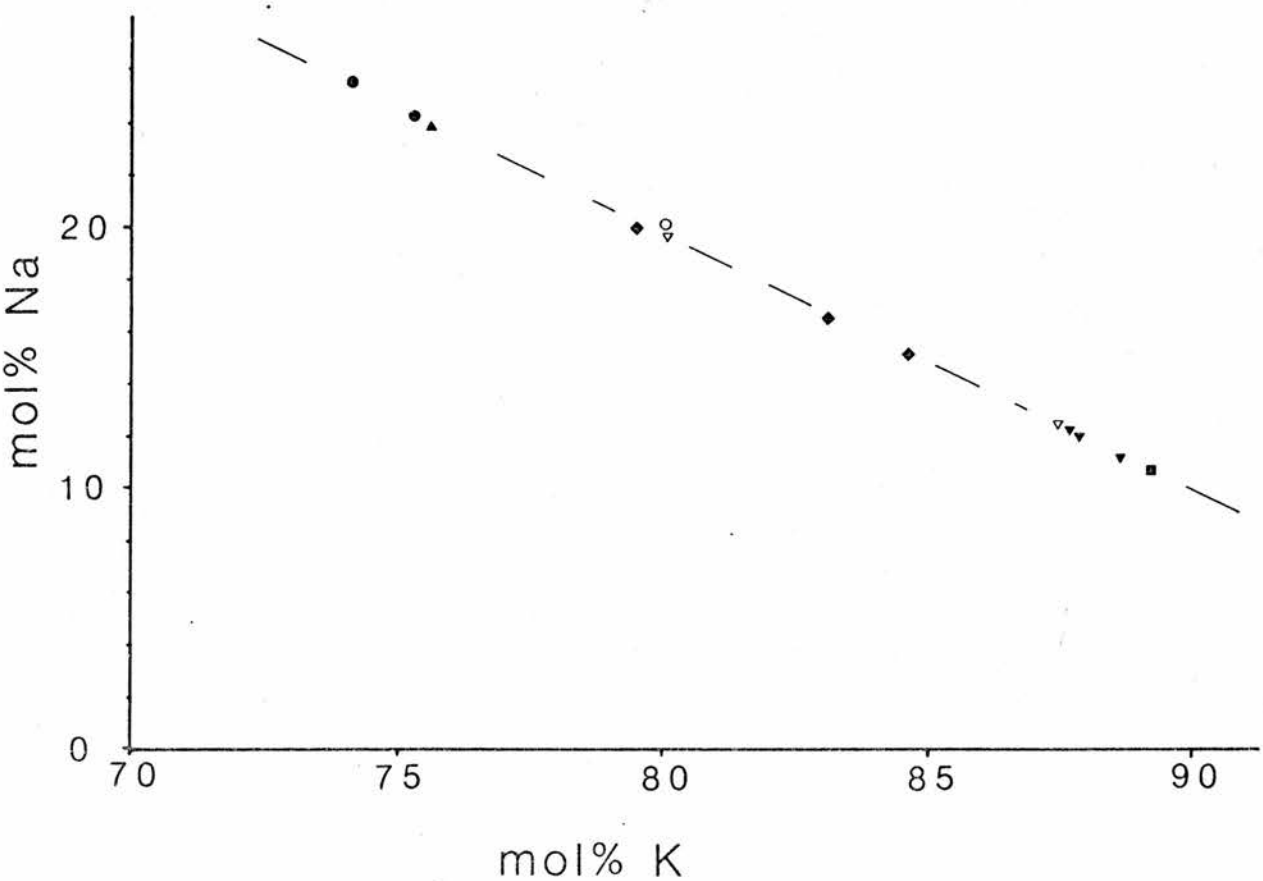

Figure 6.4.2 Plot of alkali feldspar analyses with dashed line indicating best-fit of data (estimated by eye). Core to rim tie lines omitted for clarity.

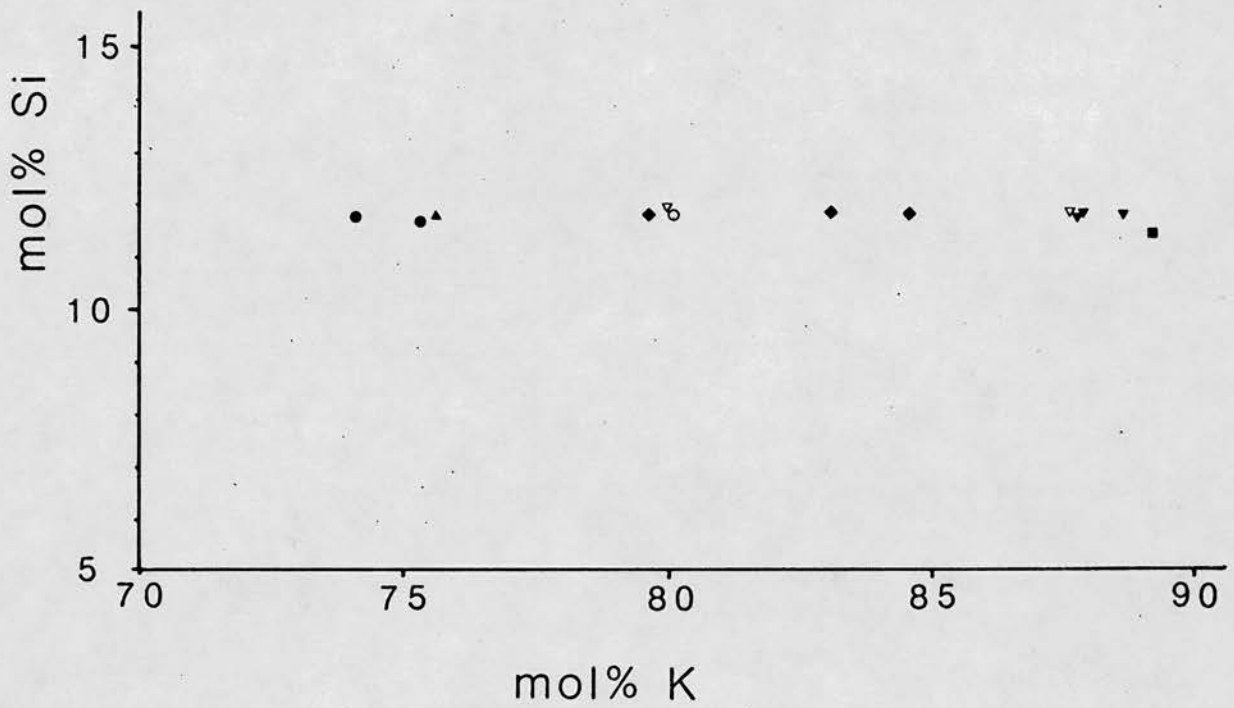

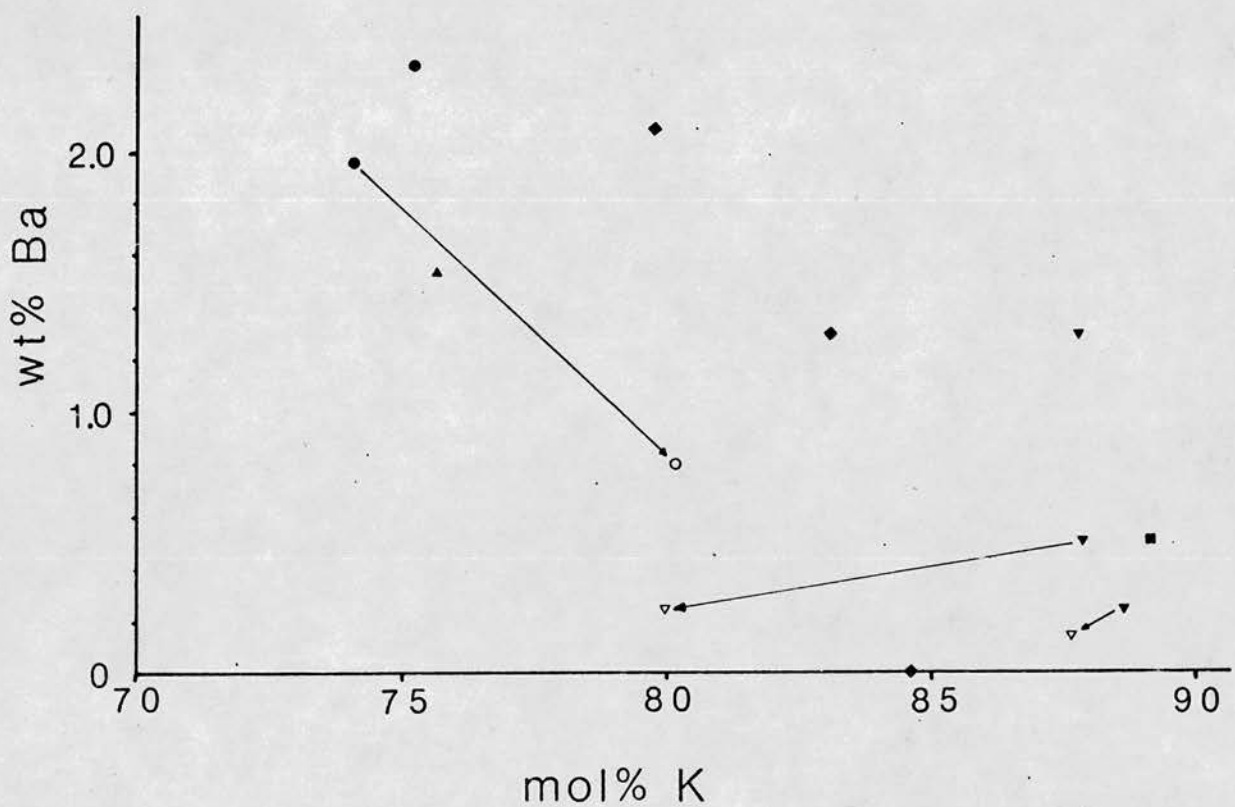

Figure 6.4.3 Plot of alkali feldspar with tie lines indicating core - rim variation. Bulk rock values of Ba added for comparison purposes.

The analysis of an alkali feldspar (RM54) optically microcline, shows the highest mol% K and the feature of increased triclinicity in the alkali feldspars appears to be common to the granodiorites. From Figs. 6.4.1, 6.4.2 & 6.4.4, compositional zoning is noted with decreasing Na and Ba from core to rim. One analysed crystal in RM36 (syenogranite) showed 'reverse zoning' with increasing Na and Ca towards the rim, but Ba behaviour followed the pattern of decreasing to the rim. This may be explained by patchy perthite development (segregation of Na and K) without invoking complex reverse zoning mechanisms.

The variation of Ca within alkali feldspar in the quartz-monzodiorites and monzogranites appears to be more regular than that of the syenogranite analysis, but the Fe content is noted as an approximately constant value in the latter (RM36) over the range Or80-88. This feature may be a function of Fe entry into the plagioclase lattice (see 6.3.2) with only a 'residual' concentration of Fe available for alkali feldspar crystallising contemporaneously.

6.2.2 Coexisting biotite and amphibole.

Throughout the Moor of Rannoch pluton, biotite is frequently found together with amphibole and is commonly mantled by green, non-weakly pleochroic amphibole of at least two distinctive habits (Chapter 4, Plates 4.1 - 4.6). This feature occurs throughout the range of petrographic types and is especially well developed in RM109

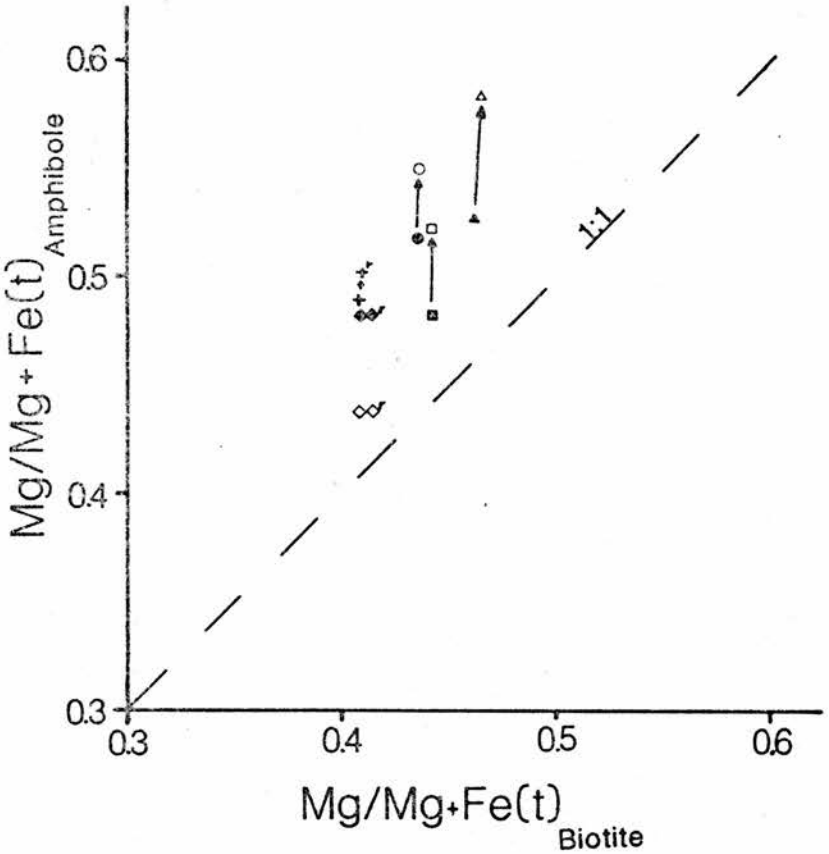

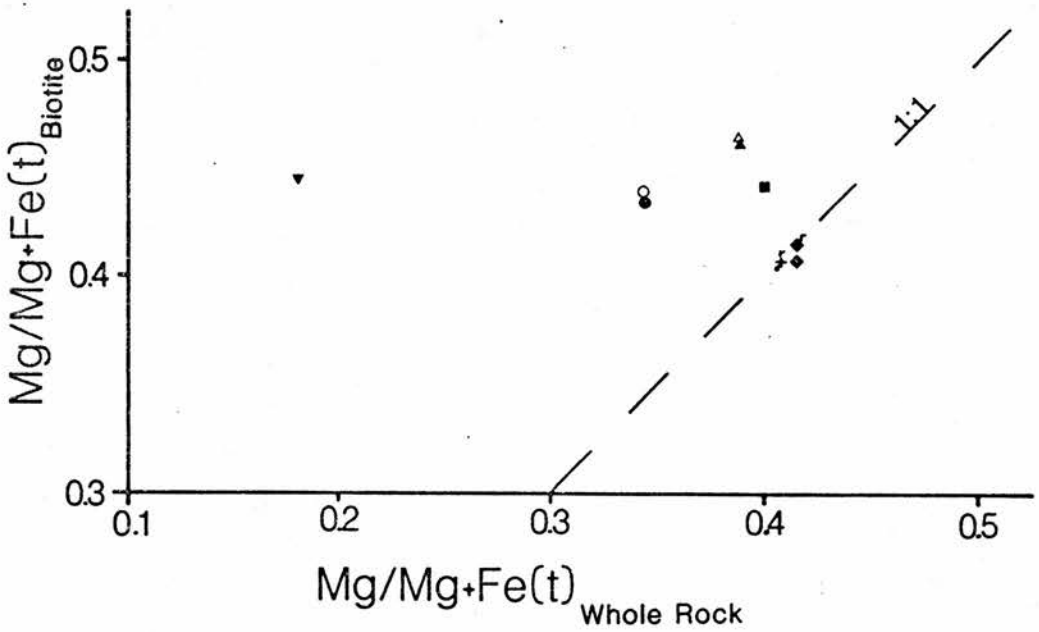

Figure 6.5.1 Plot of Mg ratio for co-existing biotite and amphiboles with unity ratio value (dashed line) added for clarity. Symbols as numbered with core - rim tie lines indicating within-crystal compositional variation.

& RM111, monzodiorites.

Comparing the distribution of Fe, Mg, Ti, Mn and Ca in biotite cores and associated amphiboles, the concentration of Mg increases slightly into the surrounding amphibole as does Mn, while both Fe and Ti significantly decrease from biotite to amphibole. The apparent distribution of Mg and Fe between biotite and amphibole (Fig. 6.5.1) indicates higher values of Mg/Mg+Fe and therefore Mg in the amphibole. Mg variation is greater in amphibole than biotite as are the overall values of the Mg ratio. This suggests that the amphiboles are of magmatic origin and may be the dominant fractionating mineral.

Comparing the Mg ratio for the xenolith with its host (RM69) quartz monzo-diorite suggests that the xenolith is composed of less refractory material than the host (ie. it is not restitic). The material may therefor represent an inclusion of metasedimentary origin which has not completely equilibrated with the host.

There is no obvious correlation between Mg and Mn indicating that their behaviour is mutually independant. If the biotite and the amphibole crystallised together, it would be expected that the distribution of Mn would be the same in both given that the Kd(Mn) is approximately similar for biotite and amphibole. The amphiboles in the samples analysed show enrichment of Mn which suggests that it crystallised earlier than the biotite.

PETROGENESIS

7.0 Introduction.

From the evidence of field relations, mineralogy and geochemistry, the Moor of Rannoch pluton has extensive chemical and petrographic variation. Thus any petrogenetic model for Moor of Rannoch magmatism must accounted for the characteristics briefly summarised below.

a) The mapped distibution of samples indicates a predominance of quartz monzodiorite and monzogranite types east of the Laidon-Ericht fault and granodiorites west of the fault.

b) There is a low volume of evolved (syenogranitic) types in the pluton, a feature common to many calc-alkaline suites, unlike the nearby Etive intrusion. The outcrop characteristics have been summarised in Chapter 3.

c) Harker plots of major and trace elements display colinear, discontinuous trends.

d) There are significantly different absolute abundances of certain trace elements and differing element ratios across the Laidon-Ericht fault.

e) Moor of Rannoch samples possess elevated Ba and Sr values and the basic rocks are also rich in Ni and Cr.

f) New isotopic data for Moor of Rannoch (presented below) shows the initial $^{87}Sr/^{86}Sr$ ratios for the syenogranites to be significantly lower than those of the intermediate and basic types. The Sr initial ratios for Moor of Rannoch are lower than those for the neighbouring

Strath Ossian pluton (Clayburn, 1981).

g) The reversal of the normal amphibole and biotite crystallisation trend, described in chapters 4 & 6, must be explained.

Four possible petrogenetic models will be examined and applied to Moor of Rannoch data in an attempt to explain the observed features of the pluton. The models under consideration are (a) in-situ fractional crystallisation of a single intrusion of magma; (b) episodic comagmatic intrusion or "pulses" of magma from a common homogeneous source, which may or may not undergo fractionation on emplacement; (c) multiple intrusion and fractionation of magma from a heterogeneous source; (d) the pluton is a composite of two disparate intrusive events not necessarily contemporaneous or spatially related until juxtaposed by movement along the Laidon-Ericht fault. Magma mixing and restite separation processes may additionally be involved.

The internal nature of calc-alkaline magma chambers and their development has been studied by many workers (eg. Read, 1956; Pitcher and Berger, 1972; Pitcher, 1978; Hildreth, 1981). The postulated magma chamber(s) at Moor of Rannoch will be considered in terms of discontinuous versus continuous evolution resulting in the observed distribution of rock types.

A model of in-situ fractional crystallisation would therefore attempt to account for the field, petrographic and geochemical evidence in terms of a single event of magma generation followed by ascent into the crust where crystallisation proceeded essentially undisturbed. Considering the continuous magma chamber evolution

hypothesis, both single and multiple events of magma generation and emplacement are encompassed.

Emplacement of magma into the crust as a single chamber may lead to the establishment of an independent convective 'cell' within the body and thus crystallisation may not proceed simply from margin inwards to core with concomitant element fractionation. The concept of density and chemical stratification within calc-alkaline magma chambers, recently reviewed by Hildreth (1981), further complicates a simple fractional crystallisation model. Magma mixing may thus result from coalescence of fractionated magma in convective cells in an essentially unique magmatic event. Disruption of chemical gradients in a graded magma chamber would also lead to a more random distribution of rock types within a single intrusive event. Fridrich and Mahood (1984) consider that significant and abrupt trace and major element differences are not due to diffusion based mechanisms (in-situ differentiation) but result from rearrangement of a vertically graded magma column.

Replenishment of a magma chamber would also give rise to an apparently random distribution of rock types and implies continued connection to depth throughout the evolution of the chamber. Differentiation may therefore have occurred at source, during ascent (reaction with earlier magmatic phases) or on emplacement as with a single magmatic event, independent of the earlier phase.

The implications of the above will be discussed later after isotopic data and computer modelling of the geochemical data has been considered.

7.1 New isotopic data.

Initial Sr ratios (assuming an age of 400 Ma.) for selected samples from each geochemical group within the complex were obtained and are presented in Table 7.1 (see also Appendix 2 for analytical details).

The close relationship between the monzogranite samples of groups III & IV (RM17A & RM17) and the group II monzodiorite sample (RM111) (0.70500 - 0.70503) suggests that the source material for the rocks was relatively homogeneous. Large scale assimilation of crustal material does not appear to have occurred. Temporal separation of the different rock types isotopically is not practicable as all three analyses lie within analytical error (+/- 4 in the fifth decimal place).

The monzo/syenogranite sample RM86 has a significantly lower Sr initial ratio which cannot be explained in terms of assimilation of Sr-poor crustal material affecting a comagmatic, cogenetic melt. A separate source for this type is therefore proposed and this is in good agreement with trace element data (Chapter 5.8.1, Table 5.1).

TABLE 7.1

MOOR OF RANNOCH: Rb-Sr ANALYSES (NEW)

SAMPLE NUMBER	Rb ppm	Sr ppm	Rb/Sr (weight)	$^{87}Rb/^{86}Sr$ (atomic)	$^{87}Sr/^{86}Sr$ (atomic)	$(^{87}Sr/^{86}Sr)_t$
RM111	34	1854	0.01834	0.061724	0.705357	0.70500±4
RM17	53	994	0.05332	0.169170	0.706021	0.70503±4
RM17A	35	1319	0.02654	0.084449	0.705506	0.70501±4
RM86	67	256	0.26172	0.782334	0.708937	0.70454±5

MOOR OF RANNOCH: Sm-Nd ANALYSIS (NEW)

SAMPLE NUMBER	Sm ppm	Nd ppm	Sm/Nd	T_{CHUR} (Ma)	t (Ma)	$(E)_t$
RM111	9	48	0.1875	1083.288	400	-6.8075
	(143/144)			TDM		
	.5118			1536.507		

Clayburn (1981) has interpreted Sr initial ratios for the neighbouring Strath Ossian pluton (0.70576 - 0.70610 for granodiorite; 0.70736 - 0.70812 for biotite granite) as being the result of upper crustal contamination of an I-type magma of lower(?) crustal origin. Harmon and Halliday (1980) analysed a sample of Moor of Rannoch (quartz monzodiorite ?) with 1581ppm Sr and one Sr initial ratio of 0.7048 at 405 Ma. Interpreting this against his data, Clayburn (1981) suggested that the unradiogenic Sr isotopic composition of Moor of Rannoch indicated this intrusion had suffered minimal upper crustal contamination, unlike the Strath Ossian intrusion. Clayburn further suggested that the high Sr abundance for the Moor of Rannoch sample indicated a greater lower crustal component.

The more detailed sampling carried out for this work suggests that the two intrusions, although spatially and petrographically related, are distinct in terms of source, intrusive history and may not be contemporaneous.

7.2 Mass balance modelling.

Computer modelling using the petrochemical blending method of Wright and Doherty (1969) was carried out with mineral and whole rock major element data on selected samples of each geochemical group from the complex. The object was to test hypotheses of fractional crystallisation between members of the complex. The results are presented in Table 7.2,a-d.

TABLE 7.2(A)

TARGET ANALYSIS: GROUP II COMPOSITION USING A GROUP I STARTING COMPOSITION

CHEMISTRY OXIDE	CALCULATED GPI RESIDUAL	TARGET GPI ANALYSIS	STATISTICS SQUARED DEVIATIONS	MINERALOGY BULK ROCK/ MINERAL	PROPORTION
SiO_2	52.82	52.82	0.0	GPII	0.0
TiO_2	1.32	1.320	0.0	MAG	0.194
Al_2O_3	17.380	17.380	0.0	Mg-AMPH	20.338
FeO(t)	6.907	6.907	0.0	Mg-BIOT	21.050
MnO	0.107	0.070	0.0014	PLAG	47.317
MgO	5.520	5.520	0.0	ALK FELD	9.731
CaO	5.456	6.120	0.4405	SPHENE	0.841
Na_2O	4.322	3.830	0.2416		
K_2O	3.500	3.500	0.0		
TOTAL	97.319	97.467	0.6835		99.472

NOTES: 10 Iterations, all Iron calculated as Fe_2O_3 mineralogy corresponds to a Monzodiorite rock type
Mg-rich mineral Probe Analyses used.

TABLE 7.2(B)

TARGET ANALYSIS: GROUP III COMPOSITION USING A GROUP II STARTING COMPOSITION

CHEMISTRY OXIDE	CALCULATED GPII RESIDUAL	TARGET GPII ANALSIS	STATISTICS SQUARED DEVIATIONS	MINERALOGY BULK ROCK/ MINERAL	PROPORTION
SiO_2	56.880	56.880	0.0	GPIII	32.769
TiO_2	0.759	0.750	0.0001	Mg-AMPH	11.886
Al_2O_3	18.850	18.850	0.0	Mg-BIOT	10.793
FeO(t)	5.162	5.162	0.0	PLAG	44.941
MnO	0.102	0.090	0.0001		
MgO	4.281	4.950	0.4480		
CaO	5.460	5.460	0.0		
Na_2O	5.553	5.490	0.004		
K_2O	2.211	2.190	0.0004		
TOTAL	99.257	99.822	Σ0.4527		100.389

NOTES: 14 Iterations, all Iron calculated as Fe_2O_3 mineralogy corresponds to a Quartz Diorite/Tonalite rock type
Mg-rich mineral Probe Analyses used.

SiO_2	56.880	56.880	0.0	GPIII	32.058
TiO_2	0.750	0.750	0.0	Fe_AMPH	11.735
Al_2O_3	18.850	18.850	0.0	Fe-BIOT	10.279
FeO(t)	5.162	5.162	0.0	PLAG	45.395
MnO	0.104	0.090	0.0002	ALK FELD	0.503
MgO	4.088	4.950	0.7432	SPHENE	0.044
CaO	5.460	5.460	0.0		
Na_2O	5.553	5.490	0.004		
K_2O	2.190	2.190	0.0		
TOTAL	99.038	99.822	Σ0.7474		100.013

NOTES: 10 Iterations, all Iron calculated as Fe_2O_3 mineralogy corresponds to a Quartz Diorite/Tonalite rock type
Fe-rich mineral Probe Analyses used.

TABLE 7.2(C)

TARGET ANALYSIS: GROUP IV COMPOSITION USING A GROUP III STARTING COMPOSITION

OXIDE	CALCULATED GPIII RESIDUAL	TARGET GPIII ANALYSIS	STATISTICS SQUARED DEVIATION	MINERALOGY BULK ROCK/ MINERAL	PROPORTION
SiO_2	59.490	59.490	0.0	GPIV	25.469
TiO_2	0.688	0.660	0.0008	MAG	0.164
Al_2O_3	18.390	18.390	0.0	Mg-AMPH	13.439
FeO(t)	4.675	4.675	0.0	Mg-BIOT	10.499
MnO	0.111	0.090	0.0005	PLAG	44.348
MgO	3.900	3.900	0.0	ALK FELD	8.152
CaO	4.960	4.960	0.0		
Na_2O	5.244	4.900	0.1186		
K_2O	2.930	2.930	0.0		
TOTAL	100.389	99.995	Σ0.1199		102.071

NOTES: 10 Iterations, all Iron calculated as Fe_2O_3 mineralogy corresponds to a Quartz Diorite/Tonalite rock type
Mg-rich mineral Probe Analyses used

SiO_2	59.490	59.490	0.0	GPIV	26.982
TiO_2	0.681	0.660	0.0005	Fe-AMPH	13.629
Al_2O_3	18.390	18.390	0.0	Fe-BIOT	10.283
FeO(t)	4.675	4.675	0.0	PLAG	42.847
MnO	0.112	0.090	0.005	ALK FELD	8.297
MgO	3.791	3.900	0.0119		
CaO	4.960	4.960	0.0		
Na_2O	5.204	4.900	0.0922		
K_2O	2.930	2.930	0.0		
TOTAL	100.234	99.995	Σ0.1051		102.038

NOTES: 12 Iterations, all Iron calculated as Fe_2O_3 mineralogy corresponds to a Quartz Diorite/Tonalite rock type
Fe-rich mineral Probe Analyses used

TABLE 7.2(D)

TARGET ANALYSIS: GROUP V COMPOSITION USING A GROUP IV STARTING COMPOSITION

CHEMISTRY OXIDE	CALCULATED GPIV RESIDUAL	TARGET GPIV ANALYSIS	STATISTICS SQUARED DEVIATIONS	MINERALOGY BULK ROCK/ MINERAL	PROPORITON
SiO_2	65.710	65.710	0.0	GPV	33.991
TiO_2	0.510	0.510	0.0	MAG	0.173
Al_2O_3	16.090	16.090	0.0	FE-AMPH	18.476
FeO(t)	3.390	3.390	0.0	FE-BIOT	-
MnO	0.087	0.070	0.003	PLAG	41.698
MgO	2.490	2.490	0.0	ALK FELD	5.960
CaO	3.474	3.780	0.0934	SPHENE	0.627
Na_2O	6.095	4.430	2.7729		
K_2O	2.600	2.600	0.0		
TOTAL	100.446	99.070	Σ2.8666		100.925

NOTES: 12 Iterations, all Iron calculated as Fe_2O_3 mineralogy corresponds to a Monzonite/Monzodiorite rock type
Fe-rich mineral Probe Analyses used

7.2(E)

GROUP I Composition, analysis of - RM68
GROUP II " " " - RM69
GROUP III " " " - RM3
GROUP IV " " " - RM54
GROUP V " " " - RM36

Matching the selected constituents with a specified target composition results in a best fit, the squared deviations (r^2) of which approach zero as the difference between the actual and calculated end-member compositions approaches zero. Values of (r^2) < 1.0 are normally taken to indicate that removal of minerals from a selected parental melt composition, in specified proportions, fits the observed end-member with only a small error. This would support fractional crystallisation as a process. Minor discrepancies will occur as all Fe is recalculated to Fe2O3 and so any differences in modal mineralogy as a result of different oxidation states will not be modelled.

Considering a group I sample RM68, and a group II sample RM69 (both quartz monzodiorites), the modelling indicates that Mg-rich biotite and amphibole compositions are more likely to be involved in any crystal fractionation along with plagioclase (andesine), minor sphene, alkali feldspar and Fe-Ti oxides. If Fe-rich mafic compositions are modelled, the 'fit' of blende to target decreases and the proportion of alkali feldspar and sphene increase significantly. From Figs. 5.2.3, 5.3.5 and 6.5.1, Mg can be seen to be the main variant.

If alkali feldspar is not considered as a fractionating mineral, the 'fit' of the target composition decreases due to increasing differences in Na and K. Alkali feldspar, from petrographic evidence, occurs both as an early mineral phase and as a late-stage pore filling phase and thus may be considered within the models.

A 'best fit' at $r^2 = 0.68$ (Table 7.2a) indicates that Mg-rich mafic minerals, plagioclase and alkali feldspar fractionating out of an originally group I composition are unlikely to generate a rock of group II composition as both Ca and Na are poorly modelled. The proportion of group II composition generated suggests that simple crystal fractionation alone could not generate the volume of group II quartz monzodiorites and quartz monzonites seen at surface.

Examining a possible relationship between groups II and III, the chemical modelling of crystal fractionation shows that Mg is the only element with a significantly poor fit between target and selected actual composition. The model indicates that Mg-rich biotite and amphibole, coupled with plagioclase (andesine) as the dominant fractionating minerals, with alkali feldspar as a minor accessory fractionating mineral. Minor amounts of sphene would reduce the differences in Ti and Mn. The overall 'fit' produced by the model is good ($r^2 = 0.45$, Table 7.2b) suggesting that crystal fractionation could link the end-member group II and III compositions.

The totals for target and constituent proportions are very similar. The proportions of minerals abstracted from the group II composition would approximate to a rock of dioritic type and probable group I composition. There is however a volume problem as the total area of group III rocks (and their spatial distribution with respect to group II types) makes it unlikely that a crystal fractionation process alone was responsible for their generation from a group II parent. The problem of modelling a complex 3-dimensional shape and

attempting to reconcile the data with 2-dimensional surface observations is considered in more detail in section 7.3.

Between geochemical groups III & IV a calculated crystal fractionation relationship is produced with Mg-rich mafic minerals involved, the proportions of which are similar to that for the link between groups II & III. The sum of deviations (r^2 = 0.119 for Mg-rich mafic minerals, 0.105 for Fe-rich mafic minerals, Table 7.2c) is low and although the total proportion of fractionating minerals and resultant end-member composition is slightly high, the target and blende compositions are very similar. Na appears to be poorly modelled but this could be explained by metasomatic processes artificially enriching or depleting the element from the selected composition. The calculated volume of end-member composition generated appears to be inconsistent with the observed spatial distribution of group IV types at surface.

Chemical modelling of any possible crystal fractionation connection between the syenogranites and rocks of intermediate composition must take into account the Fe-rich compositions of the syenogranite biotites.

If it assumed that amphibole fractionation was involved and that all amphibole was removed from the intermediate compositions, the calculated mineral and bulk-rock proportions when amphibole is considered give an improved degree of 'fit'. However, since biotite and alkali feldspar are mutually exclusive in the model, it is considered that biotite is the more likely fractionating mineral.

Regardless of choice of Fe or Mg-rich mafic minerals or selection of alkali feldspar as a fractionating mineral, Ca and Na are poorly modelled and the lack of 'fit' (r^2 = 2.866, Table 7.2d) implies that the syenogranites are not part of a series related only by crystal fractionation. Metasomatic(?) alteration of an originally related end-member composition would disrupt the ideal model - whole-rock composition 'fit'. Variable sericitisation and incipient sodic alteration has been noted for group IV and V samples (chapter 4).

7.3 Fractional crystallisation model.

Considering a simple crystal fractionation model, in-situ fractionation of a single intrusive pulse of magma would be expected to yield smooth gradations of rock type from margin to core and gradual changes in bulk-rock and mineral chemistry when plotted against silica. Antipathetic variation of Rb and Sr on a common line of descent and minor variations of Sr initial ratios would suggest that all samples were a genetically related geochemical series. From the data presented in chapters 3 through 6, together with petrochemical modelling information, this simplistic model can be rejected for the following reasons.

The mapped distribution of rock types is irregular and cross-cutting relationships of normal and reversed style between more evolved and basic intermediate types are found. Variation of bulk-rock major and trace elements indicate that petrographically distinct types are also chemically distinct. There are abrupt composition gaps between geochemical groups II & III and IV & V which are not thought

to result from sampling irregularities and are not adequately explained.

Petrochemical modelling suggests that the quartz monzodiorites of group III and monzogranites and granodiorites of group IV could be linked in a crystal fractionation scheme, but the volumes of the more acidic end-member generated do not readily equate with the mapped surface distribution of these types. The syenogranites form approximately 2% (c. 5 km^2) of the total exposed area of the pluton (c. 240 km^2).

From the mass balance modelling (Table 7.2d), the removal of amphibole and plagioclase in the calculated percentages from a group IV parent could yield a group V syenogranite whose volume would approximate to 34% of the starting volume. Group IV rocks form approximately 60% of the pluton (c. 160 km^2) and thus the calculated volume of group V syenogranite should approximate to c. 55 km^2. The sheet-like nature of the eastern syenogranites suggests a possibly larger original volume than is seen at present. Despite this, the volume of acidic end-member calculated does not readily equate with the mapped distributions for the syenogranites with the difference a factor of 10. Mass balance modelling for the Skye granites also indicates that the volume of granite visible does not equate with those calculated (Aprahamian et al., 1976) and thus trace element variability and radiogenic Sr data must be used to constrain any likely fractional crystallisation link between the different geochemical groups at Moor of Rannoch.

Trace element abundances within the pluton show variations which do not conform to a simple zoning scheme. The pattern appears to represent minor zoning resulting from fractionation modifying a spatial distribution of magmatic pulses. The relative Rb depletion of the acidic members of the suite with respect to the basic and intermediate members is distinctive and, coupled with the Rb/Sr and Ce/Y ratios, the same source is thought unlikely for the parental melt of the syenogranites from west of the Laidon-Ericht fault. The initial Sr ratio for the syenogranites (0.70454 +/-5) is significantly lower than that of the quartz monzodiorites, granodiorites and monzogranites (0.70500 - 0.70503 +/-4). This implies that either crustal contamination has selectively affected the intermediate types or that there has been a change in source for the syenogranites.

7.4 Magma mixing models.

Magma mixing of two genetically related magmas has often been proposed to explain rectilinear compositional variation on Harker diagrams (Fenner, 1926; Hall, 1972; Vogel et al., 1984). McBirney (1980) considered that two processes were involved - a deep-seated one responsible for long-term variation of successive suites and a shallow level one which gave rise to vertically zoned magma chambers. A problem with any interpretative approach to chemical data is that the spread of data points may result from sampling different pulses as well as rock types within a large complex. This situation may have occurred with Moor of Rannoch data and any magma mixing model must account for compositional variation with respect to time.

Magma mixing is a possible explanation for the amphibole textures noted previously but is a process precluded from a scheme of in-situ fractionation of a single intrusion of magma. Invoking episodic replenishment of the magma chamber, regardless of source heterogeneity, is consistent with a magma mixing event. Hall (1972) proposed that magma mixing was responsible for granitoid generation in the Caledonian as it more conveniently explained the linear continuity of geochemical data. Whalen and Currie (1984) also point out that linear chemical variation on element-element plots is intrinsic to all types of mixing processes. These features are seen on the scale of the Moor of Rannoch pluton.

If it is assumed that the Moor of Rannoch complex is a moderately high-level, mesozonal intrusion (on the basis of comparison with Etive, Droop and Treloar, 1981; Strath Ossian, Clayburn, 1981), then any magma which was the product of lower crustal partial melting would have to be relatively 'dry' to enable it to ascend significant distance.

The presence of primary amphibole and secondary amphibole mantling biotite aggregates suggests that tha magma had a moderate H2O content. Further, a magma mixing origin for these characteristic mineral textures would involve a more basic end-member which is not seen, either at surface or as mineral inclusions (eg. clinopyroxene) in the monzodiorites. Development of the texture within the basic to more evolved intermediate rock-types could be the result of magma mixing, but its widespread occurrence would require the process to

have pervaded the two magmas over large distances.

7.5 Multiple intrusion model (common parental source).

The second model proposed, multiple intrusion from a common parental source, implies periodic replenishment of the magma chamber and could better explain some of the gross discrepancies found for the first model. The common trend in major and trace element data for the different rock types, together with their field relations and distinctive geochemical grouping, suggests that the pulses were comagmatic. The field relations showing later, more basic material cutting earlier more evolved material remain unexplained and abrupt changes in trace element abundances between the facies are not consistent with simple fractionation of successive comagmatic pulses. Significant differences in certain major and trace element ratios across the Laidon-Ericht fault are not adequately explained by such a model, while the different Sr initial ratios for the syenogranites and intermediate types implies source heterogeneity or changing source composition for the parental melt.

7.6 Multiple intrusion model (changing parental source).

The third model, multiple intrusion or pulses of magma from a changing parental source with subsequent fractionation on replenishment, could account for the changes in trace element ratios (eg. Ce/Y, Fig. 5.8.1, Rb/Sr, Fig. 5.7.8) across the fault. The characteristic field evidence of later basic material east of the Laidon-Ericht fault could be interpreted as a first product of later

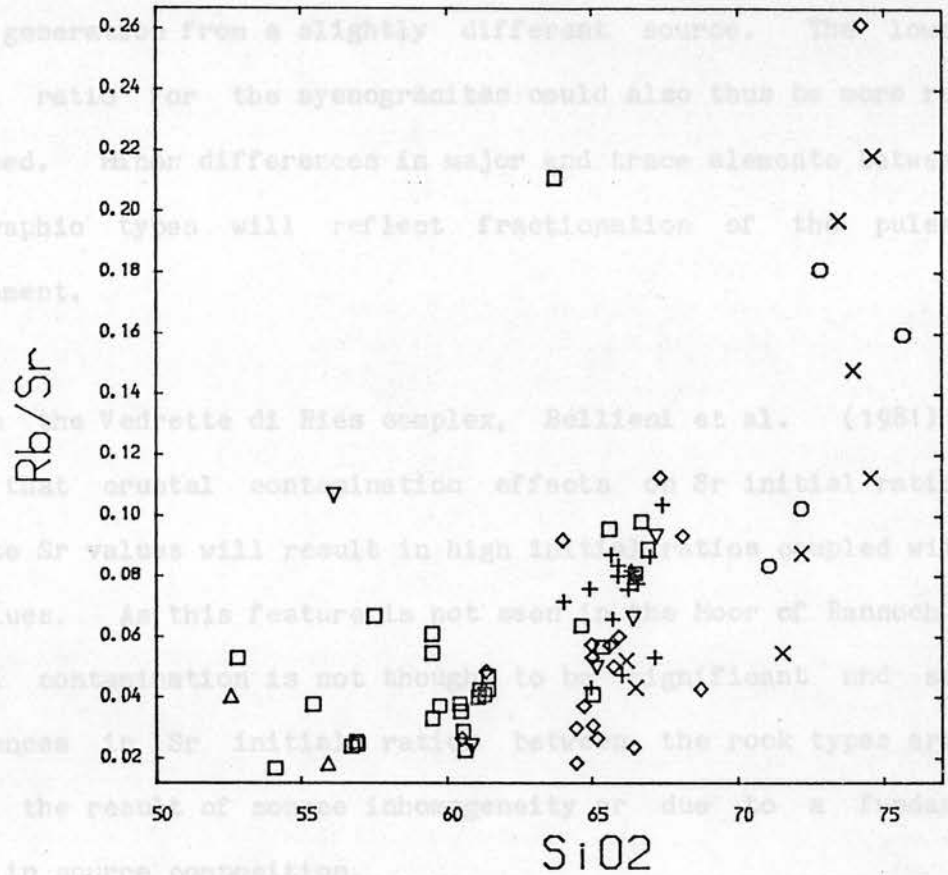
Rb/Sr
0.26
0.24
0.22
0.20
0.18
0.16
0.14
0.12
0.10
0.08
0.06
0.04
0.02
50
55
60
65
70
75
SiO2

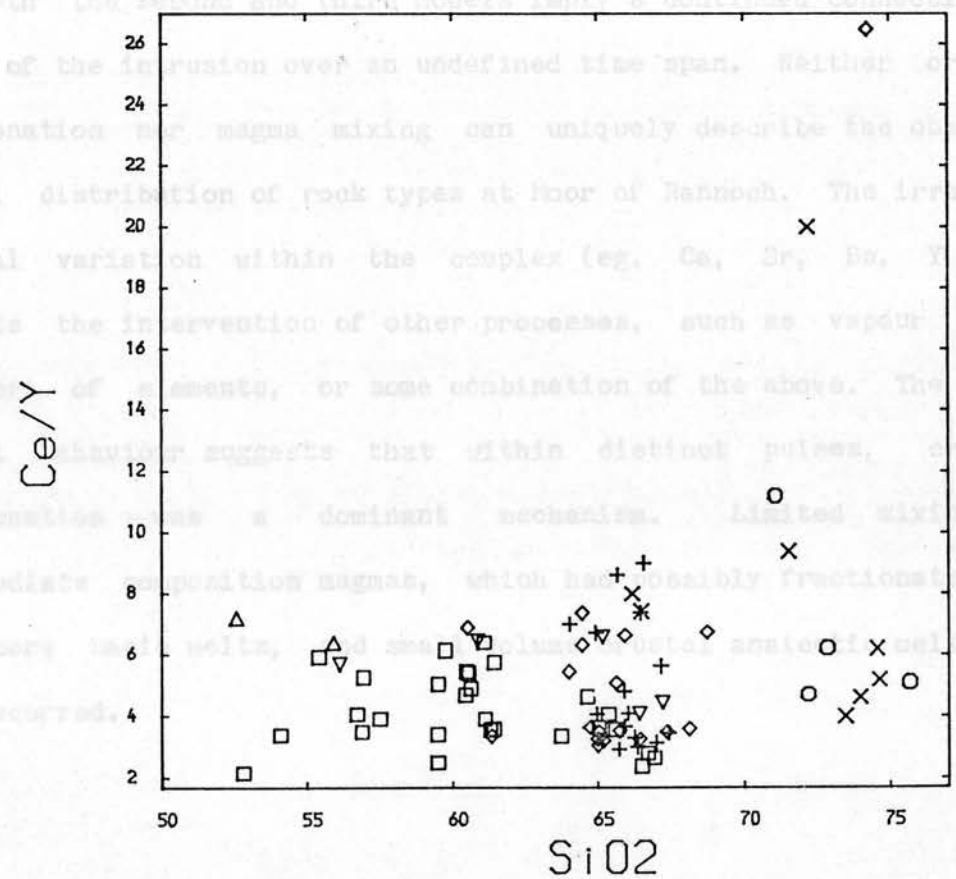
Ce/Y
26
24
22
20
18
16
14
12
10
8
6
4
2
50
55
60
65
70
75
SiO2

Late precipitation of biotite as an interstitial phase evidences a 'dry' melt which would correspond to fractionation of an anhydrous phase from an intermediate composition felsic I-type melt. However low Rb and relatively high Sr abundances are not consistent with a fractionation scheme involving plagioclase and the lower Sr initial ratio remains enigmatic. If source heterogeneity is considered then this, together with an undefined time lapse between generation of the intermediate and acidic compositions, may explain the lower ratio.

Winkler (1976) argued that granites could be the result of anatexis of metasediments, with lower temperatures (675 - 750^{o}C) and lower P_{H2O} (2 kbars) generating alkali granite compositions and higher temperature and pressure generating monzogranitic compositions. The syenogranites may result from limited evolution of an originally I-type magma, giving some characteristics which are common to both I- and A-type magmas. but their low total volume and association with predominantly I-type intermediate compositions may preclude this origin. There is no evidence of ghost stratigraphy or schlieren, which Pitcher (1979) considers to be common to all anatectic partial melts of metasediments (eg. banded semipelitic schists), except in those acidic types at the northern and western margins of the complex.

7.7 Contemporaneous fault movement and magma emplacement.

The fourth model is essentially a modification of the episodic intrusion model involving source region heterogeneity. Based on comparisons and contrasts between the two distinct parts of the Moor of Rannoch pluton divided by the Laidon-Ericht fault, this proposal seeks to establish a possible relationship between the eastern portion of the Moor of Rannoch complex and the Etive intrusive complex some 20-30 kms to the south-west.

Field evidence for a possible relationship centres on the similarity of intrusive style noted for the south-eastern part of Moor of Rannoch and south-western part of the Etive complex. As reported in Chapter 3, the margin of the Moor of Rannoch pluton is a sheeted contact with the country rocks with inward dipping attitude and a progression from more acidic to more basic material into the main mass of the intrusion. This is similar to that noted for the south-west part of the Cruachan monzodiorite in the Etive complex (Batchelor, 1984). In contrast, the eastern margin of Etive has a sharp, steep contact with the country rocks. On the eastern margins, the porphyritic Starav intrusion of Etive pinches out this outer Cruachan phase.

Trace element distributions for the Moor of Rannoch have been shown to be different across the Laidon-Ericht fault. The abundances of selected elements from the eastern part of the complex, especially towards the southeast, are similar to those for the Etive monzogranites and quartz-monzodiorites (Batchelor, 1984). Moor of Rannoch sample RM28 from the Loch Tulla outlier lies consistently

outwith the fields of main pluton samples and appears to be equivalent to Starav material, both chemically and petrographically (e.g. lower Sr abundances, porphyritic orthoclase). The leucocratic syenogranites of this eastern part of Moor of Rannoch, with low Y, Nb & Zr, show chemical affinity with the Meall Odhar type of Etive.

The aeromagnetic anomaly map (IGS, 1978; scale 1:10000) also clearly shows the Laidon-Ericht fault to be a major structural feature and the higher values of closed anomalies in the eastern part of Moor of Rannoch may be related to similar anomalies noted in the south and south-eastern parts of the Etive complex. If the south-eastern part of the Moor of Rannoch pluton was originally part of the Etive intrusion, then the sense of the fault displacement would be sinistral. This is consistent with that of the sub-parallel Great Glen Fault and would require a movement of the order of 20 - 30 kms. Displacements of varying amounts have also been postulated for the Great Glen Fault and so these values for the Laidon-Ericht fault are feasible.

7.8 Moor of Rannoch and Strath Ossian plutons compared and contrasted.

7.8.1 Strath Ossian field relations.

Hinxman (1923) and Anderson (1956) both described in detail features of the contact relationships between the Strath Ossian intrusion and the surrounding Moine quartzites and Lower Dalradian schists. The realignment of strike and increase in dip of the country rocks with increasing proximity to the intrusion is similar to that

noted for the eastern margin of the Moor of Rannoch (Chapter 3). Hinxman (1923) considered the belt of schists between the two intrusions to represent a roof pendant and thus argued that Strath Ossian was a satellite cupola of the Moor of Rannoch intrusion.

Internal contact relations between the different rock types in the northern part of the complex were described by Anderson (1956) and confirmed by Clayburn (1981). The full range of rock types has remained unknown and the reconnaissance sampling undertaken for this work has shown there to be a range from diorites in the centre of the elongate body to the more acidic varieties noted from the northern margin. Intrusive relations between the diorite and quartz-monzodiorite types have been found (O.S. grid ref. NN399731) and these indicate that the quartz-monzodiorite is later than the diorites in a cross-cutting and veining relationship. There appears to be only limited re-equilibration at the contact between the two which is restricted to a millimetric scale. The intrusive leucocratic quartz-monzodiorite has a marginal leucocratic contact with the diorite approximately 0.5-1cm wide and patches of finer-grained quartz-monzodiorite are associated with the coarser material.

Reference to the aeromagnetic and gravity anomaly (IGS, 1978;scale 1:100000) maps indicates that there are a series of closed aeromagnetic anomalies, similar to those noted for the different intrusive types at Moor of Rannoch, which are elongated parallel to the margin of the Strath Ossian pluton and may correspond to the different petrographic rock types. The gravity map shows decreasing negative values towards the northern margins where a closed anomaly,

coupled with an aeromagnetic anomaly, could represent the more acidic phenocrystic granite phase described by Clayburn (1981).

7.8.2 Strath Ossian petrography.

In this work, three distinctive types of intrusive material were noted in an oblique traverse along the length of the Strath Ossian complex. One of these, medium - coarse grained hornblende biotite monzogranite/granodiorite, corresponds to the medium grained, hornblende biotite granodiorite described by Clayburn (1981) for the northern area of the intrusion.

This type is grey with an occasional fluxion texture noted at outcrop and in thin section. Hornblende forms elongate twinned crystals up to 1.5mm in length and is optically actinolitic hornblende. Biotite is predominantly interstitial as ragged tabular to equant laths up to 1mm and often shows chlorite developed in cleavage fractures. Plagioclase, optically oligoclase, is frequently oscillatory zoned with ubiquitous albite twinning and forms crystals 0.5 - 2mm in size. Sericitisation is variable. Orthoclase forms sub - anhedral grains rarely exceeding 0.75 - 1mm in size and quartz is predominantly interstitial. Granophyric textures and consertal quartz are noted while interstitial sphene, opaques and zircon are common accessory phases.

The second type noted from this traverse is a medium-grained leucocratic hornblende biotite quartz monzodiorite, finer grained varieties of which are texturally similar to equivalent rocks in the Moor of Rannoch complex (Plates 4.10,4.12). The mafic minerals show patchy distribution in hand specimen and limited development of secondary amphibole in these aggregates.

Biotite forms predominantly tabular - equant laths interstitial to primary actinolitic hornblende which occurs as small (<1 - 1.5mm), twinned acicular crystals. Plagioclase, optically andesine, forms twinned, occasionally oscillatory zoned, subhedral crystals up to 2mm in medium-grained varieties. Orthoclase occurs as subhedral crystals (<2mm) which infrequently contain inclusions of small, discrete biotite crystals. Quartz is interstitial but also rarely occurs as inclusions in amphibole and alkali feldspar. Sphene is a common macroscopic accessory and is interstitial to plagioclase and primary amphibole.

The third type noted is a dark green, medium to coarse grained, melanocratic diorite. In thin section, amphibole is abundant and together with biotite forms >65% of the rock. Amphibole appears to be almost exclusively secondary in origin and forms light-green anhedral grains or aggregates which frequently contain quartz, minor plagioclase and biotite. Clinopyroxene is noted in the cores of the tabular shaped secondary grains along with biotite in a texture similar to that noted for the amphiboles of the Moor of Rannoch complex.

Biotite occurs as sub-anhedral crystals with ragged edges and is often chloritised along cleavage fractures. It rarely exceeds 0.75 - 1mm in size and often displays a texture similar to that recorded in Plates 4.20,4.21. Plagioclase, optically andesine/oligoclase, is present as two generations with large (up to 3mm) subhedral crystals containing small discrete biotite inclusions. Smaller tabular sub-anhedral laths form a patchy 'matrix' along with interstitial quartz grains. Sphene is a common accessory phase occasionally forming crystals up to 1.5 - 2mm in size.

7.8.3 Strath Ossian geochemistry.

Major and trace elements were analysed for 11 samples (Table 5.1) and selected elements have been plotted on Harker, triangular and chondrite normalised plots (Figs. 7.1 - 7.13). Strath Ossian samples have a range of values from 51.67 wt% to 71.2 wt% SiO2 and there is good correspondence between petrographical and geochemical groups. Due to the limited number of samples little can be said about the separation of the samples into geochemically distinct groups in the 60 - 70wt% SiO2 range.

One sample of xenolithic material, SOG2A, on the basis of major element chemistry is similar to the basic intermediate types of both Strath Ossian and Moor of Rannoch. Its trace element characteristics e.g. higher Ba, low Rb and low - intermediate values of Sr, suggests it could be a xenolith of igneous material from the Moor of Rannoch intrusion. However the absolute abundances of these elements are

significantly lower than those of 'typical' members of petrographic types from the latter and thus the xenolith may represent an earlier, more basic intrusive phase of Strath Ossian. The lower Sr abundances could also result from re-equilibration of the included material with a host which was extensively Sr depleted due to upper crust contamination, as suggested by Clayburn (1981).

Major element chemistry shows the most basic types (SOG4, SOG5) to be TiO2, FeO, MgO and CaO enriched and Al2O3 and Fe2O3 (SOG4 only) and Na2O and K2O depleted. These samples are also Ba, Rb, Sr and Zr depleted but only sample SOG4 shows Ni and Cr enrichment, Ce and Y depletion relative to the remainder of the suite. Coupled with a characteristic petrography in which hornblende occurs in prismatic phenocrystic and groundmass habit, this suggests a basic, possibly appinitic affinity, for this material. The presence of clinopyroxene as relict cores(?) in amphibole and as discrete crystals also suggests a more basic source, or one at less water pressure, with respect to the remainder of the Strath Ossian suite.

Triangular variation diagrams, Na2O+K2O - FeO+Fe2O3 - MgO and Na2O - K2O - CaO, show Strath Ossian datas to be closely related to Moor of Rannoch, with the exception of samples SOG4 & SOG5. These plot as Fe, Mg and Ca enriched relative to both intrusions as a whole and this can be explained by their amphibole (+ clinopyroxene) rich mineralogy. Strath Ossian samples show slight K enhancement with respect to Moor of Rannoch and this may be related to the amount of contamination undergone on intrusion.

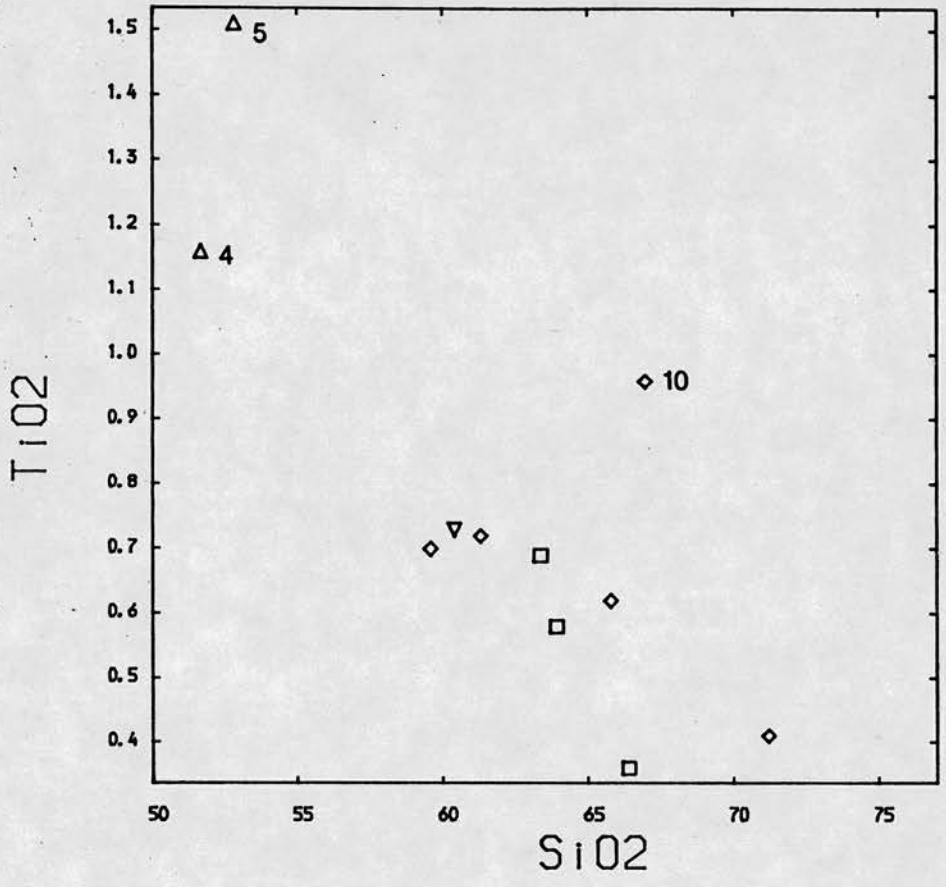

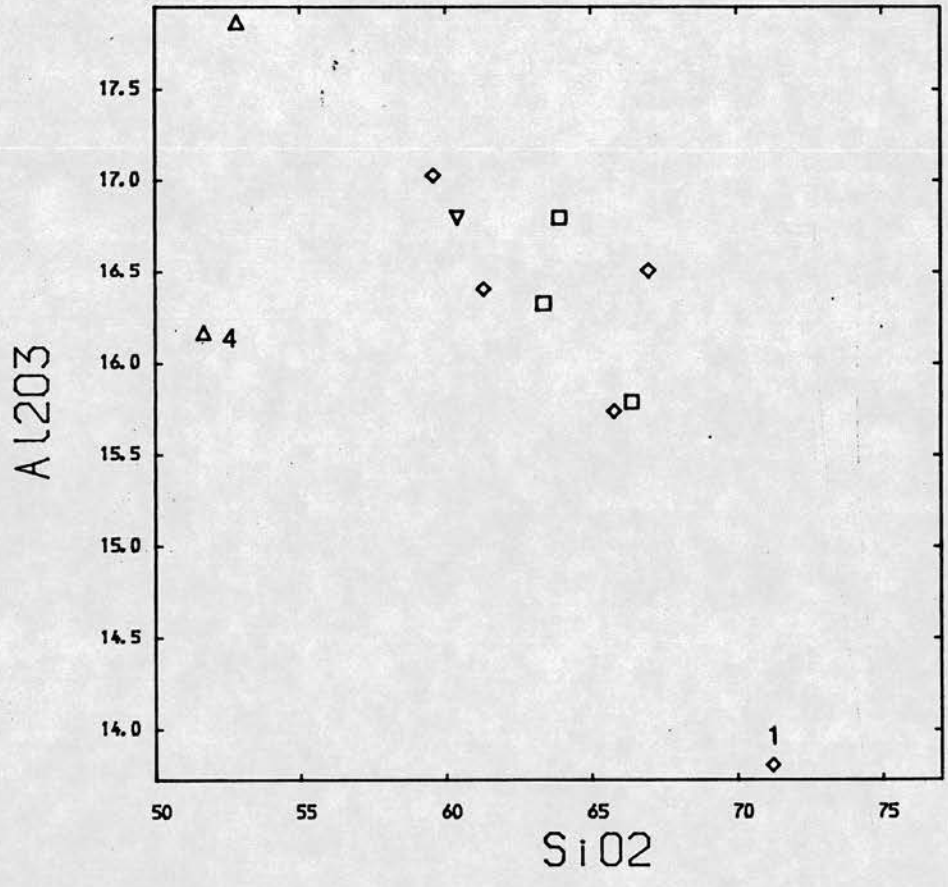

Figure 7.1 Harker plots of Ti and Al.

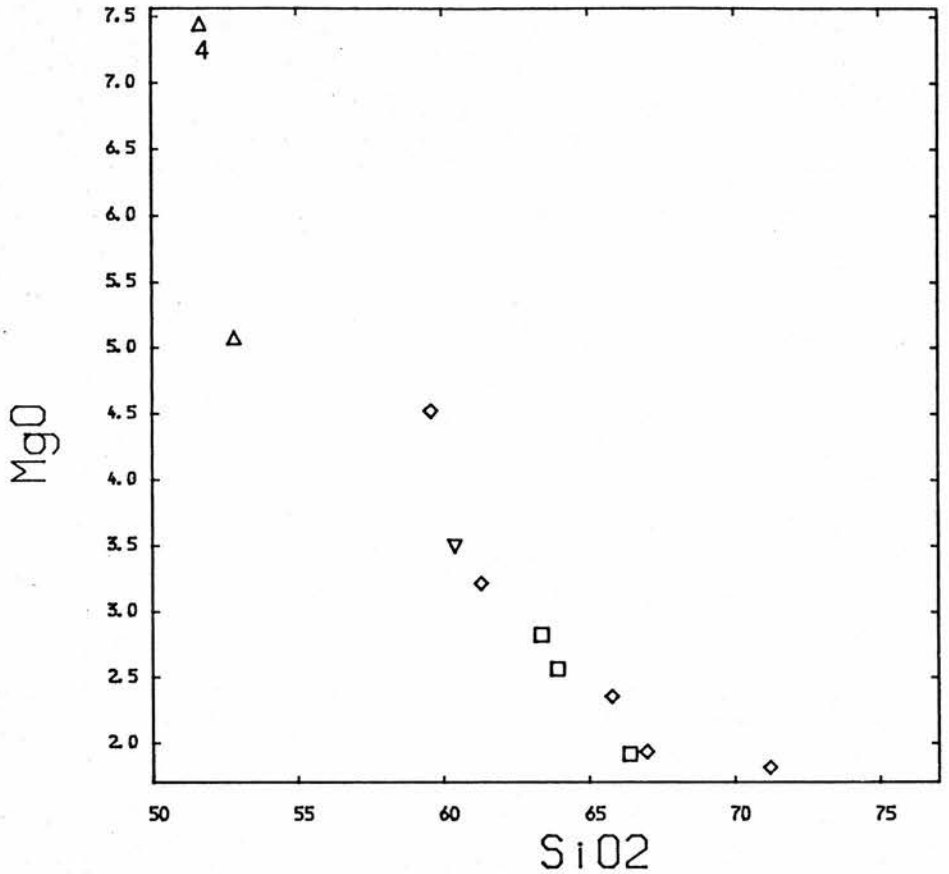

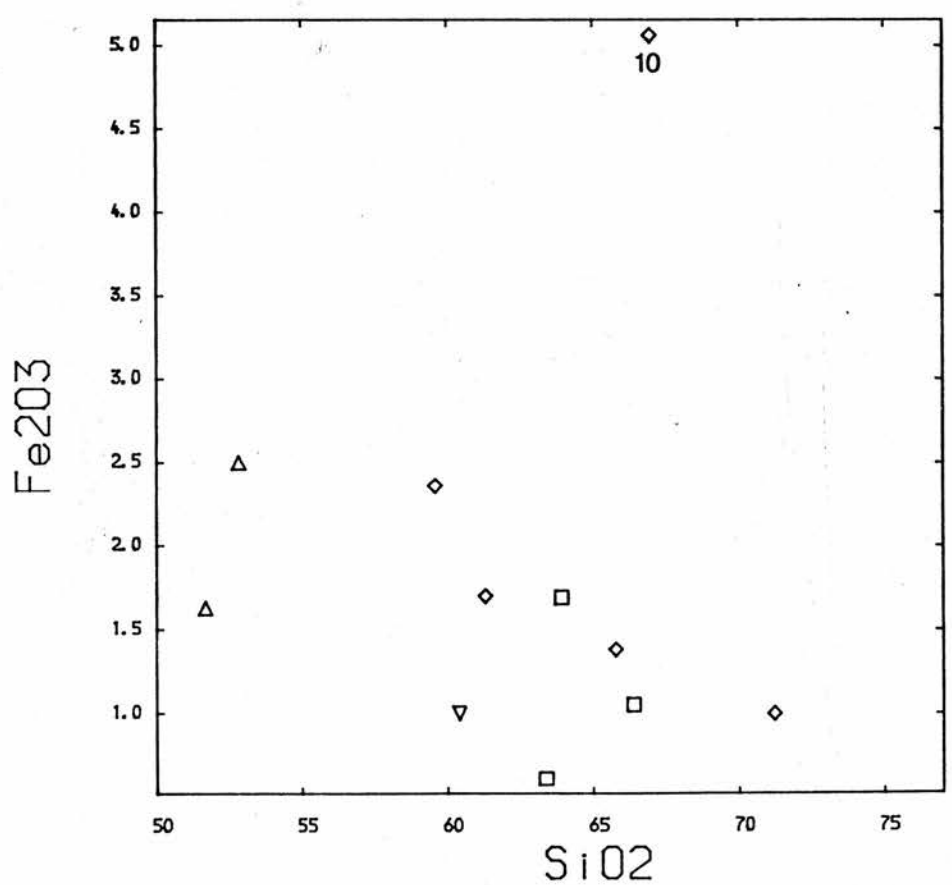

Figure 7.2 Harker plots of Mg and Fe (as Fe_2O_3)

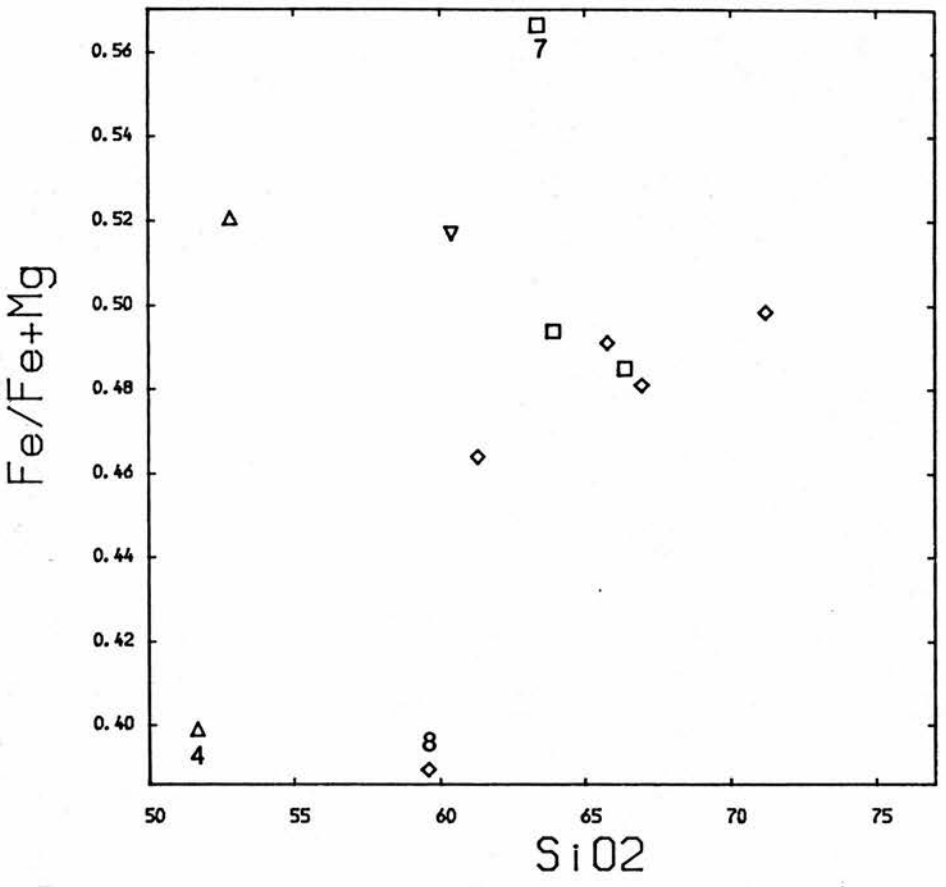

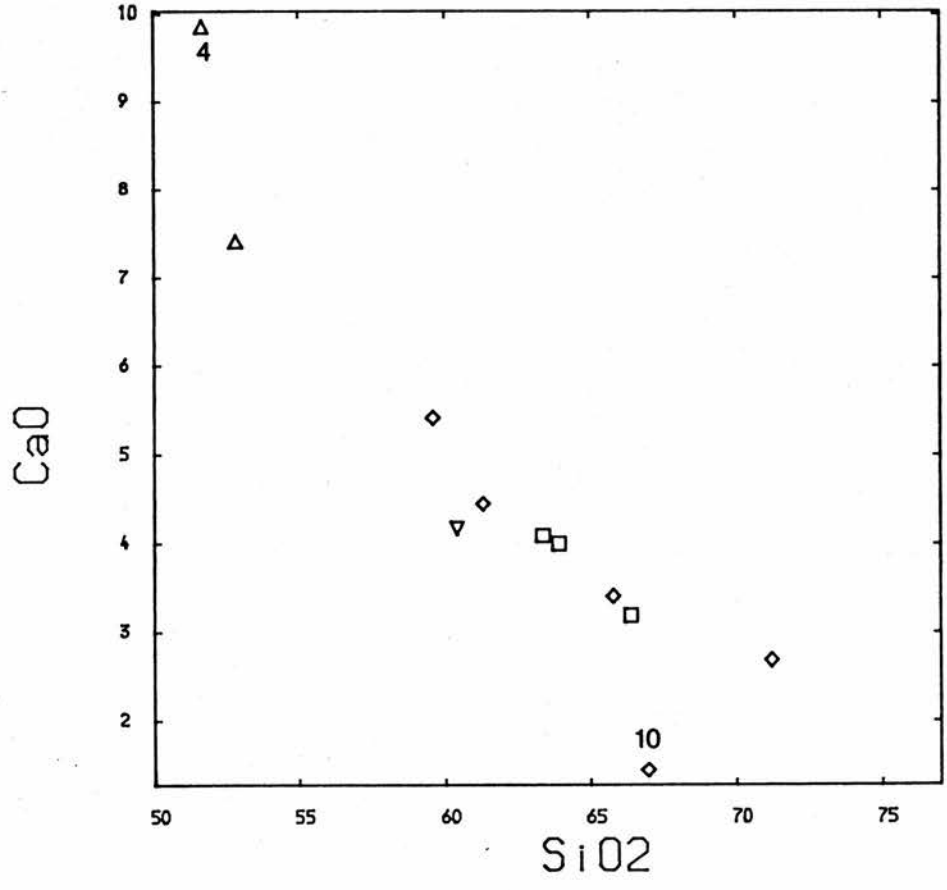

Figure 7.3 Harker plots of Fe ratio and Ca.

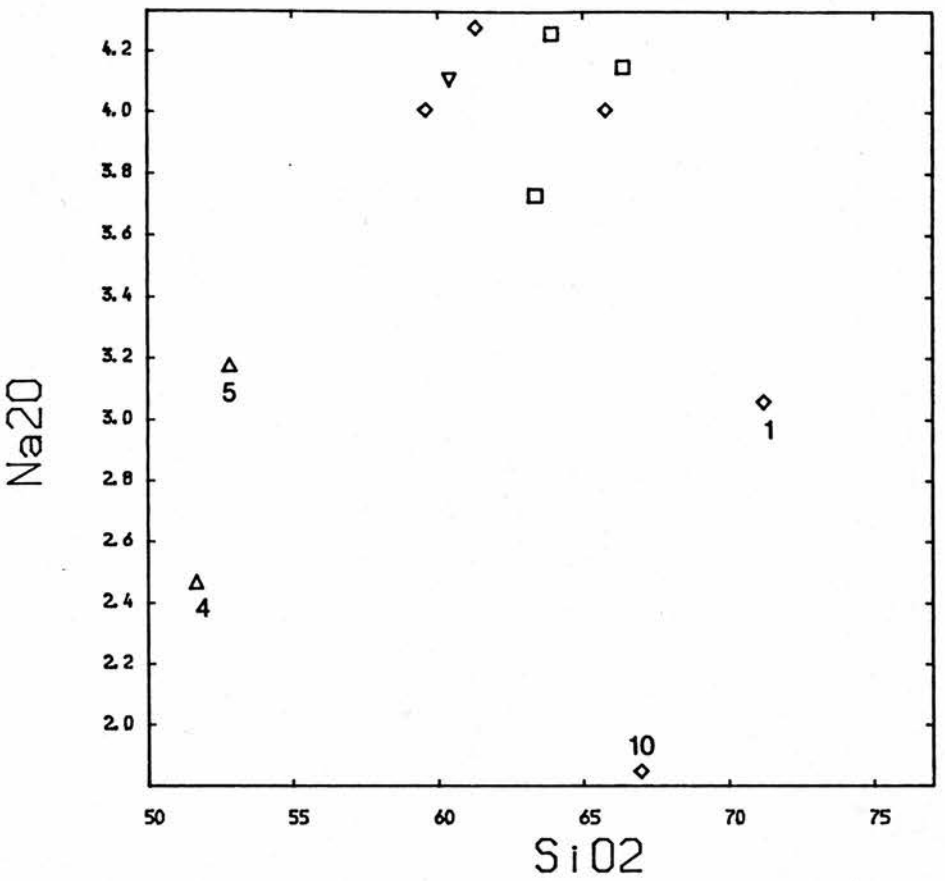

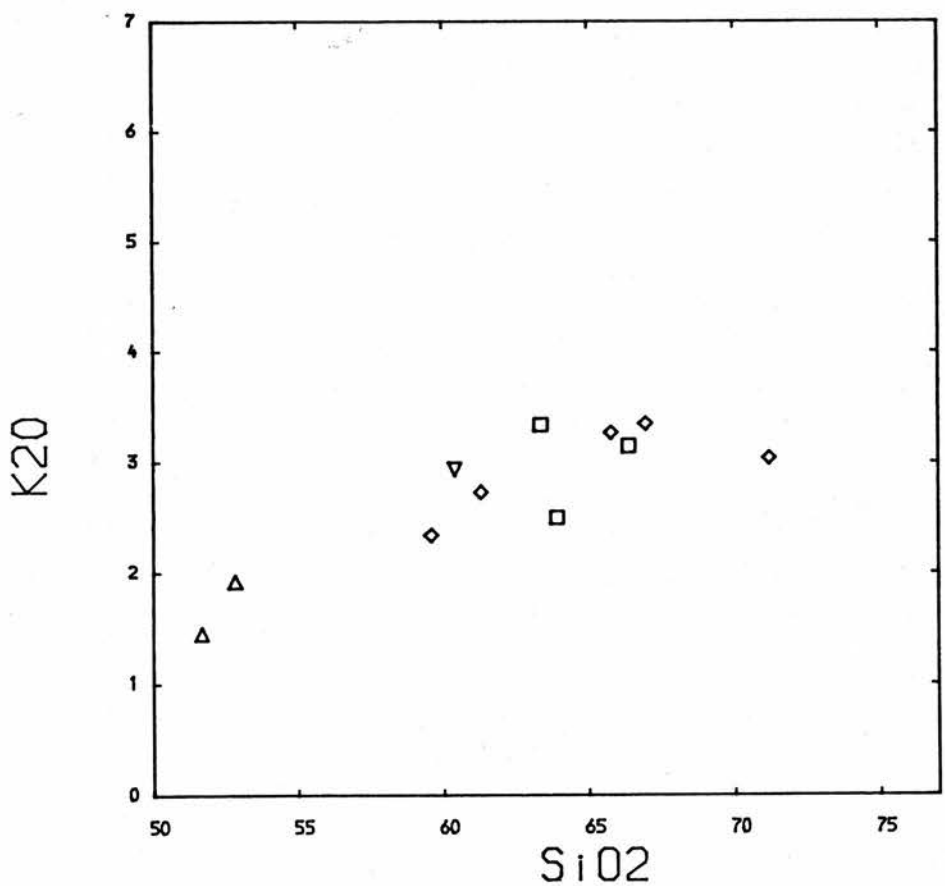

Figure 7.4 Harker plots of Na and K.

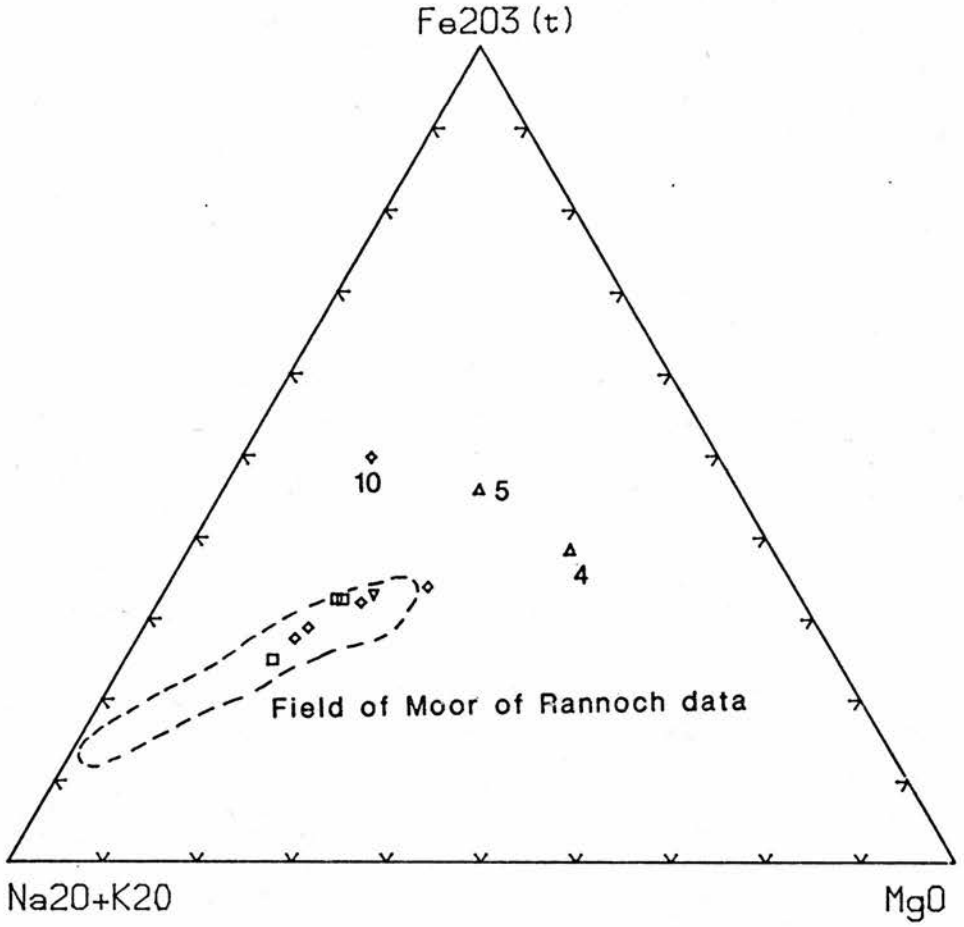

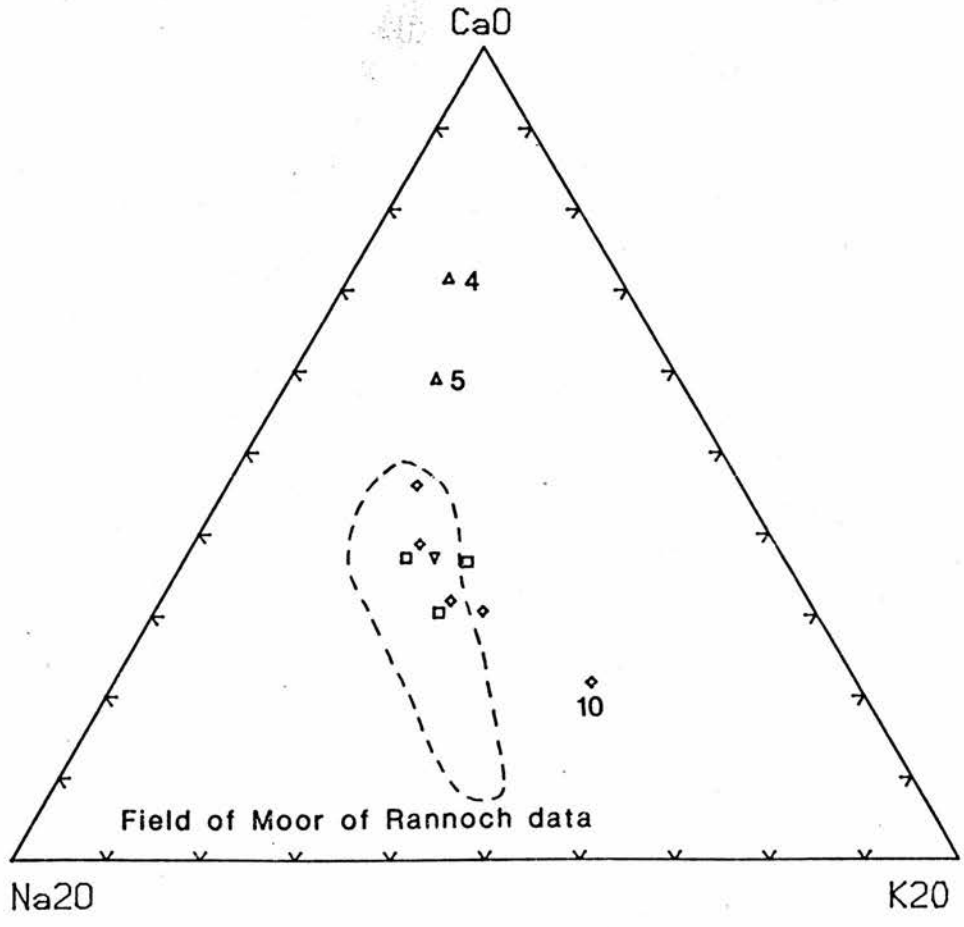

Figure 7.5 Triangular variation diagrams for $Fe_{(t)}$ - Na+K - Mg and Ca - Na - K.

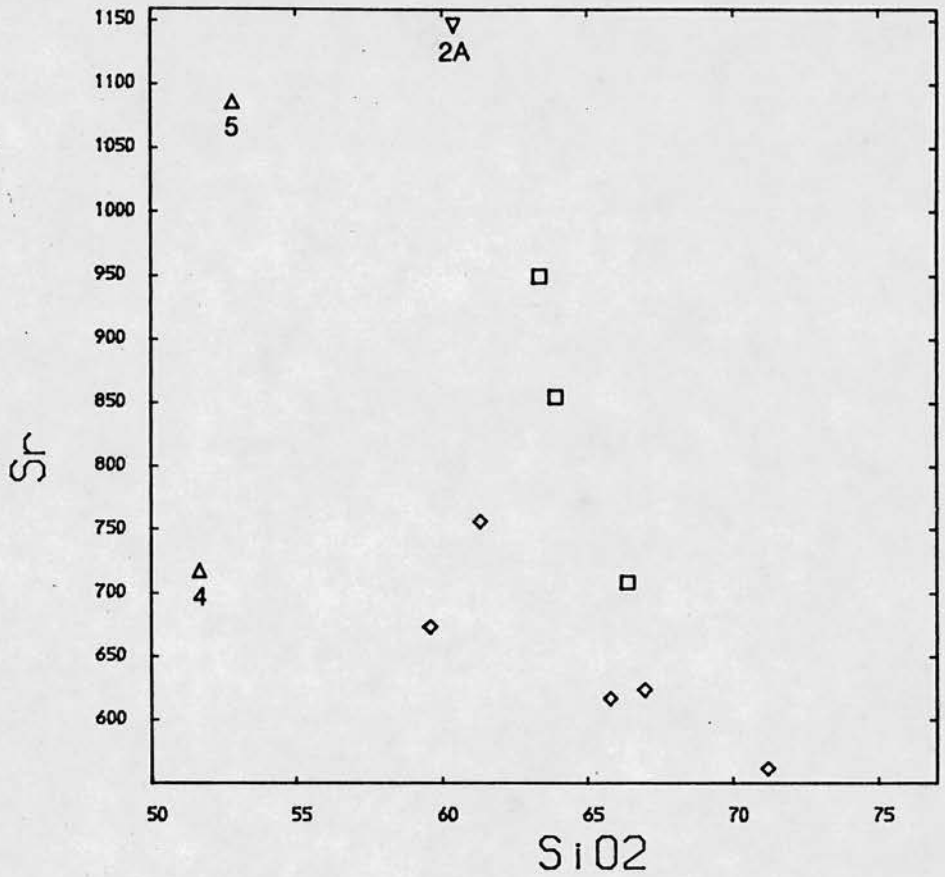

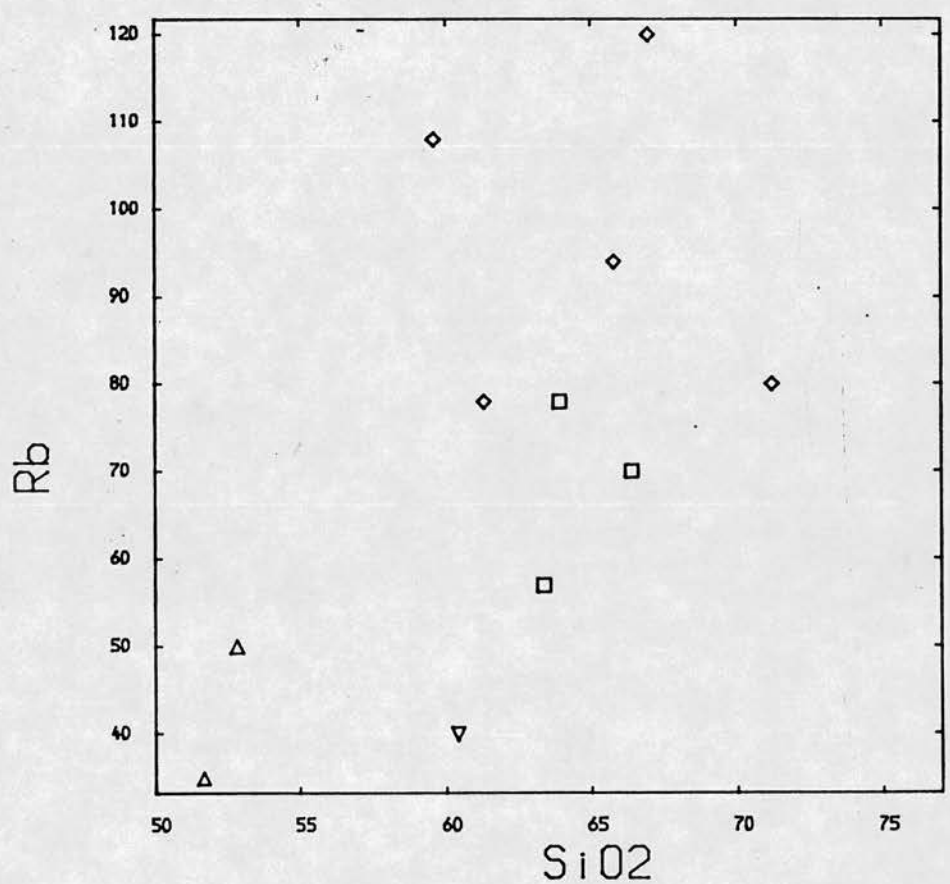

Figure 7.6 Trace element variation with SiO_2 for Sr and Rb.

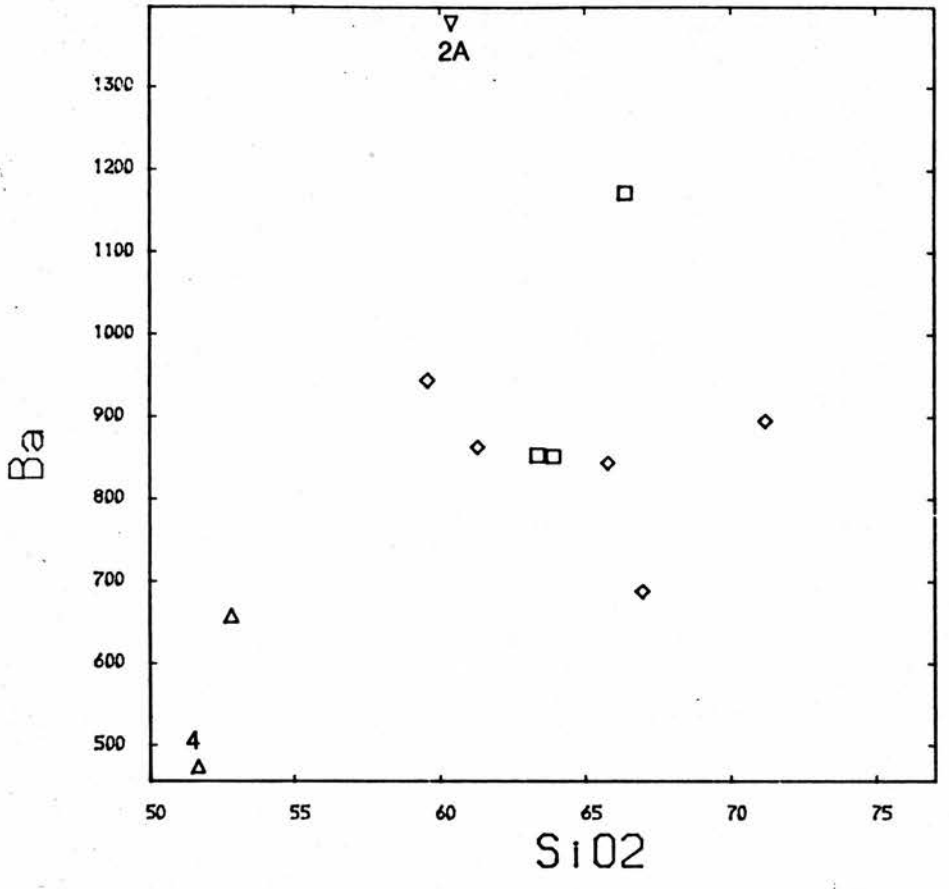

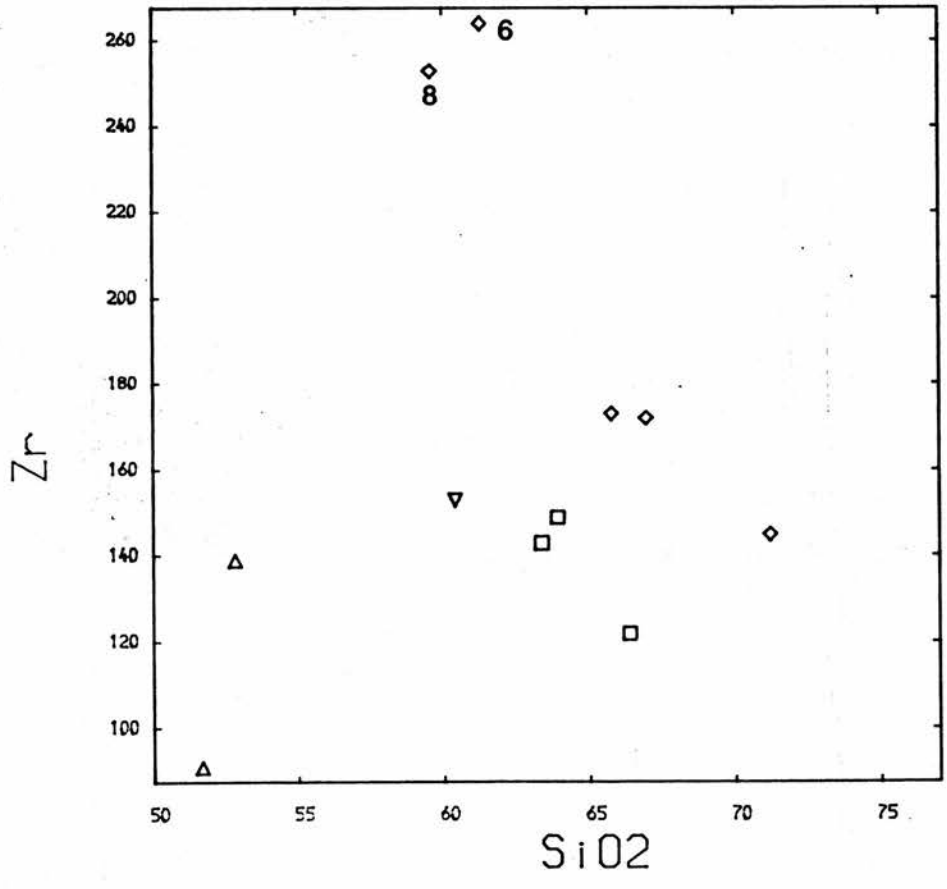

Figure 7.7 Trace element variation with SiO_2 for Ba and Zr.

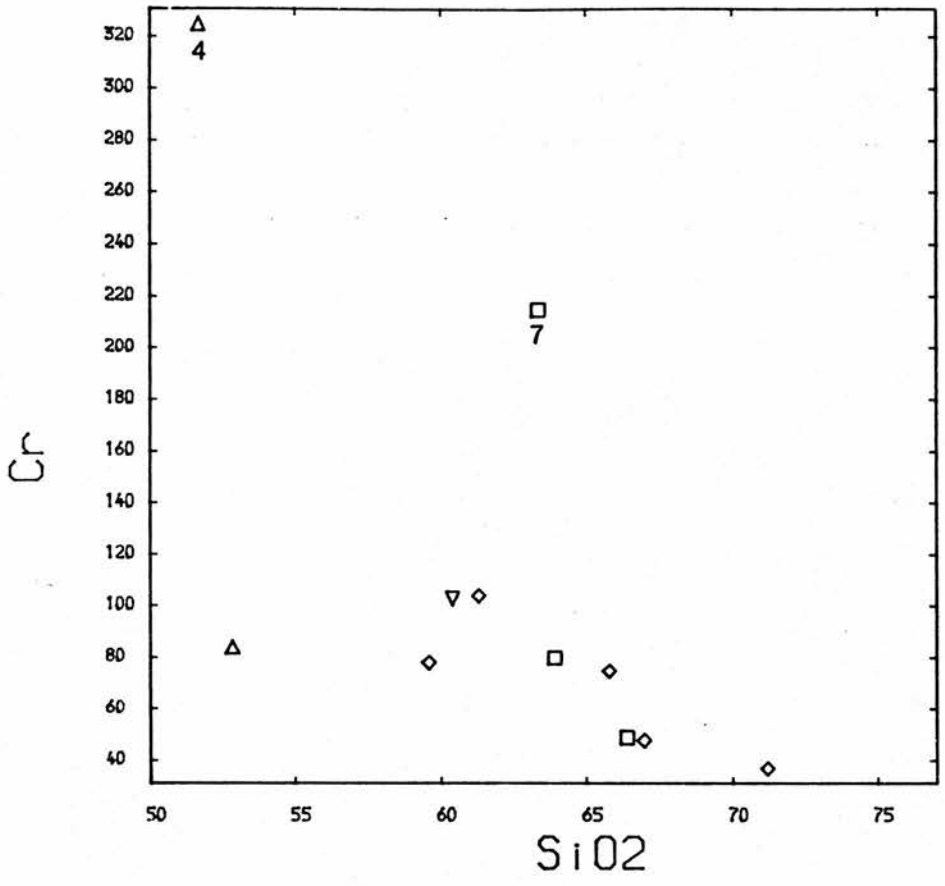

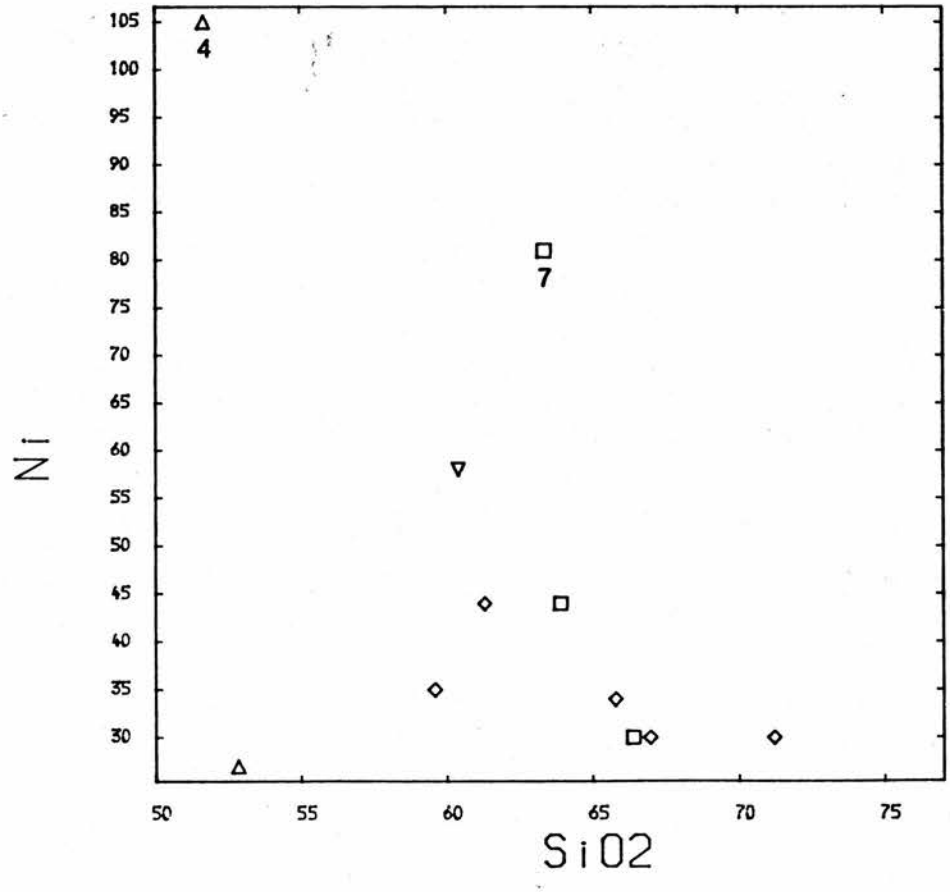

Figure 7.8 Trace element variation with SiO_2 for Cr and Ni.

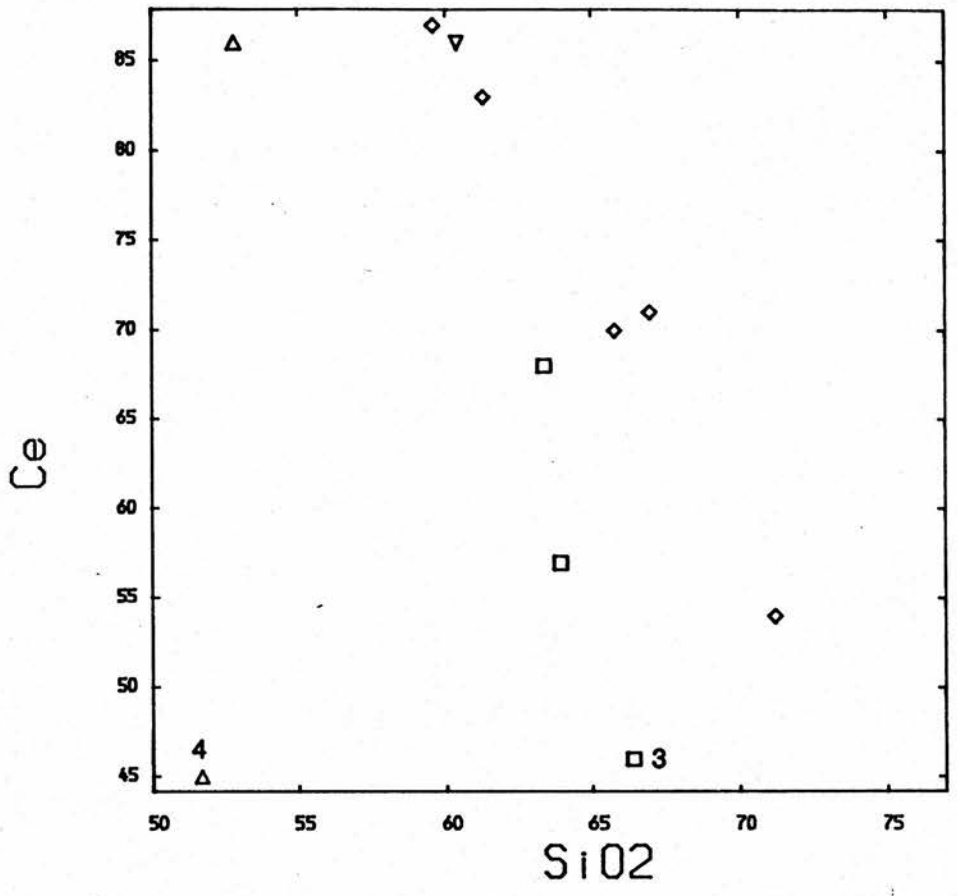

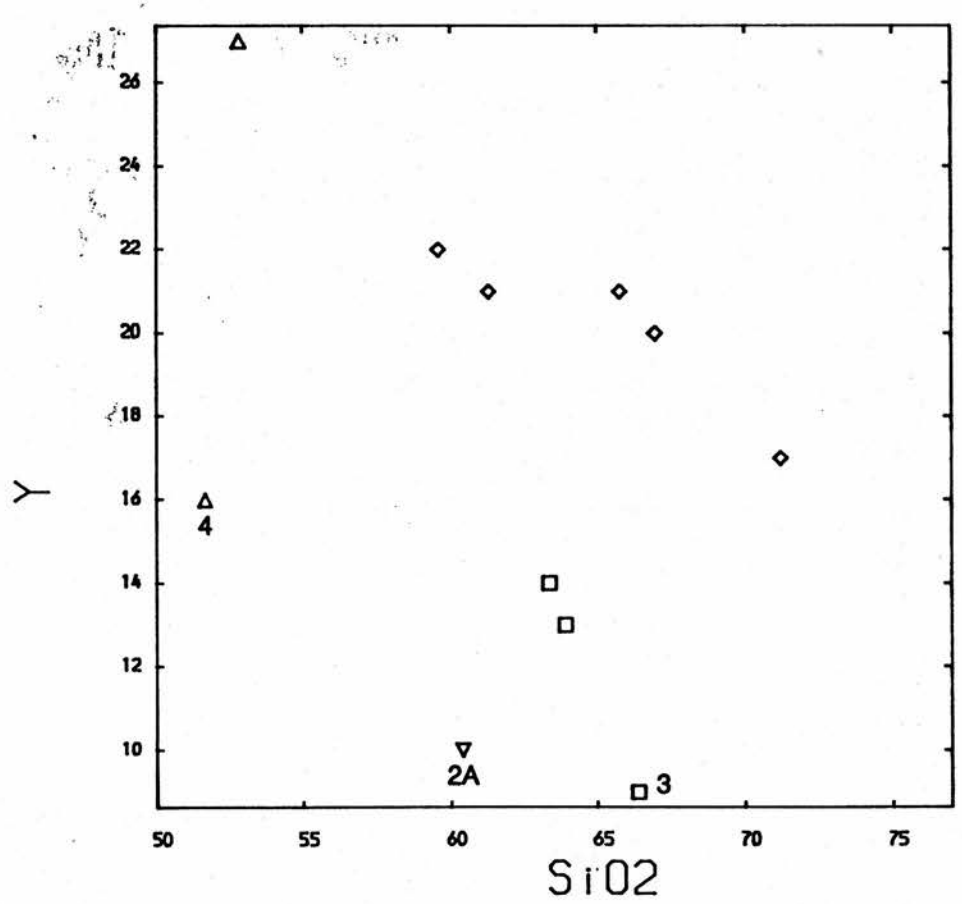

Figure 7.9 Trace element variation with SiO_2 for Ce and Y.

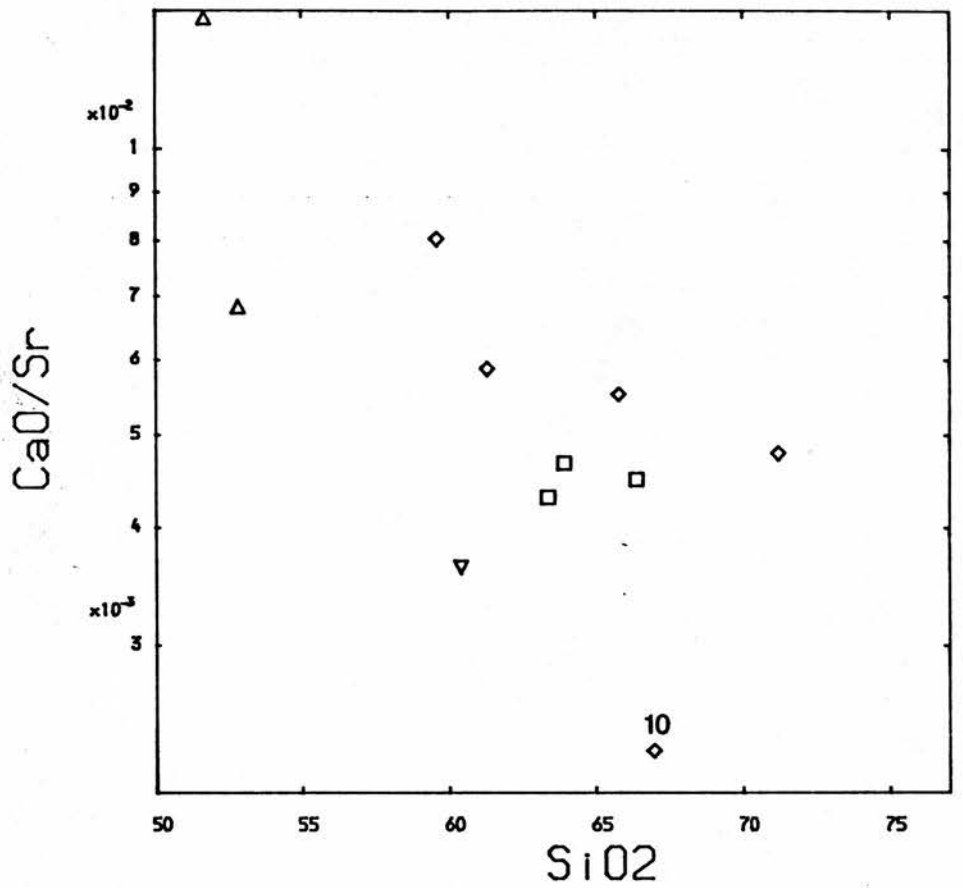

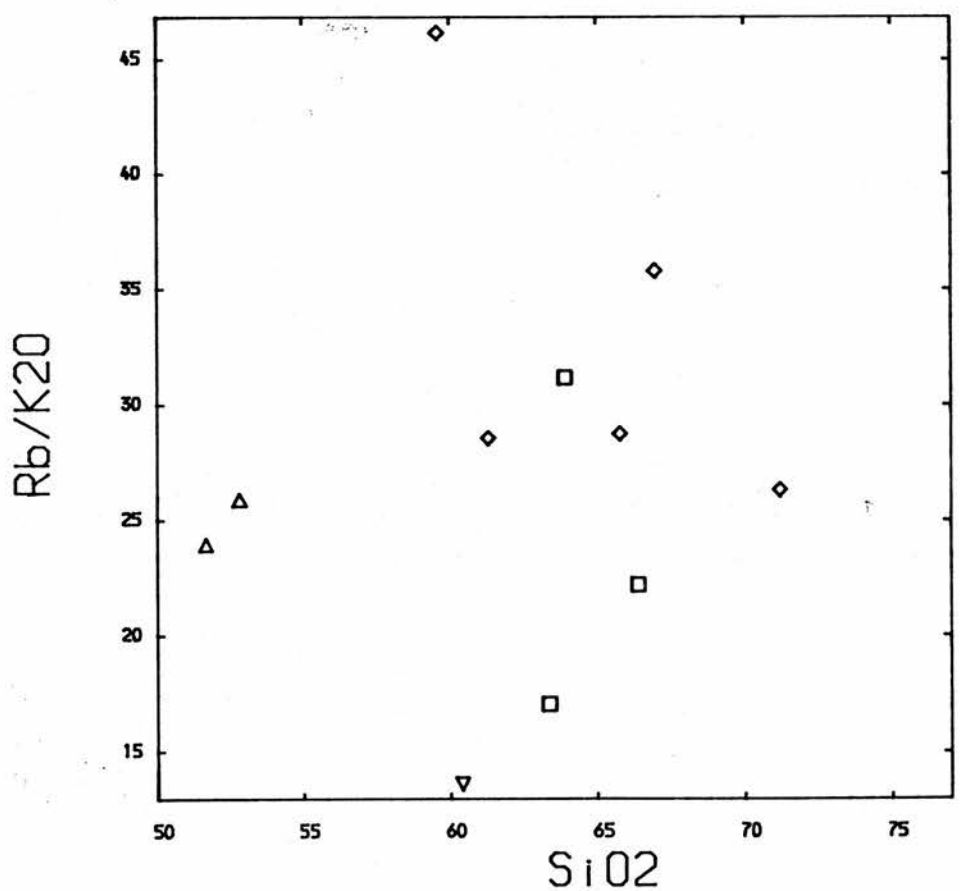

Figure 7.10 Element ratio variation against SiO_2 for CaO/Sr and Rb/K2O.

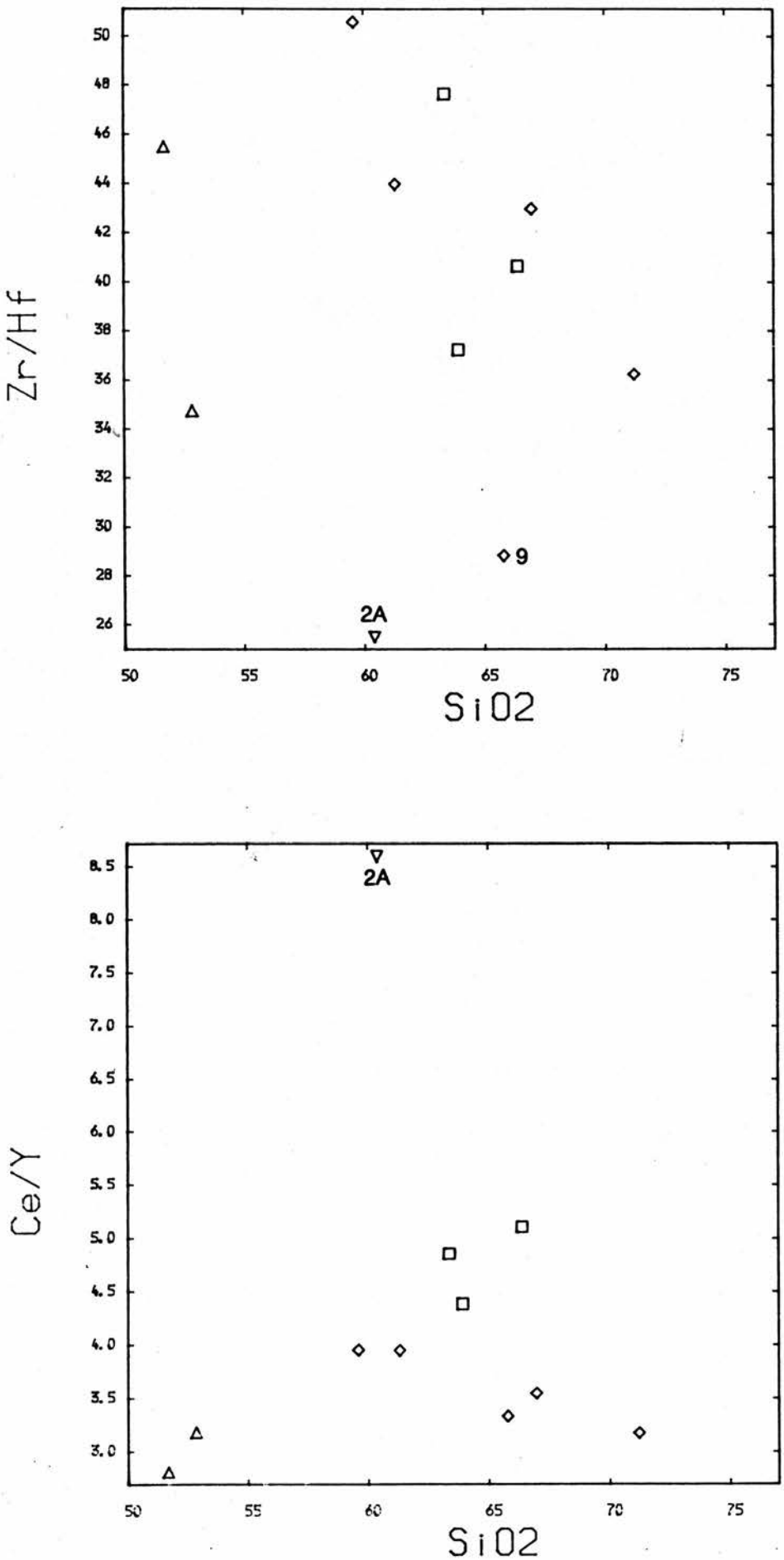

Figure 7.11 Trace element ratio variation against SiO_2 for Zr/Hf and Ce/Y.

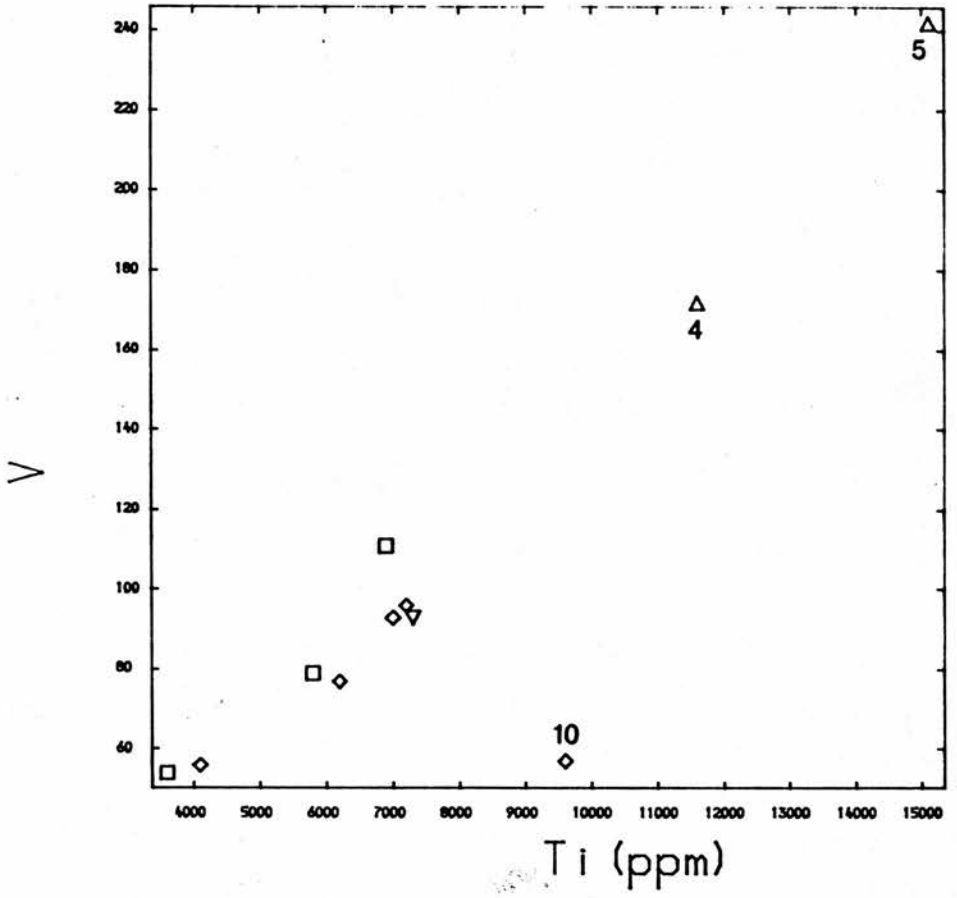

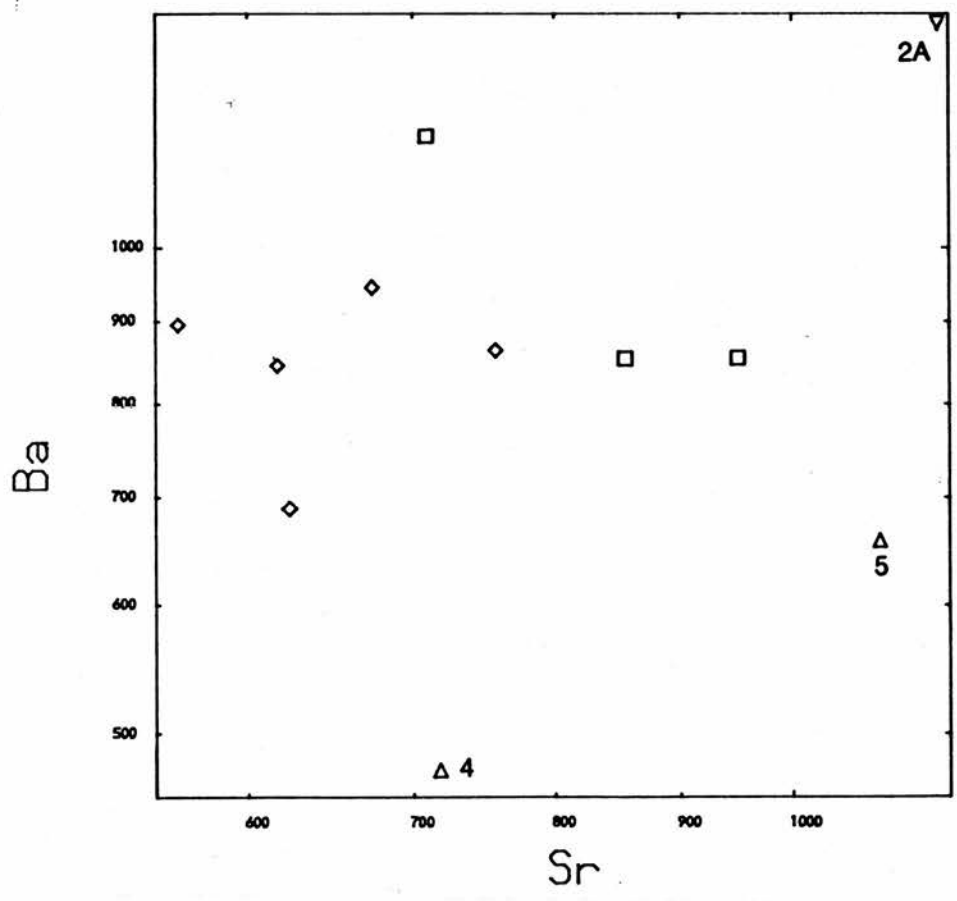

Figure 7.12 Element variation for V - Ti and log Ba - log Sr.

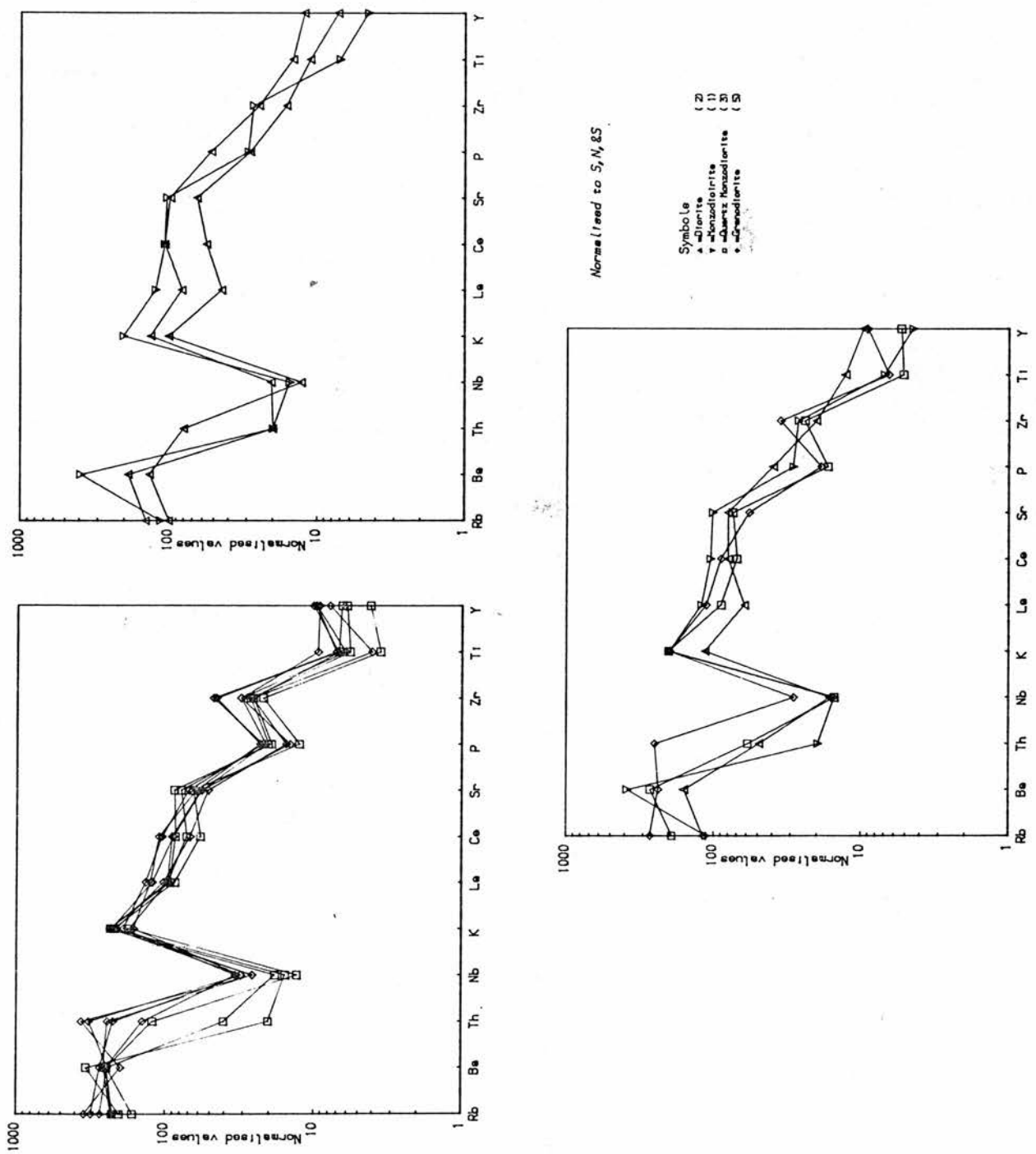

Figure 7.13 Chondrite normalised plots for petrographic types (upper diagrams) and plot of mean values for the groups (lower diagram). Symbols as per 5.6.17

7.9 Conclusions and relationships to Caledonian magmatism.

Evidence presented in this work suggests that both complexes are related within the overall framework of Caledonian plutonism. However, with reference to structural interpretations and isotopic data for Strath Ossian, the Moor of Rannoch pluton as a whole appears to have chemical, petrographical, isotopic and intrusive features distinct from the Strath Ossian pluton and is not directly related as a 'satellite cupola', as proposed by Hinxman et.al.(1923). Although more detailed internal mapping of the different phases is required at Strath Ossian, the two plutons appear to be genetically unrelated considering their trace element (this work) and radiogenic Sr datas (Clayburn, 1981). The greater abundances of unradiogenic Sr, Ba, Rb, Cr and Ni for the Moor of Rannoch intrusion suggests that it has been derived from a different source with a higher Sr content or that considerable source inhomogeneity was involved. A greater lower crustal component is most likely for the Moor of Rannoch pluton. The low Rb and initial Sr values for the syenogranites argues for a possible mantle contribution extending into the later partial melts.

Clayburn (1981) presented a two feldspar-whole rock isochron age of 405 +/-9 Ma and a biotite-two feldspar-whole rock isochron age of 400 +/-6 Ma for a hornblende granodiorite from the northern area of the Strath Ossian pluton. The Moor of Rannoch pluton, which has been shown to be more complex than previously thought, will require further isotopic analysis taking into account the significant chemical and petrographical variations across the Laidon-Ericht fault. Such work would more accurately determine the nature of this major dislocation

and could resolve the difference, if any, in age and source for the main intrusive types.

The calc-alkaline nature of the Moor of Rannoch and its relationship with nearby Argyll suite plutons (Stephens and Halliday, 1984) suggests that it represents an early phase of 'Newer granite' magmatism. However, until the timing and amount of lateral displacement along the Laidon-Ericht fault has been satisfactorily resolved, no unambiguous statements can be made concerning the temporal and spatial relationship of the Moor of Rannoch with respect to nearby 'Newer' granites.

The Late Caledonian granites were emplaced into cooling country rock after the peak of Grampian metamorphism which occurred around 480-450 Ma (van Breemen et.al., 1979b). They are predominantly post-tectonic, high level intrusives which have a greater range of magmatic types and were superimposed on earlier magmatic events. Pitcher (1979) refers to these as members of the 'high level uplift regime'. Their chemical, isotopic and petrologic heterogeneity can be seen in the high Cr and Ni, more primitive magmas of Moor of Rannoch, through to the more evolved types present at Glen Coe and Etive. Piasecki et al. (1981) suggest a 450 Ma event for reconstruction of sinistral movement on the Great Glen fault. The sub-parallel Laidon-Ericht fault may have been initiated at this time with later, smaller scale sinistral movements (10 - 30 kms) around 410 - 390 Ma.

Summary of conclusions.

When the field, geochemical and isotopic evidence from the Moor of Rannoch pluton is assessed, it is considered that the pluton can be best explained in terms of multiple intrusion of intermediate composition magmas of lower crustal origin with only limited upper crustal contamination affecting the marginal phases. The most basic phases possess characteristics of primitive magmas and their emplacement appears to be controlled by a deep-seated crustal fault, the Laidon-Ericht fault. The following conclusions are considered important for further workers:

1) A greater petrographic range of rock types is present than has been previously recorded, from monzodiorite through to syenogranite.

2) The range in major and trace element geochemistry is also greater than previously considered, from 52.6 to 75.7 wt% SiO_2.

3) New isotope data shows that the basic and intermediate rock types have similar initial Sr values and may thus be related in terms of source and subsequent evolution. The more evolved syenogranites have a lower initial Sr value arguing for a distinct source or evolution.

4) Trace element data, coupled with radiogenic Sr data, in conjunction with a comparison of data from the Etive intrusion, suggests that the Moor of Rannoch pluton is a composite of two distinct intrusive suites juxtaposed by movement of the Laidon-Ericht fault.

Appendix A

A.1 Sample collection and whole rock geochemical analysis.

Rock specimens for geochemical analysis were c.2kgs mass of freshest possible material. Due care was noted when sampling coarse-grained types so as to obtain representative specimens. All samples were examined in thin section before crushing and powdering for XRF analysis; this enabled any weathered samples to be discarded. All weathered surfaces were removed and any pieces with joint planes discarded before samples were hydraulically split and passed through a riffle splitter. One split was retained and cataloged, the other powdered in a 'TEMA' mill and passed through a 200 sieve.

A.2 XRF analysis.

X-ray flourescence spectrometry (XRF) analysis was conducted on a PHILLIPS PW1212 automatic spectrometer linked to an APPLE IIe computer in an on-line system. Software for the system and later data handling - CIPW normative mineralogy calculation, molar proportions of oxide and probe data and plotting of geochemical variation diagrams - was provided by Dr. W.E. STEPHENS.

Major oxides analysed were - SiO_2, Al_2O_3, TiO_2, $Fe_2O_3(t)$, MnO, MgO, CaO, Na_2O, K_2O - following the conditions of Norrish and Chappell (1977). Analyses were performed on fused beads of 0.5g sample powder prepared after the method of Harvey et.al.(1973) and adapted for use

at St. Andrews by R. Batchelor (Int. Pub. 1980). All beads were checked optically for quench crystals and re-fused if any found present. Bead heterogeneity gave anomalously high oxide totals.

FeO Determination.

This was performed by titration following the proceedures of Batchelor (1980) adapted from Wilson (1955). To ensure accuracy, U.S.G.S. standards were also analysed and if necessary, corrections applied to the samples.

Samples were digested in HF and then oxidised by the addition of ammonium metavanadate, any excess of which was reduced by adding excess ferrous ammonium sulphate. Any excess ferrous iron was titrated with potassium dichromate and sodium diphenylamine sulphonate indicator. Blanks of chemicals alone were titrated along with sample unknowns and FeO calculated by subtraction.

H2O Determination.

Total H2O was determined by loss-on-ignition (T>800 C) during fused bead preparation (Batchelor 1980).

A.3 Trace element XRF analysis.

Trace elements - Zr, Y, Sr, Rb, Nb, Cu, Pb, Zn, V, Th, Hf, Ce, La - were analysed seperately following the conditions of Norrish and Chappell (1977) and Leake et.al. (1970). Analysis was performed on pressed powder pellets, the powder for which had been homogenised in a 'TEMA' ball mill. This was to finely crush flakes of mica which tended to orientate themselves parallel to, and on the analysis surface of the pellet.

A.4 Sample locations.

All sample locations were recoreded on a six-figure O.S. grid reference and are listed in Table A.4

Table A.4 Moor of Rannoch sample type and locations.

Sample number	Sample type	Grid reference (Area NN)
RM2	Quartz-Monzodiorite	474548
RM3	Quartz-Monzodiorite	479554
RM4	Monzogranite	486556
RM5	Quartz-Monzodiorite	497582
RM6	Quartz-Monzodiorite	494583
RM7	Monzogranite	489586
RM8	Monzogranite	407571
RM10	Quartz Monzonite	395586
RM11	Quartz-Monzodiorite	453578
RM13	Monzogranite	482580
RM16	Quartz Monzonite	405608
RM17	Monzogranite	428598
RM17A	Monzogranite	428598
RM18	Marginal Granite	339638
RM19	Quartz-Monzodiorite	335635
RM20	Quartz-Monzodiorite	335632
RM22	Marginal Granite	381667
RM25	Marginal Granite(Loch Tulla)	263424
RM28	Quartz-Monzodiorite	268418
RM29	Quartz-Monzodiorite	304511
RM30	Syenogranite (W. margin)	242558
RM32	Granodiorite	377491
RM33	Quartz-Monzodiorite	380494
RM34	Granodiorite	385496
RM35	Quartz-Monzodiorite	392500
RM36	Syenogranite	394512
RM37	Syenogranite	393511
RM38	Syenogranite	388507
RM40	Monzogranite	368495
RM43	Quartz-Monzodiorite	261557
RM44	Quartz-Monzodiorite	328475
RM51	Granodiorite	293562
RM52	Granodiorite	304575
RM54	Granodiorite	284562
RM55	Granodiorite	271561
RM57	Monzogranite	427567
RM60	Monzogranite	424563
RM63	Monzogranite	429550
RM64	Monzogranite	435523
RM68	Quartz-Monzodiorite	443577
RM69	Quartz-Monzodiorite	461568
RM70	Quartz-Monzodiorite	460567
RM71	Granodiorite	309498
RM76	Granodiorite	259578
RM77	Granodiorite	268571
RM78	Quartz-Monzodiorite	278571
RM79	Quartz-Monzodiorite	435602
RM81	Quartz-Monzodiorite	469597
RM85	Quartz-Monzodiorite	374567
RM86	Monzogranite	376570

Sample number	Sample type	Grid reference (Area NN)
RM89	Quartz-Monzodiorite	375570
RM90	Quartz-Monzodiorite	398568
RM91	Quartz monzonite	470581
RM92	Granodiorite	487594
RM93	Granodiorite	488606
RM94	Granodiorite	490613
RM95	Quartz-Monzodiorite	498609
RM96	Granodiorite	508605
RM97	Quartz-Monzodiorite	427595
RM98	Quartz-Monzodiorite	422586
RM99	Syenogranite	383516
RM100	Monzogranite	387510
RM101	Monzogranite	382513
RM102	Quartz-Monzodiorite	363528
RM103	Monzogranite	369535
RM104	Quartz-Monzodiorite	397567
RM106	Syenogranite	362574
RM107	Syenogranite	375573
RM109	Monzodiorite	460565
RM110	Syenogranite	443578
RM111	Monzodiorite	444578
RM112	Monzogranite	426566
RM113	Quartz Monzonite	426568
RM114	Monzogranite	367575
RM115	Granodiorite	400566
RM116	Quartz-Monzodiorite	408572
RM117	Quartz Monzonite	408571
RM118	Granodiorite	395667
RM119	Marginal Granite	384668
RM120	Monzogranite	381666

A.4(b) Strath Ossian sample types and locations.

SOG1	Granodiorite	406764
SOG2	Quartz-Monzodiorite	411756
SOG2A	Igneous Xenolith	412756
SOG3	Quartz-Monzodiorite	405744
SOG4	Diorite	399737
SOG5	Diorite	399731
SOG6	Granodiorite	419702
SOG7	Quartz-Monzodiorite	409725
SOG8	Granodiorite	407805
SOG9	Granodiorite	396806
SOG10	Granodiorite	388806

APPENDIX B

B.1 Modal Analysis.

Modal mineralogy was determined by point counting 2000 points per thin section. Phenocryst concentration was estimated by eye on hand and thin sections, where necessary modal proportions being modified. Classification followed the scheme of Streckeisen (1976).

B.2 Electron microprobe mineral analysis.

Under the guidance and supervision of Dr. P Hill, selected samples were analysed on the Cambridge Microscan 5 microprobe at the Grant Institute of Geology of Edinburgh University. All analyses were made in WDS mode, with data processing by Digital computer. Using the limited time available, amphibole, mica and feldspar analyses took precedent but occassionally alkali feldspar, Fe-oxide and apatite were analysed. Due to the initially low oxide totals for biotite, BaO was analysed and recorded, with due care in interpretation as a result of possible TiO2 interference with the Ba peak.

Subsequent analyses of further samples were made at the University of St. Andrews on a Jeol 733 Superprobe under the direction of Dr. W.E. Stephens and Donald Herd. The purpose of this was to investigate in greater detail variations found on the initial analyses.

B.3 Whole rock isotopic analysis.

Four samples were analysed for $^{87}Sr/^{86}Sr_i$ ratios by P. Holden of the University of St. Andrews while engaged on his own research. All were analysed on a VG Isomass MM30B mass-spectrometer by isotope dilution as per Blaxland et al. (1978). One sample, RM111, was also analysed for Nd & Sm by the method of Richard et.al. (1976) on a VG Isomass 54E mass spectrometer following the parameters of Halliday (1980).

P. Holden is gratefully acknowledged for his time and effort in producing this valuable data.

ACKNOWLEDGEMENTS

I am indebted to W.E. Stephens for suggesting this project, acting as my supervisor and having patience to wait for its fruition. Iain and Sheila Young are remembered and thanked for their generous company, food and accomodation during my periods at St. Andrews and Joy Gray for her support.

The technical staff, Andy, Jim, Alistair, Donald, Angus and Alison are gratefully acknowledged for their help in sample preparation, drafting photomicrographs and data gathering, beyond normal requirements. All who discussed and provided comments on the thesis - Iain, Rob, Eva, Lorna, Pete, Ben, Judy, Richard - have my thanks. Pete Holden is further mentioned for his work at the S.U.R.R.C. at East Kilbride in providing Sr & Nd values at the same time as his own project work load. Kit Finlay typed the data tables and is greatly thanked.

Finally, I should like to thank Alistair and Maree Scott at the Moor of Rannoch hotel for all their help during my field work, the use of the hotel's boat and meals 'par - excellence'.

REFERENCES

de Albuquerque, C.A.R. (1973). "Geochemistry of biotites from granitic rocks, Northern Portugal." Geochim. Cosmo. Acta, 37, 1770-1802.

de Albuquerque, C.A.R. (1978). "Rare earth elements in the "Younger" granites, N. Portugal." Lithos, 11, 219-229.

de Albuquerque, C.A.R. (1977). "Geochemistry of the tonalitic and granitic rocks of the Nova Scotia southern plutons." Geochim. Cosmo. Acta, 41, 1-13.

Allegre, C.J. and Minster, J.F. (1978). "Quantitative models of trace element behaviour in magmatic processes." Earth and Planetary Science Letters, 38, 1-25.

Aprahamian, F. Ed., (1976). "Igneous Case Study, The Tertiary igneous rocks of Skye, NW Scotland." Earth Science Topics and Methods, The Open University, The Open University Press.

Ashwal, L.D., Leo, G.W., Robinson, P, Zartman, R.E. and Hall, D.J. (1981). "The Belcherstown Quartz monzodiorite pluton, West-central Massacheusets; a syntectonic Acadian intrusion." Amer. J. Sci. 279, 936-969.

Bailey, E.B. (1925). "Perthshire tectonics: Loch Tummel, Blair Atholl and Glen Shee." Trans. Roy. Soc. Edinb., 53, 671-98

Bailey, E.B. and Maufe, A.B. (1916, 1960). "The Geology of Ben Nevis

and Glen Coe." Mem. Geol. Surv. Scot. Explanation of sheet 53.

Bailey, E.B. and McCallien, W.J. (1937). "Perthshire tectonics, Schiehallion to Glen Lyon." Trans. Roy. Soc. Edinb., 59, 79-117.

Barth, T.F.W. (1969). in "Feldspars" Pub. Wiley Intersciences.

Batchelor, R.A. (1980). "Analysis of major, minor and selected trace elements in silicate rocks and minerals." Internal Publication No 80/1, Univ. St Andrews.

Bateman, P.C. and Wones, D.R. (1972). "Geological map of the Huntington Lake Quadrangle, central Sierra Nevada, California." U.S. Geol. Survey Map GQ987.

Beams, S.D. (1980). "Magmatic evolution of the Southeast Lachlan fold belt, Australia." Ph.D. Thesis, La Trobe Univ. Bundoora.

Belieni, G., Peccerillo, A. and Poli, G. (1981). "The Vedrette di Ries (Riesenferner) plutonic complex: petrological and geochemical data bearing on its genesis." Contrib. Mineral. Petrol., 78, 145-156.

Black, R.C. (1973). "The geology of the Loch Dochard - Stob Ghabhar area, Argyllshire." Unpub. Honours Research Essay, Univ. St Andrews.

Blaxland, A.B., Aftalion, M. and van Breemen, O. (1979). "Pb isotopic composition of feldspars from Scottish Caledonian granites, and the nature of the underlying crust." Scot. J. Geol., 15, 139-151

Borradaile, G.J. (1979). "Pre-tectonic reconstruction of the Islay anticline: implications for the depositional history of Dalradian rocks in the SW Highlands." Geol. Soc. Lond. Spec. Pub. 8. Eds. Harris et al.

Bowen, N.L. (1928). "The evolution of the igneous rocks." Princeton Univ. Press.

Bowes, D.R. and McArthur, A.C. (1976). "Nature and genesis of the appinite suite." Krystalinikum, 12, 31-46.

Bradbury, H.J., Harris, A.L. and Smith, R.A. (1979). "Geometry and emplacement of nappes in the central Scottish Highlands." Geol. Soc. Lond. Spec. Pub. 8, Eds: Harris et al.

Brook, M., Brewer, M.S. and Powell, D. (1976). "Grenville age for the rocks in the Moine of north western Scotland." Nature, 260, 515-517

Brown, G.C. (1979). "Geochemical and geophysical constraints on the origin and evolution of Caledonian granites." Geol. Soc. Lond. Spec. Pub. 8, Eds: Harris et al.

Brown, G.C., Cassidy, J., Tindle, A.G. and Hughes, D.J. (1979). "The Loch Doon granite: an example of granite petrogenesis in the British Caledonides." J. Geol. Soc. Lond., 136, 745-753.

Brown, G.C. and Locke, C.A. (1979). "Space-time variations in British

Caledonian granites: some geophysical correlations." Earth and Planetary Science Letters, 45, 69-79.

Brown, G.C., Plant, J.A. and Simpson, P.R. (1981). "Caledonian plutonism in Britain: a summary." J. of Geophys. Res., 86 B11, 10502-10514.

Bullard, in Discussion, Giletti et al., (1961).

Cawthorn, R.C. and O'Hara, M.J. (1976). "Amphibole fractionation in calc-alkaline magma genesis." Amer. J. Sci. 276, 309-329.

Chappell, B.W. and White, A.J.R. (1974). "Two contrasting granite types." Pacific Geology, 8, 173-174.

Clayburn, J.A.P. (1981). "Age and petrogenetic studies of some magmatic and metamorphic rocks in the Grampian Highlands." Unpub. D. Phil. Thesis, Univ. of Oxford.

Clemens, J.D. (1984). "Water contents of silicic to intermediate magmas." Lithos, 17, 273-287.

Clemens, J.D. and Wall, V.J. (1981). "Origin and crystallisation of some peraluminous (S-type) granitic magmas." Canadian Mineralogist, 19, 111-131.

Collins, W.J., Beams, S.D., White, A.J.R. and Chappell, B.W. (1982). "Nature and origin of A-type granites with particular reference to southeastern Australia." Contrib. Mineral. Petrol., 80, 189-200.

Cox, K.G., Bell, J.B., and Pankhurst, R.J. (1979). "The Interpretation of igenous rocks." George, Allen & Unwin, 450 pp.

Craig, G.Y. "The Geology of Scotland." Scottish Academic Press.

Czamanske, G.K. and Wones, D.R. (1973). "Oxidation during magmatic differentiation, Finnmarka complex, Oslo area, Norway: Part 2, The mafic silicates." J. Petrol., 14, 349-380.

Deer, W.A., Howie, R.A., and Zussman, J. (1966). "An introduction to the rock-forming minerals." Longman Group Ltd., London. 528 pp..

Dodge, F.C.W., Moore, J.G., Papike, J.T. and May, R.E. (1968). "Hornblendes from granitic rocks of central Sierra Nevada batholith, California." J. Petrol., 9, 378-410.

Doolan, B.L., Drake, J.C. and Crocker, D. (1973). "Actinolite and sub calcic hornblende from a greenstone of the Hazen's Notch Formation, Lincoln Mountain quadrangle, Warren, Vermont." Geol. Soc. Amer. Abstr. with Prog., 5, 157.

Doolan, B.L., Zen, E-an and Bence, A.E. (1978). "Highly aluminous hornblendes: composition and occurrences from southwestern Massachussets." Amer. Mineral., 63, 1088-1099.

Emmermann, R., Daieva, L. and Schneider, J. (1975). "Petrologic significance of rare earths distribution in granites." Contrib. Mineral. Petrol.,

52, 267-283.

Fettes, D.J. (1979). "A metamorphic map of the British and Irish Caledonides." Geol. Soc. Lond. Spec. Pub. 8, Eds: Harris et al.

Fleet, M.E. and Barnett, R.L. (1978). "Al^{IV}/Al^{VI} partitioning in calciferous amphibole from the Flood Mine, Sudbury, Ontario." Can. Mineral., 16, 527-532.

Fourcade, S. and Allegre, C.J. (1981). "Trace elements behaviour in granite genesis: a case study. The calc-alkaline plutonic association from the Querigut complex (Pyrenees, France)." Contrib. Mineral. Petrol., 76, 177-195.

France, D.S. (1971). "Structure and metamorphism of the Moine and Dalradian rocks in the Grampians of Scotland near Beinn Dorain between Tyndrum and Moor of Rannoch." Unpub. Ph.D. thesis, Univ. of Liverpool.

Fridrich, C.J. and Mahood, G.A. (1984). "Reverse zoning in the resurgent intrusions of the Grizzly Peak cauldron, Sawatch Range, Colorado." Geol. Soc. Amer. Bull., 95, 779-787.

Gilbert, M.C. and Troll, G. (1974). "A comparison of the stabilities of OH and F- tremolite." Int'l. Mineral. Assoc., 9th General Meeting, Berlin and Regensburg, Germany. Collected Abstracts.

Giletti, Moorbath, S. and Lambert, R.St.J. (1961). "A geochronological study of the metamorphic complexes of the Scottish Highlands." Quar. J. Geol.

Soc. Lond., 117, 233-72.

Hall, A. (1967). "The chemistry of appinitic rocks associated with the Ardara pluton, Donegal, Ireland." Contrib. Mineral. Petrol. 16, 156-171.

Halliday, A.N., Aftalion, M., van Breemen, O. and Jocelyn, J. (1979). "Petrogenetic significance of Rb-Sr and U-Pb isotopic systems in the 400 Ma old British Isles granitoids and their hosts." Geol. Soc. Lond. Spec. Pub. 8, Eds: Harris et al.

Hamilton, P.J., O'Nions, R.K. and Pankhurst, R.J. (1980). "Isotope evidence for the provenance of some Caledonian granites." Nature 287, 279-284.

Hanson, G.N. (1978). "The application of trace elements to the petrogenesis of igneous rocks of granitic composition." Earth and Planetary Science Letters, 38, 26-43.

Harmon, R.S. and Halliday, A.N. (1980). "Oxygen and Strontium isotope relationships in the British late Caledonian granites." Nature 283, 21-25.

Harris, A.L. (1978). "Dalradian rocks of Britain." in "The Orthotectonic Caledonides of Scotland." G. S. C. Paper, 78-113.

Harris, A.L. and Pitcher, W.S. (1975). "The Dalradian Supergroup." Geol. Soc. Lond. Spec. Pub. 6.

Harvey, P.K., Taylor, D.M., Hendry, R.D. and Bancroft, F. (1973). "An accurate fusion method for the analysis of rocks and chemically related materials by X-ray fluorescence spectrometry." X-ray Spectro., 5, 33-44.

Haslam, H.W. (1968). "The crystallisation of intermediate and acid magmas at Ben Nevis, Scotland," J. Petrol., 9, 84-104.

Hawthorne, F.C. (1981). "The quantitative characterization of cation ordering in minerals. A review." Amer. Mineral., 66.

Hibbard, M.J. (1979). "Myrmekite as a marker between preaqueous and post aqueous phase saturation in granitic systems." Geol. Soc. Amer. Bull., 90, 1047-1062.

Hibbard, M.J. (1981). "The magma mixing origin of mantled feldspars." Contrib. Mineral. Petrol., 76, 158-170.

Hildreth, W. (1981). "Gradients in silicic mamga chambers: implications for lithospheric magmatism." J. Geophys. Res., 86, B11 10153-10192.

Hinxman, L.W., Carruthers, R.G. and MacGregor, M. (1923). "The geology of Corrour and the Moor of Rannoch." Mem. Geol. Surv. Scot. Explanation of Sheet 54.

Hyndman, D.W. (1984). "A petrographic and chemical section through the Northern Idaho batholith." J. Geol., 92, 83-102.

Irving, A.J. (1978). "A review of experimental studies of crystal/liquid

rocks in the Chugoku District, Southwest Japan." J. Japan. Soc. Japan 83, 718-724

Lambert, R. St J., Holland, J.G. and Wichester, J.A. (1982). "A geochemical comparison of the Dalradian Leven schists and the Grampian Division Monadhliath schists of Scotland. J. Geol. Soc. Lond., 139, 71-84.

Lambert, R. St J. and McKerrow, W.S. (1976). "The Grampian orogeny." Scot. J. Geol., 12(4), 271-292.

Lameyre, J. and Bowden, P. (1982). "Classification of plutonic rocks: discrimination of various granitic series by their modal composition." J. Volcanol. Geotherm. Res., 14, 169-186.

Leake, B.E. (1978). "Nomenclature of amphiboles." Amer. Mineral., 63, 1023-1052.

Leake, B.E., Hendry, G.L., Kemp, A., Plant, A.G., Harry, P.K., Wilson, J.R., Coats, J.S., Ancott, J.W., Lunel and Howarth, R.J. (1974). "The chemical analysis of rock powders by automatic X-ray fluorescence." Chem. Geol., 5, 7-86.

Litherland, M. (1970). "The stratigraphy and structure of the Dalradian rocks around Loch Creran, Argyll." Unpub. Ph.D. thesis, Univ. Liverpool.

Loomis, T.P. and Welber, P.W. (1982). "Crystalisation processes in the Rocky Hill granodiorite pluton, California: an interpretation based

on compositional zoning of plagioclase." Contrib. Mineral. Petrol., 80, 230-239.

Luth, W.C., Jahns, R.H. and Tuttle, O.F. (1964). "The granite system at pressures of 4 to 10 kilobars." J. Geophys. Res, 69(4), 759-773.

Luth, W.C. and Tuttle, O.F. (1969). "The hydrous vapour phase in equilibrium with granite and granitic magmas." Geol. Soc. Amer. Mem., 115, 513-548.

McBirney, A.R. (1980). "Mixing and unmixing of magmas." J. Volcanol. Geotherm. Res. 7, 357-371.

McDowell, S.D. (1978). "Little Chief granite porphyry: Feldspar crystalization history." Geol. Soc. Amer. Bull., 89, 33-49.

Maaloe, S and Wyllie, P.J. (1975). "Water content of a granite magma deduced from the sequence of crystallisation determined experimentally with water-undersaturated Contditions." Contrib. Mineral. Petrol., 52, 175-191.

Munoz, J.L. and Luddington, S.D. (1974). "Fluoride-hydroxyl exchange in biotite." Amer. J. Sci., 274, 396-413.

Naney, M.T. and Swanson, S.E (1980). "The effect of Fe and Mg on crystallisation in granitic systems." Amer. Mineral., 65, 639-53.

Nockolds, S.R. and Mitchell, R.L. (1948). "The geochemistry of some

Caledonian plutonic rocks: and study in the relationship between the major and trace elements of igneous rocks and their minerals." Trans. Roy. Soc. Edin., 61, 533-575.

Norrish, K. and Chappell, B.W. (1977). pages 201-272 in "Physical methods in Determinative mineralogy." Ed. Zussman, J. Academic Press.

Pankhurst, R.J. (1975). Discussion of Harris and Pitcher (1975).

Pankhurst, R.J. (1979). "Isotope and trace element evidence for the orgin and evolution of Caledonian granites in the Scottish Highlands." in "Origin of Granite Batholiths, Geochemical evidence." Atherton and Tarney (Eds.).

Pankhurst, R.J. and Pidgeon, R.T. (1976). "Inherited isotope systems and the source region pre-history of early Caledonian granites in the Dalradian series of Scotland." Earth and Planetary Science Letters, 31, 55-68.

Pankhurst, R.J. and Sutherland, D. "Caledonian granites and diorites of Scotland and Ireland." in "Igneous rocks of the British Isles." (Ed. Sutherland).

Parsons, I. (1978). "Feldspars and fluids in cooling plutons." Min. Mag., 42, 1-19.

Peach, B.N. and Horne, J. (1930). in "Chapters on the Geology of Scotland."

Oxford Univ. Press.

Pearce, J.A. and Norry, M.J. (1979). "Petrogenetic implications of Ti, Ar, Y and Nb variations in volcanic rocks." Contrib. Mineral. Petrol., 69, 33-47.

Peccerillo, A. and Taylor, S.R. (1976). "Geochemistry of Eocene calc-alkaline volcanic rocks from the Kastamonu area, Northern Turkey." Contrib. Mineral. Petrol., 58, 63-81.

Phillips, W.E.A., Stillman, C.J. and Murphy, T. (1976). "A Caledonian plate tectonic model." J. Geol. Soc. Lond., 131, 579-609.

Phillips, W.J., Fuge, R. and Phillips, N., (1981). "Convection and crystallisation in the Criffell-Dalbeattie pluton." J. Geol. Soc. Lond., 138, 351-366.

Piasecki, M.A.J. and van Breemen, O. (1979). "The central Highland granulites: cover-basement tectonics in the Moine." Geol. Soc. Lond. Spec. Pub. 8. Eds. Harris et al.

Piasecki, M.A.J. and van Breemen, O. (1979). "A Morarian age for the "Younger Moines" of central and western Scotland." Nature, 278, 734-736.

Piasecki, M.A.J. (1980). "New light on the Moine rocks of the central Highlands of Scotland." J. Geol. Soc. Lond., 137, 41-59.

Rast, N. (1963). "Structure and metamorphism of the Dalradian rocks of Scotland." in "The British Caledonides." Eds. Johnson and Stewart.

Read, H.H. (1956). "Mylonisation and cataclasis in acidic dykes in the Insch gabbro and its aureole." Proc. Geol. Assoc. Lond., 62, 237-47.

Read, H.H. (1961). "Aspects of Caledonian magmatism in Britain." Liverpool & Manchester Geol. Jour., 2, 653-83.

Roberts, J.L. and Treagus, J.E. (1977b). "Polyphase generation of nappe structures in the Dalradian rocks of the South-west Highlands of Scotland." Scot. J. Geol., 13 237-54.

Roberts, J.L. and Treagus, J.E. (1979). "Stratigraphical and structural correlation between the Dalradian rocks of the SW and Central Highlands of Scotland." Geol. Soc. Lond. Spec. Pub. 8 Eds: Harris et al.

Shackleton, R.M. (1979). "The British Caledonides: comments and summary." Geol. Soc. Lond. Spec. Pub. 8. Eds. Harris et al.

Sibley, F., Vogel, T.A., Walker, B.W. and Byerly, G. (1976). "The origin of oscillatory zoning in plagioclase: a diffusion and growth controlled model." Amer. J. Sci., 276, 275-284.

Smith, J.V. (1974). Feldspar minerals. 1. Crystal structure and physical properties." Springer-Verlag, New York.

Smith, R.K. and Lofgren, G.E. (1983). "An analytical and experimental study of zoning in plagioclase." Lithos, 16, 153-168.

Stephens, W.E. and Halliday, A.N. (1979) "Compositional variation in the Galloway plutons." in "Origin of Granite Batholiths, Geochemical evicence." Altherton and Tarney (Eds.)

Stephens, W.E. and Halliday, A.N. (1984). "Geochemical contrasts between late Caledonian granitoid plutons of northern, central and southern Scotland." Trans. Roy. Soc. Edin., 65.

Streckeisen, A. (1976). "To each plutonic rock its proper name." Earth and Planetary Science Letters, 12, 1-33.

Sturt, B.A. (1961). "The geological structure of the area south of Loch Tummel." Quar. J. Geol. Soc. Lond., 117, 131-56

Sun, S-S., Nesbitt, R.W. and Sharaskin, A.Ya. (1979). "Geochemical characteristics of mid-ocean ridge basalts." Earth and Planetary Science Letters 44, 119-138.

Swanson, S.E. (1978). "Petrology of the Rocklin pluton and associated rocks, western Sierra Nevada, California." Geol. Soc. Amer. Bull., 89, 679-686.

Tagiri, M. (1977). "Fe-Mg partition and miscibility gap between co-existing calcic amphiboles from the Southern Abukuma Plateau, Japan." Contrib. Mineral. Petrol., 62, 271-281.

Thirwall, M.F. (1981). "Implications for Caledonian plate tectonic models of chemical data from volcanic rocks of the British Old Red Sandstone." J. Geol. Soc. Lond., 138, 123-138.

Thomas, P.R. (1965). "The structure and metamorphism of the Moinian rocks in the Glen Garry, Glen Tilt and adjacent disricts of Scotland." Unpub. Ph.D. thesis, Univ. Liverpool.

Thomas, P.R. (1979). "New evidence for a Central Highland root zone." Geol. Soc. Lond. Spec. Pub. 8, Eds. Harris et al.

Thornton, C.P. and Tuttle, O.F. (1960) "Chemistry of igneous rocks, 1. Differentiation index." Amer. J. Sci., 258, 664-84.

Tindle, A.G and Pearce, J.A. (1981). "Petrogenetic modelling of in-situ fractional crystallisation in the zoned Loch Doon pluton, Scotland." Contrib. Mineral. Petrol., 78, 196-207.

Treagus, J.E. (1964). "The structural and metamorphic history of an area of Moine and Dalradian rocks south of Loch Rannoch, Perthshire." Unpub. Ph.D. thesis, Univ. Liverpool.

Treagus, J.E. and King, G. (1978). "A complete Lower Dalradian succession in the Schiehallion district, central Perthshire." Scot. J. Geol., 14.

Tuttle, O.F. and Bowen, N.L. (1958). "Origin of granite in the light of experimental studies in the system $NaAlSi_3O_8$ - $KAlSi_3O_8$

- SiO_2 - H_2O." Geol. Soc. Amer. Mem., 74, 153pp.

van Breemen, O., Pidgeon, R.T. and Johnson, M.R.W. (1974). "Precambrian and Paleozoic pegmatites in the Moines of northern Scotland. J. Geol. Soc. Lond., 130, 493-509.

van Breemen, O. and Bluck, B.J. (1981). "Episodic granite plutonism in the Scottish Caledonides." Nature 291, 113-117.

Vance, J.A. (1962). "Zoning in igneous plagioclase: normal and oscillatory zoning." Amer. J. Sci. 260, 746-760.

Vance, J.A. (1965). "Zoning in igneous plagioclase: patchy zoning." J. Geol. 73, 636-651.

Vance, J.A. (1969). "On synneusis." Contrib. Mineral. Petrol., 24, 7-29.

Wells, P.R.A. (1979). "P and T conditions in the Moines of the central Highlands of Scotland." Jour. Geol. Soc. Lond., 136, 663-671.

Wells, P.R.A. and Richardson, S.W. (1979). "Thermal evolution of metamorphic rocks in the cenral Highlands of Scotland." Geol. Soc. Lond. Spec. Pub. 8. Eds. Harris et al.

Wiebe, R.A. (1968). "Plagioclase stratigraphy: a record of magmatic conditions and events in a granitic stock." Amer. J. Sci. 266, 690-703.

White, A.J.R. and Chappell, B.W. (1977). "Ultrametamorphism and granitoid genesis." Tectonophysics, 43, 7-22.

Winchester, J.A. (1974). "The zonal pattern of regional metamorphism in the Scottish Caledonides." J. Geol. Soc. Lond., 130, 509-524.

Winchester, J.A. (1981). "The zonal pattern of metamorphism in the pre-Dalradian rocks of the Scottish Caledonides." J. Geol. Soc. Lond., 138, 635-636.

Wones, D.R. (1981). "Mafic silicates as indicators of intensive variables in granitic magmas." Mining Geology, 31, 191-212.

Wyllie, P.J., Huang, W.L., Stern, C.R. and Maaloe, S. (1976). "Granitic magmas: possible and impossible sources, water conents and crystallisation sequences." Journal of Earth Sciences, 13, 1007-1019.

Wyllie, P.J. (1977). "Crustal antexis: an experimental review." Tectonophysics, 43, 41-71.

Yund, R.A. and Ackermand, D. (1979). "Development of perthite microstructures in Storm King granite, New York." Contrib. Mineral. Petrol., 70, 273-280.

Zaleski, E. (1982). "The geology of Speyside and lower Findorn granitoids." Unpub. M.Sc. thesis, Univ. of St Andrews.